Lecture Notes in Civil Engineering

T. Thyagaraj *Editor*

Ground Improvement Techniques and Geosynthetics

IGC 2016 Volume 2

Springer

Lecture Notes in Civil Engineering

Volume 14

Lecture Notes in Civil Engineering (LNCE) publishes the latest developments in Civil Engineering - quickly, informally and in top quality. Though original research reported in proceedings and post-proceedings represents the core of LNCE, edited volumes of exceptionally high quality and interest may also be considered for publication. Volumes published in LNCE embrace all aspects and subfields of, as well as new challenges in, Civil Engineering. Topics in the series include:

- Construction and Structural Mechanics
- Building Materials
- Concrete, Steel and Timber Structures
- Geotechnical Engineering
- Earthquake Engineering
- Coastal Engineering
- Hydraulics, Hydrology and Water Resources Engineering
- Environmental Engineering and Sustainability
- Structural Health and Monitoring
- Surveying and Geographical Information Systems
- Heating, Ventilation and Air Conditioning (HVAC)
- Transportation and Traffic
- Risk Analysis
- Safety and Security

More information about this series at http://www.springer.com/series/15087

T. Thyagaraj
Editor

Ground Improvement Techniques and Geosynthetics

IGC 2016 Volume 2

Springer

Editor
T. Thyagaraj
Department of Civil Engineering
Indian Institute of Technology Madras
Chennai, Tamil Nadu
India

ISSN 2366-2557 ISSN 2366-2565 (electronic)
Lecture Notes in Civil Engineering
ISBN 978-981-13-0558-0 ISBN 978-981-13-0559-7 (eBook)
https://doi.org/10.1007/978-981-13-0559-7

Library of Congress Control Number: 2018941217

Printed on acid-free paper

This Springer imprint is published by the registered company Springer Nature Singapore Pte Ltd.
The registered company address is: 152 Beach Road, #21-01/04 Gateway East, Singapore 189721, Singapore

Foreword

The Indian Geotechnical Society (IGS) was started as the Indian National Society of Soil Mechanics and Foundation Engineering in the year 1948, soon after the Second International Conference on Soil Mechanics and Foundation Engineering held at Rotterdam. The Society was affiliated to the International Society in the same year, and since then, it has strived to fulfil and promote the objectives of the International Society. In December 1970, the name 'Indian Geotechnical Society (IGS)' was adopted.

The Society conducted several symposia and workshops in different parts of India since its inception in 1948. It was in the year of 1983, the Indian Geotechnical Society organized its first annual conference IGC 1983 in Indian Institute of Technology Madras.

Several local chapters of the Society were established over the years, and gradually, the annual conferences were held in different cities under the leadership of the respective local chapters. The conferences were well utilized as the venue for showcasing the research works and the case studies on geotechnical engineering and geoenvironmental engineering, and the papers presented during the deliberations were being published as conference proceedings volume.

The annual conferences IGC 1996 and IGC 2006 were organized by IGS Chennai Chapter, and the papers were published as printed volumes. The practice of printing the volumes was later discontinued in view of large expenditure involved and also because of the easy access to the electronic storage media. The papers then became not accessible to the rest of the geotechnical community.

The responsibility of organizing the annual conference of 2016 was taken up by IGS Chennai Chapter, and the conference was held during 15–17 December 2016. It was felt necessary to publish selected papers for the benefit of the entire geotechnical engineering community as well as of the contributing authors. The Chapter approached Springer with a request to take up this responsibility, and with the great help of Springer, about 150 selected papers are being published in four volumes under the series 'Lecture Notes in Civil Engineering'. The selected papers are distributed among these volumes depending upon the topic of discussion.

Volume 1—Geotechnical Characterisation and Geoenvironmental Engineering
Volume 2—Ground Improvement Techniques and Geosynthetics
Volume 3—Soil Dynamics and Earthquake Geotechnical Engineering
Volume 4—Geotechnical Applications

I am thankful to all the general editors and the reviewers of these papers who provided valuable review comments for the betterment of the papers published in these volumes. The support provided by the former President of the Indian Geotechnical Society, the late Prof. Sreerama Rao, and the former Honorary Secretary of IGS, Shri Jai Bhagwan, is gratefully acknowledged here.

Bringing out these volumes under the banner of prestigious publishers, Springer will immensely improve the visibility of these conference proceedings volumes. The Chennai Chapter of the Indian Geotechnical Society places on record its acknowledgement of the efforts put forth by Springer for bringing out these volumes for the benefit of the geotechnical engineering community.

Chennai, India

Prof. A. Boominathan
Chairman, Indian Geotechnical Conference 2016
Department of Civil Engineering, IIT Madras

Preface

The demand for land is increasing day by day owing to the rapid urbanization and industrialization in developing countries, in particular India. This leads to the unavailability of good construction sites, and thus, it becomes inevitable to construct on problematic soils or unsuitable soils, such as soft soils, expansive soils and collapsible soils. Construction on problematic soils requires either expensive foundations such as pile foundations or adoption of shallow foundations with suitable ground improvement techniques.

The objective of the ground improvement techniques is to improve the engineering properties of the soil to suit the specific project requirements, which include an increase in dry density and thus the shear strength characteristics of soil and the reduction in compressibility of soil which decreases the settlements, and to control the permeability characteristics. The volume change control using various methods is important in case of expansive soils.

Ground improvement can be broadly categorized into four groups, namely mechanical modification, hydraulic modification, physical and chemical modification and modification by geosynthetics and inclusions. In the last five decades, significant advances have been made in the ground improvement techniques and modelling of improved materials. Invention of new methods of ground improvement and improvement of the existing ground improvement methods continue as long as the demand for the land exists.

This volume presents 45 contributing papers pertaining to 'Theme 3: Ground Improvement and Geosynthetics' of Indian Geotechnical Conference 2016. The papers cover wide range of topics of ground improvement, which include chemical modification using admixtures, microbial-induced carbonate precipitation, geopolymers, fly ash and other industrial wastes, modification using geosynthetic materials such as natural and synthetic fibres, EPS geofoam, prefabricated vertical drains, geosynthetic-encased granular columns and mechanical densification through sand columns.

I thank all the reviewers for their constructive review of these papers. I am grateful to the technical committee of IGC 2016 for giving me the opportunity to edit this volume of the proceedings.

Chennai, India

Dr. T. Thyagaraj
General Editor

Contents

About the Editor

Dr. T. Thyagaraj is currently an associate professor at the Department of Civil Engineering, Indian Institute of Technology Madras, Chennai. He obtained his B.E. (Civil) from Osmania University, Hyderabad, and M.Sc. (Eng.) and Ph.D. from the Indian Institute of Science, Bangalore. His major areas of research interest include unsaturated soil behaviour, ground improvement techniques, geoenvironmental engineering and use of waste materials in civil engineering applications. He has published 24 papers in repute international journals. He received the IGS-Prof. Dinesh Mohan Award in 2016. Currently, he is an editorial board member of the International Journal of Geotechnical Engineering.

Behaviourial Study on Geopolymer Column in Soil

M. Somu Alias Ramya and S. P. Jeyapriya

Abstract Geopolymer soil column is one of the advancements in Ground improvement techniques. The study is aimed at the comparison of Geopolymer soil column and untreated sand in the load carrying capacity and settlement behavior of footing resting on loose sand. The effects of Geopolymer soil column and untreated sand are investigated by conducting experimental studies. The parameters involved in this study include soil column spacings and curing periods. A load test was carried out on a model footing resting on sand with Geopolymer soil column and untreated sand. Load test is repeated on the footing with Geopolymer soil column at varying curing periods of 7, 14, and 28 days. The load-settlement curve for different curing periods day were compared. It was observed that the Geopolymer soil column has high bearing capacity improvement factor compared to untreated sand. Settlement also considerably reduced while using Geopolymer soil column. A parametric study has been carried out to compare the settlement of Geopolymer soil column and untreated sand by finite element modelling using PLAXIS 2D Software and the results are agreeable with the experimental results.

Keywords Geopolymer · Column spacings · Curing periods · Bearing capacity Settlement

1 Introduction

The term "Geopolymer" was formed by a Davidovitis in 1978 to describe the wide range of materials characterized by networks of inorganic molecules. Geopolymerization is an innovative technology that can transform several aluminosilicate materials into useful products called Geopolymer (or) inorganic polymers. The name geopolymerisation refers to the dissolution of alumina and silica from some

M. Somu Alias Ramya · S. P. Jeyapriya (✉)
Government College of Technology, Coimbatore, India
e-mail: jeyapriyagct@yahoo.co.in

M. Somu Alias Ramya
e-mail: ramyagcecivil@gmail.com

T. Thyagaraj (ed.), *Ground Improvement Techniques and Geosynthetics*, Lecture Notes in Civil Engineering 14, https://doi.org/10.1007/978-981-13-0559-7_1

materials in an alkaline environment and their subsequent polymerization to form new materials (Cristelo et al. 2011). Geopolymer contains combination of fly ash mixed with Potassium Hydroxide (KOH) and Potassium Silicate (K_2SiO_3) or Sodium Hydroxide and Sodium Silicate as alkaline activator (Davidovits 1999; Paloma et al. 1999; Chindaprasirt et al. 2011). Reactions occur at a high rate when the alkaline liquid contains soluble silicate, either sodium or potassium silicate, compared to the use of only alkaline hydroxides. Abdullah et al. (2011) concluded that the Geopolymer cement is produced by totally replacing the Ordinary Portland Cement (OPC). Therefore, the use of Geopolymer technology not only substantially reduces the CO_2 emissions by the cement industries, but also utilizes the waste materials such as fly ash in improving weak soils. Flyash was investigated as a basic ingredient of geopolymeric material (Swanepoel and Strydom 2002). It is to be noted that fly ash, one of the possible sources for making Geopolymer binders is available abundantly worldwide, and yet its usage to date is very limited. An attempt has been made in this research to utilize Geopolymer as an additive to improve soil by forming it as a column similar to stone/sand/lime column with the usage of fly ash and alkaline activators.

2 Geopolymer Preparation

To prepare the Geopolymer the following materials were used

(1) Sand
(2) Flyash
(3) Water
(4) Alkaline activators.

1. Sand

The soil sample was collected from Cauvery river near Lalakudi at Karur district. Various properties such as grain size analysis, Specific gravity, minimum and maximum void ratio, maximum and minimum dry unit weight and last shearing resistance of sand was found out using IS codes and tabulated in Table 1.

2. Flyash

Flyash of class 'F' was used as source material in this study. It was collected from Mettur thermal power plant.

3. Water

The water used for preparing Geopolymer is distilled water.

4. Preparation of alkaline solutions

The alkaline solutions used in this study were Potassium Hydroxide and Potassium Silicate. Potassium Hydroxide pellets are dissolved in water to get Molar concentrations of 1, 5, 10, and 15. Potassium silicate is available in solution form. Both the solutions were mixed together and the alkaline liquid was prepared.

Table 1 Properties of sand

Sl. No	Properties	Values
1.	Coarse sand	8%
2.	Medium sand	61%
3.	Fine sand	31%
4.	D_{10} (mm)	0.28
5.	D_{30} (mm)	0.40
6.	D_{60} (mm)	0.70
7.	C_u	2.5
8.	C_c	0.82
9.	Specific gravity of soil particles	2.65
10.	Maximum dry unit weight (kN/m^3)	16.86
11.	Minimum dry unit weight (kN/m^3)	15.22
12.	Maximum void ratio (e_{max})	0.708
13.	Minimum void ratio (e_{min})	0.542
14.	Angle of internal friction	31°

Table 2 Triaxial test results

Shear strength parameters	Geopolymer specimen			
	1 M	5 M	10 M	15 M
Cohesion (kN/m^2)	40	150	230	290
(φ) (degrees)	29	14	5	3
Shear strength (kN/m^2)	248	277	343	364

2.1 Shear Strength Parameters of Geopolymer Specimen

The proportion of soil to Geopolymer was taken as 60%:40%. (Sharmistha et al. 2012). The Molar strength of KOH is selected for Geopolymer was 1, 5, 10, and 15 M. The results obtained for different molarities are shown in Table 2. It can been seen that the cohesion of Geopolymer stabilized soil increases with the increase of molar strength of KOH solution. Unconsolidated undrained triaxial test was conducted for the Geopolymer Specimen.

3 Experimental Study

3.1 Model Test Tank

The dimension of model tank was selected based on the dimension of the model footing. The model footing used was a mild steel circular plate of 60 mm diameter and thickness 5 mm. As per IS1888-1982, the diameter of model tank was fixed as equal to five times the diameter of model footing. Hence, a circular tank of 300 mm diameter and depth 150 mm was used.

3.2 Loading Setup

A loading frame consisting of proving ring of 25 kN capacity and two numbers of LVDTs were placed diagonally opposite was mounted on the plate for settlement observations and is shown in Fig. 1.

Fig. 1 Laboratory model load test on soil treated with Geopolymer column

3.3 Preparation of Geopolymer Soil Column

Geopolymerisation treatment of soil with KOH of 15 M strength and Potassium silicate was used as this trial has given the maximum Shear strength among the tested samples. The diameter of Geopolymer soil column was 12 mm and the length of the column was 75 mm. The water content of soil in all the tanks was maintained as 4%, for the ease of making hole in the sandy soil with a PVC pipe of external diameter of 12 mm. The density of soil achieved in moist condition is 15.55 kN/m^3. Geopolymer solutions was poured in the holes so that Geopolymer soil columns were formed. Totally nine columns were made for 2, 2.5 and 3*d* spacing, where *d* is diameter of Geopolymer soil column. The geopolymer soil column is placed in equilateral triangular pattern arrangement.

4 Results and Discussions

The ultimate load, bearing capacity and improvement factor for Geopolymer column at different spacings after 7, 14, and 28 days curing periods as shown in Table 3. The load vs settlement of Geopolymer soil column placed at different spacings and at 7 days of curing is presented in Fig. 2.

From Fig. 2, it was observed that as the spacing is increased, the load carrying capacity decreases and the settlement increases. Similarly the same trend was observed after 14 and 28 days of curing. The spacing should be kept minimum and maximum curing should be given for treated sand to get higher bearing capacity as observed from the bearing capacity values and improvement factor. Earlier research reported that increase in strength was observed with increase in curing periods (Palomo et. al. 1999).

Table 3 Ultimate bearing capacity of Geopolymer soil column for different spacing and curing periods

Curing periods	Spacing	Ultimate load (kN)	Bearing capacity (kN/m^2)	Improvement factor
Untreated sand	–	0.25	88.65	–
7 days	2D	0.42	148.93	1.679
	2.5D	0.39	138.29	1.559
	3D	0.33	117.02	1.320
14 days	2D	0.46	163.12	1.840
	2.5D	0.43	152.48	1.720
	3D	0.36	127.66	1.440
28 days	2D	0.49	173.75	1.959
	2.5D	0.45	159.57	1.80
	3D	0.38	134.75	1.520

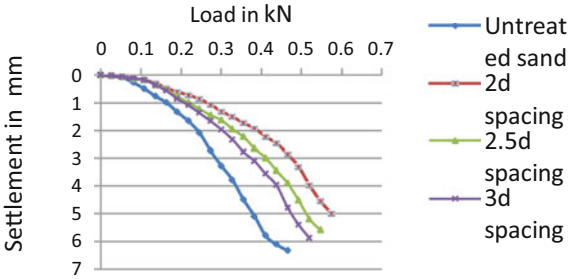

Fig. 2 Load settlement curve for Geopolymer column after 7 days of curing

5 Software Analysis

5.1 Introduction

PLAXIS is a finite element package intended for the two-dimensional analysis of deformation and stability studies in Geotechnical Engineering.

5.2 Input of Soil Data

In this study, axisymmetry model is used to analyse the load-settlement behavior. Soil hardening model is adopted for the soil medium. Footing is modelled as a plate element. Prescribed load method is used to obtain the ultimate settlement. The soil parameters obtained from the laboratory investigations are used as input in PLAXIS. Other data required are taken as standard values from the program. The property given as input to run the model for loose sand condition is shown in Table 4.

Table 4 Input of soil data

Parameters	Values
Material model	Hardening soil model
Drainage condition	Drained
γ_{unsat} (kN/m^3)	17.18
γ_{sat} (kN/m^3)	20.70
Φ (degree)	31
Material type	Saturated
Material state	Loose condition

6 Software Analysis

The vertical displacement of footing was taken by considering Axisymmetry is shown in Figs. 3 and 4. In order to analyse the settlement characteristics by using PLAXIS 2D a comparison was made between the settlement of model footing resting on untreated sand and Geopolymer soil column at an ultimate load of 22 kN/m^2. The corresponding settlement was found to be 2.13 mm for footing with untreated sand and 1.24 mm for footing with Geopolymer soil column at 2*d* spacing. This showed that formation of Geopolymer column improved the bearing capacity with reduction in settlement.

Capacity is shown in Figs. 3 and 4.

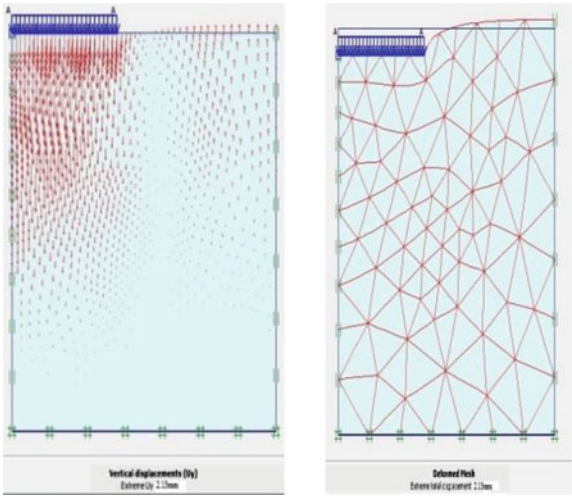

Fig. 3 Vertical displacement without Geopolymer

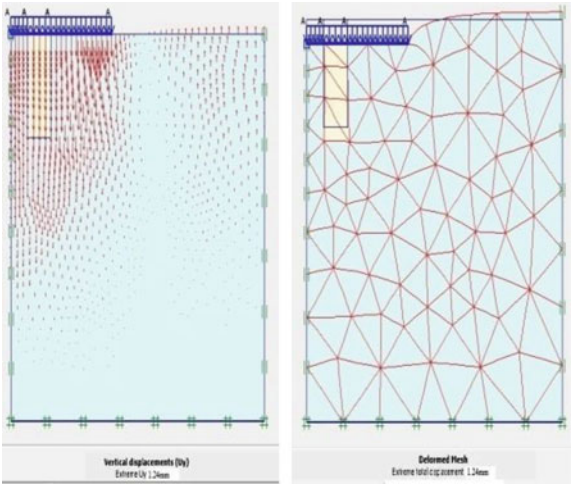

Fig. 4 Vertical displacement with Geopolymer at 2*d* spacing

Table 5 Settlement values for experimental and numerical analysis

Spacing	Experimental analysis	Numerical analysis
Untreated sand	1.9	2.13
2*d*	1.0	1.24
2.5*d*	1.4	1.51
3*d*	1.66	1.83

PLAXIS model was made to validate the experimental results. Among the Selected spacings 2 D spacing was found to be effective in terms of ultimate load and Bearing capacity (Table 5).

7 Conclusions

Based on this model study, the following conclusions are drawn.

1. Geopolymer is one of the promising techniques employed for improving loose cohesionless sand.
2. Geopolymer column prepared using Potassium Silicate and Potassium Hydroxide of 15 M showed increased cohesion of soil thereby increasing the shear strength of soil.
3. From the experimental study on Geopolymer soil column on varying curing periods, it was observed that the load carrying capacity of Geopolymer soil column increased with increase in curing days. Increase in spacing decreases the load carrying capacity.
4. The improvement of bearing capacity of Geopolymer soil column for 2*d* spacing was increased by 68, 84 and 96% after 7, 14, and 28 days respectively.
5. It is observed both from experimental and PLAXIS the settlement of the footing can be considerably reduced with the inclusion of Geopolymer soil column is in loose sand.

References

Abdullah, M. M. A., Hussian, K., Bnhussain, M., Ismail, K. N., & Ibrahim, W. M. W. (2011). Mechanism and chemical reaction of flyash geopolymer cement—A review. *International Journal of Pure and Applied Sciences and Technology*, 35–37.

Chindaprasirt, P., Chareerat, T., Hatanaka, S., & Cao, T. (2011). High strength geopolymer using fine high-calcium fly ash. *Materials In Civil Engineering, ASCE*, 1055–1061.

Cristelo, N., Glendinning, S., & Teixeira Pinto, A. (2011). Deep soft soil improvement by alkaline activation. *Ground Improvement, 164*, 1–10.

Davidovits, J. (1999). Chemistry of Geopolymeric systems, terminology. In *Proceedings of 2nd International Conference on Geopolymer*, pp. 9–40.

Palomo, A., Blanco-Varela, M. T., & Granizo, M. L. (1999). Chemical stability of cementious materials based on metakaolin. *Cement and Concrete research, 29*(7), 997–1004.

Paloma, A., Grutzeck, M. W., & Blanco, M. T. (1999). Alkaliactivated fly ashes: A cement for the future". *Cement and Concrete Research, 29*(8), 1323–1329.

Sharmistha, R. P., Aminul I. L., & Ashim, K. D. (2012). Application of geopolymer in foundation. In *Proceedings of Indian Geotechnical Conference*, Delhi, pp. 73–76.

Swanepoel, J. C., & Strydom, C. A. (2002). Utilisation of fly ash in a geopolymeric material. *Applied Geochemistry, 17,* 1143–1148.

A Study of Parameters Influencing Efficiency of Micropile Groups

Binu Sharma, Sushanta Sarkar and Zakir Hussain

Abstract Micropiles support loads individually, as group or as a network. In cases of groups and networks, the micropiles and the surrounding soil will form a composite block to resist the applied loads. This may lead to a group capacity or network capacity that is different from the total capacity of individual piles consisting of the group or network. The group effect of piles in granular soil has been studied by many researchers, the results of which so far have been inconsistent. Therefore, it is difficult in practice to compare the performance of micropile groups from one test program with other, without considering all the factors together. This work consists of a model experimental study of group behaviour in sand. In this paper three important parameters, namely length-to-diameter ratio (L/D), spacing of piles and relative density of sand were considered. For this purpose 12 micropile groups with each group arranged in a square grid of four piles, with centre-to-centre spacing of 2D, 4D, and 6D and with L/D ratio of 20, 35, 50, and 65 were installed in sand bed having relative density of 50%. The group effect of ultimate total resistance on contractive (loose) sand was studied by installing the same number of micropile groups in sand having relative density of 30%. Similarly the group effect on dilative (dense) sand was studied by installing another twelve groups in sand having a relative density of 80%. The model micropile groups were subjected to axial compressive loading. The group efficiency came out to be high at 4D spacing for the entire different L/D ratio for the loose and the medium dense sand. Positive group effect was observed in most cases but in case of micropile group in 80% relative density, mostly negative group effect was observed. Most importantly the group efficiency was found to be a function of L/D ratio, spacing of the micropile groups and relative density of sand.

B. Sharma (✉) · S. Sarkar · Z. Hussain
Department of Civil Engineering, Assam Engineering College, Guwahati, India
e-mail: binusharma78@gmail.com

S. Sarkar
e-mail: santac7409@gmail.com

Z. Hussain
e-mail: zakirhussain.ray@gmail.com

T. Thyagaraj (ed.), *Ground Improvement Techniques and Geosynthetics*, Lecture Notes in Civil Engineering 14, https://doi.org/10.1007/978-981-13-0559-7_2

Keywords Micropiles · Length-to-diameter ratio (L/D) · Spacing of piles
Relative density of sand

1 Introduction

Micropiles are small diameter piles having diameter less than 250 mm and it is constructed by pressure grouting technique by pumping mortar or concrete into reinforcement (Φ 16–32 mm). It is widely used in view of the facts that its construction equipment is light, employs a flexible layout, requires a low headroom area, exhibits adaptability to construction sites, and has less environmental effect. In cases of groups and networks, the micropiles and the surrounding soil will form a composite block to resist the applied loads. This may lead to a group capacity or network capacity that is different from the total capacity of individual piles consisting of the group or network.

Very few works exist in the literature on efficiency of micropile groups. Lo (1967) observed that the group effect was not consistent, but most of piles presented positive group effect. In case of loose sand the maximum efficiency was found at 3D spacing. Whereas, in dense sand for rough piles, maximum efficiency was found at a closer spacing and then the efficiency decreases with the increase in spacing. Overall efficiency of pile groups was found to be more in loose sand than dense sand in most of the cases except for the pile groups with closer spacing the efficiency was higher in case of dense sand. Plumelle (1984) demonstrated that a negative group effect will develop in a micropile group, with the vertical displacement of the micropile group being greater than the vertical displacement of a single pile under axial loading equivalent to the axial loading per micropiles of a group. Lizzi (1985) reported model test results of group efficiency of micropile on coarse sand. The result showed a positive group effect at spacing between 2 and 6 times the pile diameter and for length of 50D–200D. Thus maximum efficiency was obtained at 4D spacing and at L/D ratio of 200D. The micropile groups in loose and medium dense sand showed similar trend.

In 2006, FHWA (Federal Highway Administration) reported in the case of contractive sands, group effects will result in the reduction of side resistance as compared to an isolated pile case. The opposite will be true in the case of dilative sands. Overlap of shear stresses is the second mechanism effecting side resistance in group piles. Thus, the overlap of shear stresses might contribute to positive increase in side resistance in group piles regardless of the state. Overall side resistance in group piles is dependent on both dilatancy (volume change) and stress overlap mechanisms. In the case of dilative sands, both mechanisms produce a positive effect resulting in increased overall side resistance. However, in the case of contractive sands, increase or decrease in the overall side resistance in group piles would depend on the dominant mechanism. O'Neill's (1983) studies concluded that, for loose soils, the efficiency coefficient of the group was always higher than 1 and reaches a maximum for spacing of Spacing/Diameter ratio of 2 (S/B = 2) and

the coefficient increases with the increase in number of piles in a group. However, the efficiency coefficient was slightly greater than unity for dense sand with a spacing of $2 < S/B < 4$.

This work consists of a model experimental study of group behaviour in sand having three different relative densities. The model micropile groups were subjected to axial compressive loading.

2 Experimental Program

2.1 Experimental Set up

For the experimental study, dry sand (Table 1) was filled up in a model tank with physical dimensions of 1.7 m × 1.5 m × 0.93 m. To fill up the tank at a uniform relative density, the rainfall technique of pluviations was utilized. The tank was filled up by pouring sand uniformly through a strainer and keeping the height of fall of the sand particles constant. It was determined that when the height of fall was 40, 60, and 100 cm, the obtained relative density of the sand was 30, 50 and 80% respectively.

2.2 Installation of Micropiles

Micropiles were installed in a square group of four piles in each group, with a spacing 2D, 4D, and 6D and at L/D ratio of 20, 35, 50, and 65. The piles were casted through a steel casing pipe of external diameter 1.2 cm and internal diameter of 1.0 cm. At the lower end of the pile a 60° wooden conical shoe was attached to

Table 1 Properties of sand

	Properties	Values
1.	Effective grain size	
(i)	D10	0.22
(ii)	D30	0.32
(iii)	D60	0.46
2.	Uniformity coefficient, C_u	2.08
3.	Coefficient of curvature, C_c	0.98
4.	Specific gravity of sand, G_s	2.67
5.	Maximum void ratio, e_{max}	0.88
6.	Minimum void ratio, e_{min}	0.68
7.	Void ratio (e), under relative density 50%	0.78
8.	Φ-value for relative density 30, 50 and 80% respectively	34°, 38°, 43.5°

prevent sand from entering the casing during installation. A 1.5 mm diameter mild steel rod was used as reinforcement. The steel casing pipe along with the steel rod and the wooden shoe was pushed inside the sand manually, using a wooden template having holes at 2D, 4D, and 6D spacing, maintaining the pipe vertical. Maintaining a fluid head of 100 cm inside the casing as it was extracted in 2 cm lift, the pile was grouted using a simple cement slurry mixture with a water-to-cement ratio of 0.5. This process was repeated until the pile was grouted and the casing extracted.

2.3 Loading Arrangement

Vertical load was applied by a mechanical jack system. One end of the proving ring of capacity 0.99 kg/division was attached to a mechanical jack and other end of the proving ring was fixed to the top of the pile cap by ball and socket arrangement shown in Fig. 1.

3 Experimental Results

The micropile groups and single micropiles having length to diameter (L/D) ratio of 20, 35, 50, and 65 were installed in a sand bed of relative density of 30, 50, and 80% in a square grid pattern of four piles per group, with a spacing of 2D, 4D, and 6D, where, D is the diameter of the micropile. Altogether 36 micropile groups and 12 single micropiles were grouted. Ultimate resistance of pile under vertical load has been taken as the point on the load versus displacement curve at which the curve maintains a continuous displacement increase with no further increase in load. Typical load settlement plots of single micropile and micropile group are shown in Figs. 2 and 3. Efficiency of the micropile groups were then calculated as that of conventional piles.

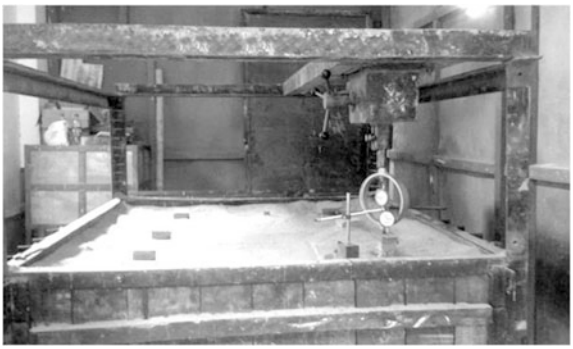

Fig. 1 Loading arrangement

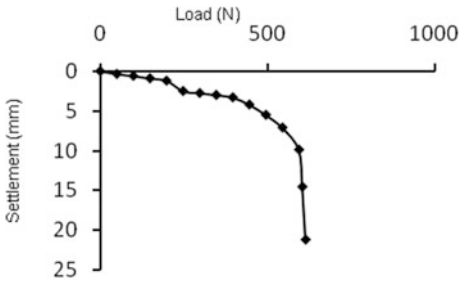

Fig. 2 Load-settlement plot of single micropile at 30% relative density, L/D = 65

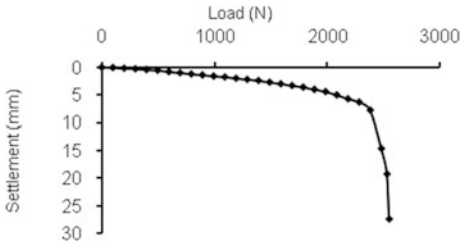

Fig. 3 Load-settlement plot at 2D spacing, at 30% relative density, L/D = 65

3.1 Variation of Efficiency with L/D Ratio

After calculation of efficiency for each of the micropile groups tested, efficiency versus L/D ratio were plotted as shown in Fig. 4. It was found that efficiency of the groups increased with the increase in L/D ratio. All the micropile groups having L/D ratio of 20 exhibited negative group effect, except the group having 4D spacing at 50% relative density. Micropile groups having L/D ratio of 35 and 50 exhibited similar trend. Micropile groups at 4D and 6D spacing having 30 and 50% relative density exhibited positive group effect and the rest showed negative group effect. For L/D ratio of 65, negative group effect was observed at 80% relative density for

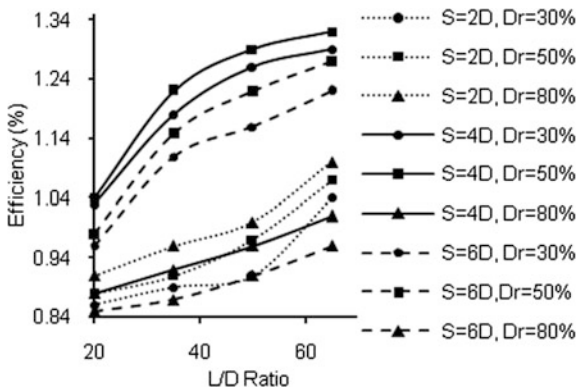

Fig. 4 L/D ratio versus efficiency plot

4D and 6D spacing and the rest exhibited positive group effect. Hence L/D ratio of the micropiles can be assumed as a governing factor affecting the efficiency of the micropile groups.

3.2 Variation of Efficiency with Respect to Relative Density

The trend of efficiency with relative density is plotted in Fig. 5. Efficiency was found to increase from 30 to 50% relative density and then decrease at 80% relative density for 4D and 6D spacing. The trend changes at 2D spacing and the efficiency was found to increase with increase in relative density. For 30 and 50% relative density negative group effect was observed for L/D ratio of 20, 35, and 50 for 2D spacing between the micropile groups. For 80% relative density almost all the group showed negative group effect, irrespective of different spacing between the micropiles. Positive group effect was observed at higher L/D ratios for all the three relative densities. So, relative density is also one of the key factors that influence the efficiency of the micropile groups.

3.3 Variation of Efficiency with Spacing/Diameter Ratio

Figure 6 shows the plot of spacing/diameter ratio versus efficiency of four-pile groups with spacing of 2D, 4D, and 6D. At 30 and 50% relative density, minimum efficiency is observed at 2D spacing and maximum efficiency is observed 4D spacing. Whereas at 80% relative density, maximum efficiency is observed at 2D spacing and it gradually reduces at 4D and 6D spacing. This observation is similar to that of Lo (1967). Group effect of Lizzi's (1985) might not be similar to the present investigation, because of dissimilarity among the parameters but the trend of efficiency was seen almost similar to that of Lizzi (1985) where the maximum efficiency was obtained at 4D spacing and at higher L/D ratio of 200D.

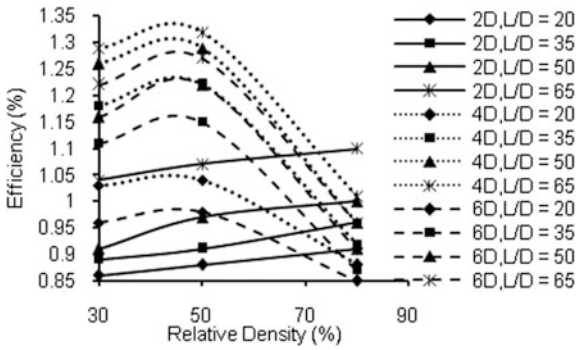

Fig. 5 Relative density versus efficiency plot

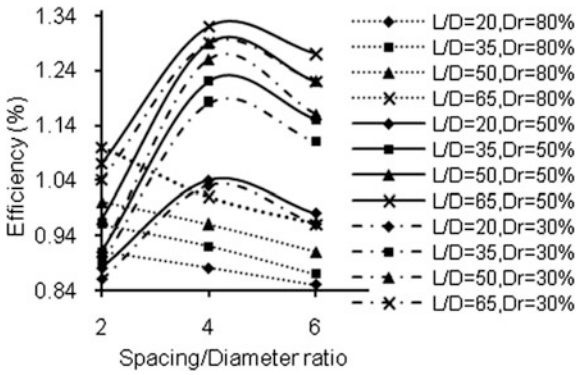

Fig. 6 Spacing/diameter ratio versus efficiency

Table 2 Percentage variation of efficiency with the increase in relative density

L/D ratio	Increase in relative density from (%)	2D in (%)	4D in (%)	6D in (%)
20	30–50	2.32	0.97	2.08
35	30–50	2.24	3.39	3.60
50	30–50	6.60	2.38	5.17
65	30–50	2.90	2.32	4.10
20	30–80	5.81	−14.50	−11.46
35	30–80	7.86	−22.03	−21.62
50	30–80	9.89	−23.81	−21.55
65	30–80	5.80	−21.70	−21.31
20	50–80	3.41	−15.40	−13.30
35	50–80	5.50	−24.60	−24.35
50	50–80	3.10	−25.60	−25.40
65	50–80	2.81	−23.50	−24.41

The micropile groups in loose and medium dense sand showed similar trend in Lizzi's (1985) work which is also observed in this work. Similar agreement with O'Neill's (1983) work is not observed in the present investigation.

Table 2 shows the percentage variation in efficiency, with the increase in relative density. In case of 2D spacing, there is insignificant increase in efficiency with increase in relative density. Again in case of 4D and 6D spacing, percentage increase in efficiency from 30 to 50% relative density is not significant. However for 4D spacing and 6D spacing, percentage decrease in efficiency with increase of relative density from 30 to 80% and from 50 to 80% is found to be significant.

Hence it is observed that the micropile group effect is dependent on many factors and the results so far are inconsistent. Length-to-diameter ratio, state of the sand and relative density are important factors. Moreover the FHWA (Federal Highway

Administration), 2006, has shown that the state of the sand, whether dilative or contractive and overlap of shear stresses are important parameters affecting micropile group effects. Further studies are needed to know better, factors effecting efficiency of micropile groups.

4 Conclusions

Length-to-diameter ratio (L/D), relative density of the sand and spacing of the micropiles in the groups are governing factors affecting the efficiency of the micropile groups. Efficiency of the groups increases with the increase in L/D ratio. At 30 and 50% relative density, minimum efficiency is observed at 2D spacing and maximum efficiency is observed 4D spacing. Whereas at 80% relative density, maximum efficiency is observed at 2D spacing and it gradually reduces at 4D and 6D spacing. Efficiency was found to increase from 30 to 50% relative density and then decrease at 80% relative density for 4D and 6D spacing. The trend changes at 2D spacing and the efficiency was found to increase with increase in relative density.

References

Lizzi, F. (1985). *Pali radice root piles and reticulated pali radice, underpinning* (pp. 84–151). Glasgow (Lanark): Surrey University Press.

Lo. (1967). Discussion to paper by Y. O. Beredugo. *Canadian Geotechnical Journal, 4*, 353–354.

Muhunthan, B., Shu, S., & Marek, A., FHWA Research Report. (2006). Sand state and performance analysis of micropiles' by Balasingham contract DTFH61–03-C_00104, research Task No. 4, Investigation of soil structure interaction and performance of micropiles in seismic retrofitting.

O'Neil. (1983). Group action in offshore piles. In *Proceedings of ASCE Conference, Geotechnical Practice in offshore engineering*, Austin, pp. 25–64.

Plumelle, C. (1984). Improvement of the bearing capacity of soil by insertion of group and reticulated micropiles. In *Proceedings, International Conference on In-situ soil and Rock Reinforcement*, Paris, France, pp. 83–89.

Alteration of CBR Values in Soft Soils Using Enzymatic Lime

Greeshma Nizy Eujine, S. Chandrakaran and N. Sankar

Abstract Natural soil samples were treated and cured with lime, enzyme and enzymatic lime. The cured samples were subjected to various laboratory tests. The optimum dosages were calculated based on the results of Unconfined Compressive Strength Tests. Later samples were mixed with optimum dosages and compacted in Proctor moulds and were subjected to CBR tests at different stages of curing. Significant improvement was observed in enzymatic lime stabilized soils over lime stabilized and enzyme stabilized soils. CBR tests were also done by varying the percentage of clay in the soil specimens. In all tests enzymatic lime stabilized soils exhibited superior improvement of properties.

Keywords CBR · Enzyme stabilization · Ground improvement
Lime stabilization

1 Introduction

During the construction of highways, most often good earth is brought from ex situ or the in situ clayey soil is compacted. In the case of compacted soils, the monsoon season moistens the soil subgrade and the performance of the pavement, or in other words affects its CBR. The CBR or California Bearing Ratio is a measure of pavement stability/thickness or a technique of strength comparison between treated and untreated soils. The CBR of stabilized soils ends to be higher than of untreated soils. In this paper CBR values are compared to study the effect of enzymatic compound extracted from sugar molasses, on soils stabilized with lime.

G. N. Eujine (✉) · S. Chandrakaran · N. Sankar
NIT Calicut, Kozhikode, India
e-mail: nizy_123@yahoo.com

S. Chandrakaran
e-mail: chandra@nitc.ac.in

N. Sankar
e-mail: sankar@nitc.ac.in

T. Thyagaraj (ed.), *Ground Improvement Techniques and Geosynthetics*, Lecture Notes in Civil Engineering 14, https://doi.org/10.1007/978-981-13-0559-7_3

While numerous research works are and have been done to understand the behavior of soil–lime mixtures in the presence of other salts/chemicals, no literature has been found on enzymatic lime soil stabilization. On the other hand a number of case studies have been reported (Vedula et al. 2002) stating that sugar molasses enzyme by itself improves soil properties. The scope of the paper includes observation of the changes in CBR values of cured lime and enzyme treated soil systems and the possible savings in pavement design and construction.

2 Mechanism of Stabilization

As mentioned, the paper describes the use and effect of chemical agents lime and a bioenzyme on the index properties of stabilized soils. The utilization of lime in soil modification is not a novel technology. It is a traditional means in a variety of construction applications since the time of Romans and has never entirely disappeared. When used in soil, lime modification describes an increase in strength brought by cation exchange capacity rather than cementing effect brought by pozzolanic reaction (Sherwood 1993).

It alters the clay surface mineralogy, producing a reduction in plasticity and moisture holding capacity, and an improvement in soil stability. But the disadvantages of lime stabilization include lime carbonation and sulfate salt reactions which may lead to disintegration of bonds on aging. To account for the negative impacts, a number salts and chemicals have been added with lime to soil and tested. Among these already tried and proved agents include cement, fly ash, rice husk, etc.

It was hence decided to mix an enzyme with lime for the purpose of soil stabilization and to study its effects on soil properties. Enzymes are organic molecules that catalyze very specific chemical reactions if conditions are conducive to the reaction. They are typically used in low concentrations as they are not consumed by the reactions they make possible. Enzyme additives attach with large organic molecules that are attracted to the clay mineral's net negative surface charge (Scholen 1992). The enzyme used in the work like other enzymes is costly and a method to reduce the amount of enzyme, while obtaining the same degree of improvement, if achievable would be greatly advantageous. And since lime and enzyme use the same mechanism of cation exchange to improve soil properties, the idea to add both lime and enzyme together in the soil and to investigate the alterations in soil properties seemed feasible.

3 Materials Used and Methodology

The materials used in the present study is a natural clay soil obtained from Pantheerancavu, 12 km south of Calicut, lime purchased from local market in Kunnamagalam at Calicut and bioenzyme acquired from Avijeet agencies, Chennai.

Table 1 Engineering properties of soil

Property	Value
Liquid limit (%)	79
Plastic limit (%)	48
Shrinkage limit (%)	27
Bulk density (kN/m^3)	13.25
Optimum moisture content (%)	32
Soil type	Kaolinitic
Unconfined compressive strength (kPa)	64
Clay content (%)	22.17

Table 2 Properties of bioenzyme

Property	Value
Boiling point	212 F
pH	2.8–3.5
Vapor pressure (mmHg)	As water
Melting point	Liquid
Vapor density (Air = 1)	1
Solubility in water	Infinite
Evaporation rate	As water
Specific gravity (H_2O = 1)	1.00–1.10
Appearance and odor	Lt. gold liquid, characteristic odor

The physical properties of soil used are given in Table 1 and the basic properties of bioenzyme (provided by the supplier) are given in Table 2.

4 Methodology

All the specimens tested in this study were prepared and tested using standard procedures described in the Bureau of Indian Standards—IS 2720 (Part 5):1985, IS 2720 (Part 10):1991, and IS 2720 (Part 16):1987. Soil sample was air dried for a week, pulverized manually using weights, sieved through 425 micron sieve and preserved in large containers in an enclosed room. Lime was sieved using 425 micron sieve and preserved in an air-tight container to prevent carbonation. Bioenzyme was preserved in an air-tight bottle in its original liquid form.

It is known that the Optimum Lime Content of soils vary from 2 to 6% of weight with higher percentages required for soils with higher clay content. Thus soil and lime were mixed from 0 to 10%. The variations in Liquid Limit and Optimum Moisture Content were observed for each fraction within 24 h. The minimum amount of lime that did not further reduce the Liquid Limit i.e. 3.5% was chosen as

approximate Optimum Lime Content. Unconfined Compression Tests were done on soils mixed with lime in the ranges 2–5%, and cured up to four weeks in air-tight bags. The actual optimum lime content was inferred from the results of unconfined compressive strength tests.

Similar tests were also done to determine the optimum dosage of Bioenzyme in the soil. A dilution ratio chart provided by Avijeet agencies (that calculated the required dosage of Bioenzyme for a particular soil based on particle size and plasticity index) served as a reference to determine the range of optimum Enzyme Content. Literature shows that enzymes provide 80% of their final strength in three to four weeks. Hence soil specimens were mixed with Bioenzyme dosages between 70 and 90 ml/m^3, cured up to four weeks in air-tight bags and tested for Unconfined Compressive Strengths. The Optimum Bioenzyme Content was determined from the test results.

Various combinations of soil + lime + enzyme mixtures were cast, cured, and tested at the optimum moisture content of untreated soil. The amount of Bioenzyme was kept close to Optimum Bioenzyme Content predominantly in all cases and percentage lime was varied from 1 to 6%. After several trials and combinations, and comparison of unconfined compressive strength of these specimens, the optimum enzymatic lime dosage was inferred.

From the results of unconfined compression tests, the optimum dosages for soil–lime mixtures, soil enzyme mixtures and soil enzyme lime mixtures were chosen. The CBR tests were performed at these dosages.

5 Results of CBR Tests

A series of experiments were conducted to understand the variation in CBR values of soil lime, soil enzyme, and soil enzyme lime mixtures. The optimum dosages were 3% lime for soil–lime mixtures, 80 ml/m^3 Bioenzyme for soil enzyme mixtures and 70 ml/m^3 Bioenzyme + 1.75% lime for soil enzyme lime mixtures. It was observed that the CBR values increased in comparison to the CBR values of untreated soils. Tables 3 and 4 describe the modification of unsoaked and soaked CBR of natural clay treated with the three stabilizing agents. The CBR values

Table 3 Variation in CBR of soil treated with stabilizers (unsoaked)

Specimen type	CBR values w.r.t period of curing in weeks			
	1	2	3	4
Untreated soil	3.6			
Soil–lime mixture	5.8	8.5	12.9	16
Soil enzyme mixture	4.2	6.2	10.1	13.2
Soil enzyme lime mixture	7.1	14.3	16.3	19.6

Table 4 Variation in CBR of soil treated with stabilizers (soaked)

Specimen type	CBR values w.r.t period of curing in weeks			
	1	2	3	4
Untreated soil	2.7			
Soil–lime mixture	4.2	6.2	8.5	11.5
Soil enzyme mixture	3.8	4.0	5.2	6.8
Soil enzyme lime mixture	4.3	10.2	12.0	13.4

increased up to 5 times when treated with lime alone, up to 3 times when treated with enzyme alone and more than 6 times when treated with enzymatic lime under unsoaked conditions

Figures 1 and 2 describe the load verses penetration curve of unsoaked and soaked CBR samples of untreated and stabilized soil samples at four weeks curing. It is observed that the enzymatic lime-stabilized soils gave higher CBR values under both unsoaked and soaked conditions. Although the improvement remains marginal, it is to be noted from Tables 3 and 4 that the CBR of enzymatic lime stabilized soils at two weeks curing is higher than the CBR of lime treated and enzyme treated soils at four weeks curing. Several studies have been done on lime and enzyme treated soils. However studies on enzymatic lime treated soils have not yet been done.

Yong (2007) studied the effect of lime on Marl Clay and reported that CBR reduced up to 78% under soaked conditions. While in this paper it was observed that CBR reduced up to 29% for lime treated soil, almost 50% for enzyme treated soils and nearly 32% for enzymatic lime-stabilized soils. Bell (1996) found that expansive clays respond more quickly to the lime treatment. In this case montmorillionitic clay has responded quite well to all three additives. The lime in the presence of enzyme has enhanced the soil properties better than lime-stabilized

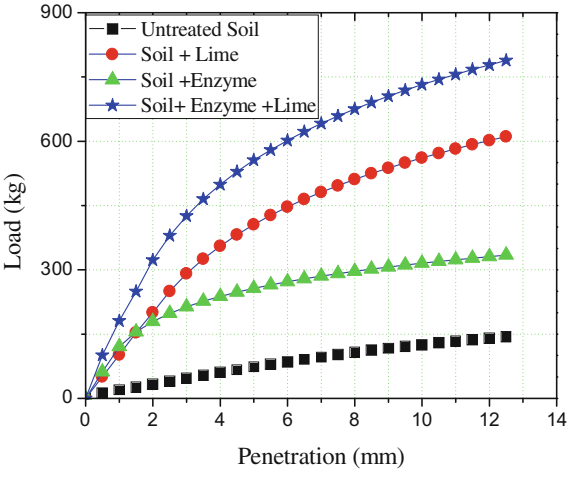

Fig. 1 Load verses penetration graph for soil samples under soaked condition (at 28 days)

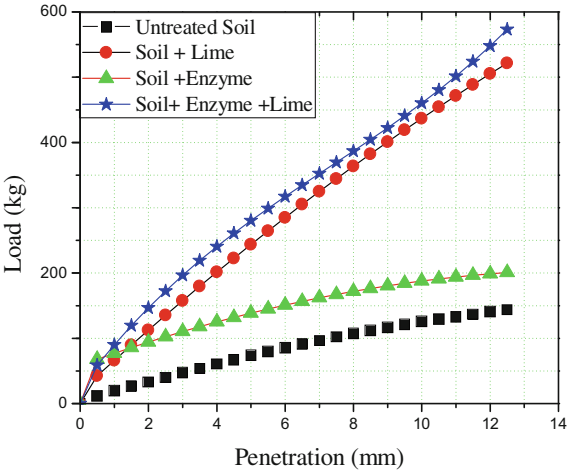

Fig. 2 Load verses penetration graph for soil samples under soaked condition (at 28 days)

soils. Nugent et al. (2009) evaluated the interactions between exo-polymers and kaolinite clay to determine effects on the behavior of the kaolinite. The nano-scale interactions between the kaolinite and the cations and biopolymers used in the study were evaluated and it was found, inter alia, that biopolymer-induced aggregation of clay particles formed a clay-polymer interconnected network through cation bridging and hydrogen bonds. When the soil is combined with lime and enzyme, the cation bonds may be formed at an accelerated rate, bringing bout an increase in strength in shorter duration.

6 Modified Flexible Pavement

A good pavement design enables vehicles to pass through safely and economically. The granular materials are often affected by changes in moisture. The reason soil stabilization improves the pavement performance is because the changes in soil subgrade at the micro level affect the pavement behavior at a macro level (Steyn 2011). A sustainable pavement reduces the use of natural resources and energy consumption. It limits pollution and ensures a high level of user comfort and safety (Maher et al. 2006). Consider the design of flexible pavement of enzymatic lime stabilized soil subgrades, as compared to conventional lime stabilized soils.

Figure 3 describes the thickness of flexible pavement based on the CBR values of underlying subgrade and is a very rudimentary rule-of-thumb check from AUSTROADS (2001). The untreated soil used in this work has an initial CBR of 4, a pavement thickness requirement of 560 mm for an equivalent single axle (ESA) value of 4e7 (Line 1). For the same ESA, while conventional lime treatment increased the CBR to 16, requiring a pavement thickness of 285 mm (Line 2), the enzymztic lime stabilized soil with CBR value 19.6 will require a pavement

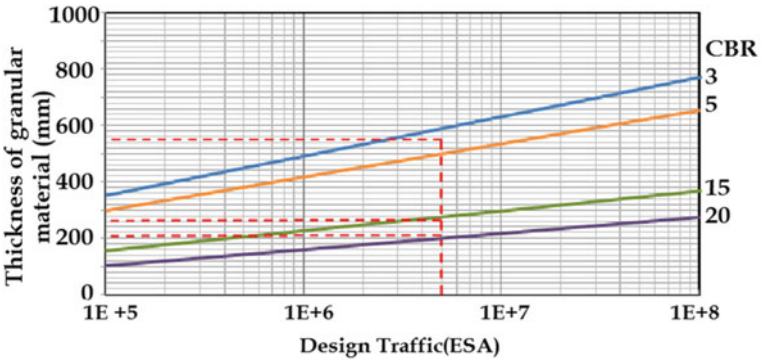

Fig. 3 Design thickness of flexible pavement on varying subgrades

thickness of only 240 mm (Line 3). A considerable savings of 45 mm is possible, along with a reduced curing period of two weeks. The use of this enzymatic lime stabilization system in the field has certain economic advantages on cost. Using local soil as much as possible instead of bringing the material from outside, the digging of the local soil and exchanging with the material brought from outside and avoiding the cost of both transportations, etc., being some. One of the most important advantages of this system is the opportunity to use and develop the local material that generally causes costs to increase, when local material needs to be exchanged with the material that is brought from outside, the opportunity to pre-mixing the material and saving construction time.

It can be concluded that using enzymatic lime stabilization for the construction of pavements, a cost saving up to 20% may be obtained as compared to lime-stabilized methods. The above cost is calculated without considering the maintenance costs which will further reduce the cost of enzymatic lime stabilized soil.

7 Conclusion

Enzymatic Lime Stabilization of soils can be used in improving the bearing capacity of the subgrade, with noticeable savings on both aggregate and disposal charges. Exposure to water has significantly reduced the CBR of all treated soils, with enzyme treated soil being affected the most. CBR of enzymatic lime treated soils have improved by more than 450% in unsoaked condition as compared to untreated soils. Economic advantages of using enzymatic lime stabilization technique include:

- Using local soil as much as possible
- Avoiding transportation cost

- Reduction in construction time
- Reduction in construction materials.

References

Bell, F. G. (1996). Lime stabilization of clay minerals and soils. *Engineering Geology, 42*(1996), 223–237.

Maher, M., Uzarowski, L., Moore, G., & Aurilio, V. (2006). Sustainable pavements—Making the case for longer design lives for flexible pavements. In *Proceedings 51st Annual Conference of the Canadian Technical Asphalt Association*, Charlottetown, Prince Edward Island, Canada, pp. 44–56.

Nugent, R. A., Zhang, G., & Ganbrell, R. P. (2009). The effect of exopolymers on the liquid limit of clays and its engineering implications. *Journal of Transportation Research Board*, 210134–210143.

Scholen, D. E. (1992). *Nonstandard stabilizers*. Report FHWA-FLp-92-011 US Department of Transportation.

Sherwood, P. (1993). *Soil stabilization with cement and lime. State of the art review*. London: Technical Report of Transport Research Laboratory; HMSO.

Steyn, W. J. (2011). Applications of nanotechnology in road pavement engineering. In *Nanotechnology in civil infrastructure* (pp. 49–83). Berlin: Springer.

Vedula, M., Nath, P., & Chandrashekar, B. P. (2002). A Critical Review of Innovative Rural Road Construction Techniques and Their Impacts. National Rural Roads Development Agency, New Delhi.

Yong, R. N., Vahid, R., & Ouhadi, B. (2007). Experimental study on instability of bases on natural and lime/cement—stabilized clayey soils. *Applied Clay Science, 35*, 238–249.

Factors Influencing PVD Performance in Soft Clay Consolidation

R. Radhakrishnan and C. Gunasekaran

Abstract Soft clay consolidation is an important aspect to be considered for large construction projects undertaken in or near coastal areas. Pre-fabricated Vertical Drain or PVD has gained considerable importance in accelerating soft clay consolidation for major civil engineering construction projects worldwide, as it is economical with proven efficiency. However, there is still some confusion and uncertainty in selecting the right type of PVD for a particular project as well as the design procedure to be adopted. As a result, specification for PVD in many cases are made without considering many factors which may influence the performance of such drains for a project. This paper considers the PVD design theory and evaluates various parameters which influence PVD performance such as soil, soil disturbance due to installation, PVD materials, etc., and recommends a procedure for PVD design and selection of PVD and installation method for a project.

Keywords Soft clay · PVD · Consolidation

1 Consolidation Theory

The main objective of soft clay consolidation with PVD is to achieve the desired degree of consolidation within a specified period of time. In classical one-dimensional consolidation theory (Terzaghi 1943), consolidation due to vertical drainage only to natural drainage boundaries is considered. However, the classical one-dimensional consolidation theory can be extended to include vertical as well as horizontal or radial drainage taking place using vertical drains. Average degree of consolidation, U, then is calculated for combined vertical and radial drainage (Carrillo 1942) as follows:

R. Radhakrishnan (✉) · C. Gunasekaran
Geo-Enviro Engineers P Ltd, Chennai, Tamil Nadu 600 041, India
e-mail: geoenviro2012@gmail.com

C. Gunasekaran
e-mail: gunageoenviro@gmail.com

T. Thyagaraj (ed.), *Ground Improvement Techniques and Geosynthetics*, Lecture Notes in Civil Engineering 14, https://doi.org/10.1007/978-981-13-0559-7_4

$$U = 1 - (1 - U_h)(1 - U_v), \tag{1}$$

where

U = overall average degree of consolidation

U_h = average degree of consolidation due to radial drainage

U_v = average degree of consolidation due to vertical drainage.

A general equation for computing average degree of consolidation employing vertical drains due to horizontal or radial drainage was first proposed by Barron (1948) as follows:

$$t = (D^2/8C_h)\,F(n)\ \text{In}\ (1/(1 - U_h), \tag{2}$$

where

C_h = coefficient of consolidation for radial drainage

t = time required to achieve U_h

D = diameter of the cylinder of influence of the drain

$F(n)$ = drain spacing factor = $\ln(D/d_w) - 3/4$, where

d_w = equivalent diameter of drain.

Hansbo (1979) modified Barron's equation to suit consolidation with PVD, incorporating soil disturbance due to drain installation and drain resistance in the following "general" case.

$$t = (D^2/8C_h)\,(F(n) + F_s + F_r)\ \text{In}(1/(1-U_h)), \tag{3}$$

where

F_s = factor for soil disturbance = $((k_h/k_s) - 1)\ \ln(d_s/d_w)$, where

k_h = the coefficient of permeability in the horizontal direction in the undisturbed soil

k_s = the coefficient of permeability in the horizontal direction in the disturbed soil

d_s = diameter of the idealized disturbed zone around the drain

F_r = factor for drain resistance = $\pi\ z\ (L - z)\ (k_h/q_w)$

z = distance below top surface of the compressible soil layer

L = effective drain length

q_w = discharge capacity of the drain (at gradient = 1.0).

In the simplified "ideal" case where soil disturbance and drain resistance are both ignored, the above general case simplifies to Eq. (2) with only function of soil properties (C_h), design requirements (U_h) and design variables (D, d_w).

2 Parameters Which Influence PVD Performance

2.1 Drain Influence Zone, D

The time to achieve a given degree of consolidation is a function of the square of the diameter of the influence cylinder, D. D is a variable in the drain spacing factor, $F(n)$, which is used in both the "general" and "ideal cases". Unlike the other parameters which influence soil consolidation with the exception of d_w, D is a controllable variable since it is a function of drain spacing only. Vertical drains are usually installed in square or triangular patterns. The distance between the drains or drain spacing, S, establishes D with $D = 1.13\ S$ for Square Pattern and $D = 1.05\ S$ for Triangular Pattern. A triangular pattern is usually preferred, since it provides more uniform consolidation between drains when compared with equivalent square pattern.

2.2 Equivalent Drain Diameter, d_w

For practical considerations, assumption is made that both band shaped drain and a circular drain with the same circumference will result in similar soil consolidation. It is therefore reasonable to calculate the equivalent circular diameter of PVD to be:

$d_w = (2(a + b)/\pi)$, where a & b = width & thickness respectively of the rectangular PVD. For commonly available PVD at present, d_w varies from 50 to 75 mm.

2.3 Drain Discharge Capacity, q_w

The drain discharge capacity is mainly influenced by the size of drain, soil confining pressure, and effects of vertical compression on the shape of the drain. During consolidation, soil settlement causes the installed PVD to deform or "buckle". Considerable reduction in drain discharge capacity may result after buckling. It has been noticed that rigid drains cause larger reduction in discharge capacity as buckling starts at relatively lower vertical compression.

2.4 Horizontal Coefficient of Consolidation, C_h

$C_h = C_v\ (k_h/k_v)$, where

k_v = vertical coefficient of permeability.

As laboratory test results are very sensitive to soil sample disturbance, they depend very much on the quality of the soil samples tested. Special equipment and

procedure are required for laboratory determination of C_h. Determination of k_h is therefore usually made from special in situ tests with good-quality tests and equipment. Accuracy of results depends therefore on several factors and in many cases may not be quite reliable. It has been found that even tests carried out with care may result in variable values from the same site (Bergado et al. 2008).

Therefore, in most cases the practice is to determine C_v from laboratory soil consolidation tests and estimate the value of k_h/k_v from field and laboratory tests for PVD design.

Based on several field and laboratory tests in different soil conditions, for most sedimented clays the value of k_h/k_v may vary from 2 to 5 (FHWA 1986). Studies at the Indian Institute of Technology Madras (Sridhar et al. 2014) have shown that for coastal marine clays, a value of $k_h/k_v = 2$ was found applicable, based on special laboratory tests and back analysis of instrument data from a number of project sites. k_h/k_v back-calculated from field instrument data suggest values between 2 and 3 for coastal marine clays (Radhakrishnan and Suriyanarayanan 2010).

2.5 *Soil Disturbance Due to PVD Installation*

Soil consolidation due to combined horizontal and vertical drainage for the "general case" considers both soil disturbance due to drain installation and drain resistance (Eq. 3).

2.5.1 Disturbed Soil Zone or Smear Zone, d_s

For PVD installation, a steel mandrel is used to protect the drain during installation. The mandrel has a cross sectional area larger than that of the drain and it causes shear strains and displacements within the soil surrounding the drain. Accompanied by re-moulding of the surrounding soft soil, it increases the pore pressure and decreases the shear strength in the zone of disturbance (Holtz and Holme 1973). Besides, the hydraulic conductivity of the disturbed soil is reduced and consequently the flow of pore water into the drain and rate of soil consolidation are reduced.

Many researchers have investigated the properties of the disturbed zone using laboratory investigation on large soil samples as well as by numerical methods. Studies by Chai and Miura (1999) and others suggest that the size of the smear zone may vary between 1 and 4 times the equivalent mandrel radius. FHWA (1986) suggests soil disturbed zone, d_s = 5–6 times r_m, where r_m is the radius of circle equivalent in area of mandrel cross section.

Evaluation of soil properties within the disturbed zone is extremely complex. In addition, the following factors also affect drain performance due to soil disturbance resulting from PVD installation which should be minimized as far as possible.

2.5.2 Effect of Mandrel Size and Shape

As disturbance increases with increase in mandrel cross sectional area, it should be as close to the drain cross sectional area to minimize soil displacement, but without affecting stiffness necessary to install the drain to design depths. Mandrel tip and anchor should be as tapered as possible to minimize disturbance. Most mandrels used currently are of rectangular in shape even though some use rhombic shaped mandrels. It has been considered that to minimize soil disturbance, mandrel cross sectional area should not exceed 65 cm^2 (FHWA 1986).

2.5.3 Drain Installation Method

The method of installation causes soil disturbance around the drain. Drain installation disturbs the soil and may reduce the shear strength of the deposit. Vibratory or jetting methods cause increased disturbance to soft soil than static pushing. PVD installation should therefore be by static pull down force where possible. For design purpose it may be considered that within the disturbed soil zone, the soil is completely remoulded.

2.6 PVD Material Parameters

Besides the above, material parameters of PVD used may influence PVD performance.

2.6.1 Drain Filter

PVD filter fabric is exposed to ground water and remoulded fine grained soil after its installation. The fabric serves as a filter when the preloading increases pore pressures and the pore water seeps horizontally into the drain core. The potential therefore exists for the filter fabric to "cake" or clog due to mobility of fines in the remoulded soil.

Filter permeability should be greater than that of the surrounding soil in order not to retard the pore water flow into the drain. However, very high permeability of filter may lead to large inflow of water and may not be effective in preventing fines from passing into the core. It may therefore be more effective to consider filter permittivity, which is defined as the volumetric flow rate per unit area under a given hydraulic head, instead of permeability.

2.6.2 Drain Strength, Flexibility, and Durability

Stress–strain characteristics of drain filter and core should be compatible. The drain core or filter should not break when subjected to handling and installation stresses, which are typically higher than in situ stresses in soil except in cases where sub-grade instability can occur. Therefore, a relatively high rupture strain is considered more important than high tensile strength of the drain.

Durability of the geosynthetic materials throughout the consolidation period is generally not a concern. However, if ground water is suspected to contain solvents or other chemical pollutants, the drain integrity needs to be checked.

Even though individual drain characteristics mentioned above help to select a particular drain, the most important consideration should be that the selected drain will help to achieve the required consolidation within the required period considering the whole system. No drain should be rejected on the basis of one characteristic alone, as there may be compensations when other factors are taken into consideration. For example, one drain may have relatively low filter permeability or discharge capacity which may be offset by a larger equivalent diameter (FHWA 1986).

2.6.3 Drain Length

Drain length should be sufficient to consolidate the soft soil deposit or portions of the deposit to the extent necessary to achieve the design objectives. In some cases, it may not be necessary to fully penetrate the compressible stratum to achieve the necessary shear strength gain or amount of consolidation. Also, as drain length becomes very large, say greater than 25 m, additional length may not improve the consolidation rate considering the effects of drain resistance.

3 Major Parameters Affecting Performance

The "general" case for PVD design considers drain spacing, soil disturbance, and drain resistance. It is noted that the greatest potential effect on t_{90} is due to changes in C_h and D (FHWA 1986). The value of C_h, which can easily vary by a factor of 10, has the most dominant influence on t_{90}. D, which can vary by a factor of about 2–3, has a considerable influence due to the D^2 term. The influence of the properties of the disturbed zone (k_s and d_s), although very difficult to quantify, can be very significant. The equivalent diameter, d_w has only a minimal influence on t_{90}.

For typical values the ratio $F_r/F(n)$ is generally less than 0.05. Therefore, typically the theoretical effect of drain resistance is considerably less than the effect of drain spacing or soil disturbance. As Eq. (3) suggests, the length of PVD may influence drain resistance. It is generally considered that except for PVD deeper than say, 25 m, F_r may not have much influence on PVD performance (FHWA 1986).

4 Suggested Design Procedure

Evaluation of effects of soil disturbance requires determination of (k_h/k_s) as well as diameter of the disturbed zone, d_s. As mentioned above, research indicates that the ratio of (k_h/k_s) may vary from 2 to 5. Both soil sensitivity and condition of soil micro fabric have been found to affect this ratio. Careful consideration, engineering judgement and special testing are necessary to make realistic assessment of (k_h/k_s) for a particular project.

Except for very important major projects where time–settlement relationship has to be established with greater accuracy, such extensive investigation may prove time consuming and expensive. In any case, unless special techniques are adopted for soft soil sampling, soil sample disturbance is a reality and laboratory test results to establish C_v and k_h/k_v values are also subject to error. It may therefore be concluded that except for special projects, consideration of soil disturbance due to PVD installation as proposed in the "general" case for PVD design may not be viable. In the light of this, the following procedure for PVD design is proposed.

4.1 Category—A

For the majority of projects involving ground improvement using PVD, the "ideal" case for PVD design provides reasonable time–settlement relationship where smear and drain resistance effects are ignored. As mentioned earlier, laboratory determination of k_h/k_v values compared well with back-calculated values from field instrument data giving k_h/k_v = 2–3. For conservative analysis, a value of C_h/C_v = 1–2 may be appropriate for use. This procedure may be adopted for PVD design to arrive at reasonably acceptable time-settlement relationship for the majority of ground improvement projects involving coastal marine clays and other soft coastal clays. However, it is important to consider precautions to minimize soil disturbance due to PVD installation and adopt recommended values for other parameters including PVD material parameters as discussed earlier.

4.2 Category—B

For more critical projects where more accurate time-consolidation prediction is required, extensive field and laboratory investigation will be required to establish C_v and k_h/k_v values applicable for a specific project site. As mentioned, evaluation of soil disturbance effects due to PVD installation is complex and may be established either by suitable laboratory investigations or by appropriate numerical analysis method. Recommended values for disturbance as mentioned earlier may be used in lieu.

5 Conclusions

1. Paper discusses theories and procedures currently available for PVD design. Significant parameters which affect PVD performance have been discussed.
2. As evaluation of soil disturbance due to PVD installation as well as drain resistance, which affect time-settlement prediction, is extremely complex and require special and expensive sampling, laboratory investigations and in situ tests.
3. For the majority of projects involving PVD in coastal marine clays, the time-consolidation relationship can be predicted with sufficient accuracy considering the "ideal" case, i.e. C_v value from normal laboratory consolidation tests and considering $k_h/k_v = 2$ or 3.
4. As disturbance to soil due to PVD installation is a major parameter affecting PVD performance, it is important to consider various measures to minimize soil disturbance during PVD installation.

References

Barron, R. A. (1948). Consolidation of fine grained soils by drained wells. *Transmission ASCE, 113,* 718–742.

Bergado, D. T., Balasubramaniam, A. S., Fannin, R. J., & Holtz, R. D. (2008). Innovations & performance of PVD soft ground improvement: A case of the second Bangkok International Airport Project. In *Indian Geotechnical Conference,* Bangalore, pp. 110–134.

Carrillo, N. (1942). Simple two and three dimensional cases in the theory of consolidation of soils. *Journal of Mathematics and Physics, 21*(1), 1–5.

Chai, J. C., & Miura, N. (1999). Investigation of factors affecting vertical drain behavior. *Journal of Geotechnical and Geoenvironmental Engineering, ASCE, 125*(3), 216–226.

FHWA. (1986). Prefabricated vertical drains engineering guidelines. In *FHWA/RD-86/168. Federal Highway Administration* (Vol. 1). Washington. DC.

Hansbo, S. (1979). Consolidation of clay by band-shaped prefabricated drains. *Ground Engineering, 12*(5), 16–25.

Holtz, R. D., & Holme, B. G. (1973). Excavation and sampling around some sand drains in Ska-Edeby. *Sweden Sartryck och Preliminara Rapporter, 51,* 79–85.

Radhakrishnan, R., & Suriyanarayanan, N. S. (2010). Embankment construction over reclaimed land using pre-fabricated vertical drains. In *Proceedings of IGC-2010.*

Sridhar, G., Robinson, R. G., Rajagopal, K., & Radhakrishnan, R. (2014). Comparative Study on Horizontal Coefficient of Consolidation determined using Rowe and Conventional Consolidation Cell. *International Journal of Geotechnical Engineering, 9,* 388–402.

Terzaghi, K. (1943). *Theoretical soil mechanics*. New York: Wiley Inc.

Experimental Study of Heave Control Technique for Expansive Soil Using Micropiles and Geotextile Layers

B. M. Badaradinni, A. M. Hulagabali, C. H. Solanki and G. R. Dodagoudar

Abstract Heaving of expansive soil is a crucial phenomenon due to their excessive volume changes with variation in moisture regime, which in turn leads to substantial distress to the structures built on them. The main objective of this study is to evaluate the effectiveness of micropile and performance of geotextile to resists upward movement of structures built over expansive soil. For this study, the expansive clay compacted in a steel box of size 50 cm × 50 cm × 50 cm to a depth of 20 cm and analyzed with two different methods to control heaving of soil. Firstly, four micropiles of 16 and 20 mm in diameter were inserted into the soil with and without frictional resistance. The micropiles were fastened to the corners of footing of size 15 cm × 15 cm × 0.5 cm, with nut and bolt system. Further, Geotextiles were reinforced below the footing at a vertical spacing of 0.1B and 0.3B as single and double layers. Then the soil was saturated with water and the upward movement of model footings (swelling) was monitored with time. Test results showed that maximum heave reduction was 79% for 20 mm diameter micropiles with frictional resistance.

Keywords Expansive soil · Geotextile · Micropile · Footing
Frictional resistance

B. M. Badaradinni (✉) · A. M. Hulagabali
Department of Civil Engineering, Basaveshwar Engineering College, Bagalkot, Karnataka, India
e-mail: bbharamagoud@gmail.com

A. M. Hulagabali
e-mail: anandmhulagabali@gmail.com

C. H. Solanki
Applied Mechanics Department, SVNIT Surat, Surat, Gujarat, India
e-mail: chs@amd.svnit.ac.in

G. R. Dodagoudar
Department of Civil Engineering, IIT Madras, Chennai, Tamilnadu, India
e-mail: goudar@iitm.ac.in

T. Thyagaraj (ed.), *Ground Improvement Techniques and Geosynthetics*, Lecture Notes in Civil Engineering 14, https://doi.org/10.1007/978-981-13-0559-7_5

1 Introduction

The most of central India and part of south India is covered with expansive soil. Expansive soil swells and shrinks due to seasonal variation, when subjected to changes in the moisture regime causing, substantial distress to the structure built on them. Lightweight reinforced concrete structures built over expansive soils are subjected to significant upward movement, which may cause undesirable damages to the structure (Ali and Ahmed 2011). The cracks appear in the structures are well recognized that swelling of expansive soils may cause significant distress and severe damage to overlying structures. To prevent damages to the structures over expansive soil, laboratory studies was conducted to improve the expansive soil against swelling, various reinforcing techniques were compared for the footing that was placed over the expansive soil reinforced with micropiles, geotextile layers. The soil was reinforced with micropiles with frictional resistance and without; sand was used as frictional material. The layers of geotextiles were reinforced into the soil at predetermined optimum depth, which reduces swelling of expansive soil due to their pushing action.

1.1 Mechanism of Heave Control

The micropile technique is based on inserting 16 and 20 mm diameter mild steel bars as piles in pre-drilled holes of larger diameter than that of the mild steel piles in an expansive soil, which are then filled with and without sand to improve the frictional resistance of the micropiles. The top sections of each micropile were fastened to the footing. Upon water absorption by the underlying clay, the generated lateral swelling pressure is added to the initial horizontal normal stress at the micropile surface. The induced vertical swelling pressure tends to push the footing upwards and to pull the micropiles upwards with respect to the surrounding sand which mobilizes frictional resistance (Nusier and Alawneh 2004). The magnitude of mobilized frictional resistance decreases with lateral distance away from the interface and therefore may be sufficient for some minimum thickness of sand around the micropiles. In the second case, geotextiles of size 136 GSM and tensile strength of 26 kN/m was placed below the footing with optimum vertical spacing, which acts as reinforcement and pushes the soil below the footing; this pushing effect by the geotextiles tends to prevent heaving of soil below the footing or foundation.

2 Experimental Methodology

2.1 Materials

SOIL: Expansive soil was used in this study, which is abundantly available semiarid region, which was collected from Hebsoor village near Navalagund taluk in Gadag district, Karnataka state. The basic geotechnical properties of the testing soil sample were known by conducting laboratory tests in compliance to Indian Standard Codes as shown in Tables 1 and 2.

Table 1 Geotechnical properties of expansive soil

Sl. No	Properties	Value
1.	Specific gravity, G	2.53
2.	Grain size distribution (%) Clay Silt	68 32
3.	Consistency limits (%) Liquid limit, W_L Plastic limit, W_P Shrinkage limit, W_S Plasticity index, IP	84.50 33 9.71 51.50
4.	IS soil classification	CH
5.	Swelling properties Free swell index (%) Swell potential	100 Very high
6.	Compaction characteristics Maximum dry density (g/cc) Optimum water content (%)	1.29 28
7.	Hydraulic conductivity, K (m/sec)	1×10^{-6}

Table 2 Geotechnical properties of sand

Sl. No	Properties	Value
1.	Specific gravity, Gs	2.68
2.	Grain size (mm) D_{10} D_{30} D_{60}	0.38 0.59 0.85
3.	IS classification	SP
4.	Uniformity coefficient (Cu)	2.24
5.	Coefficient of curvature (Cc)	1.07
6.	Angle of internal friction Loose state Dense state	37° 34^{0}

2.2 Experimental Setup

See Fig. 1 and Table 3.

2.3 Experimental Procedure for Micropile Technique

The soil which has been brought for investigating purpose was prepared by pulverizing air dried soil using hammer, and then sieved by 4.75 mm IS sieve. The

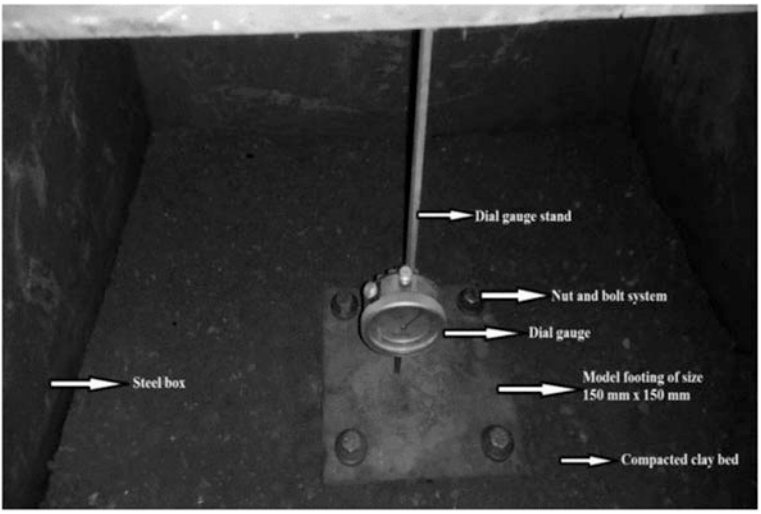

Fig. 1 Complete experimental setup with nut and bolt system, micropile fastened to the corners of square footing

Table 3 Specifications of geotextiles

Properties	Unit	GWF 26–136
Mass per unit area	GSM	136
Mechanical properties		
Tensile strength	kN/m	26
Elongation at specified tensile strength	%	25
Trapezoid tearing strength	N	300
Puncture strength	N	250
Hydraulic properties		
Apparent opening size	microns	75
Water flow rate	$L/m^2/s$	10
Packaging		
Roll width	m	3.5 or 5
Roll length	m	100

prepared soil for testing was mixed thoroughly with calculated optimum moisture content. The surrounding wall and bottom of steel box was lubricated using waste oil to reduce sidewall friction. Steel pipes of 22 mm diameter were installed vertically inside the box. Then soil was compacted by placing it in steel box with 136 blows per each layer and height of fall of hammer was 100 mm with standard proctor compaction hammer to achieve required density, compacted thickness of clay was 50 mm of four layers. After this, steel rods are removed leaving hole in compacted soil. The micropiles of 16 mm diameter were inserted into the previously drilled 22 mm diameter hole and then frictional materials as sand was filled around the micropile to improve the frictional resistance during heaving. The footing was placed above the compacted soil the micropiles were fastened to the footing with nut and bolt system. Similarly, the procedure of 16 mm diameter micropile was conducted for 20 mm diameter micropile. Moreover, for frictionless the same diameter micropiles were directly inserted into soil. To measure the heave dial gauge was placed over the footing. The sufficient amount of water was allowed in compacted soil in box. Heave readings were monitored with time to reach maximum swell percentage. Initially, heave reading were recorded at an interval of 5 min for first one hour. After that readings were noted for every 30 min up to 3 h and then subsequent to every 24 h.

2.4 Experimental Procedure for Geotextile Reinforcement

The procedure up to compaction of soil is same as done in micropile technique but geotextile layer was placed at a depth of 0.1B (15 mm) below footing, for single layer. Two layers were placed at depths of 0.1B (15 mm) and 0.3B (45 mm) respectively, where B is width of footing. Results are monitored is same as micropile technique (Fig. 2; Tables 4 and 5).

3 Results and Discussions

The semi log graph plotted with Heave (mm) against log time (min). The percentage reduction in heave for each combination of the test variables was calculated using the following expression.

$$RH(\%) = \frac{Hu - Hr}{Hu} \times 100$$

RH (%) = percentage reduction in heave with reinforcement
Hu = Heaving of unreinforced soil
Hr = Heaving of reinforced soil.

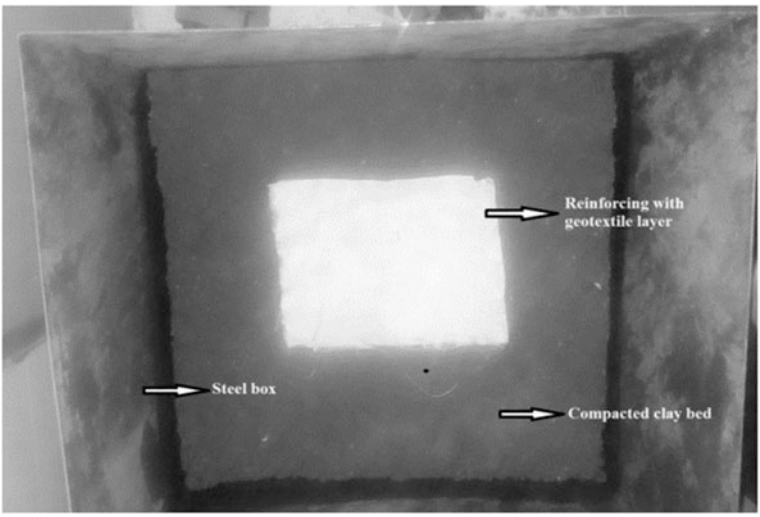

Fig. 2 Expansive Soil reinforcing with geotextile layers

Table 4 Results of micropile reinforcement

Micropile diameter (mm)	Heave of unreinforced soil (mm)	Maximum heave reduction	
		Without frictional resistance (mm)	With frictional resistance (mm)
16	31.29	18.88	10.33
20		15.83	6.73

Table 5 Results of geotextile reinforcement

Number of layers	Depth of placing	Heave of unreinforced soil (mm)	Maximum heave reduction (mm)
One	0.1B	31.29	25.26
Two	0.1B and 0.3B		8.43

Figure 3 shows the heave (mm) plotted against logarithmic time (min) for clay bed without any reinforcement methods. Heave gradually increases with increase in time and attained equilibrium. Maximum heave recorded was to be 31.29 mm.

Figure 4 shows the percentage reduction in the swelling by using of 16 mm diameter micropiles was 66.98 and 39.66% respectively.

Figure 5 the percentage reduction in the swelling by using of 20 mm diameter micropiles was 78.49 and 49.40% respectively.

Figure 6 indicates the proportional results for the swelling assessment conducted on the expansive soil by reinforcing geotextile layers. The percentage reduction in

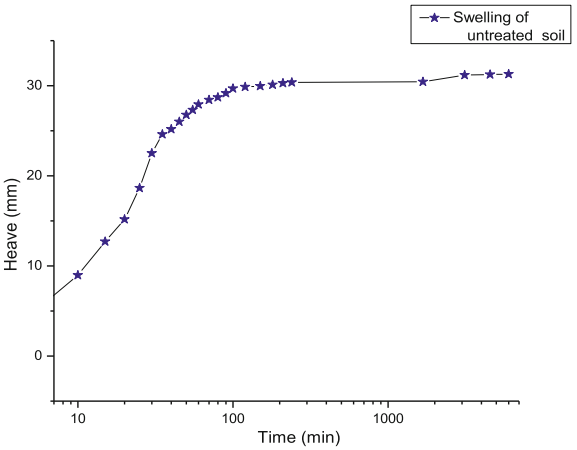

Fig. 3 Experimental result for heave test on untreated soil

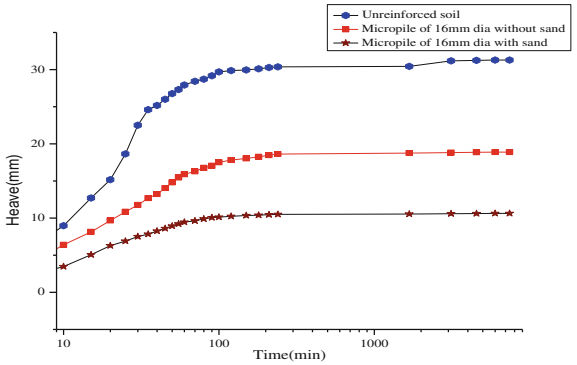

Fig. 4 Comparative results of 16 mm micropile diameter

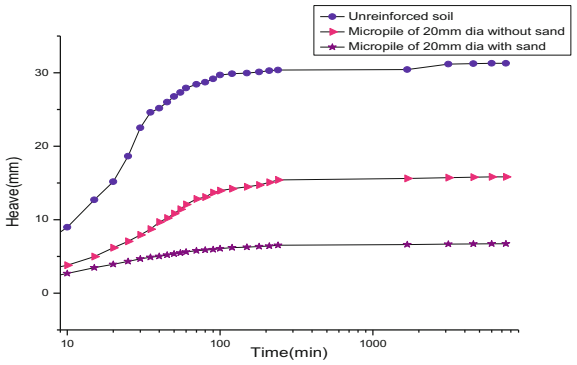

Fig. 5 Comparative results of 20 mm micropile diameter

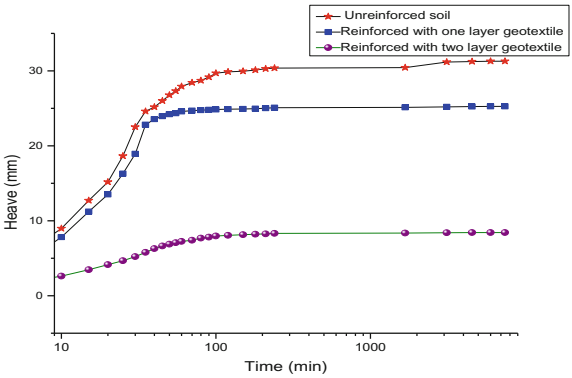

Fig. 6 Comparative results of geotextile layer

the swelling by using one and two layers of geotextile at optimum depths (0.1B) and combination of (0.1B & 0.3B) was 19.42 and 73.05% respectively.

3.1 Summary of Results and Discussions

Overall summary drawn from the results and discussions are described briefly in following subsections.

3.1.1 Effectiveness of Micropile Diameter on Swelling

The increase in micropile diameter heave reduction is increases. For four numbers of micropiles of diameter 16 mm with and without frictional resistance the reduction in swelling varies between 35 and 50%. Further four numbers of micropiles of diameter 20 mm with and without frictional resistance the reduction in swelling varies between 40 and 80% respectively.

3.1.2 Performance of Expansive Clay with and Without Micropile Reinforcement

The experimental results of average upward movement of footing laid over expansive clay bed with and without micropile reinforcement plotted against time are shown in Figs. 4 and 5 that indicates use of micropile reinforcement as almost 80% heave reduced. The micropile with frictional resistance is very effective in clayey soil and gives better results.

3.1.3 Effectiveness of Geotextile Layers on Swelling

The increase in number of layers of geotextile swelling is increases. For one and two layer of geotextile at depths the reduction in swelling from 20 to 70%. The heave reduction also increases with increase in properties of geotextile such as tensile strength and thickness.

4 Conclusions

An intensive laboratory tests were conducted to evaluate the effectiveness and performance of micropile and geotextile in reducing the heaving of expansive soil. Based on their experimental results following conclusions have been drawn.

- Maximum percentage reduction in swelling was found to be 79%, when use of micropile diameter of 20 mm with frictional resistance.
- As the micropile diameter increases, percentage reduction in heave increases.
- Percentage reduction in heave increases with the increase in the number of geotextile layers at optimum depths.
- About 73% of heave reduction takes place when use of two layers of geotextiles at optimum depths of 0.1B and 0.3B.

References

Ali, M., & Ahmed, S. M. (2011). Micropile technique to control heave on expansive soils. In *Proceedings of Indian Geotechnical Conference* (paper No. D-311).

Nusier, O. K., & Alawneh, A. S. (2004). Micropile technique to control upward movement of lightweight structures over expansive soils. *Geotechnical and Geological Engineering, 112* (22), 89–104.

Effect of Underground Void on the Internal Stress Distribution in Soil

J. Jayamohan, Thasneem Shajahan and Aswathy Sasikumar

Abstract Underground voids may develop due to natural causes and due to human activity. The presence of underground void can cause severe instability to foundation and damages to the structure. In this paper the effect of an underground void on the load-settlement behaviour of a strip footing is investigated by carrying out a series of laboratory scale load tests. The parameters varied for the study are depth of void below the footing and eccentricity of void from the centre of footing. It is observed that the effect of void is considerable only when it is within a critical depth and eccentricity. The results of loading tests are compared with those obtained from finite element analyses for validation. The addition of Foundation bed and Reinforced foundation bed improves the load-settlement behaviour of the soil with void. It is observed from the results of finite element analyses that the presence of underground void can cause stress concentration inside the soil mass which leads to failure. The stress concentration factor around the void on the side nearer to loading is more than that on the farther side. Also with increase in depth parameter the stress concentration factor goes on decreasing. The distribution of internal stress and location of stress concentration depends upon the relative positions of the footing and void.

Keywords Eccentricity · Finite element analyses · Laboratory scale load tests Load-settlement behaviour · Reinforced foundation bed · Stress concentration Underground void

J. Jayamohan (✉)
Department of Civil Engineering, LBS Institute of Technology for Women, Thiruvananthapuram 695012, India
e-mail: jayamohan7@gmail.com

T. Shajahan · A. Sasikumar
Department of Civil Engineering, Marian Engineering College, Thiruvananthapuram 695582, India
e-mail: thasneems89@gmail.com

A. Sasikumar
e-mail: aswathy273@gmail.com

T. Thyagaraj (ed.), *Ground Improvement Techniques and Geosynthetics*, Lecture Notes in Civil Engineering 14, https://doi.org/10.1007/978-981-13-0559-7_6

1 Introduction

Underground voids may be encountered as a result of underground cavities such as natural caves, water and gas networks, old conduits, tunnel and mine workings, due to tension cracks in unsaturated cohesive soils, differential settlement of municipal solid waste, and settlement of poorly compacted trench backfill. The presence of these underground voids may impose threat to the foundations stability and can cause serious engineering problems leading to severe damages to the superstructure. When the void is located beneath the footing, serious bearing capacity and settlement problems arises which results in expensive and dangerous consequences. When void is found in the foundation soil, the designer may adopt some remedial measures like filling the void with competent material through grouting, using piles to bypass the voids and transmitting the load to a competent layer underneath. The most economical solution will be placing the foundation at a suitable depth so that the distance of void from the base of footing will be more than the critical depth and the performance of the proposed foundation is not affected. But in many cases the depth of soil cover available above the void will be less than the critical depth. In low-budget projects, the use of pile foundations will be a very expensive alternative as far as the whole project is concerned. So, in such cases, it will be most economical to provide an additional layer of soil over the weak soil with voids. This additional layer usually consists of granular beds (GB) or Reinforced Granular Beds (RGB) which could enhance the performance of the footing. This method could be adopted in cases where it is not possible to totally abandon the site after the detection of underground voids or it will be completely uneconomic to go for pile foundations. Also, no suitable design procedures have been developed so far for foundations on soils with underground voids. Hence granular beds (GB) with and without reinforcement will be the most suitable and economic option for laying foundations on soils with underground natural defects. There could be considerable stress concentration surrounding the underground voids. Stress concentration is defined as the localized stress considerably higher than the average stress due to abrupt changes in geometry or localized loading. The effect of stress concentration can be determined quantitatively by determining the stress concentration factor. It is defined as the ratio of maximum stress in element to the average stress.

Baus and Wang (1983), Jayamohan et al. (2015), Shivashankar and Jayamohan (2015), Wang and Badie (1985) and Wang and Hseigh (1987) reported that the soil below the loaded footing collapses in the form of a wedge into the void and the footing stability will be affected by the underground void only when it is located within the critical depth. Kiyosumi et al. (2007, 2011) reported that there could be three modes of failure such as: bearing failure without void failure, bearing failure with void failure and void failure without bearing failure. Azam et al. (1991) conducted Finite element studies to investigate the behaviour of strip footings on homogeneous soil and stratified soil with and without void and demonstrated that the effect of void on the performance of footing depends upon the void location. Mohamed (2012) carried out a series of numerical studies to evaluate the effect of a

buried rock presence under a strip footing on the stress concentration and settlement and reported that pre-stressing the geosynthetic reinforcement can decrease the reduction in bearing capacity due to the formation of underground voids.

In this investigation, finite element analyses and laboratory scale load test are carried out to study the Effect of Underground Void on the Internal Stress Distribution in Soil. The eccentricity of the void is defined by the parameter "*X*" and depth of void by the parameter "*Y*".

2 Experimental Programme

2.1 Materials Used

The material used as weak soil is locally available clay and for foundation bed is river sand. Reinforcement used is Biaxial Geogrid. The properties of weak soil and river sand are given in Table 1 and the properties of geogrid are mentioned in Table 2.

2.2 Test Setup

The load tests are conducted in a loading frame. The internal dimension of the test tank is 100 cm × 75 cm × 75 cm, which has 23 cm thick brick masonry walls on the three sides. The front side of tank is formed using a frame work of steel channels and angles, in which an opening where the void is to be formed can be provided.

The model strip footing used for the test is an inverted Tee beam with dimensions 65 cm × 10 cm. The footing is loaded by a hand operated Mechanical jack of 50 kN capacity. The load is measured using a proving ring and deformation using two dial gauges of 0.01 mm sensitivity kept diametrically opposite to each other. The experimental setup is shown in Fig. 1.

Table 1 Properties of soil

Properties	Weak soil	Sand
Specific gravity	2.63	2.65
Average dry unit weight (kN/m^3)	15.61	16.13
Friction angle (ϕ°)	5	31.2
Cohesion (kPa)	25	0
Liquid limit (%)	58	–
Plastic limit (%)	22	–
Soil classification	CH	SW

Table 2 Properties of geogrid

Properties	
Colour	Black
Coating type	PVC
Textile type	High tenacity low shrinkage polyester yarn
Tensile strength (kN/m)	30
Aperture size (mm)	26 × 20
Mass per unit area (g/m^2)	225
Roll size (m × m)	100 × 2.40
Pull out interaction coefficient, *C*i	0.8

Fig. 1 Experimental setup and void formed in the weak soil

2.3 Procedure

The clay is filled and compacted in layers to the required level in the test tank to achieve the predetermined density. After completing the compaction the model footing is kept at the centre of the tank and subjected to loading. The subsequent tests are carried out by positioning the void in clay bed. The shape of void is circular and diameter is taken as 0.5 times the width of footing. The void is created by placing a lubricated GI pipe of required shape and diameter at the specified location during filling the clay in test tank. This pipe is carefully pulled out after completing the filling and compaction of clay in the test tank. After preparing the bed the surface is levelled and the footing is placed at the centre to avoid eccentric loading. The load is applied in small increments. The loading is continued until the footing failure occurs. The tank is emptied and refilled for each test to maintain standard conditions throughout the testing programme. The tests are carried out for different positions of void. The parameters varied are given in Table 3.

Table 3 Positions of void

Depth parameter (*Y*/*B*)	1, 1.5, 2, 2.5, 3
Eccentricity parameter (*X*/*B*)	0, 0.5, 1, 1.5, 2, 2.5, 3

3 Finite Element Analyses

Finite element analyses are carried out using the finite element software PLAXIS 2D. Settlement of the rigid footing is simulated using vertical prescribed displacements. The foundation system is simulated using plain strain model and the continuous void is modelled as a tunnel without lining. The boundary conditions are taken as full fixity at the base of the geometry and smooth conditions at the vertical sides. To simulate the behaviour of the soil, material parameters and appropriate soil model are chosen. The Mohr–Coulomb model is adopted as the soil model for all analyses. The properties of locally available clay are assigned as the material parameters of weak soil and for granular bed the properties of sand are assigned. Geogrid is used as the reinforcement. The size of reinforcement is taken as 5B for all cases. The properties of weak soil and sand are mentioned in Table 1. The soil is modelled using 15-node triangular elements. Poisson's ratio of the soil is taken as 0.25 for all cases. The various positions of void considered in the analysis are given in Table 3.

The geometrical parameters defining the position of void are shown in Fig. 2.

The distribution of vertical stress along a horizontal section passing through the void is presented in Fig. 3. It is seen that there is considerable stress concentration at the periphery of the void.

4 Results and Discussions

4.1 Effect of Depth of Void from the Surface of Weak Soil

Vertical stress versus Normalized settlement curves for footing at different depth of void at zero eccentricity ($X/B = 0$) is presented in the Fig. 4. The curve for clay without void is also shown in the figure so that the reduction in strength due to the presence of void can be clearly understood. From the figure it is seen that as the

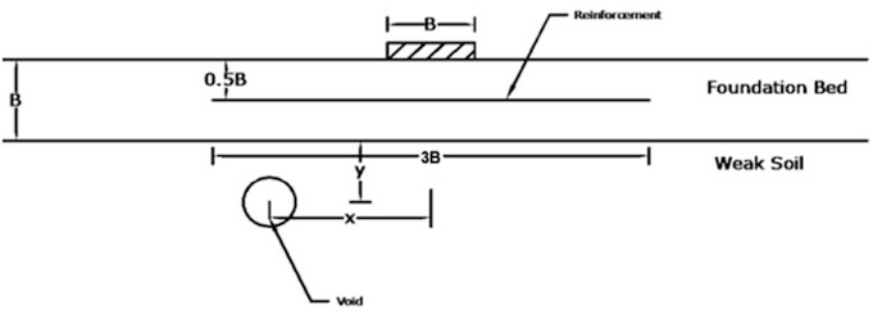

Fig. 2 Parameters defining the position of void

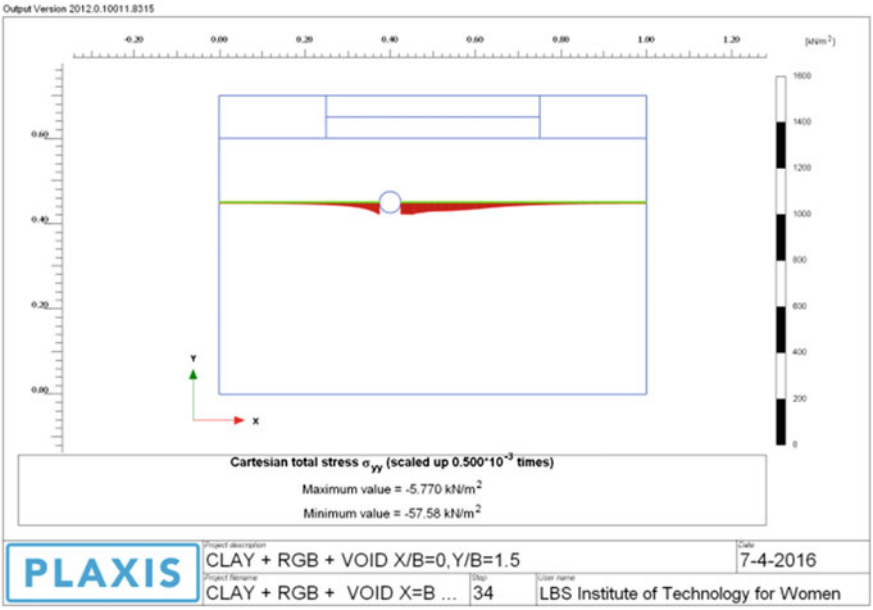

Fig. 3 Typical distribution of vertical stress along a horizontal section through void

depth of void from the surface of weak soil increases, the influence of void diminishes and the effect of void is negligible when its depth from the surface of weak soil is equal to twice the width of footing. The results obtained from Finite element analyses are also presented and these results are in reasonably good agreement with the experimental results.

4.2 Effect of Eccentricity of Void from the Centre of Footing

Vertical stress versus Normalized settlement curves for footing at different eccentricity of void at a depth $Y/B = 1$ is shown in the Fig. 5. The curve for clay without void is also shown in the figure so that the reduction in strength due to the presence of void can be clearly understood. It is seen that as the eccentricity of void from the centre of footing increases, the influence of void diminishes and the effect of void is negligible when its eccentricity is equal to twice the width of footing.

The results obtained from Finite element analyses are also presented and these results are in reasonably good agreement with the experimental results.

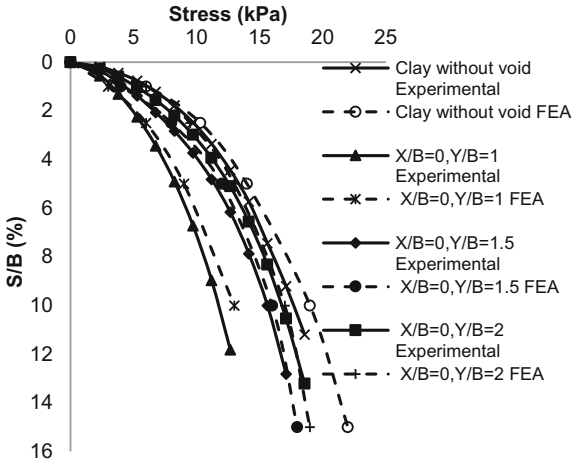

Fig. 4 Vertical stress versus normalized settlement curves for clay

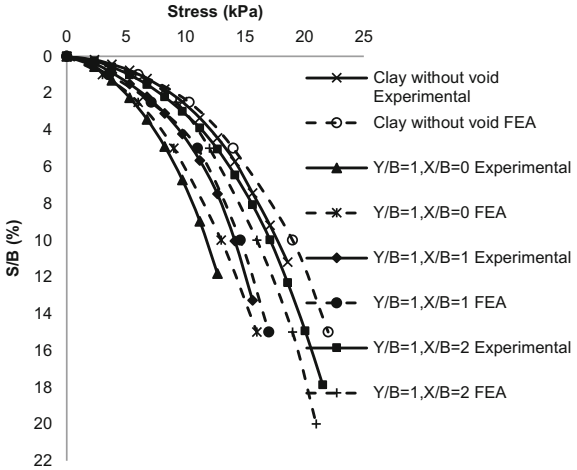

Fig. 5 Vertical stress versus normalized settlement curves for clay

4.3 Effect of Foundation Bed and Reinforced Foundation Bed

Figure 6 presents the Vertical Stress versus Normalized settlement for various cases when there is no void. The curves obtained from the finite element analyses are also presented in the figure. From the figure it is observed that the addition of granular bed and reinforced granular bed over the weak soil considerably improves the load-settlement behaviour of footing. Also the results obtained from finite element analyses are in reasonably good agreement with the experimental results. At 5% settlement the maximum load-settlement behaviour is observed for Clay with

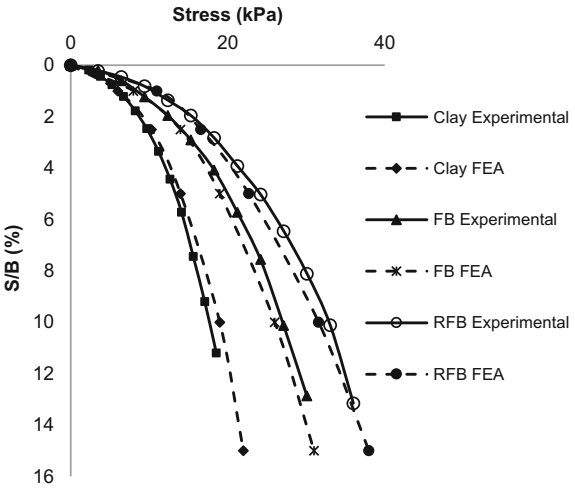

Fig. 6 Vertical stress versus normalized settlement for clay, GB and RGB without void

Reinforced granular bed than that of unreinforced granular bed. The percentage improvement for clay with RGB is about 85% and for clay with GB is about 54%.

4.4 Effect of Depth of Void on Stress Concentration

The variation of stress concentration factor (SCF) for various vertical position of void, when eccentricity is zero ($X/B = 0$) is presented in Fig. 7. It is observed that stress concentration factor is decreasing with the depth of void from the surface of weak soil for all the three cases. Also it is seen that for the depth of void less than 1.5 times the width of footing the Stress Concentration Factor is maximum and however the depth of void greater than 1.5 times the width of footing the Stress Concentration Factor is minimum for clay with RGB.

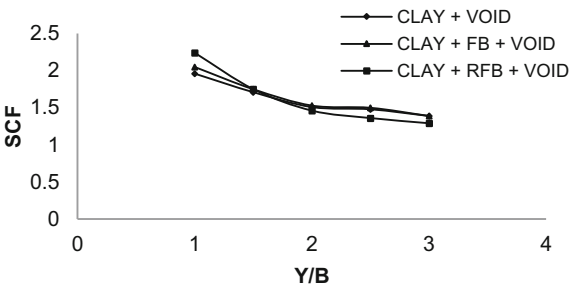

Fig. 7 Stress concentration factor versus Y/B at $X/B = 0$

4.5 Effect of Eccentricity of Void on Stress Concentration

Figure 8 shows the variation of Stress Concentration Factor with the eccentricity of void at a depth equal to the width of footing when the footing is on the right side of void. The stresses around the void to the left and to the right sections are different for different eccentricities. It is seen from the figure that the stress concentration is more on the nearer side of the footing than that of the farther side of the footing. In the nearer side of load for clay and clay with RGB the stress concentration reaches a peak value when eccentricity equal to 0.5 times the width of footing. With further increase of eccentricity the stress concentration reduces and reaches a minimum value when eccentricity equal to the width of footing. With the further increase in eccentricity it is seen that the stress concentration increases till $X/B = 1.5$ and thereafter it remains constant. In the farther side of load the stress concentration is decreasing when eccentricity increases up to $X/B = 1$ and further increase in eccentricity the stress concentration slightly increases and later at $X/B = 2.5$ it becomes constant. Also the stress concentration factor is more when the foundation bed is reinforced.

4.6 Distribution of Internal Stress in Soil

The variations of stress at the nearer side of footing with different eccentricity are presented in Fig. 9. It is seen that for clay, clay with unreinforced and reinforced GB the stress is first decreases and then increases to a peak value at $X/B = 1$. With further increase in X/B nearer stress has a steep variation and thereafter it increases and remains constant.

Figure 10 presents distribution of stresses at the farther side of footing. For clay with GB and RGB the farther stress has a steep decreasing variation up to $X/B = 1$.

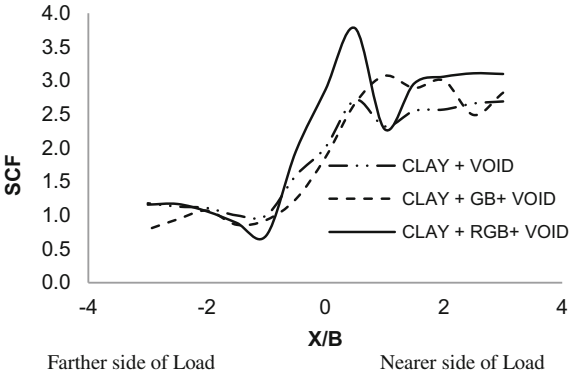

Fig. 8 Stress concentration factor versus eccentricity parameter

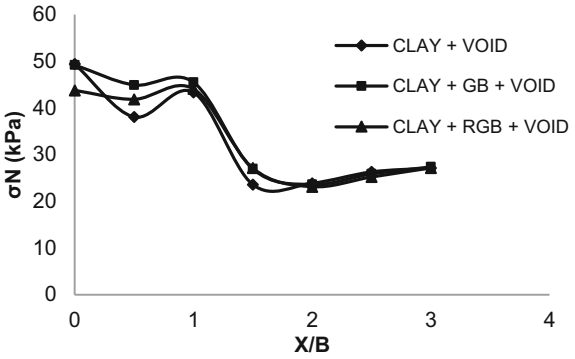

Fig. 9 σ_N versus eccentricity parameter

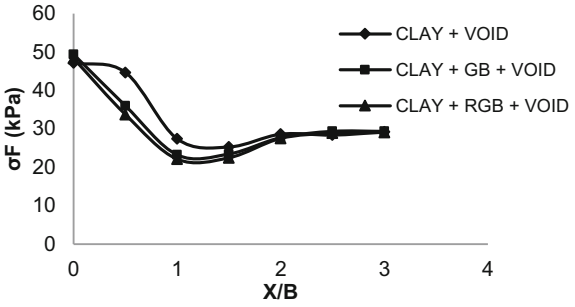

Fig. 10 σ_F versus eccentricity parameter (X/B)

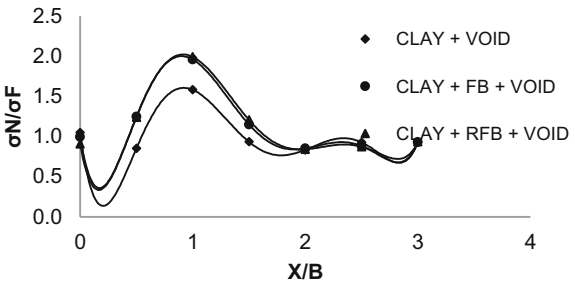

Fig. 11 σ_N/σ_F versus X/B at $Y/B = 1$

For clay the farther stress is constant up to $X/B = 0.5$ and then it has a steep decreasing variation up to $X/B = 1$. Further increase in X/B shows almost a constant variation in farther stress.

The effect of eccentricity of void on the ratio of stresses at the nearer side (σ_N) to that of farther side (σ_F) of the footing when $Y/B = 1$ is shown in the Fig. 11. It is seen that the ratio (σ_N/σ_F) is more when providing foundation bed and reinforced foundation bed. It is observed that the ratio (σ_N/σ_F) decreases when (X/B) increases from 0 to 0.25 and then increases and reaches its maximum value when (X/B) = 1.

A further increase of (X/B) causes a reduction in (σ_N/σ_F). The equation of best fit curve for all the cases is obtained. The equation of best fit curve for clay with void is given in Eq. (1), foundation bed overlying clay with void is given in Eq. (2) and reinforced foundation bed overlying clay with void is given in Eq. (3).

$$(\sigma_N/\sigma_F) = 0.788(X/B)^6 - 7.653(X/B)^5 + 28.26(X/B)^4 - 48.91(X/B)^3 + 38.57(X/B)^2 - 10.53(X/B) + 1.047 \quad (1)$$

$$(\sigma_N/\sigma_F) = 0.740(X/B)^6 - 7.214(X/B)^5 + 26.72(X/B)^4 - 46.04(X/B)^3 + 35.31(X/B)^2 - 8.558(X/B) + 0.995 \quad (2)$$

$$(\sigma_N/\sigma_F) = 0.669(X/B)^6 - 6.59(X/B)^5 + 24.68(X/B)^4 - 43.01(X/B)^3 + 33.20(X/B)^2 - 7.878(X/B) + 0.905 \quad (3)$$

5 Conclusion

Based on the results of experimental studies and finite element analyses, the following conclusions are made:

- The presence of void has only negligible effect when the void is located at a depth equal to twice the width of footing and at an eccentricity equal to twice the width of footing.
- The addition of Foundation Bed and Reinforced Foundation Bed improves the load-settlement behaviour of clay with underground voids.
- There is considerable stress concentration surrounding the underground void.
- The stress concentration factor will decrease as the depth of the void increases from the base of the footing.
- The stress concentration factor will vary asymmetrically with the increase in eccentricity of void from the centre of footing for a given depth.

References

Azam, G., Hseigh, W., & Wang, M. C. (1991). Performance of strip footing on stratified soil deposit with void. *Journal of Geotechnical and Geoenvironmental Engineering, ASCE, 117*, 753–772.

Baus, R. L., & Wang, M. C. (1983). Bearing capacity of strip footing above void. *Journal of Geotechnical and Geoenvironmental Engineering, ASCE, 109*, 1–14.

Jayamohan, J., Rajeev Kumar, P., & Vimal, A. (2015). Effect of underground void on the behaviour of strip footing resting on reinforced foundation bed. In *Indian Geotechnical Conference*, Pune, India, December 17–19, 2015.

Kiyosumi, M., Kusakabe, O., Ohuchi, M., & Peng, F. L. (2007). Yielding pressure of spread footing above multiple voids. *Journal of Geotechnical and Geoenvironmental Engineering, ASCE, 133*, 1522–1531.

Kiyosumi, M., Kusakabe, O., & Ohuchi, M. (2011). Model tests and analyses of bearing capacity of strip footing on stiff ground with voids. *Journal of Geotechnical and Geoenvironmental Engineering, ASCE, 137*, 363–375.

Mohamed, A. K. (2012). Numerical study for the behaviour of strip footing on sand in the existence of a buried rock. *Journal of Engineering Sciences, 40,* 1611–1624.

Shivashankar, R. & Jayamohan, J. (2015). Effect of formation of voids on the behaviour of prestressed reinforced granular beds overlying weak soil. In *Geosynthetics 2015*, Portland, USA, February 15–18, 2015.

Wang, M. C., & Badie, A. (1985). Effect of underground void on foundation stability. *Journal of Geotechnical and Geoenvironmental Engineering, ASCE, 111*, 1008–1019.

Wang, M. C., & Hseigh, C. W. (1987). Collapse load of strip footing above circular void. *Journal of Geotechnical and Geoenvironmental Engineering, ASCE, 113*, 511–515.

Influence of Properties of Infill Material on the Behaviour of Geocells

J. Jayamohan, S. Aparna and Aswathy Sasikumar

Abstract This paper investigates the influence of properties of infill material on the load-settlement behaviour of geocell mattresses by carrying out a series of laboratory scale-load tests on a model strip footing resting on clay reinforced with confined geocells. The parameters varied include aspect ratio of the aperture of geocell, infill materials and relative density of the infill material. The infill materials used in this study are sand, 6 mm aggregates and 12 mm aggregates. The experimental results are compared with the results obtained from Finite Element Analyses carried out using the software Plaxis 2D. It is observed that the load-settlement behaviour is considerably influenced by the properties of infill material. An increase in grain size of the infill material considerably improved the load-settlement response of the geocell. However an increase in the aspect ratio of the aperture of the geocell caused a reduction in bearing capacity. It is also observed that an infill material of sand, compacted to a relative density of 88% gives better improvement than 6 mm aggregate.

Keywords Geocell · Load-settlement behaviour · Infill material
Laboratory scale-load tests · Finite element analyses

J. Jayamohan (✉)
Department of Civil Engineering, LBS Institute of Technology for Women,
Thiruvananthapuram 695012, India
e-mail: jayamohan7@gmail.com

S. Aparna · A. Sasikumar
Department of Civil Engineering, Marian Engineering College,
Thiruvananthapuram 695582, India
e-mail: aparnas182@gmail.com

A. Sasikumar
e-mail: aswathy273@gmail.com

T. Thyagaraj (ed.), *Ground Improvement Techniques and Geosynthetics*, Lecture Notes in Civil Engineering 14, https://doi.org/10.1007/978-981-13-0559-7_7

1 Introduction

Due to rapid urbanization, there has been an increase in demand for land space all over the world. This has resulted in an increase in the need to construct on soft soil grounds, which were considered unsuitable for construction a couple of decades ago. The stability of such structures on soft soil deposits is a challenging task due to high settlement and heaving tendency of soft soil. In such cases, ground improvement techniques have to be adopted to improve the load-carrying capacity and to reduce the settlement of the soft foundation bed (Zou and Wen 2008). The introduction of geosynthetics as reinforcement has significantly reduced the cost of ground improvement and simplified the construction procedure. Geocell is the latest development in the field of geosynthetics and its benefits have been highlighted by several researchers (Pokharel 2010; Dash et al. 2004).

Geocell is a three-dimensional, polymeric, honeycomb like structure of cells interconnected at the joints that provide effective confinement of the encapsulated soil against being pushed away from the region under loading. The filled cells being interconnected, the panel acts like a large mat that spreads the applied load over an extended area leading to an improvement in the overall performance (Bathurst et al. 1998; Carter and Dixon 1995) as shown in Fig. 1.

Webster (1979) mentioned in his studies that the concept of lateral confinement by cellular structures dates back to 1970s where the United States Army Corps of Engineers developed this idea for providing lateral confinement to soil to improve the bearing capacity of poorly graded sand. At present, high density polyethylene (HDPE) is the most common polymer used to make geocells by welding extruded HDPE strips together to form honey combs (De Garided and Morel 1986). The geocell reinforcement arrests the lateral spreading of the infill soil and creates a stiffened mat to support the foundation thereby giving rise to higher load-carrying capacity (Bush et al. 1990; Latha et al. 2009).

In this investigation, a series of Finite Element Analyses is carried out to investigate the influence of ratio of the aperture of geocell, infill materials and relative density of the infill material on the load-settlement behaviour of a geocell mattress. The results obtained are compared with laboratory scale-loading tests for validation.

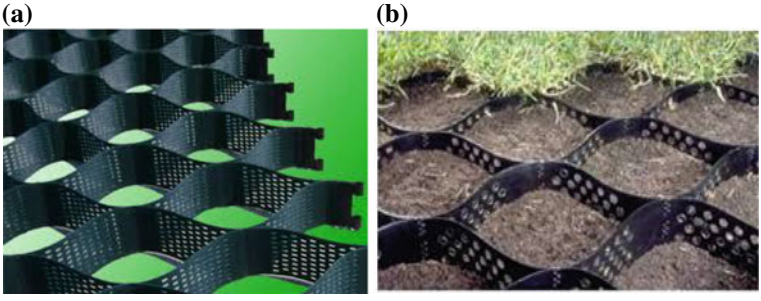

Fig. 1 **a** Geocell **b** soil reinforced with geocell

2 Laboratory Model Tests

2.1 Test Setup

Model tests are conducted in a test bed comprising of a test tank, a loading system and dial gauges to measure deformation. The general arrangement of the laboratory test setup is shown in Fig. 2. The testing tank is designed as a rigid box 1000 mm in length, 750 mm in height and 750 mm in width, encompassing the reinforced soil and model foundation.

The loading system includes a loading frame and a mechanical jack of 50 kN capacity. The loading frame consists of four stiff and heavy steel columns and a horizontal cross head that supports the mechanical jack. Settlements are measured using two dial gauges placed diametrically opposite to each other.

2.2 Materials

Locally available clay is used as weak soil in all the tests. Infill materials used are sand, 6 mm aggregate and 12 mm aggregate.

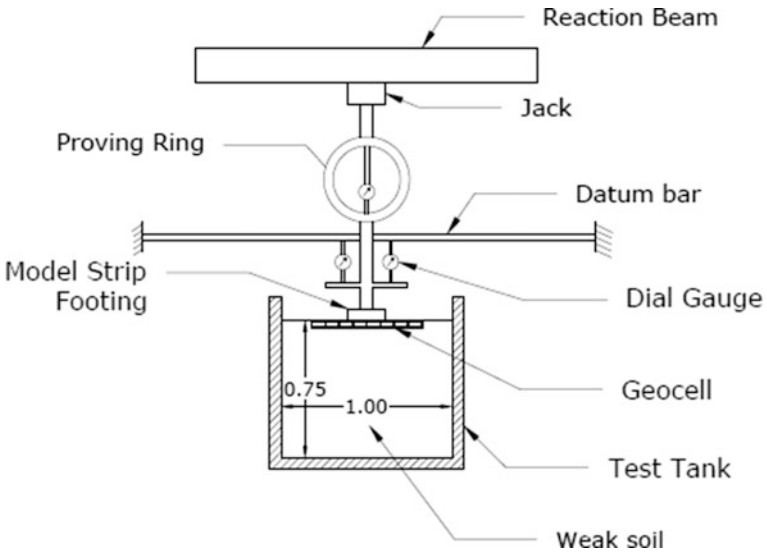

Fig. 2 Laboratory test setup

2.3 Reinforcement

Vertical and horizontal geogrid elements are prepared by cutting geogrids to the required length and height from full rolls. The geogrid elements are then joined together using threads resulting in the formation of geocell mattress. The properties of geogrid used is given in Table 1.

2.4 Test Parameters and Testing Program

The width of geocells adopted in the study is $3B$, where B is the width of the footing. The width of model strip footing is taken as 100 mm in this study. Various aspect ratios of a/b = 0.33, 0.5, 1, 2, and 3 are adopted in this study. The geocell mattress is placed centrally below the footing without any eccentricity. The infill materials of various particle sizes were used in the geocell mattress. Geocell mattresses were prepared from geogrids and geotextiles. The geometry of geocell for the load test is shown in Fig. 3. The length of the aperture opening is taken as 'a' and its width as 'b'.

Aspect ratio is defined as the length to width ratio of the geocell aperture. Sand is compacted for two relative densities to understand the effect density of infill material on the load-settlement behaviour of the geocell reinforced footing resting on clay. The parameters studied are indicated in Table 1.

3 Finite Element Analyses

Finite element analyses are carried out using the FE software PLAXIS 2D. The width and depth of soil mass is taken as 1000 mm × 750 mm and the width of the strip footing (B) is taken as 100 mm. The size of soil mass is taken equal to the test

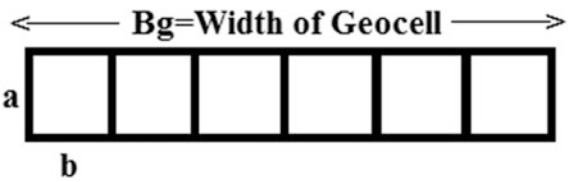

Fig. 3 Geometry of geocell for the load test

Table 1 Parameters varied

Aspect ratio of the aperture (a/b)	0.33, 0.5, 1, 2, 3
Infill materials	Sand, 6 and 12 mm aggregates
Relative density (sand) (%)	64, 88

tank and width of strip footing equal to the size of model strip footing used for the laboratory-scale load tests. The settlement of the rigid footing is simulated using vertical prescribed displacements and the foundation system is simulated using plain strain model. The boundary conditions are taken as full fixity at the base of the geometry and smooth conditions at the vertical sides. To simulate the behaviour of the soil, material parameters and appropriate soil model are chosen. Mohr–Coulomb model is adopted as the soil model for all analyses. The properties of materials used for the laboratory tests are assigned as the material parameters in the FE analyses. The soil is modeled using 15-node triangular elements. Poisson's ratio of the soil is taken as 0.25 for all cases. The geogrid reinforcement is combined with an interface to appropriately model the interaction with the surrounding soil. The parameters varied for the finite element analyses are also the same as those varied during the laboratory model study as given in Table 1. Figures 4, 5, and 6 shows the deformed mesh, stress distribution in soil and typical distribution of vertical stress along a horizontal section through the bottom of geocell during the finite element analyses.

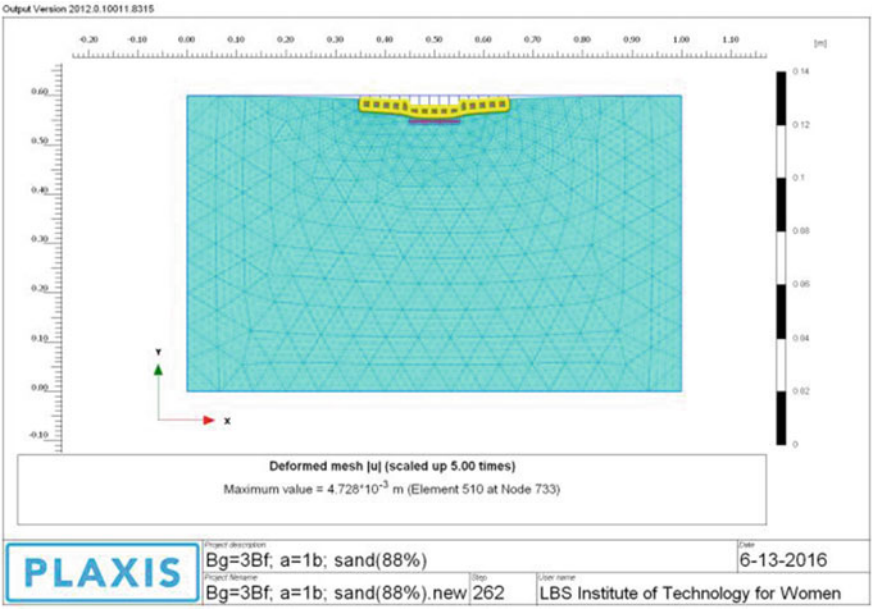

Fig. 4 Deformed mesh after loading

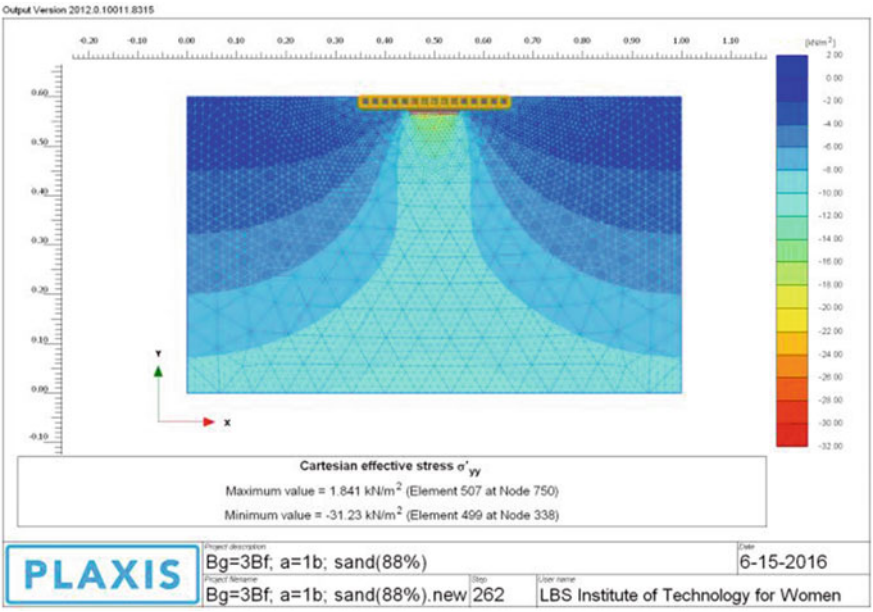

Fig. 5 Typical stress distribution in soil after loading

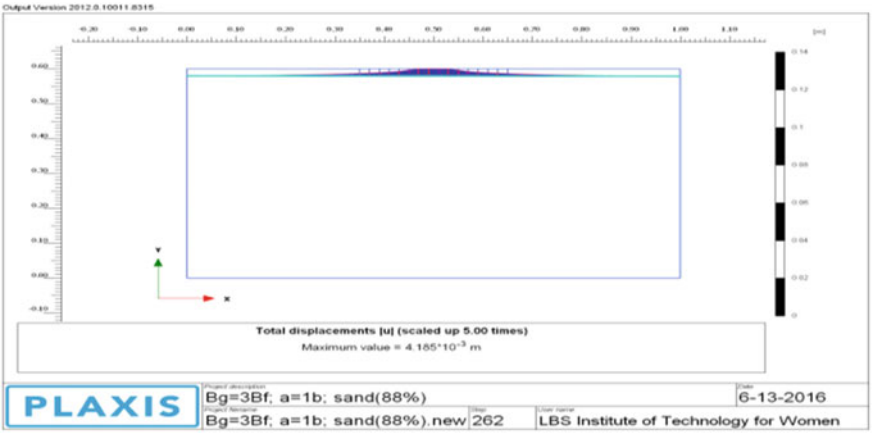

Fig. 6 Typical distribution of vertical stress along a horizontal section through the bottom of geocell

4 Results and Discussions

4.1 Effect of Gradation of Infill Material

Figure 7 represents Vertical stress versus normalized settlement curves obtained from experimental and finite element results on the effect of different infill materials on the load-settlement behaviour of footings for aspect ratio 0.5. It is seen from the figure that geocell with infill 12 mm aggregates gives better results than other infill materials. It is seen from the figure that the improvement in load-carrying capacity is more for 6 mm aggregates than for sand compacted to a relative density of 88%. A similar variation of bearing pressure with footing settlement is observed for other aspect ratios 0.33, 1, 2, and 3.

4.2 Effect of Aspect Ratio

Vertical stress versus normalized settlement curves for various aspect ratios of aperture of geocell made with geogrids with infill material of sand compacted to 88% relative density is presented in Fig. 8. It is seen that an increase in aspect ratio reduces the load bearing capacity. The ultimate load taken by the geocell increased with the relative density of infill material. It can also be seen from the figure that the there is improvement in load-settlement behaviour as the aspect ratio reduces up to 0.5 and a further reduction in aspect ratio is not beneficial. The experimental results were in good agreement with the finite element results. Similar behaviour is seen for geogrids with infill material sand compacted to a relative density of 64%.

From Fig. 9, which presents the behaviour of geocell with infill material of size 12 mm, it is seen that improvement in load-settlement response is maximum when

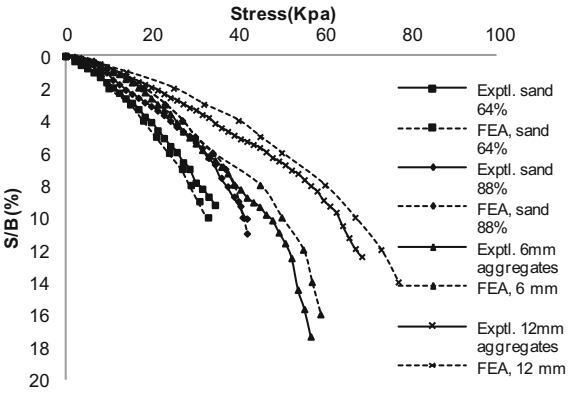

Fig. 7 Effect of gradation of infill material for aspect ratio 0.5

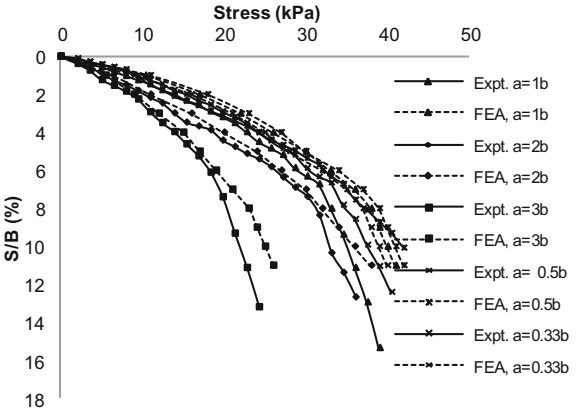

Fig. 8 Comparison of aspect ratio of the aperture of geocell for sand with relative density 88%

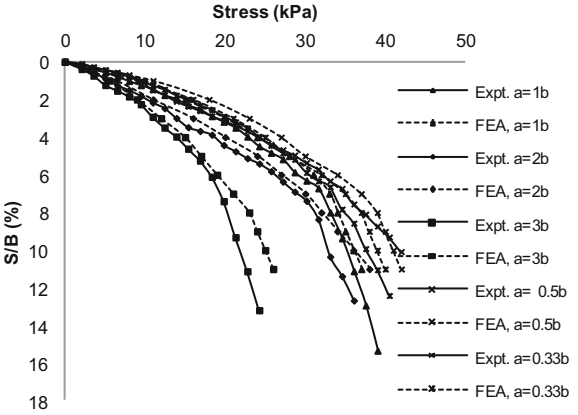

Fig. 9 Comparison of aspect ratio of the aperture of geocell for 12 mm aggregates

aspect ratio is equal to one. A similar behaviour is observed when 6 mm aggregate is also used as the infill material. It is also seen that the load-carrying capacity of geocell with infill material of 12 mm aggregate is more than that with infill material of 6 mm aggregate.

As the aspect ratio increases the number of reinforcing geogrid elements within the geocell mattress decreases which results in a decrease in the efficiency of the geocell mattress to distribute the load laterally. As the aspect ratio decreases, the height of the geocell increases, the beam or plate effect and confinement of the geocell increases the stiffness of the reinforced base thus having a wider stress distribution.

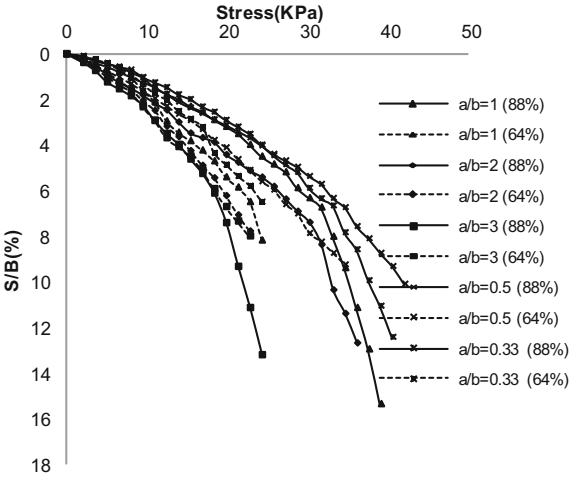

Fig. 10 Effect of relative density on bearing capacity of footings

4.3 Effect of Relative Density of the Infill

Vertical stress versus normalized settlement curves with two different relative densities, for different aspect ratios are presented in Fig. 10. The curves for sand with relative density 88% is shown in solid lines and that with relative density 64% is shown in dotted lines. It is seen that the load-settlement behaviour improves with an increase in the relative density of infill material. It is seen from the figure that sand compacted to a relative density of 88% for aspect ratios 0.33, 0.5, and 1 gives more improvement than sand compacted to a relative density of 64% for aspect ratio 0.5.

5 Conclusions

From the results of loading tests carried out, the following conclusions are drawn.

Due to three-dimensional structure, geocell mattress provides lateral confinement to soil particles within the geocell which is due to friction between the infill material and the geocell. As particle size of infill material increases there is an improvement in soil properties. It is also observed that sand when compacted to a relative density of 88%, it could take more load than for 6 mm chips.

As the aspect ratio of the aperture is increased, the number of reinforcing geogrids in the geocell decreases which results in the decrease in bearing capacity of the soil. As the aspect ratio decreases, the height of the geocell increases, the beam or plate effect and confinement of the geocell increases the stiffness of the reinforced base thus having a wider stress distribution.

It is observed that the load-settlement behaviour improves with an increase in the relative density of infill material. Sand when compacted to a relative density of 88% for aspect ratios 0.33, 0.5, and 1 gives more improvement than sand compacted to a relative density of 64% for aspect ratio 0.5.

References

Bathurst, R. J., Nernheim, A., Walters, D. L., Allen, T. M., Burgess, P., Saunders (1998). Influence of reinforcement stiffness and compaction on the performance of four geosynthetic-reinforced soil walls. *Geosynthetics International 16*(1), 43–49.

Bush, D. L., Jenner, C. G., & Basett, R. H. (1990). The design and construction of a geocell foundation mattress supporting embankments over soft ground. *Geotextiles and Geomembranes, 9,* 83–98.

Carter, G. R., & Dixon, J. H. (1995). Oriented polymer grid reinforcement. *Construction and Building Materials, 9*(6), 389–401.

Dash, S. K., Krishnaswamy, N. R., & Rajagopal, K. (2004). Behaviour of geocell-reinforced sand beds under strip loading. *Geotextiles and Geomembranes, 21*(4), 905–916.

De Garided, R., & Morel, G. (1986). New strength techniques by textile elements of low-volume roads. In *Proceeding of Third International Conference on Geotextiles* (pp. 1027–1032), Vienna, Austria.

Latha, G. M., Rajagopal, K., & Somwanshi, A. (2009). Numerical simulation of the behavior of geocell reinforced sand in foundations. *Geotextiles and Geomembranes, 9*(4), 143–152.

Pokharel, S. K. (2010). Investigation of factors influencing behaviour of single geocell-reinforced bases under static loading. *Geotextiles and Geomembranes, 28*(6), 570–578.

Webster, S. L. (1979). *Investigation of beach sand trafficability enhancement using sand-grid confinement and membrane reinforcement concepts* (Report GL-79–20 (1)). Vicksburg, MS: US Army Engineer Waterways Experiment Station.

Zou, L., & Wen, Y. (2008). Bearing capacity of geocell reinforcement in embankment engineering. *Geotextiles and Geomembranes, 28*(5), 475–482.

Investigation of Glass Fiber Reinforcement Effect on the CBR Strength of Cohesive Soil

Suchit Kumar Patel and Baleshwar Singh

Abstract An experimental study was carried out to investigate the application suitability of randomly distributed glass fiber-reinforced cohesive soil as subgrade material. Glass fiber of 20 mm length with varying fiber contents (f_c = 0.25, 0.5, 0.75 and 1% by dry weight of soil) was used as reinforcement. The effects of fiber content variation on compaction parameters of soil, and the effect of fiber content and soaking time variation on CBR strength were investigated. The soaking time was varied from 4 to 40 days. The CBR and secant modulus were calculated at different penetration depths ranging from 2.54 to 12.7 mm. Test results have shown that the glass fiber content has insignificant effect on the OMC and MDD of the soil. The CBR strength is found to increase with penetration depth up to 7.62 mm penetration and thereafter remains almost constant at all fiber contents. The CBR strength and secant modulus of soil have improved significantly with fiber content up to an optimum fiber content value of 0.75%, and decrease with increase in soaking time at any fiber content. The maximum improvement in CBR strength is found out as 2.48, 2, and 1.5 times for 4, 20, and 40 days soaking for 0.75% fiber inclusion. It has been found that the glass fiber-reinforced soil can be extensively used as subgrade material.

Keywords Fiber-reinforced soil · CBR test · Fiber content · Secant modulus Soaking time

S. K. Patel (✉) · B. Singh
Department of Civil Engineering, Indian Institute of Technology Guwahati, Guwahati 781039, India
e-mail: skpmit@gmail.com; p.suchit@iitg.ac.in

B. Singh
e-mail: baleshwar@iitg.ac.in

T. Thyagaraj (ed.), *Ground Improvement Techniques and Geosynthetics*, Lecture Notes in Civil Engineering 14, https://doi.org/10.1007/978-981-13-0559-7_8

1 Introduction

Lack of good quality soil at site and escalating cost of materials has motivated geotechnical engineers to explore new alternative materials for constructing geotechnical structures. Design and construction of pavement over weak soil is quite challengeable and problematic for geotechnical engineers. Application of synthetic materials like geotextiles, geogrids, and fibers have evoked considerable interest among geotechnical engineers and manufacturers for using these materials as reinforcing element to improve the bearing capacity of weak soils. Among several ground improvement techniques, reinforcing the subgrade soils with short fibers appears to have the greatest potential for successful application in the design of flexible pavements. These benefits can be in terms of extending the service life of the pavement or reduction in subbase or base thickness.

Fiber-reinforced soil has some advantages such as low cost, light weight, capability of maintaining strength isotropy within soil mass. Its application in construction is also not significantly affected by weather conditions.

The objective of this study is to investigate the suitability of glass fiber-reinforced cohesive soil as a subgrade material through laboratory CBR tests. The effects of fiber content and soaking period variation on CBR and secant modulus were studied. An optimum soil-fiber mix which will give the maximum strength as a subgrade material is to be determined.

2 Earlier Work

Lawton and Fox (1992) noted that sand reinforced with multioriented geosynthetics results in increasing California Bearing Ratio (CBR). The multioriented elements also proved useful in reducing rutting and providing increased mobility and trafficability in soft and loose soils. Benson and Khire (1994) showed an increase in CBR and secant modulus of sand when cut pieces of waste milk jugs was used as reinforcement. Kumar et al. (1999) reported an increase in the CBR value and ductility of silty sand and pond ash specimens reinforced with randomly distributed polyester. The optimum fiber content for both silty sand and pond ash was found to be approximately 0.3–0.4% of dry unit weight.

Zahran and Fatani (1999) reported that reinforcing asphalt paving mixture with glass fiber enhanced the overall performance of the pavement structure in terms of reducing the frequency of future rehabilitation costs and resulting in a more economical pavement. Tingle et al. (2002) observed that fiber stabilization of medium sand improved the CBR by about sixfold, and the improvement was attributed to

the confinement of sand particles by discrete fibers. Chandra et al. (2002) reported that CBR values of clayey, silty and silty sand soils were found to be 1.16, 1.95, and 6.20%, respectively, which increased to 4.33, 6.42, and 18.03%, respectively, with 1.5% fiber content of propylene fiber.

Dutta and Sarda (2007) observed that application of waste plastic strip reinforced stone dust-fly ash overlying saturated clay appreciably increased the CBR and the secant modulus up to 2% plastic strip reinforcement. Addition of geofibers with synthetic fluid was noted to effectively increase the CBR performance of fine-grained soil under both soaked and unsoaked conditions and the optimum geofiber content was found to be between 0.2 and 0.5% depending on the sample condition and geofiber type (Hazirbaba and Gullu 2010). Kalantari et al. (2010) found that the 0.15% of polypropylene fiber reinforcement in cement stabilized peat soil caused maximum CBR increases by a factor of 22 for unsoaked condition and by a factor of 15 for the soaked condition. Srinivas Rao and Jayalekshmi (2010) found that addition of 1% polyester fiber of aspect ratios 200 and 400, increases the CBR by 1.54 and 1.25 times respectively.

3 Materials and Methodology

A cohesive soil having 25% sand, 55% silt and 20% clay size particles with 25 and 47% as its plastic and liquid limits was used in this study. The soil is classified as intermediate plastic clay (CI). The optimum moisture content (OMC) and maximum dry density (MDD) of the soil are 19.4% and 16.8 kN/m^3. Commercially available glass fiber of 20 mm length and different fiber content (f_c = 0.25, 0.5, 0.75, and 1% by dry weight of soil) was used as reinforcing material. The average diameter and specific gravity of fiber is 0.15 mm and 2.57, respectively.

Soil and fibers as per their designated weights were manually mixed in different stages with appropriate amount of water in a steel tray. Fibers were segregated carefully during mixing as they tended to form lumps by sticking together with increasing fiber content. As the laboratory test results highly depend on the sample preparation method, proper care was taken at every step while preparing reinforced specimen. The uniform soil-fiber mix was prepared prior to compaction of test specimens.

CBR tests on compacted specimens were performed in accordance with ASTM D 1883 (1999). The CBR value was calculated at different penetration depths ranging from 2.54 to 12.70 mm at an interval of 2.54 mm in order to check the response of penetration depth on the behavior of fiber reinforcement. The soaking period was varied as 4, 20 and 40 days.

4 Results and Discussion

4.1 Compaction Behavior

Standard proctor compaction tests were carried out on parent soil and fiber-reinforced soil according to ASTM D 698 (2012). The effect of glass fiber inclusion on OMC and MDD was insignificant. The maximum variation in OMC and MDD with glass fiber inclusion was 1 and 0.24% from that of unreinforced soil. The reason might be due to the fact that the specific gravity of glass fiber (2.57) is close to that of parent soil (2.62) and that the water absorption capacity of the glass fiber is nil.

4.2 Load Penetration Behavior

Figure 1 shows typical load penetration curves obtained from the CBR tests on fiber-reinforced specimens of varying fiber content are shown in Fig. 1 for specimen soaking period of 4 days. The penetration resistance of the specimens is found to increase substantially with fiber inclusion. This resistance is observed to increase with fiber content and maximum resistance is found with 0.75% fiber content up to 9 mm penetration. With 1% fiber content, the penetration resistance decreases. The effect of strength increment can be noted from the initial small penetration level of 1 mm indicating that the fiber benefit is obtained as soon as specimen is subjected to vertical loading. As the penetration depth increases, the effect of fiber benefit is observed to increase. The CBR and secant subgrade modulus were calculated from this load penetration response

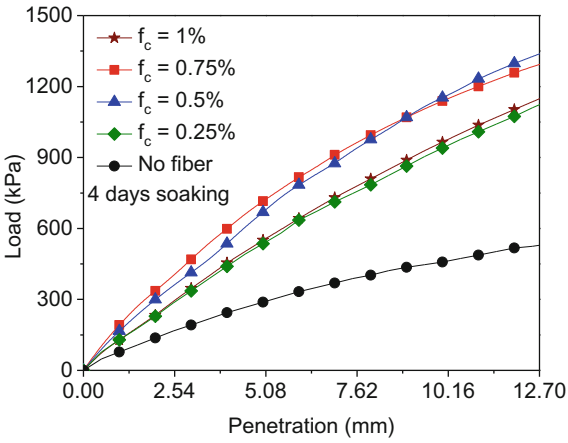

Fig. 1 Effect of fiber content on load penetration response

In general for field applications, CBR value is reported for either 2.54 or 5.08 mm depth of penetration. This may sometimes not give the real resistance of reinforced soil, and possible failure may take place at greater penetration. Keeping this in view, for fully capturing the modification of soil behavior after glass fiber reinforcement, the CBR value has been examined at greater penetration depths up to 12.70 mm.

4.3 *Effect of Fiber Content on CBR*

Variations of CBR values at different penetration depths are presented in Fig. 2 with different fiber contents. The CBR has increased with fiber content up to 0.75% dose. Soil-fiber surficial interaction seems to have reached its saturation point at 0.75% fiber content. At any fiber content, the CBR of specimen increases with penetration depth up to 7.62 mm, thereafter the value remain constant or CBR increment is very small.

It can be noted that the CBR value at 5.08 mm penetration is higher for all fiber content with maximum value of 7.16% for 0.75% fiber content (Fig. 2). The CBR value of unreinforced soil is 2.81%. This increases to 5.22, 6.51, 6.97 and 5.97% with 0.25, 0.5, 0.75, and 1% fiber content, respectively. The maximum increase in CBR strength is almost 2.48 times that of unreinforced specimen with 0.75% fiber content.

4.4 *Effect of Soaking Period on CBR*

Soaking of specimens has been carried out to simulate the worst condition in the field during rainy season. The effect of soaking period variation on CBR is shown

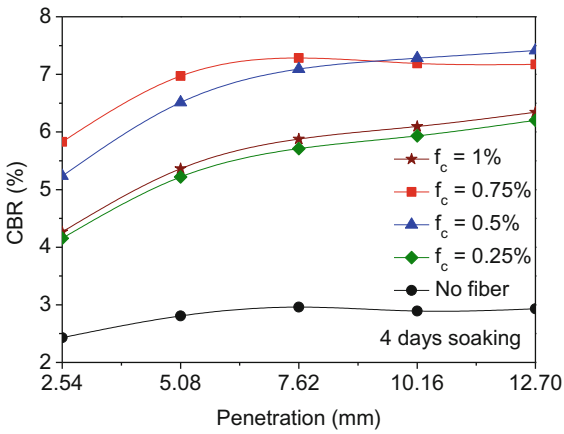

Fig. 2 CBR versus penetration depth at varying fiber contents

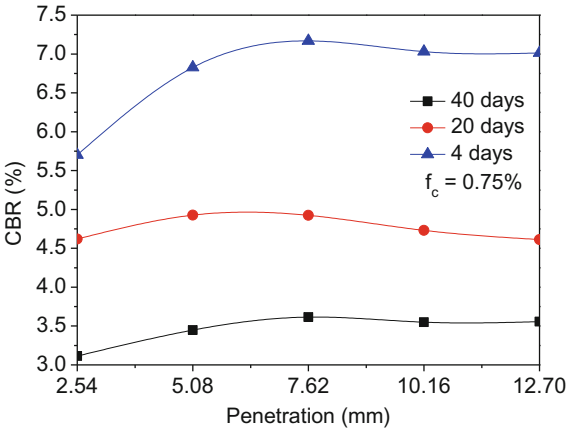

Fig. 3 CBR versus penetration depth for different soaking periods

in Fig. 3 for the specimens reinforced with 0.75% fiber content. The CBR value is found to decrease considerably as the soaking time is increased. With increasing moisture content, the surfacial interaction between soil-fiber and soil–soil particles get reduced, and the full mobilization of fiber tensile strength does not take place resulting decrease of CBR strength. The CBR values at 5.08 mm penetration are 6.97, 4.92 and 3.95% with 0.75% fiber reinforcement for 4, 20, and 40 days soaking, respectively, representing 43% reduction in CBR at 40 days soaking than that of 4 days. From Figs. 2 and 3, it can be noted that the CBR value of reinforced specimen even after 40 days soaking is higher than the CBR value of unreinforced specimen after 4 days soaking.

4.5 Secant Modulus Variation

The effect of penetration depth on secant modulus of fiber-reinforced specimens is shown in Fig. 4 for 4 days soaking. The secant modulus was calculated from the following expression:

$$k_s = \frac{\sigma_\Delta}{\Delta}, \tag{1}$$

where, σ_Δ is stress (kPa) at any penetration depth Δ.

At any fiber content, the secant modulus of specimen is noted to decrease with increasing penetration depth. However, at any penetration depth the secant modulus of specimen is found to increase with fiber content up to 0.75% fiber content and then decreases with 1% fiber content. The secant modulus at 2.54 mm penetration depth is 7.71 MN/m^3 for unreinforced specimen which increases to 13.20, 16.63, 18.51, and 13.54 MN/m^3 for 0.25, 0.50, 0.75 and 1% fiber content, respectively.

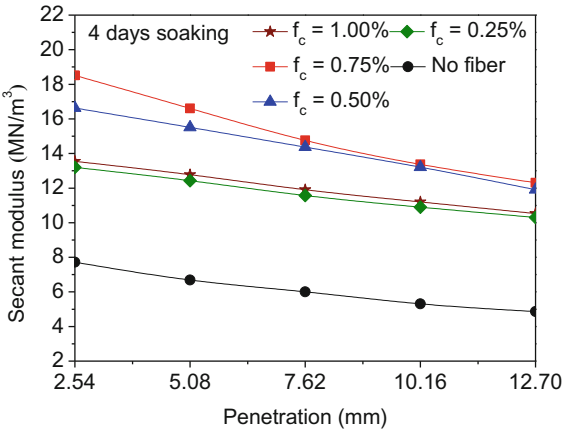

Fig. 4 Secant modulus versus penetration depth at varying fiber contents

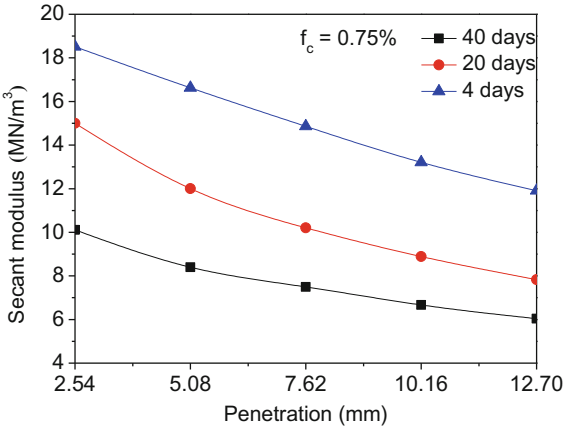

Fig. 5 Secant modulus versus penetration depth at varying soaking periods

These values decrease to 4.87 MN/m^3, for unreinforced soil and 10.30, 11.91, 12.31, and 10.53 MN/m^3 for 0.25, 0.50, 0.75, and 1% fiber contents, respectively at 12.70 mm penetration depth.

Effect of soaking period on secant modulus response of specimens reinforced with 0.75% fiber content at varying penetration depth is presented in Fig. 5. The secant modulus of specimen is noted to decrease with increasing soaking period at any penetration depth. The secant modulus values at 2.54 mm penetration for 4, 20, and 40 days soaking are 18.51, 15.00, 10.11 MN/m^3. The values decrease gradually with increasing penetration depth and increasing soaking days to 11.91, 7.83, and 6.04 MN/m^3, respectively at 12.70 mm penetration depth.

5 Conclusions

Based on the test results, following conclusions are drawn:

- The maximum dry density and optimum moisture content of the soil are insignificantly affected by glass fiber inclusion.
- At any fiber content, the penetration resistance of reinforced specimen increases even from a small penetration depth of 1.0 mm.
- With increasing penetration depth, CBR increases significantly up to 7.62 mm penetration and thereafter the increment is very small.
- The CBR increases with fiber content up to 0.75% and the corresponding CBR improvement over unreinforced soil is 2.48 times. With increasing soaking period, the CBR value decreases.
- At any fiber content, the secant modulus of the reinforced soil specimen decreases with penetration depth
- With increasing soaking period, the secant modulus of specimen decreases for all soil-fiber mix.

Overall, it has been found that the CBR value and secant modulus of fiber-reinforced specimens have increased significantly, and glass fiber-soil mix of 0.75% fiber content can serve the purpose of a better subgrade material. Large scale mixing at site can be carried out by using rotary mixer before compaction.

References

ASTM D 698-12. (2012). *Standard test method for laboratory compaction characteristics of soil using standard effort* (12,400 ft-lbf/ft^3 (600 kN/m^3)). West Conshohocken, PA, USA: ASTM International.

ASTM D 1883-99. (1999). *Standard test method for CBR (California Bearing Ratio) of laboratory-compacted soils*. West Conshohocken, PA, USA: ASTM International.

Benson, C. H., & Khire, M. V. (1994). Reinforcing sand with strips of reclaimed high-density polyethylene. *Journal of Geotechnical Engineering, ASCE, 12*(5), 838–855.

Chandra, S., Viladkar, M. N., & Nagrale, P. P. (2002). Mechanistic approach for fiber-reinforced flexible pavements. *Journal of Transportation Engineering, ASCE, 134*(1), 15–23.

Dutta, R. K., & Sarda, V. K. (2007). CBR behaviour of waste plastic strip-reinforced stone dust/fly ash overlying saturated clay. *Turkish Journal of Engineering and Environmental Science, 31,* 171–182.

Hazirbaba, K., & Gullu, H. (2010). California Bearing Ratio improvement and freeze–thaw performance of fine-grained soils treated with geofiber and synthetic fluid. *Cold Regions Science and Technology, 63,* 50–60.

Kalantari, B., Huat, B. B. K., & Prasad, A. (2010). Effect of polypropylene fibers on the California Bearing Ratio of air cured stabilized tropical peat soil. *American Journal of Engineering and Applied Sciences, 3*(1), 1–6.

Kumar, R., Kanaujia, V. K., & Chandra, D. (1999). Engineering behaviour of fiber-reinforced pond ash and silty sand. *Geosynthetics International, 6*(6), 509–518.

Lawton, E. C., & Fox, N. S. (1992). Field experiments on soils reinforced with multioriented geosynthetic inclusions. In *Transportation research record, 1369* (pp 44–53). Washington, D.C.: Transportation Research Board.

Srinivas Rao, B., & Jayalekshmi, S. (2010). Fiber reinforcement of soil subgrade beneath flexible pavements. In *Indian Geotechnical Conference (IGC 2010)*, Bombay, India.

Tingle, J. S., Santoni, R. L., & Webster, S. L. (2002). Full-scale field tests of discrete fiber-reinforced sand. *Journal of Transportation Engineering, ASCE, 128*(1), 9–16.

Zahran, S. Z., & Fatani, M. N. (1999). Glass fiber reinforced asphalt paving mixture: feasibility assessment. *Journal of King Saud University: Engineering Sciences, 11*(1), 85–98.

Bearing Capacity of Strip Footing on Clay Soil Reinforced with Metal Strips and with Anchors

P. V. S. N. Pavan Kumar

Abstract Experiments were conducted on model strip footings resting on clay soil reinforced with horizontal layers of strip reinforcement with and without end plate anchors. Load and corresponding settlements were measured and results presented in the form of pressure–settlement curves. Model strip footing was a rigid steel plate while galvanized iron sheet strips of 1 mm thickness were used as reinforcement with 16% coverage. Anchor plates were attached on either side of strip reinforcement. Tests were conducted for three arrangements of reinforcement, i.e., length increasing with depth, constant length, and length decreasing with depth. Bearing capacity increased by 38 and 370% respectively compared to unreinforced soil for without and with anchor conditions. Maximum increase was observed for the case of constant length of reinforcement. Provision of end anchors increases the bearing capacity significantly and permits use of shorter reinforcement with low coverage ratio.

Keywords Bearing capacity · Clay · Reinforcement · Anchor
Steel strip

1 Introduction

Reinforced soil bed is a soil foundation containing horizontal layers of tensile reinforcement. Such an inclusion in foundation soil increases load carrying capacity and the load settlement stiffness of foundation soil system (Binquet and Lee 1975a; Athavan 1995). The construction of reinforced soil bed involves refilling the excavation with good quality frictional soils such as such as sand, gravel, and/or crushed stone. Binquet and Lee (1975b) observed three modes of failure of

P. V. S. N. P. Kumar (✉)
Department of Civil Engineering, Guru Nanak Institutions Technical Campus, Hyderabad, India
e-mail: pavankumar.pvsn@gmail.com

T. Thyagaraj (ed.), *Ground Improvement Techniques and Geosynthetics*, Lecture Notes in Civil Engineering 14, https://doi.org/10.1007/978-981-13-0559-7_9

reinforced soil beds. These are shearing of soil above the reinforcement, pullout, and rupture of reinforcement.

Importing good quality friction fill material may become uneconomical and unavailable. Under these circumstances one is compelled to make use of locally available low-quality cohesive soils by treatment or inclusion of reinforcement. Samtani and Sonpal (1989) studied the bearing capacity of strip footing resting on cohesive soil reinforced with metallic strips and observed that the circular failure surface tend to become shallow with increase of linear density ratio of reinforcement. Mandal and Sah (1992) conducted bearing capacity tests on clay subgrades reinforced with geogrids and observed an improvement of bearing capacity or decrease of settlements. It is well known that saturated soil under undrained conditions develop very poor bond between the soil and reinforcing material (Jewell and Wroth 1987). This Condition is further aggravated when high pore pressures develop during compaction. Rajyalakshmi et al. (2012) presented a method to estimate the bearing capacity of a strip footing resting on the surface of a geosynthetic reinforced foundation bed laid over soft foundation clay.

In order to increase the load carrying capacity of saturated cohesive fill it is preferable to provide end plate anchors. When a reinforced cohesive soil bed is provided with end plate anchors, on either side of reinforcement layers, the load carrying capacity of such system is expected to increase with development of passive earth pressure resistance provided by the action of end plate anchors (Kumar 2002). Rowe and Davis (1982) conducted model tests to study the pullout of vertical anchor plates and developed charts to estimate the pullout failure load for anchor plates.

2 Experimental Studies

Soil beds were prepared in a steel tank with inside dimensions of 1200 mm length, 332 mm width and 700 mm height (Fig. 1). Two sides of the tank were made of 15 mm thick perspex sheet and were braced on the outer surface with mild steel angles to avoid yielding during tests. Model footing was made of a rigid steel plate and measured 330 mm length $\times$ 100 mm width $\times$ 25 mm thickness. A rough base condition was achieved by cementing a thin layer of sand on to the base of model foundation with epoxy glue. Footing was centered in the tank with length of the footing parallel to the width of the tank.

On each side of the tank 1 mm gap was given to prevent contact between footing and the side walls. Effect of side wall friction was reduced by coating the inside of the perspex wall with grease. Two ends of the footing plate were polished to have smooth surface and coated with grease to minimize the end friction effects. To ensure uniform distribution of applied load on the model footing, two rollers of 10 mm diameter and 330 mm length made of high strength steel were placed on the two parallel grooves made at the top of the footing. These grooves were made along the length footing, each at a distance of 32.5 mm from the centre line of the footing

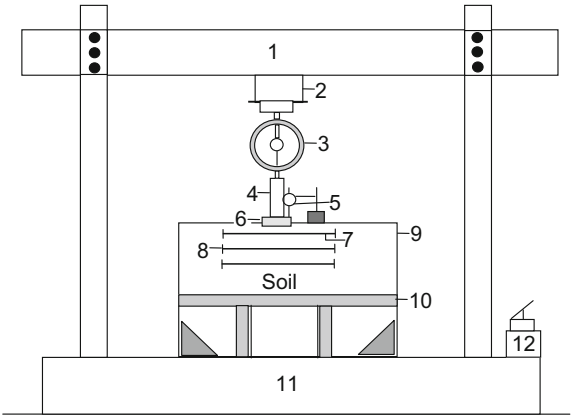

Fig. 1 Schematic of Experimental setup. 1. Self-straining loading frame, 2. Hydraulic jack, 3. Proving ring, 4. Spacer block, 5. Dial gauge fixed by magnetic base, 6. Strip footing, 7. Strip reinforcement, 8. Anchor, 9. Test tank, 10. Angles supporting the tank, 11. Platform, 12. Oil pump for jack

on either side. A 10 mm thick steel plate having the same plan dimensions and grooves as the model footing was mounted on the rollers. Grooves at the bottom of this steel plate ensured the perfect seating of it over the rollers. Footing was loaded with a hand operated hydraulic jack supported against the upper cross head of reaction frame. The reaction frame is anchored to the concrete floor by means of base plates and anchor bolts independent of the test container.

Upon filling the whole tank, the top surface was leveled and the footing was placed on a predefined alignment such that the loads from the jack and loading frame would be transferred concentrically to the footing. Hydraulic jack was connected to the footing through a proving ring to measure the load applied on the footing. Load was applied to the footing through a rigid spacer (made of steel) of 60 mm diameter and 60 mm height centered on the top plate below the proving ring. A ball bearing was positioned between the proving ring and the spacer to ensure that no extraneous moment was applied to the footing.

Load applied to the footing was measured by a calibrated proving ring suspended from the spindle of the jack through an adopter and resting on the footing through a ball bearing. Footing settlement was measured by means of dial gauges one at each end on opposite sides. Index properties of cohesive soil were determined and presented in Table 1. Average cohesion of the soil was found to be 40 kN/m^2 and the angle of internal friction of the soil was 10°.

Table 1 Properties of clay used in the model test

Property	Value
Liquid limit (%)	56.5
Plastic limit (%)	21.96
Shrinkage limit (%)	10.62
Maximum dry unit weight (kN/m^3)	16.1
Optimum moisture content (%)	18.5
Specific gravity	2.75
Soil classification from plasticity chart	CH

Galvanized iron sheets of 1 mm thickness were used for model testing. Three different patterns of reinforcement without and with anchors were adopted (Figs. 2, 3, 4, 5, 6 and 7). They are (i) Reinforcement length increasing with depth (ii) length decreasing with depth (iii) Equal length. For the above arrangement of the reinforcement galvanized iron sheets have been cut into strips of lengths 0.13, 0.21, 0.28, 0.33, 0.375, and 0.4 m. To the above reinforcement the end anchors of 3.5 cm height and 5 cm width have been welded on either side.

Soil is compacted with a known compaction effort using 5 kg drop hammer falling from a height of 500 mm over a square base plate of size 150 mm. Soil is compacted in 75 mm thick layers. Clay soil was placed in the tank at optimum moisture content. Undisturbed soil samples were collected from the test tank using open tubes for determining the strength and stiffness properties of the soil.

For arrangement of reinforcement at the required level, filling of the soil was stopped and the reinforcement was arranged at the middle of tank. Above the top of

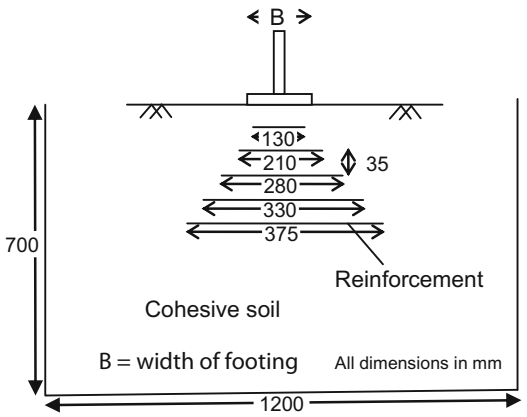

Fig. 2 Reinforcement length increasing with depth

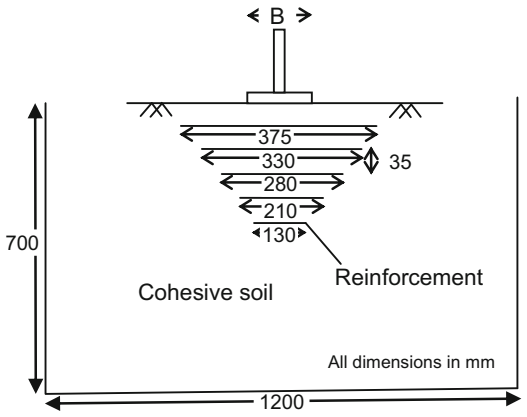

Fig. 3 Reinforcement length decreasing with depth

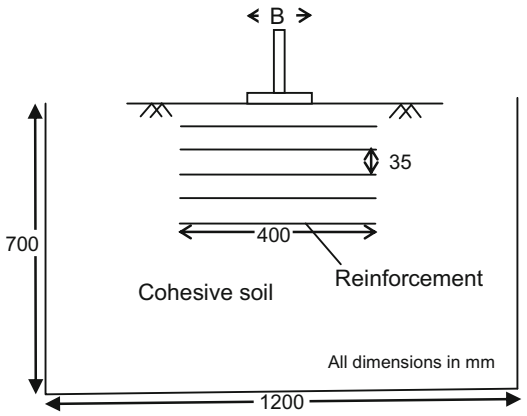

Fig. 4 Equal length of reinforcement

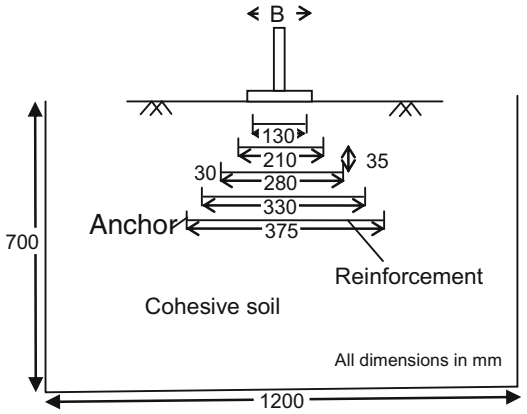

Fig. 5 Reinforcement length increasing with depth and with end anchors

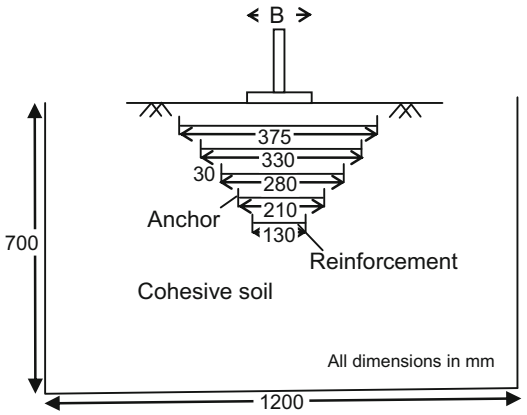

Fig. 6 Reinforcement length decreasing with depth and with end anchors

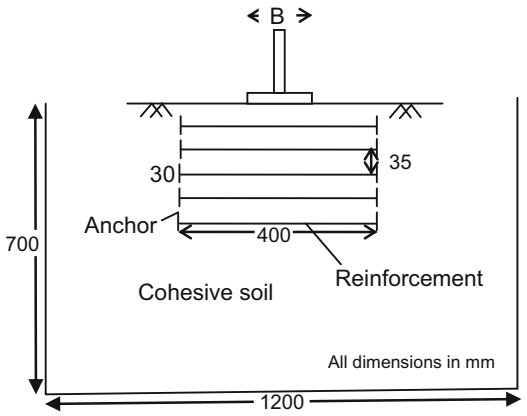

Fig. 7 Equal length of reinforcement and end anchor

reinforcement soil was laid and compacted to the required degree. Height of each compacted layer was equal to 75 mm. Footing was placed at the middle of the tank on top of compacted soil bed.

Spacer was placed on the model footing to fill up the gap between the footing and loading cell. Proving ring was attached to the self-straining loading frame and two dial gauges were attached to the model footing on either side to measure the average settlement of footing.

3 Results and Discussion

Results of the experimental work were presented in the form pressure versus settlement curves (Figs. 8 and 9). Different patterns of reinforcement were abbreviated as follows UR = Unreinforced condition, IL = Increasing length of reinforcement without anchors, DL = Decreasing length of reinforcement without anchors, EL = Equal length of reinforcement without anchors, IL = Increasing length of reinforcement with anchors, DL = Decreasing length of reinforcement with anchors, EL = Equal length of reinforcement with anchors.

Ultimate bearing capacity for unreinforced soil is indicated in Fig. 8 by continuous settlement of footing at a pressure of 122 kN/m^2. Inclusion of strip reinforcement and end anchors increases the pressure to be applied on the footing for a given settlement. Ultimate bearing capacity is determined from tangent intersection method for the cases with reinforcement and end anchors. Results are reported in Table 2.

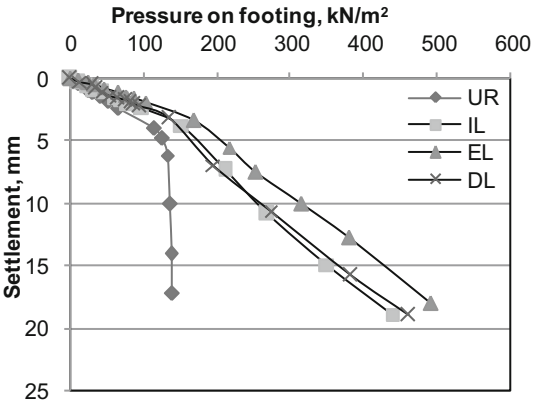

Fig. 8 Pressure versus settlement of footing for reinforcement without anchors

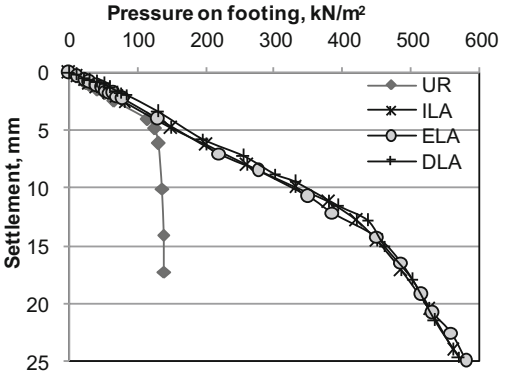

Fig. 9 Pressure versus settlement of footing for reinforcement with anchors

Table 2 Ultimate bearing capacity for different reinforcement arrangement

Reinforcement arranment	Ultimate bearing, kN/m^2
Unreinforced Case	122
Increasing length of reinforcement, IL	152
Equal length of reinforcement, EL	168
Decreasing length of reinforcement, DL	150
Increasing length of reinforcement with Anchor, ILA	460
Equal length of reinforcement with Anchor, ELA	462
Decreasing length of reinforcement with Anchor, DLA	456

4 Conclusions

Improvement of bearing capacity of clay soil using reinforcing strips with and without end anchors is studied. Bearing capacity increased by a minimum and maximum of 23 and 38% respectively for the cases with decreasing depth of reinforcement and equal length of reinforcement. Marginal improvement of bearing capacity is due to low coverage of reinforcement of 16%. Provision of end plate anchors on either side of reinforcement increases the bearing capacity by 370%. Mobilization of passive resistance in front of anchor improves the bearing capacity of reinforced clay bed. An analytical solution for improvement of bearing capacity of reinforced clay bed with anchors is developed by Kumar (2002). Based on the results of the experimental investigation and the analytical solution it is concluded that provision of end anchors with reinforcement and subsequent improvement of bearing capacity economizes the cost of foundation construction in clay soils of low bearing capacity. Permits use of reinforcement with low coverage ratio.

References

Athavan, M. A. (1995) *Analytical and experimental investigations on soil-geosynthetic composites as foundation beds (M.S thesis)*. Civil Engineering Department, Indian Institute of Technology, Madras.

Binquet, J., & Lee, K. L. (1975a). Bearing capacity tests on reinforced earth slabs. *Journal of Geotechnical Engineering Division, ASCE, 101*(12), 1241–1255.

Binquet, J., & Lee, K. L. (1975b). Bearing capacity analysis of reinforced earth slabs. *Journal of Geotechnical Engineering, ASCE, 101*(12), 1257–1276.

Jewell, R. A., & Wroth, C. P. (1987). Direct shear tests on reinforced sand. *Geotechnique, 37,* 53–68.

Kumar, P. V. S. N. P. (2002). *Studies on load carrying capacity of footings on reinforced cohesive soil beds (M.Tech thesis)*. Indian Institute of Technology Madras.

Mandal, J. N., & Sah, H. S. (1992). Bearing capacity tests on geogrid-reinforced clay. *Geotextiles and Geomembranes, 11,* 327–333.

Rajyalakshmi, K., Madhav, M. R., & Ramu, K. (2012). Bearing capacity of strip foundation beds on compressible clay. *Indian Geotechnical Journal, 42*(4), 294–308.

Rowe, R. K., & Davis, E. H. (1982). The behaviour of anchor plates in clay. *Geotechnique, 32*(1), 9–23.

Samtani, N. C., & Sonpal, R. C. (1989). Laboratory tests of strip footing on reinforced cohesive soil. *Journal of Geotechnical Engineering Division, ASCE, 115*(9), 1326–1330.

Application of Microbial-Induced Carbonate Precipitation for Soil Improvement via Ureolysis

Siddhartha Mukherjee, R. B. Sahu, Joydeep Mukherjee and Suchandra Sadhu

Abstract The challenges to develop or strengthen the weak soil always prompted the need for further research investigation to develop a new, eco-friendly, and sustainable method of ground improvement. The MICP (microbially induced carbonate precipitation) technique is one such method in which metabolic pathways of microorganism are utilized to form calcite precipitation inside the soil matrix leading to improve the engineering properties of soil. Ureolysis or urea hydrolysis is the most efficient process among all MICP methods of carbonate generating reaction, as it has the potential to produce large amount of calcite ($CaCO_3$) within a short period of time. This study aims to investigate the effectiveness of MICP technique on fine grained soil as clayey sandy silt or loam in improving its shear strength. In this study, three species of urease positive, alkaliphelic aerobic bacteria, namely *Sporosarcina pasteurii*, *Bacillus megatarium,* and *Morganella morgani* were used for ureolysis and microbially induced calcite precipitation. Quantitative analysis of calcite precipitation in the soil samples was done by Piper method. The target soil was mixed with each microorganism individually before it was compacted into the mould. In the experimental programm, four different treatment conditions were considered for each types of microorganism such as (1) untreated, (2) treated with cementation reagent (mixture of 0.5 M $CaCl_2$ and 0.5 M urea), (3) treated with bacteria only and (4) treated with both bacteria and cementation reagent. These experiments revealed that all these three types of microorganism can induce sufficient amount of calcite precipitation that can result in measurable improvement of the strength of soil.

S. Mukherjee (✉) · R. B. Sahu
Department of Civil Engineering, Jadavpur University, Kolakata 700032, India
e-mail: sidd.m@rediffmail.com

R. B. Sahu
e-mail: rbsahu_1963@yahoo.co.in

J. Mukherjee · S. Sadhu
School of Environmental Studies, Jadavpur University, Kolakata 700032, India
e-mail: joydeep_envstu@school.jdvu.ac.in

S. Sadhu
e-mail: mailtorimu@rediffmail.com

T. Thyagaraj (ed.), *Ground Improvement Techniques and Geosynthetics*, Lecture Notes in Civil Engineering 14, https://doi.org/10.1007/978-981-13-0559-7_10

Keywords Microbially induces carbonate precipitation · Ureolysis
Calcite · Urease positive · Shear strength

1 Introduction

Due to rapid infrastructural demand for the ever-growing population in the country like India, development activities has to be carried out on the weak and problematic soil due to the shortage of competent land space. Grouting is one of the commonly used methods which are widely adopted for soil stabilization technique. Traditional grouting method for ground improvement employs particulate (cement/bentonite) or chemical grout. These methods are effective only near vicinity of grouting equipment and are not useful to treat large volumes of soil. On the other hand most of the chemical grouting methods are harmful to the environment. Synthetic chemical grouting techniques are even more toxic or hazardous except sodium silicate (Karol 2003). Hence, this technology does not provide effective and economical solutions considering issues of environmental pollution of air and underground water.

Therefore, this recent issues of environmental degradation has prompted the development of new, eco-friendly, and sustainable technology for ground improvement. Bio-mediated soil improvement technique is one of such new and innovative research field within geotechnical engineering which can be applied as an alternative approach of ground improvement technique taking care of the concerning of environmental issues. In this technique, calcium carbonate precipitation has been induced inside the soil matrix by microorganism through their metabolic process to improve the engineering properties of soil. Hence, this technique is also called as microbial induced carbonate precipitation or MICP.

Though the application of this technology in ground improvement is relatively young, many studies has been reported including DeJong et al. (2006), Whiffin et al. (2007), Harkes et al. (2010), Kim et al. (2012) etc. Dejong et al. (2006) found higher initial stiffness and shear capacity at failure for treated sand specimen than untreated loose specimen. Whiffin et al. (2007) have been successful to consolidate 5 m long sand column by applying MICP treatment. Harkes et al. (2010) investigated on the methodology to distribute and fix *Sporosarcina pasteurii* homogeneously in sand bed and found that two phase injection procedure (injection of bacteria followed by fixation fluid) can be applied to achieve homogeneous distribution of bacteria. Most of the researchers use *S. pasteurii* as microorganism and sand as soil material for MICP treatment. It is reported that the presently available method of MICP treatment is not favorable for fine grained soil due to small pore throat size. Therefore the aim of this study is to investigate the effectiveness of MICP technique by using different urease positive microorganism on fine grained soil as clayey sandy silt or loam in improving its undrained shear strength.

2 Theoretical Background

Several metabolic pathways of microorganism are identified in nature which can produce cementatious compound such as calcite. Among all, urea hydrolysis or ureolysis is the most efficient process through which large amount of calcite can be precipitated within a short period of time. In ureolysis, urea is decomposed via hydrolysis to ammonium and carbonate ions by urease enzyme produced by urease positive bacteria under aerobic condition. This mechanism yields higher pH along with high concentration of carbonate ions and create an environment favorable for the precipitation of calcium carbonate or calcite. Calcite is precipitated through the reaction between carbonate ions (CO_3^{2-}) from the urea hydrolysis and calcium ions (Ca^{2+}) from the supplied calcium chloride. Following equations describe the entire pathway of carbonate generation through urea hydrolysis (Castanier et al. 1999; Hammes and Verstraete 2002; Whiffin 2004).

$$CO(NH_2)_2 + 2H_2O \xrightarrow{\text{Urease}} 2NH_4^+ + CO_3^{2-} \quad (1)$$

$$Ca^{2+} + CO_3^{2-} \rightarrow CaCO_3 \quad (2)$$

3 Material and Methodology

3.1 Selection of Bacteria and Batch Cultivation

Considering the potentiality of calcite precipitation, three non-pathogenic species of urease positive, alkalifilic, aerobic bacteria have been chosen in this study. These are **(1) *Sporosarcina pasteurii (MTCC-1761)*, (2) *Bacillus megatarium (MTCC-428)* and (3) *Morganella morgani (MTCC-662)***. All the microbes were procured from Microbial Type Culture Collection Centre and Gene Bank housed at IMTECH, Chandigarh, Govt. of India.

All these three microorganism were cultivated in nutrient broth, growth medium no. 3(MTCC) [Composition: Beef extract 1.0 gm/L, Yeast extract 2.0 gm/L, Peptone 5.0 gm/L, NaCl 5.0 gm/L, Agar 15.0 gm/L]. Incubation temperature for *S. pasteurii (MTCC-1761)* and *B. megatarium (MTCC-428) was* 30 °C, whereas for *M. morgani (MTCC-662),* it was 37 °C. For all bacteria the incubation period was 24 h.

3.2 Soil Sample

Soil sample was collected from the surface layer of sediments on the banks of river Hooghly during low tide time. The physical and engineering properties of the soil

Table 1 Engineering properties of soil sample

Properties	Values
MDD	16.97 kN/m^3
OMC	17%
Liquid limit (LL)	37%
Plastic limit (PL)	21%
Grain size	10% Sand, 70% Silt, 20% Clay (D_{50} = 0.02 mm)
IS classification	MI

specimens were determine as per Indian Standard (IS 2720) and tabulated in Table 1. Standard proctor test was performed to establish moisture-density relationship of the test soil.

3.3 Cementation Reagent

For MICP process, cementation reagent serves as the essential raw materials. In this study, cementation reagent comprises of the mixture of the solutions of 0.5 M urea ($CO(NH_2)_2$) and 0.5 M Calcium Chloride ($CaCl_2$). All the chemicals used in this research were analytical grade to ensure the consistency of the test results.

3.4 Preparation of Soil Specimen

Prior to prepare the specimen, the test soil samples were air dried for several days. To maintain the reasonable pore space for smooth percolation of reagent solution through the soil specimen, the density of the test sample was kept lower than the MDD. In this study the soil specimens were compacted in the mould (38 mm dia) by applying the equivalent energy as per the Standard Proctor Test at a density of 15.79 kN/m^3 (93% of MDD). The water content was taken from the Proctor density curve corresponding to the desired density. To inoculate the soil specimen, soil samples were mixed with each cultivated bacteria directly at a time and compacted into mould. In that case quantity of water to be mixed with the soil was replaced by the growth medium with the bacteria. Length to diameter ratio for all the test specimens was maintained approximately as 2:1.

3.5 Quantitative Analysis of Calcite Precipitation

Quantitative determination of precipitated calcium chloride was done following modified Piper's method or acid neutralization method (Piper 1966). In this method sodium hydroxide is used to titrate the excess hydrochloric acid applied to dissolve the precipitated calcium carbonate

$$\% \text{ of } CaCo_3 = \frac{5x\,(B - S) \times N \times \text{mcf}}{\text{Samplewt}\,(\text{gm})}, \tag{3}$$

where, B = Vol in ml NaOH used for blank, S = Vol in ml of NaOH used for sample, N = Normality of NaOH and mcf = moisture correction factor

3.6 Experimental Variables

In this investigation four different treatment conditions were considered for each type of microorganism. (1) Untreated in which the specimen was prepared at desired density and made saturated before testing for comparison purpose. (2) Specimen prepared at desired density and treated with cementation reagent. (3) Specimen prepared with bacterial solution and made saturated before testing to observe the effect of bacterial cell on the strength of soil. (4) Specimen inoculated with bacterial solutions during preparation and then treated with cementation reagent.

3.7 Experimental Procedure

MICP treatment was done by injecting the reagent solution (0.5 M urea/$CaCl_2$) into the soil specimen through a pressurized tank containing reagent solution. Figure 1 shows the laboratory test setup for MICP treatment of soil specimen. Total volume of reagent solution injected into the soil specimen was 4 L in 72 h. The pressure was maintained at 100 kPa throughout the treatment for all the specimens. After completion of treatment the soil specimens were extruded from the mould for strength determination by unconfined compression test.

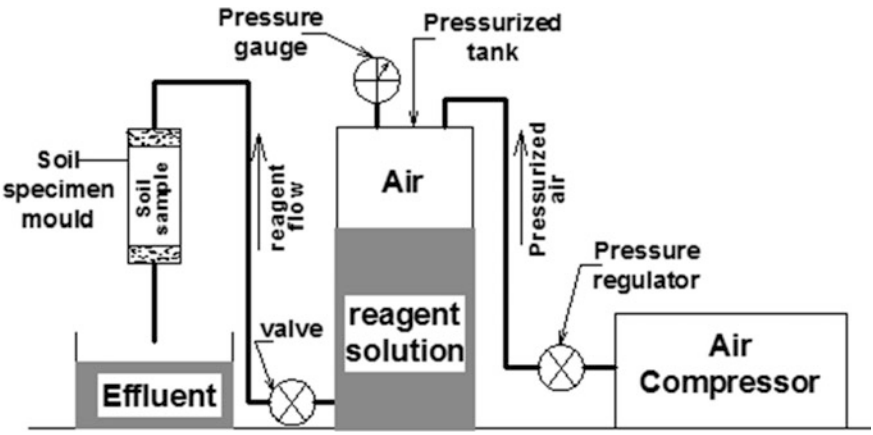

Fig. 1 Test setup for MICP treatment

4 Results and Discussion

The stress strain curves of all the soil specimens tested in the unconfined compression testing machine are shown in Fig. 2. Unconfined compressive strength or UCS (q_u) is defined as the peak stress or the stress corresponding to 20% axial strain whichever is lower. Undrained cohesion (C_u) is taken as half of the UCS value, i.e., ½ q_u. It was observed that unconfined compression strength was improved for all MICP treated soil specimen as compared to the untreated samples.

Carbonate content in the soil specimen was determined by averaging the calcite content value of three different positions (top, middle, and bottom) of the soil specimen. Percentage calcium carbonate content of different soil samples (untreated and MICP-treated) are tabulated in Table 2. It was also found that some carbonate (0.698%) was present in the untreated soil sample. The carbonate content is slightly increased (0.86%) in the samples treated with cementation reagent only. Therefore the actual amount of carbonate precipitation for MICP treated soil specimens with MTCC662, MTCC1761, and MTCC428 were 0.495, 1.042, and 1.752% respectively.

Comparison of strength improvement ratio of different test specimens with respect to untreated specimen is given in Fig. 3. The improvement ratio is maximum (1.49) for the sample treated with MTCC428 (*B. megatarium*) among all the bacteria used in this investigation. The specimen treated with cementation reagent only also exhibited a slight (15%) improvement in shear strength. This implies that the existing bacteria inhabited in the soil samples may have favoured the MICP process though it was not appreciable. Furthermore, no measurable improvement was observed in UCS strength for the soil specimen treated with microorganism only. Therefore, those results were not included in Figs. 2 and 3.

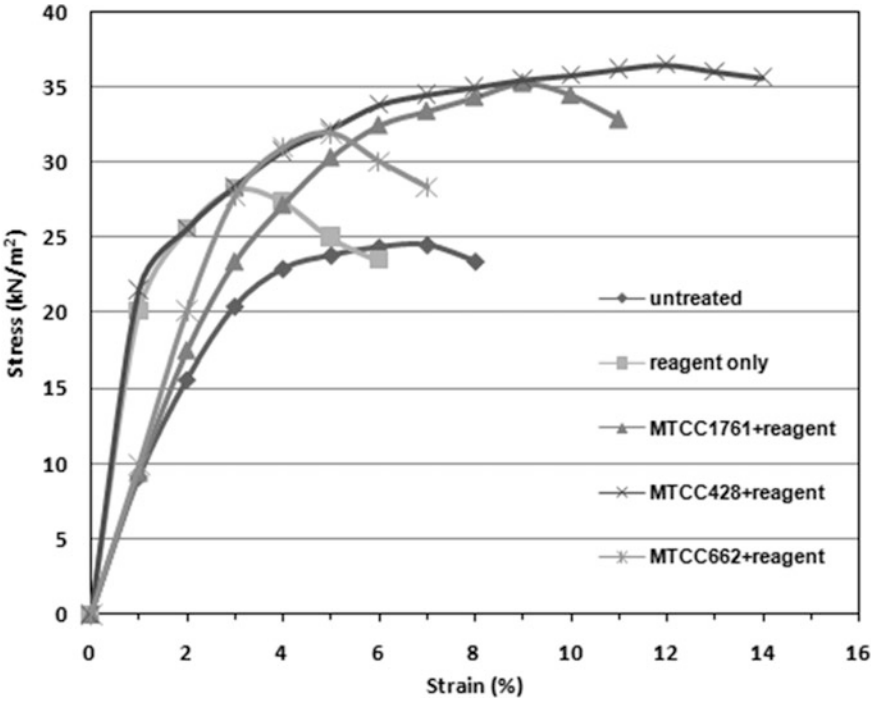

Fig. 2 Stress–strain curves in UCS test

From the test result, it was also observed that the unconfined compression strength is increased with higher percentage of carbonate content. This phenomenon can be attributed to the fact that the more amount of calcite precipitation reduces the pore volume and improve the inter-particle bonding between soil grains and hence the greater shear strength value observed.

5 Conclusions

From this preliminary investigation, the following conclusions can be drawn:

1. All the three microorganism (*S. pasteurii*, *B. megatarium,* and *M. morgani)* can be used for soil improvement by MICP technique. In this particular soil as clayey sandy silt or loam, *B. megatarium* proved to be the most effective microorganism for MICP treatment.

Table 2 Percentage carbonate content in the soil specimens

	Untreated	Treated with cementation reagent only	Treated with MTCC662 + cementation reagent	Treated with MTCC1761 + cementation reagent	Treated with MTCCC428 + cementation reagent
Calcium cobonate content (%)	0.698	0.860	1.193	1.740	2.450

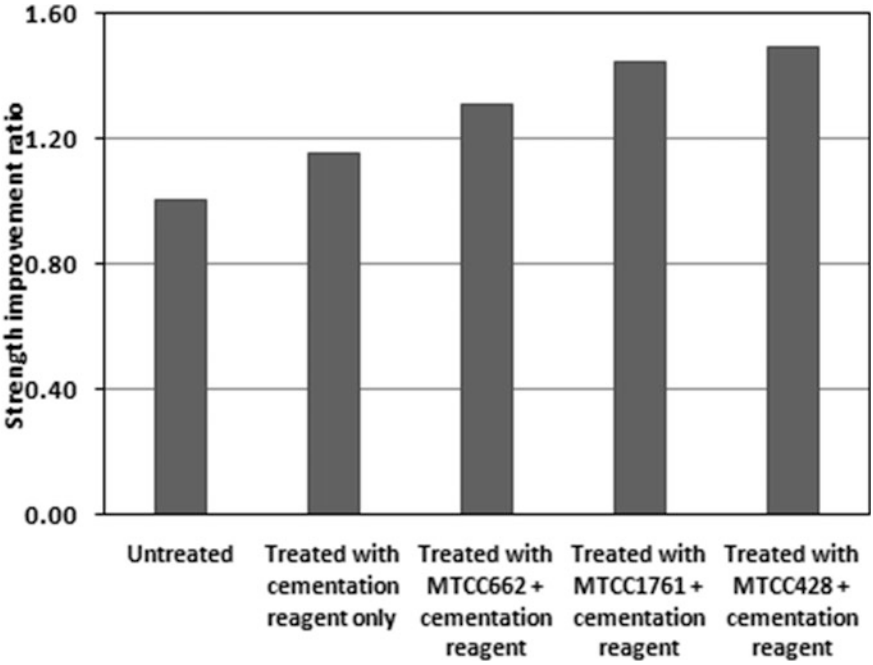

Fig. 3 Shear strength improvement of soil specimen

2. The MICP-treated soil specimen exhibited moderate improvement in shear strength, i.e., 49%. This improvement is estimated for a specified density of soil specimen. To know the effect of density on strength improvement by MICP application more investigations are required.
3. The amount of calcite precipitation in the treated soil specimen ranged from 0.495 to 1.752%. The maximum amount was observed for the soil specimen treated with the microorganism *B. megatarium* (MTCC428)
4. The soil specimen treated with cementation reagents only exhibited slight improvement in shear strength. This result indicated the fact that some calcite forming microorganism was present in the original soil.
5. The presence of biomass only in the soil specimen didn't have any significant effect in improving the strength of the soil.

References

Castanier, S., Le Metayer-Levrel, G., & Perthuisot, J. P. (1999). Ca-carbonates precipitation and limestone genesis-the microbiogeologist point of view. *Sedimentary Geology, 126*(1–4), 9–23.

Dejong, J. T., Fritzges, M. B., & Nüsslein, K. (2006). Microbially induced cementation to control sand response to undrained shear. *Journal of Geotechnical and Geoenvironmental Engineering, 132*(11), 1381–1392.

Hammes, F., & Verstraete, W. (2002). Key roles of pH and calcium metabolism in microbial carbonate precipitation. *Reviews in Environmental Science & Biotechnology, 1*(1), 3–7.

Harkes, M. P., Van Paassen, L. A., Booster, J. L., Whiffin, V. S., & Van Loosdrecht, M. C. M. (2010). Fixation and distribution of bacterial activity in sand to induce carbonate precipitation for ground reinforcement. *Ecological Engineering, 36*(2), 112–117.

Karol, R. H. (2003). *Chemical grouting and soil stabilization* (3rd ed.). New York: M. Dekker.

Kim, D. H., Park, K. H., Kim, S. W., & Mun, S. H. (2012). A novel approach to induce cementation of loose soils. *Advanced Science Letters, 9,* 545–550.

Piper, C. S. (1966). *Soil and plant analysis*. Bombay: Hans Publications.

Whiffin, V. (2004). *Microbial $CaCO_3$ precipitation for the production of biocement* (Ph.D. thesis). Mudroch University, Perth, Western Australia. 154 p.

Whiffin, V., van Paassen, L., & Harkes, M. (2007). Microbial carbonate precipitation as a soil improvement technique. *Geomicrobiology Journal, 24*(5), 417–423.

Influence of Organic Content on Fly Ash Stabilization of Clay

T. V. Sanu Vasudevan and V. Jaya

Abstract The engineering behavior of soil is affected by the presence of organic content in the soil. Previous studies have shown that organic content in clay is a key factor which affects the index properties, unconfined compressive strength and compaction behavior. Fly ash stabilization of clay is a commonly used stabilization method in pavement construction. Presence of organic content affects the stabilization of clay using fly ash, because organic content influences the pH of clay and hence the pozzolanic reaction is also affected. Kaolinite clay with different organic content (9–5%) is stabilized using Class C fly ash. The variation in index properties, unconfined compressive strength and compaction behavior of clay with different organic contents which is stabilized with fly ash is presented. Optimum fly ash requirement is also affected by the presence of organic content in clay. The optimum fly ash content for stabilization of kaolinite with different organic content is also presented in this paper.

Keywords Organic content · Chemical stabilization · Fly ash · Kaolinite

1 Introduction

Organic content in the soil results in high compressibility, low shear strength, and low unit weight (Saride et al. 2010; Kolay et al. 2010). It has a significant role in the engineering and index properties of soil (Thiyyakkandi and Annex 2011). Fly ash can be used to stabilize organic soils also. But the resulting unconfined compressive

T. V.S. Vasudevan (✉)
Department of Civil Engineering, College of Engineering Trivandrum, Trivandrum, India
e-mail: sanugeck@gmail.com

V. Jaya
Department of Civil Engineering, Government Engineering College Barton Hill, Trivandrum, India
e-mail: jayasraj@gmail.com

T. Thyagaraj (ed.), *Ground Improvement Techniques and Geosynthetics*, Lecture Notes in Civil Engineering 14, https://doi.org/10.1007/978-981-13-0559-7_11

strength depends on properties of soil and fly ash and the strength of soil-fly ash mixture decreases when organic content of soil increases (Tastan et al. 2011). Therefore organic content is an important factor to be considered during fly ash stabilization. Little is known about the engineering properties of organic soils when stabilized with fly ash. Hence the variation in physical properties, index properties, compaction behavior and shear strength of fly ash stabilized kaolinite at different organic contents are determined in this paper. The percentage of fly ash required for the organic kaolinite to attain maximum shear strength was also determined.

2 Material Properties and Experimental Procedure

Kaolinite used in the study purpose is moderately plastic and inorganic in nature. Table 1 shows the initial properties of kaolinite. Locally available biogas slurry was added to kaolinite to increase the organic content. The pH value of the slurry was obtained as 7.5. Carbon: Nitrogen ratio was 12:1.

Fly ash used in this study was of ASTM class C specifications (ASTM C618 2015). Initial properties of fly ash are summarized in Table 2. Table 3 shows the chemical composition of fly ash. Grain size distribution curves are shown in Fig. 1.

Slurry was initially air-dried and then powdered for uniform mixing. It was added to kaolinite at different percentages (10, 20 and 30%) to prepare kaolinite of different organic contents. Organic content of the mix was determined as per ASTM D 2974-14. On addition of biogas slurry organic content of kaolinite was found to varying between 14–18%.

Kaolinite mixed with biogas slurry was kept for 7 days for testing. Tests on index properties, compaction behavior and shear strength characteristics were conducted as per respective IS codes.

Table 1 Properties of Kaolinite

Properties of kaolinite	Value
Water content (%)	00.98
Specific gravity	02.42
Organic content (%)	09.00
Liquid limit (%)	42.00
Plastic limit (%)	25.00
Plasticity index (%)	17.00
Optimum moisture content (%)	23.47
Maximum dry density (g/cc)	01.46
pH	03.22
Unconfined compressive strength (kN/m^2)	72.00
Clay content (%)	75.00
Silt content (%)	23.00
Soil classification	CI

Table 2 Properties of fly ash

Properties	Value
Water content (%)	00.72
pH	08.50
Specific gravity	02.10
Clay content (%)	04.00
Silt content (%)	70.00
Sand content (%)	26.00

Table 3 Chemical composition of fly ash (laboratory test result)

Parameter	Type I
SiO_2 (%)	38.40
Al_2O_3 (%)	14.60
Fe_2O_3 (%)	04.50
CaO (%)	22.70
MgO (%)	04.80
CaO/SiO_2	00.59
Loss on ignition (%)	00.80
Classification	Class C

Fly ash was added to kaolinite in different percentages to determine the optimum percentage for which maximum shear strength was obtained. 8% was obtained as optimum and this optimum percentage of fly ash was added to kaolinite of different organic contents.

3 Results and Discussions

Figure 2 shows the classification of soils as per plasticity chart. When the organic content of kaolinite is 14% and above, it is organic. Therefore 14% organic content is considered here as the boundary separating inorganic and organic soil. The properties of kaolinite added with different percentages of slurry are shown in Table 4.

3.1 Effect of Organic Content on Index Properties

Figure 3 shows the variation in specific gravity with organic content. The specific gravities of kaolinite and fly ash were 2.42 and 2.1 respectively. Fly ash particles are light weight, hollow spheres compared to soil particles. Its specific gravity is much lower. Therefore the overall weight of the soil-fly ash mix will be less. Hence the resulting decrease in specific gravity is obtained on fly ash treatment.

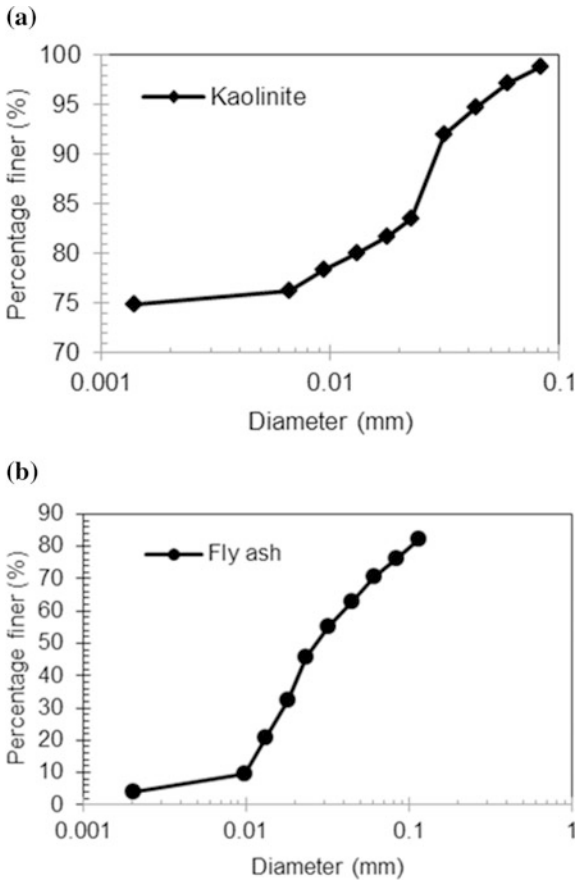

Fig. 1 Grain size distribution curves **a** Kaolinite, **b** fly ash

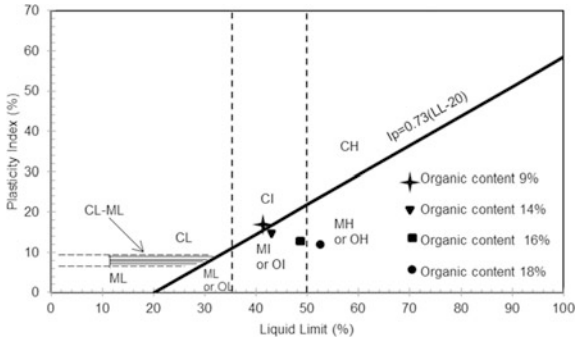

Fig. 2 Soil classification as per plasticity chart

Table 4 Properties of organic soil

Property	Kaolinite	Kaolinite + 10% slurry	Kaolinite + 20% slurry	Kaolinite + 30% slurry
Organic content (%)	09.00	14.00	16.00	18.00
Specific gravity	02.42	02.08	01.98	01.93
pH	03.22	03.75	04.17	05.24
Liquid limit (%)	42.00	43.20	48.60	52.40
Plastic limit (%)	25.00	27.22	36.19	40.35
Plasticity index (%)	17.00	15.68	12.41	12.05
Optimum moisture content (%)	23.47	26.12	27.20	29.00
Maximum dry density (g/cc)	01.46	01.36	01.29	01.20
Unconfined compressive strength (kN/m^2)	72.00	65.00	62.00	48.00
Classification	CI	OI	OI	OH

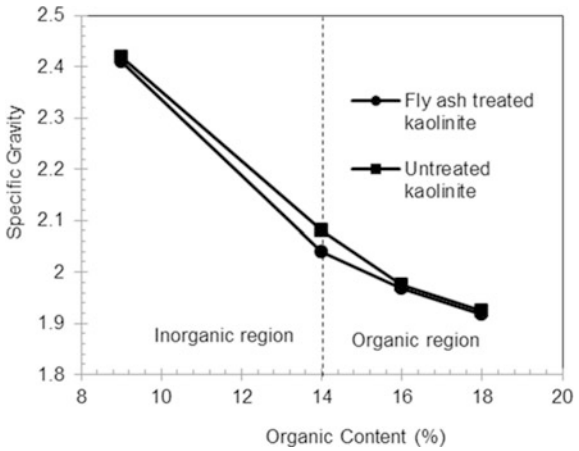

Fig. 3 Variation in specific gravity with organic content

Variation in liquid limit, plastic limit, and plasticity index are represented in Figs. 4, 5 and 6 respectively.

Organic content raises the liquid limit and plastic limit. Since the organic particles are colloidal in nature, their water adsorption capacity will be very high.

Therefore the addition of organic matter increases the demand for water. (Malkawi et al. 1999). Soil behaves as plastic or liquid at higher water contents.

Fly ash particles are coarse grained with lower surface area. Therefore fly ash treatment reduces the liquid limit. Lime content in the fly ash increases the plastic

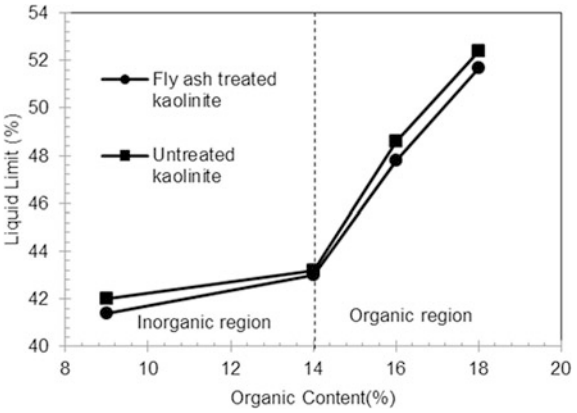

Fig. 4 Variation in liquid limit with organic content

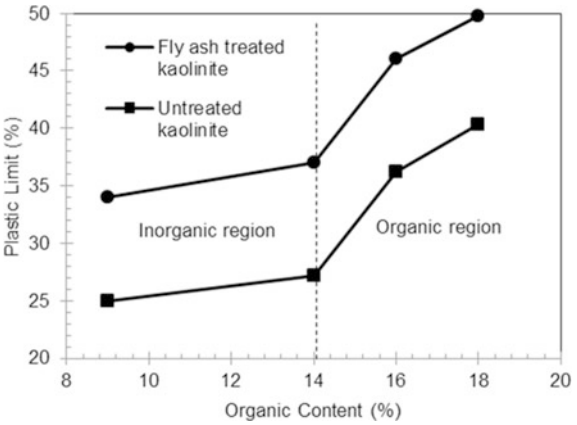

Fig. 5 Variation in plastic limit with organic content

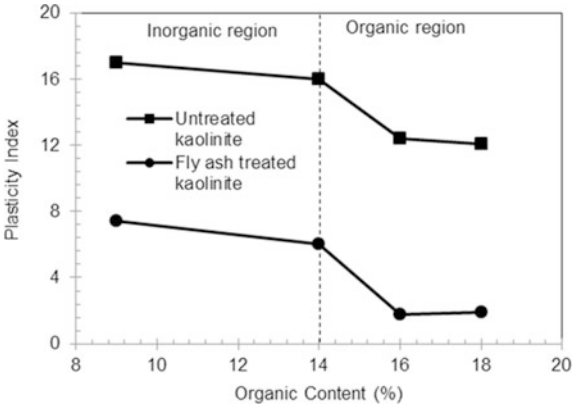

Fig. 6 Variation in plasticity index with organic content

limit. Variations in liquid limit and plastic limit are reflected in plasticity index also. Plasticity and cohesion of organic matter are very low compared to soil.

3.2 *Effect of Organic Content on Compaction Characteristics*

Variations in optimum moisture content and maximum dry density are plotted in Figs. 7 and 8 respectively.

The water adsorption capacity of organic matter is high. Therefore it demands more water, thus raising the optimum moisture content. Presence of broken hollow spheres in fly ash also increases the optimum moisture content.

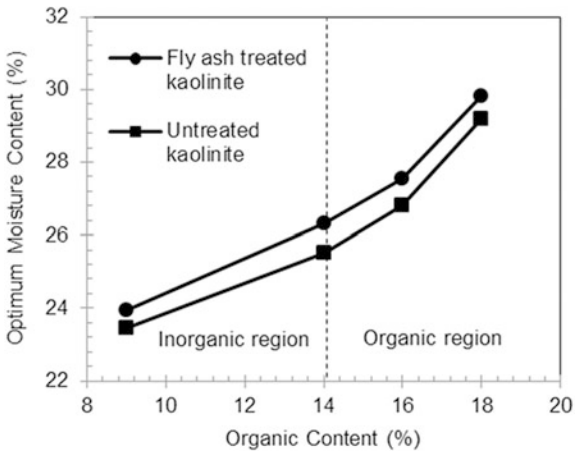

Fig. 7 Variation in optimum moisture content with organic content

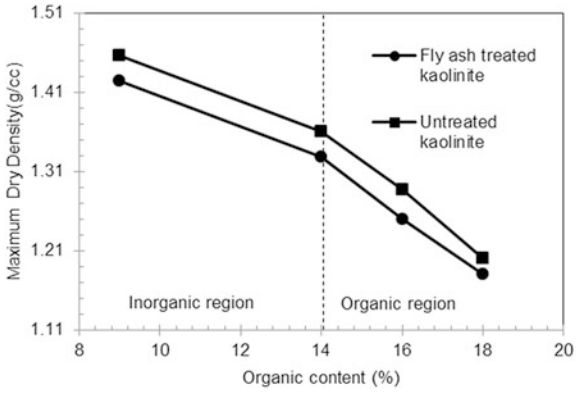

Fig. 8 Variation in maximum dry density with organic content

The decrease in dry unit weight on fly ash addition may be due to lower specific gravity, poor gradation and immediate formation of cemented products on fly ash treatment.

3.3 *Effect of Organic Content on Shear Strength Characteristics*

Variation in unconfined compressive strength is shown in Fig. 9. Treatment with 8% of fly ash increased the shear strength of kaolinite by 87.5%. This 8% was obtained as the optimum fly ash above which shear strength goes on decreasing.

Kaolinite of different organic contents was treated with this optimum percentage (8%) of fly ash. But the rate of increase was reduced with increase in organic contents. Even the shear strength of fly ash treated sample was lower than that of untreated kaolinite at higher organic content. A notable variation in all the properties was obtained in the organic region whereas in the inorganic region the variation is gradual.

4 Variation of Optimum Fly Ash with Organic Content

Different percentages of fly ash were added to kaolinite samples (varying organic content). Table 5 shows the unconfined compressive strength of kaolinite samples treated with respective optimum percentage of fly ash.

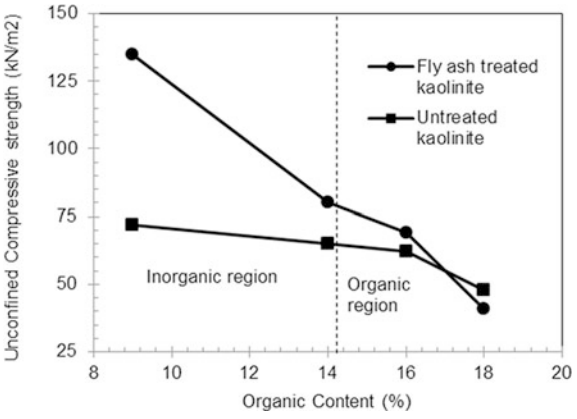

Fig. 9 Variation in unconfined compressive strength with organic content

Table 5 UCC strength at optimum fly ash

Organic content (%)	Optimum fly ash (%)	UCC strength at optimum fly ash (kN/m^2)
9	8	135
14	6	120
16	4	101
18	4	92

5 Conclusions

From the laboratory test results, the following conclusions were made:

- Optimum percentage of fly ash for stabilization of kaolinite decreases with increase in organic content. Also the maximum shear strength of fly ash stabilized kaolinite is decreasing with increase in organic content.
- Index properties, compaction behavior and shear strength of kaolinite are affected by the presence of organic content. Below 14% of organic content (inorganic region) the variation is gradual whereas a prominent variation is obtained for higher organic contents (organic region).
- Index properties, compaction behavior and shear strength of fly ash treated kaolinite also varies with organic content.
- Organic content is an important parameter to be considered during fly ash stabilization. There is possibility for shear strength of fly ash treated samples to be lower than that of untreated samples if, the presence of organic content is not taken care of.

References

ASTM C618. (2015). Standard for coal fly ash and raw or calcined natural pozzolan for use in concrete. United States: ASTM International.

Kolay, P. K., Aminur, M. R., Taib, S. N. L., & Zain, M. I. S. M. (2010). Correlation between different physical engineering properties of tropical peat soils from Sarawak. In *GeoShanghai International Conference on Soil Behavior and Geo-Micromehanics*, 3 June–5 June 2010, Shanghai, China.

Malkawi, A. I. H., Alawneh, A. S., & Abu-Safaqah, O. T. (1999). Effects of organic matter on physical, and physiochemical properties of illitic soil. *Journal of Applied Clay Science, 14,* 257–278.

Saride, S., Chikyala, S. R., Puppala, A. J., & Harris, P. J. (2010). Effects of organics on stabilized expansive subgrade soils. In *GeoShanghai International Conference on Ground Improvement and Geosynthetics*, 3 June–5 June 2010, Shanghai, China.

Tastan, E. O., Edil, T. B., Benson, C. H., & Aydilek, A. H. (2011). Stabilization of organic soils with fly ash. *Journal of Geotechnical and Geoenvironmental Engineering, ASCE, 137*(9), 819–833.

Thiyyakkandi, S., & Annex, S. (2011). Effect of organic content on geotechnical properties of Kuttanad clay. *Electronic Journal of Geotechnical Engineering EJGE, 16,* 1653–1663.

Strength Behaviours of the Clayey-Silt Soil Mixed with Fly Ash and Sand

RaiBahadur Reang and Sujit Kumar Pal

Abstract Fly ash and sand, both the materials have been added in the percentages of 10, 20, 30, 40, 50 and 60% with the clayey-silt soil by dry weight. Modified Proctor compaction was chosen for the California bearing ratio (CBR) tests and applied to soil-fly ash and soil–sand mixes. Un-soaked and soaked CBR of the soil are found as 54.50 and 3.90% respectively under modified Proctor compaction. Both fly ash and sand improved the CBR of the clayey-silt soil but addition of sand show the better result under both un-soaked and soaked conditions. However, the addition of 40% sand to the soil shows the maximum un-soaked CBR value as 70.07%. An addition of fly ash decreases the unconfined compressive strength (UCS) of the clayey-silt soil and increases in UCS observed at 40 and 20% addition of sand to the soil at standard and modified Proctor compaction respectively. The addition of both fly ash and sand to the soil increase the shear strength of the clayey-silt soil at standard Proctor compaction. Depending on availability of the material either fly ash or sand, it can be said that strength of the weaker clayey-silt soil can be improved using any of the additives.

Keywords Fly ash · Sand · Clayey-silt soil · California bearing ratio
Proctor compaction

1 Introduction

Generally clayey-silt soils are soft and weak. So, while any geotechnical engineering construction encounters such a soil it put the site civil engineers into trouble making them unable to bring out the accurate strength of the soil. Amongst the

R. Reang (✉) · S. K. Pal
Department of Civil Engineering, National Institute of Technology,
Agartala 799046, India
e-mail: raireang@gmail.com

S. K. Pal
e-mail: skpal1963@gmail.com

T. Thyagaraj (ed.), *Ground Improvement Techniques and Geosynthetics*, Lecture Notes in Civil Engineering 14, https://doi.org/10.1007/978-981-13-0559-7_12

solutions, addition of some additives is one kind of approach. In the present paper fly ash and sand were used as additives to the clayey-silt soil to study the change in strength in the soil.

Few works had been carried out in the past to study the strength of the soft soils as well as in terms of CBR with the inclusion of fly ash and sand. The addition of fly ash to the fine-grained soil showed significant improvements in the CBR values (Prabhakar et al. 2004); so, fly ash beneficial for a pavement construction. Addition of fly ash increased the unconfined compressive strength of the highly compressible fine-grained soil (Phani Kumar and Sharma 2004). Fly ashes can be used with different types of soft soil subgrade since it increased the unconfined compressive strength and CBR values of the soils (Senol et al. 2005). In both soaked and un-soaked condition, an addition of sand showed increase in CBR values (Bera 2011). Minimal addition of fly ash to expansive soil (i.e. sodium bentonite) increased both unconfined compressive strength and CBR values of the soil (Bose 2012). The addition of certain amount of fly ash and bottom ash increased the shear strength and unconfined compressive strength of the kaolin (Marto et al. 2013). Soaked and un-soaked CBR values of the clay increased when it was mixed with both fly ash and sand (Prasad and Sharma 2013). Sandy clay of high plasticity showed the highest CBR values when mixed with 6% lime and 3% palm oil fly ash (Khalid et al. 2014). With optimal amount of class F fly ash both soaked and un-soaked CBR values of the clay increased (Sreekumar and Unnikrishnan 2014). Clayey subgrade stabilized using fly ash (Athanasopoulou 2014).

2 Experimental Programme

2.1 Materials and Samples Preparation for Testing

In this study three materials are considered. Sands are collected from a local river, namely Ghoramara, passing near NIT Agartala, Tripura, India. The clayey-silt soil is collected from Gulaghati, Tripura, India. Fly ash is collected from Kolaghat thermal power station, Kolaghat, West Bengal, India. For testing of the mixes the oven dried fly ash and sand are mixed with the oven dried soil in different percentages (i.e. 10, 20, 30, 40, 50 and 60%). The tests conducted as per ASTM standards are shown in Tables 1, 2 and 3.

Table 1 Physical and engineering properties of the sand

Properties	Experimental results
Specific gravity	2.67
Relative density (R_D), %	5.06
Degree of compactness Fraction smaller than 75-μm IS Sieve, %	Very loose sand 0.515
Uniformity coefficient, C_u	2.00
Coefficient of curvature, C_c	1.07
Classification	SP-SW
Plasticity Cohesion (c) (kPa) Angle of internal friction (ϕ) (in°)	Non-plastic 0.306 29.90

Table 2 Physical and engineering properties of the clayey-silt soil

Properties	Experimental results
Specific gravity	2.57
Sand (4.75–0.075 mm), %	1.40
Silt (0.075–0.002 mm), %	61.00
Clay (<0.002 mm), %	37.60
Classification of soil	Clayey-silt soil with
(ASTM Standard)	medium plasticity
Name of soil group	CI (Inorganic Clay)
Natural water content, %	36.60
Liquid limit, %	45.20
Plastic limit, %	28.71
Shrinkage limit, %	23.21
Plasticity	Medium plastic
Light compaction:	
MDD, (kN/m^3)	15.76
OMC, (%)	21.60
Cohesion (c), (kPa)	45.00
Angle of internal friction (ϕ), (in°)	0.105
Heavy compaction:	
MDD, (kN/m^3)	18.05
OMC, (%)	13.50

Table 3 Physical and engineering properties of the fly ash

Properties	Experimental results
Specific gravity	2.09
Sand size, %	14.40
Silt size, %	77.3
Clay size, %	8.3
Plasticity index (PI), %	Non-plastic
Coefficient of uniformity, C_u	3.895
Coefficient of curvature, C_c	0.925
Name of the group	Sandy-silt
Name of the group symbol	SM
Light compaction:	
MDD, (kN/m^3)	12.46
OMC, (%)	25.80
Cohesion (c) (kPa)	0.201
Angle of internal friction (ϕ) (in°)	31.93
Heavy compaction:	
MDD, (kN/m^3)	16.58
OMC, (%)	18.50

3 Results and Discussions

3.1 Effect on Unconfined Compressive Strength

The unconfined compressive strengths (UCS) of the clayey-silt soil are found as 300 and 430 kPa at standard and modified Proctor compaction respectively. The addition of fly ash decreased the UCS values as the amount of fly ash has been increased in the mix at both standard and modified compaction effort. The reason may be the flocculation in the particles. The flocculated particles become repulsive to each other and hence the UCS value decreases in both standard and modified Proctor compaction. The similar trend was examined by Bose (2012). But Senol et al. (2005) observed that Class C fly ash increased the UCS values at standard Proctor test of soft clayey soils. It is so because Class C fly ash has self-cementing properties, and so it does not require any activator. But in this study the additive was Class F fly ash which requires a cementing agent to produce cementitious compounds. As a result, it decreased the UCS of the soil of the present study when used with Class F fly ash. The typical stress–strain curves of the soil-fly ash mixes are shown in the Figs. 1 and 2 at standard and modified Proctor compaction respectively. Table 4 shows the various results of UCS values of the clayey-silt soil and its mixes. When sand is added to the clayey-silt soil the voids present in the soil filled gradually by the finer particles of the sand as the sand percentage increased, after which the finer particles of the sand become as an excess and therefore not

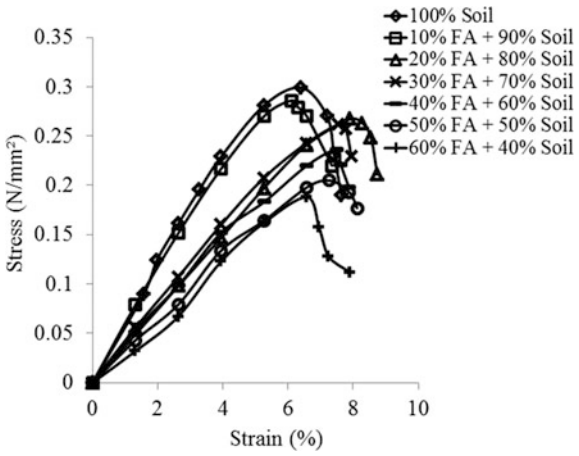

Fig. 1 Typical stress–strain curves for UCS of the clayey-silt soil and soil-fly ash mixes at standard Proctor compaction

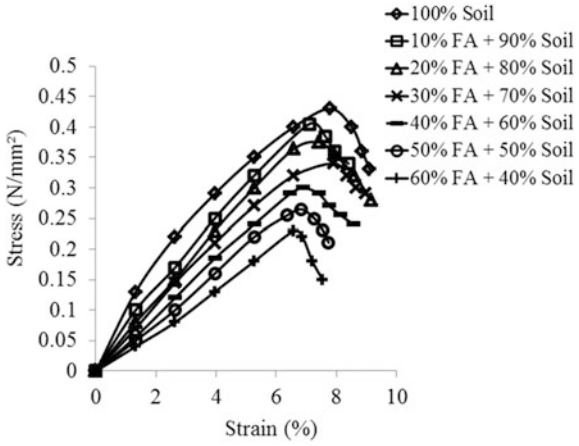

Fig. 2 Typical stress–strain curves for UCS of the clayey-silt soil and soil-fly ash mixes at modified Proctor compaction

participate in filling the voids, due to which unconfined compressive strength value of the soil decreased after 40 and 20% addition of sand at standard Proctor and modified Proctor compaction respectively.

3.2 Effect on Shear Strength

The shear strength of the clayey-silt soil, fly ash and sand are found as 45.27, 91.90 and 85.32 kPa respectively at standard Proctor compaction. The addition of both fly ash and sand increases the angle of internal friction and decreases the cohesion value of the clayey-silt soil. However, the shear strength of the soil increases as the percentages of the fly ash or sand increases at standard Proctor

Table 4 Laboratory test results on strength of the clayey-silt soil and its mixes

Materials	UCS (kPa) (at SPT)	UCS (kPa) (at MPT)	Shear strength (kPa) (at SPT)	Un-soaked CBR values (%) (at MPT)	Soaked CBR values (%)
100S	300	410	45.27	54.50	3.90
100FA	–	–	91.90	66.18	15.08
100SA	–	–	85.32	–	–
90S + 10FA	285	405	48.93	55.47	4.86
80S + 20FA	265	375	54.67	56.44	6.08
70S + 30FA	250	340	60.25	57.42	7.30
60S + 40FA	230	300	65.43	58.88	8.27
50S + 50FA	205	265	73.41	61.31	9.24
40S + 60FA	190	230	79.14	62.77	10.21
90S + 10SA	320	416	48.63	57.54	6.32
80S + 20SA	350	425	51.84	63.26	8.76
70S + 30SA	375	390	53.99	66.66	10.70
60S + 40SA	400	315	57.10	70.07	12.65
50S + 50SA	270	260	61.19	60.34	15.08
40S + 60SA	180	200	65.44	50.26	18.16

Note UCS Unconfined compressive strength, S Soil, SA Sand, FA Fly ash, SPT Standard Proctor test, MPT Modified Proctor test

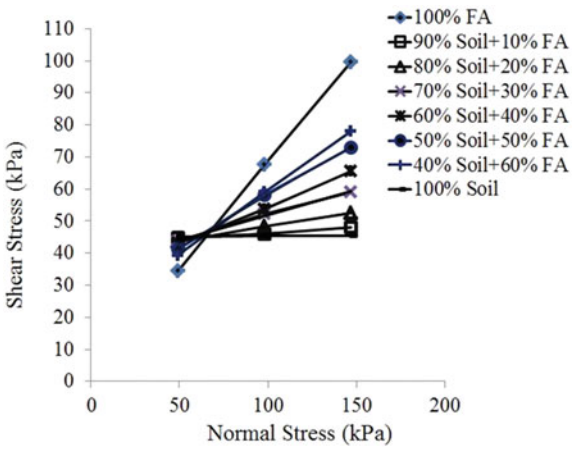

Fig. 3 Typical shear stress-normal stress curve of clayey-silt soil, fly ash and soil-fly ash mixes at standard Proctor compaction

compaction; because both of them increase the angle of internal friction between the particles of the mixes. It can be said that the material having higher frictional resistance will show the greater shear strength value. The typical shear stress versus normal stress curve for soil-fly ash mixes is shown in the Fig. 3 at standard Proctor compaction. The results of shear strength of the clayey-silt soil and of the mixes

have been represented in the Table 4. From the table, it is observed that fly ash increased the shear strength of the soil more than sand. This may be due to the angle of internal friction of the fly ash which is greater in value compared to that of the sand. From this it can be said that the material which has the greater angle of internal friction shows the higher shear strength.

3.3 *Effect on Un-Soaked CBR Value*

The un-soaked CBR values of the clayey-silt soil and fly ash under modified Proctor compaction are 54.50 and 66.18% respectively. Fly ash increases the un-soaked CBR of the soil but at slow rate. The flocculation in the particles of soil-fly ash mix broken due to increment of the energy; hence density increases and un-soaked CBR also increases. Also the cation exchange between the particles becomes lower due to which the rate of increment in CBR value become slow. The similar trend was observed by Prasad and Sharma (2013) and Athanasopoulou (2014). The sand increased the CBR value of the soil up to 40% addition and after that the same values decrease. Sand particles filled the voids in the soil mass and become well graded as a result the CBR values increases which are greater compared to soil-fly ash mixes. The typical load versus penetration curves for soil-fly ash mixes has been shown in the Fig. 4. The various results obtained from the laboratory tests on the soil and its mixes are shown in the Table 4. The similar trend was observed by Prasad and Sharma (2013) for CI type of soil-sand as well as soil-fly ash mixes at standard Proctor test and Athanasopoulou (2014) for CH type soil-fly ash mixtures and also by Bera (2011) for CL type soil-sand mixes.

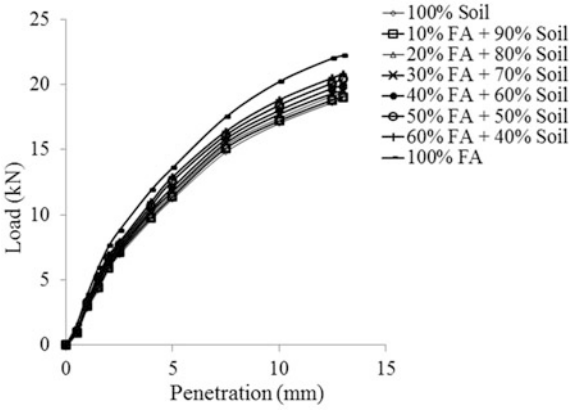

Fig. 4 Typical load-penetration curves for un-soaked CBR of clayey-silt soil and soil-fly ash mixes at modified Proctor compaction

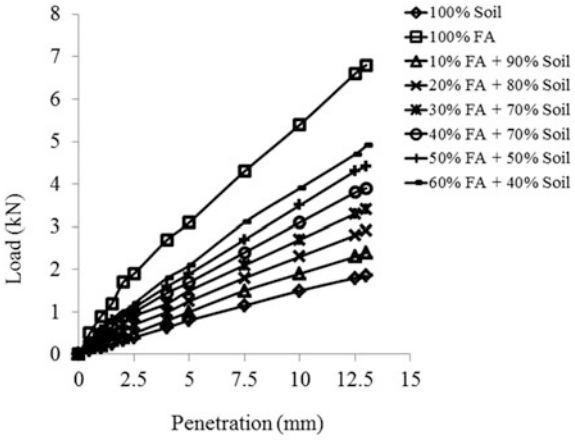

Fig. 5 Typical load-penetration curves for soaked CBR of clayey-silt soil and soil-fly ash mixes at modified Proctor compaction

3.4 Effect on Soaked CBR Value

Soaked CBR values of the soil and fly ash are 3.90 and 15.08% respectively at modified Proctor compaction. Both fly ash and sand increase the soaked (4 days) CBR values of the clayey-silt soil. The fly ash as well as sand particles filled the gaps of the soil mass, and as such the CBR values of the soil-fly ash mixes and soil-sand mixes increase.

The CBR values of the soil-sand mixes are found greater than that of the soil-fly ash mixes because there are no formations of flocculation or cation exchange takes place in case of soil-sand mixes. The typical load versus penetration curve for soil-fly ash mixes is shown in Fig. 5. The various results on soaked CBR tests are shown in the Table 4. The similar trend was observed by Prasad and Sharma (2013) for CI type of soil-sand as well as soil-fly ash mixes at standard Proctor test and also by Bera (2011) for CL type soil-sand mixes.

4 Conclusions

Based on the results and discussions made above, following conclusions may be drawn:

- Sand can be used as an additive to the clayey-silt soil up to 40 and 20% by weight at light and heavy Proctor compaction respectively to obtain the maximum unconfined compressive strength. However, fly ash decreased the unconfined compressive strength; fly ash is not that much of suitable additive during an embankment construction with this type weaker soil.

- Since both fly ash and sand increased the shear strength of the clayey-silt soil, both materials are suitable for increasing the bearing capacity of the soil for a shallow foundation.
- Both fly ash and sand increased the un-soaked and soaked CBR value of the clayey-silt soil at modified Proctor compaction. However, addition of sand should be limited to 40% to get the maximum un-soaked CBR.
- The material shows the higher shear strength which has the greater angle of internal friction even though the two chosen materials are of same kind.

References

Athanasopoulou, A. (2014). Addition of lime and fly ash to improve highway subgrade soils. *Journal of Materials in Civil Engineering*, pp. 773–775, ASCE.

Bera, A. K. (2011). Effect of sand content on engineering properties of fine-grained soil mixed with sand. *Electronic Journal of Geotechnical Engineering, 16*, pp. 1275–1286.

Bose, B. (2012). Geo-engineering properties of expansive soil stabilized with fly ash. *Electronic Journal of Geotechnical Engineering, 17*, pp. 1339–1353.

Khalid, N., Mukri, M., Arshad, M. F., & Kamarudin, F. (2014). The California bearing ratio value for banting soft soil subgrade stabilized using lime-pofa mixtures. *Electronic Journal of Geotechnical Engineering, 19*, pp. 155–163, Malaysia.

Marto, A., Hassan, M. A., Makhtar, A. M., & Othman, B. A. (2013). Shear strength improvement of soft clay mixed with tanjung bin coal ash. *APCBEE Procedia, 5,* 116–122.

Phani Kumar, B. R., & Sharma, R. S. (2004). Effect of fly ash on engineering properties of expansive soil. *Journal of Geotechnical and Geoenvironmental Engineering, ASCE, 130*(7), 764–767.

Prabhakar, J., Dendorkar, N., & Morchhale, R. K. (2004). Influence of fly ash on strength behaviour of typical soils., Vol. 18, pp. 263–267. Elsevier. ISSN 0950-0618.

Prasad, C. R. V., & Sharma, R. K. (2013). Influence of sand and fly ash on clayey soil stabilization. *International Conference on Advances in Engineering & Technology*, pp. 36–40.

Senol, A., Edil, T. B., Bin-Shafique, Md. S., Acosta, H. A., & Benson, C. H. (2005). Soft subgrades stabilization by using various fly ashes. *Resources, Conservation and Recycling*, Vol. 46, pp. 365–376. Elsevier. ISSN 0921-3449.

Sreekumar, N. R., & Unnikrishnan, R. (2014). Effect of class F fly ash and sludge ash on the geotechnical properties of clayey soil. In *Indian Geotechnical Conference*, Dec 2014, Kakinada, India.

Strength Behaviour of Expansive Soil Treated with Quarry Dust and Ferric Chloride

H. Venkateswarlu, D. S. V. Prasad and G. V. R. Prasada Raju

Abstract The main objective of this investigation is to present the variations in index and engineering properties of expansive soil such as liquid limit, plastic limit, compaction characteristics, CBR and shear strength parameters when it is mixed with different percentages of Quarry dust (0, 5 and 10%) and Ferric chloride by dry weight of soil. Quarry dust has been chosen, as it is problematic to the environment and public due to its improper disposal. Quarry dust exhibits high shear strength, good permeability which is highly beneficial for its use as a geotechnical material. Ferric Chloride can be used because of its capability to easily exchange cations and ready dissolvability in water. Initially, expansive soil is mixed with different percentages of Quarry dust and Optimum percentage of Quarry dust were determined on the basis of Compaction and CBR tests. From the test results, it is observed that up to the addition of 5% of Quarry dust there is an increase in strength parameters such as Maximum Dry Density and California Bearing Ratio beyond that it is not effective. This investigation is further carried out by mixing Ferric chloride varying from 0 to 2% with an increment of 0.5% to the Quarry dust treated expansive soil (at its optimum 5%) and same series of experiments were conducted. From the results, it is observed that at optimum percentages, i.e. 5% Quarry dust and 1% ferric chloride, there is a marked improvement in the strength characteristics of soil.

Keywords Expansive soil · Quarry dust · Ferric chloride · Stabilization and CBR

H. Venkateswarlu
Department of Civil Engineering, BVC Engineering College, Odalarevu, AP, India
e-mail: venki.hasthi@gmail.com

D. S. V. Prasad (✉)
BVC Engineering College, Odalarevu, AP, India
e-mail: drdsvp9@gmail.com

G. V. R. Prasada Raju
JNT University Kakinada, Kakinada 533003, India
e-mail: gvrp_raju@yahoo.com

T. Thyagaraj (ed.), *Ground Improvement Techniques and Geosynthetics*, Lecture Notes in Civil Engineering 14, https://doi.org/10.1007/978-981-13-0559-7_13

1 Introduction

Social and economic development of the country depends upon transportation facilities and the construction projects. Construction of projects everywhere in India is not possible, because it has diverse geological conditions. And also some soils exhibit peculiar behaviour with their chemical composition or the presence of minerals. We cannot avoid such places, we need to improve by adopting suitable technique and make them suitable for the proposed construction. Expansive soil is the one which shows drastic volumetric changes with the variation in moisture content. The present study describes the improvement of expansive soil by blending with different percentages of quarry dust (i.e. 5, 10 and 15%) and ferric chloride (i.e. 0.5, 1.0, 1.5 and 2.0%) by dry weight of soil.

2 Literature Review

In the recent past some of the researchers have did excellent research on utilization of quarry dust and ferric chloride for the Expansive soil stabilization. Number of studies has been conducted by various researchers on the use of industrial waste materials to improve the performance of weak soils. Naman Agarwal (2015) has carried out different tests such as compaction, specific gravity and CBR in the laboratory on expansive clays with different proportions of stone dust by dry weight of soil as 10, 20, 30, 40 and 50%. From the test results addition of stone dust to BC soil decreases its OMC, increases its MDD, increased CBR of soil by nearly 50% and Adding 30% stone dust is found to be optimum in case of specific gravity. Jagmohan Mishra et al. (2014) has studied the effect of granite dust on the index properties of Black Cotton Soil stabilized with 5% lime and 0, 10, 20 and 30% of granite dust and conducted laboratory tests liquid limit, plastic limit and differential free swell. The test results showed significance decrease in the expansive behaviour of the black cotton Soil. With the increase in the granite dust percentage the liquid limit decrease from 57 to 28%, plasticity index decrease from 37.2 to 3.7%, shrinkage limit values increases from 8.15 to 18% and differential free swell decreased drastically from 56.6 to 4.1%. From the test results it can be concluded that the addition of granite dust to lime stabilized BC soil decreases its swelling behaviour to a great extent. Prasada Raju (2001), has conducted field studies on expansive soil subgrades treated with KCl, $CaCl_2$ and $FeCl_3$. It was observed that $FeCl_3$ treated test track showed the best performance. Bharambe and Patil (2013) observed that CBR value increased by 155% for the combination of flyash and ferric chloride stabilized black cotton soil. In view of the limitations of lime stabilization and recent trends to utilize electrolytes, it was found that $FeCl_3$ was quite effective in minimizing swelling of expansive soils.

3 Materials Used

3.1 Expansive Soil

Expansive soil collected from Amalapuram, East Godavari Dt., Andhra Pradesh was used for this investigation. The disturbed soil samples collected from above locations were air dried and pulverized thoroughly prior to laboratory testing. A Series of tests were conducted in the Laboratory as per Indian Standard Specifications and the results are given in Table 1.

3.2 Quarry Dust

Quarry Dust for this study was collected from Rajahmundry, East Godavari District of Andhra Pradesh, India. The engineering properties of the quarry dust were determined as per IS code specifications and the results were given in Table 2.

Table 1 Properties of expansive soil

Laboratory test	Result
Atterberg's limits	
Liquid limit (W_L)	86%
Plastic limit (W_P)	41.21%
Plasticity index (I_p)	44.79%
Specific gravity (G)	2.56
Compaction parameters	
OMC	22%
MDD	16.6 kN/m^3
Un soaked CBR	2.02
Shear strength parameters	
Cohesion (c)	78.95 kN/m^2
Angle of internal friction ($\acute{\emptyset}$)	11.475^0
Differential free swell (%)	120

Table 2 Properties of Quarry dust

Laboratory test	Result
Specific gravity	2.56
Grain size analysis	
Coefficient of uniformity	18.57
Coefficient of curvature	3.95
Compaction parameters	
OMC	12.16%
MDD	15.58 kN/m^3
Un soaked CBR	7.00

3.3 Ferric Chloride

Laboratory grade Ferric Chloride consisting of 96% $FeCl_3$ was collected from Amalapuram, Andhra Pradesh was used in this work. The Quantity of Ferric Chloride is varied from 0 to 2% by dry weight of the Expansive Soil.

4 Laboratory Investigation

Various tests were carried out in the laboratory for finding the index and Engineering properties of Expansive soil and Expansive soil treated with Different percentages of Quarry dust and Ferric Chloride for finding optimum percentages. The details of these tests are given in the following sections.

4.1 Atterberg's Limits

Standard procedures recommended in the respective I.S. Codes of practice [IS: 2720 (Part-5)-1985; IS: 2720 (Part-6)-1972], were followed while finding the Index properties viz. Liquid Limit and Plastic Limit and of the various samples tried in this investigation.

4.2 Compaction Properties

Optimum moisture content and maximum dry density of black cotton soil and stabilized black cotton soil with different percentages of quarry dust and ferric chloride mixes were determined according to I.S heavy compaction test IS: 2720 (Part VIII).

4.3 California Bearing Ratio Test

CBR test was carried out on prepared soil samples of untreated Expansive soil and treated Expansive soil with various percentages of quarry dust and Ferric chloride under unsoaked conditions as per recommendations of IS 2720 part XVI-1987.

4.4 Direct Shear Test

The direct shear test were conducted in the laboratory as per IS Code (IS: 2720 (Part-13)-1986). The required percentage of quarry dust by dry unit weight of soil was mixed uniformly with the soil. The soil was compacted to maximum dry density (MDD) of untreated soil. The specimens were tested in a 6 cm × 6 cm square box at different normal stresses (N/mm^2) for each percentage of quarry dust with expansive soil and sheared at a rate of 1.25 mm/min.

5 Results and Discussions

5.1 Effect of Quarry Dust on Index Properties

The Index properties liquid limit and Plastic limit goes decreasing from 86 to 45 & 58 to 41.5 with the addition of different % of quarry dust by dry weight of expansive soil and the variations of Index properties of expansive soil treated with different percentages of quarry dust are shown in Fig. 1.

5.2 Effect of Quarry Dust on Compaction

The Maximum Dry Density increases from 16.6 to 18.1 kN/m^3 up to the addition of 5% quarry dust, after the value decreased with the further addition of quarry dust and OMC decreased from 22 to 18.2% with the addition of different percentages of quarry dust varying from 0 to 20% with an increment of 5% as shown in Fig. 2.

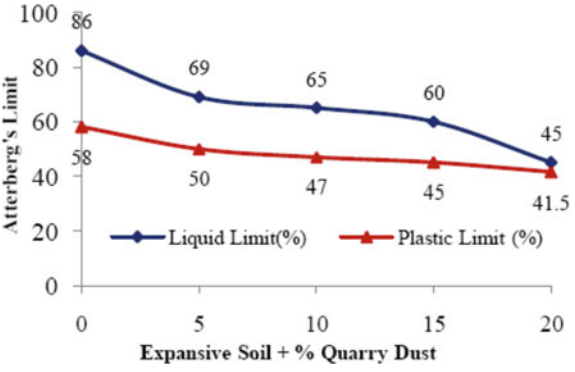

Fig. 1 Atterberg's limits of expansive soil treated with different % of Quarry dust

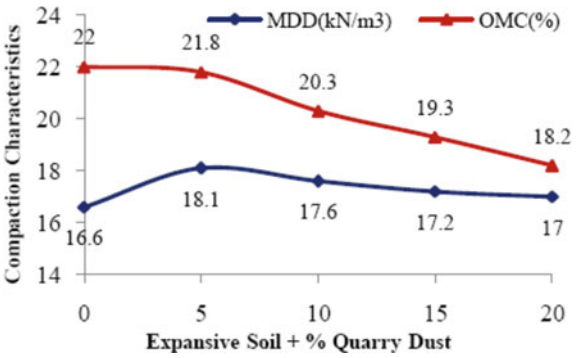

Fig. 2 Compaction characteristics of expansive soil treated with different % of Quarry dust

5.3 *Effect of Quarry Dust on CBR*

The CBR of Expansive soil increased from 2.02 to 7.04 up to the addition of 5% quarry dust, and further addition of quarry dust decreased the CBR to 6.35 and 5.3 with 10 and 15% quarry dust to the expansive soil as shown in Fig. 3

From the CBR test results, it is decided that 5% quarry dust is optimum for enhancing the strength characteristics of Expansive soil.

5.4 *Effect of Quarry Dust on Shear Strength*

The shear strength parameters of expansive soil, cohesion decreased from 29.9 to 8.47 kN/m^2 and Angle of internal friction increased from 11.475° to 54.15° with the addition of different percentages of quarry dust varying from 0 to 15% with an increment of 5% as shown in Fig. 4.

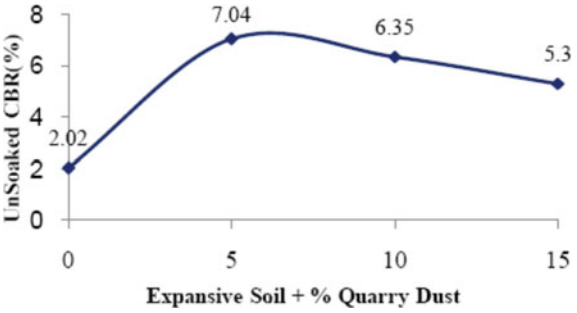

Fig. 3 Unsoaked CBR value of expansive soil treated with different % of Quarry dust

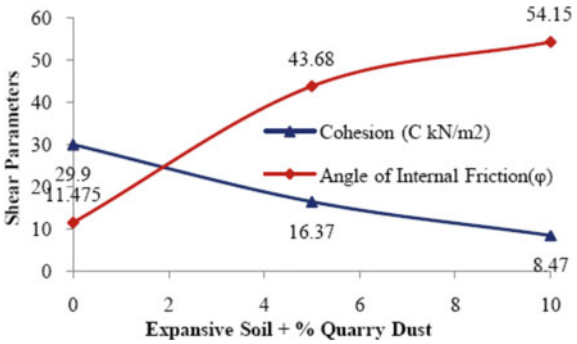

Fig. 4 Shear strength parameters of expansive soil treated with different % of Quarry dust

5.5 *Effect of $FeCl_3$ on Compaction Parameters of Expansive Soil with Optimum % of Quarry Dust*

Compaction Characteristics of quarry dust treated expansive soil at its optimum percentage, i.e. 5% such as OMC increasing from 21.8 to 29.8% and MDD decreasing from 18.1 to 15.65 kN/m^3 respectively with the addition of different percentages of ferric chloride varying from 0 to 2.0% with an increment of 0.5% as shown in Fig. 5.

5.6 *Effect of $FeCl_3$ on CBR Values of Expansive Soil with Optimum % of Quarry Dust*

For the optimum mix of expansive soil treated with quarry dust, different percentages of $FeCl_3$ varying from 0 to 2% with an increment of 0.5% by the dry weight of soil, the CBR value increased from 7.04 to 8.41 up to the addition of 1% ferric chloride, then it is declined to 6.87 with the addition of 1.5% ferric chloride to the quarry dust treated expansive soil shown in Fig. 6.

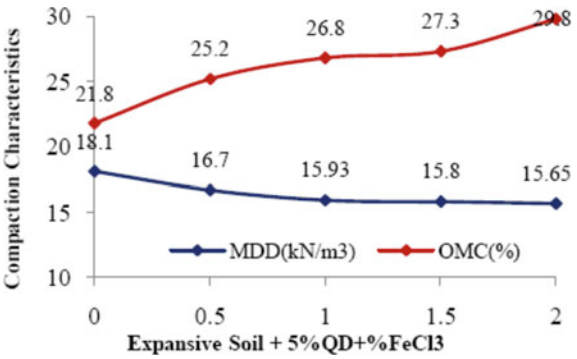

Fig. 5 Compaction parameters of expansive soil with 5% Quarry dust and different % of $FeCl_3$

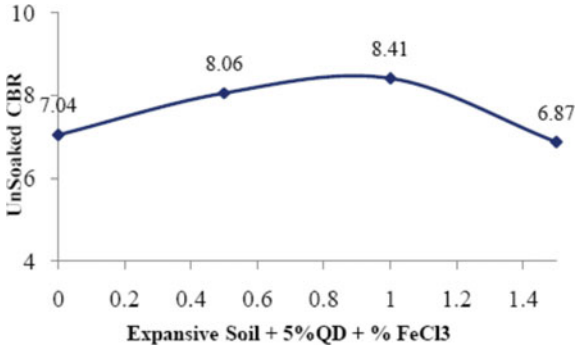

Fig. 6 Unsoaked CBR of expansive soil treated with 5% Quarry dust and different % of $FeCl_3$

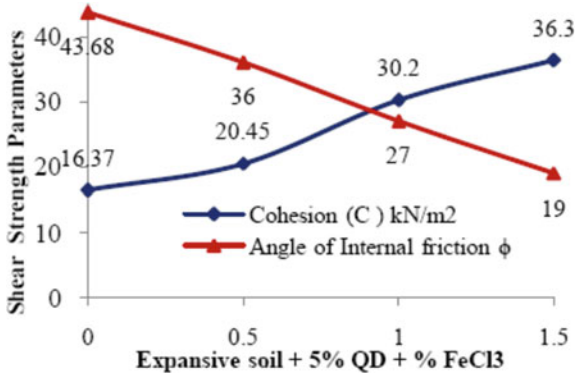

Fig. 7 Shear strength of expansive soil with 5% Quarry dust and different % of $FeCl_3$

5.7 *Effect of $FeCl_3$ on Shear Strength of Expansive Soil with Optimum % of Quarry Dust*

The Shear strength parameters of optimum mix of expansive soil and quarry dust, i.e. 5%, cohesion increasing from 16.37 to 36.3 kN/m^2 and Angle of internal friction decreasing from 43.68° to 19° with the addition of different % of ferric chloride varying from 0 to 1.5% with an increment of 0.5% as shown in the Fig. 7.

6 Conclusions

On the whole, this study has attempted to provide an insight into the compaction characteristics, shear parameters and CBR behaviour of expansive soil stabilized with varying proportions of Quarry dust and $FeCl_3$ chemical. Utilizing some portion of the industrial waste like Quarry dust will reduce environmental-related

problems. The study yielded the following conclusions based on the laboratory experimentation carried out in this investigation.

(1) The Liquid Limits values are decreasing due to the addition of Quarry dust (i.e. 0–20% by dry weight of soil) from 86 to 45% and Plastic Limits also shows gradual decreases from 58 to 41.5% respectively.
(2) Compaction characteristics of the expansive soil are improved to a greater extends, i.e. Max. Dry Density increases from 16.6 to 18.1 kN/m^3 up to the addition of 5% Quarry dust and decreases with further addition of Quarry dust by 5% increment up to 20% shows decreasing from 18.1 to 17.1 kN/m^3.
(3) Expansive treated with optimum 5% of Quarry dust is mixed with different % of $FeCl_3$ (i.e. 0, 0.5, 1, 1.5 & 2%), the MDD decreasing from 18.1 to 15.65 kN/m^3 and OMC increases from 12.9 to 29.8%
(4) The unsoaked CBR Value increased from 2.02 to 7.04% by the addition 5% quarry dust and further decrease.
(5) Treated expansive soil with optimum 5% of Quarry dust, with different % of $FeCl_3$, the optimum unsoaked CBR value of 8.41 is obtained at 1% $FeCl_3$.
(6) Addition of quarry dust to expansive soil from 0 to 10% by dry weight of soil, shear parameters like Cohesion decreases from 29.4 to 8.47 kN/m^2 and internal friction angle increases from 11.475° to 54.15° that indicates enhancement in bearing capacity.
(7) Expansive treated with 5% optimum of Quarry dust and with different percentages of $FeCl_3$ (i.e. 0, 0.5, 1 & 1.5%), cohesion increasing from 16.37 to 36.3 kN/m^2 and the angle of internal friction decreases from 43.68° to 19°.

References

Agarwal, N. (2015). Effect of stone dust on some geotechnical properties of soil. *IOSR Journal of Mechanical and Civil Engineering (IOSR-JMCE), 12*(1), 61–64. Ver. I (Jan–Feb 2015).

Prasada Raju, G. V. R. (2001). *Evaluation of flexible pavement performance with reinforcement and chemical stabilization of expansive soil subgrade* (Ph. D. thesis). Kakatiya University, Warangal, (AP).

Mishra, J., Yadav, R. K., & Singhai, A. K. (2014). Effect of granite dust on index properties of lime stabilized black cotton soil. *International Journal of Engineering Research and Science & Technology, 3*(1), 19–23, Feb 2014.

Bharambe, V. R., & Patil, G. K. (2013). A study on stabilization of black cotton soil using ferric chloride. *IOSR Journal of Mechanical and Civil Engineering, 10*(1), 26–30.

Lime Stabilization of Subgrade with Waste Sand as Partial Soil Replacement

Laya N. Nair and U. Salini

Abstract Stabilization of problematic soils using waste materials is a solution to waste disposal and can be cost-effective as well as sustainable. English Indian Clays Ltd, one of the largest clay producers, generates huge amount of waste sand during Kaolin processing and poses the problem of disposal of this waste. Hence a study is conducted on the feasibility of utilizing this waste material in improving the properties of soil in conjunction with lime. The study involved experimental investigations to characterize subgrade soil (highly compressible silty soil found in Changanaserry, Kerala) and waste sand. An effort was made to study the effect of waste sand, individually and combined, on compaction behavior, Atterberg limits, California Bearing Ratio and Unconfined Compressive Strength of soil, so as to assess its usefulness for modifying the soil. Waste sand of varying proportions was used to replace soil. It was found that the properties of subgrade improved considerably on replacing soil with waste sand. For the optimum soil–waste sand mixture, further improvement in its strength was attained by treating it with lime. The results showed a marked improvement in the strength of the mix on treating with lime and with increase in curing period.

Keywords Subgrade · Waste sand · Lime · Soil stabilization

L. N. Nair
Sarabhai Institute of Science and Technology, Thiruvananthapuram, India
e-mail: layanarayanan@gmail.com

U. Salini (✉)
Scientist B, National Transportation Planning and Research Centre, Thiruvananthapuram, India
e-mail: saliniu@gmail.com

T. Thyagaraj (ed.), *Ground Improvement Techniques and Geosynthetics*, Lecture Notes in Civil Engineering 14, https://doi.org/10.1007/978-981-13-0559-7_14

1 Introduction

There has been a great deal of concern about land pollution since the onset of industrialization. The attention is mainly because of incidents of contamination, the scarcity of usable land and increased general concern about the effect of industrial activities on the environment. Bulk utilization of industrial solid waste in various applications can be an alternative to land disposal. One such potential application is for infrastructure development works in civil engineering. For example, stabilization of problematic soils using waste can achieve great deal of economy and environmental safety. For many years, different types of admixtures have been used to improve the qualities of readily available local soils. This has opened the door for researchers to find alternate admixtures such as plastic, fibers, liquid enzymes, micro-bacteria, etc. In view of this a lot of researchers are working on utilization of industrial waste in different construction operations. There are many research works done with inert materials like sand, fly ash, etc. The present study deals with the use of waste from English Indian Clays Ltd. (EICL). EICL, a company incorporated in India, specializes in the extraction of Kaolin clay. Kaolin mining and processing industry generates two types of wastes, of which the major one is the waste sand produced during the separation of sand from ore. The mechanical stability of weak soil is improved due to the modification of its various fractions on stabilizing it with sand (Muktabhant and Ongskul 1969). The plasticity and swelling of a fine-grained soil reduces on stabilizing it with sand while for a coarse grained soil–sand stabilization leads to volume stability and improvement in its strength due to reduction in volume of voids. Louafi and Bahar (2012) found out that the addition of sand reduces the swelling of expansive clays due to the changes occurring the porosity of clay on addition of sand. Shemy et al. (2010) studied the effect of addition of waste sand in stabilizing clayey soil and thus finding a cost-effective way to improve the properties of soil. Lime is a calcium-containing inorganic material in which carbonates, oxides, and hydroxides predominate. Strictly speaking, lime is calcium oxide or calcium hydroxide. The aluminous and siliceous material in the clayey soils reacts with lime in presence of water to form cementitious gels, which increases the strength and durability of mixtures. These pozzolanic actions are slow and extend over a long period of time, several years in some instance. Hydrated lime is used extensively for the stabilization of soil, especially soil with a high clay content where its main advantage is in raising the plastic limit of the clayey soil. Many studies have been conducted to study the effectiveness of stabilizing soil with lime. Brooks et al. (2011) evaluated the potential of limestone dust and coal fly ash to stabilize some problem soil. Bhuvaneshwari et al. (2014), made an effort to study the microstructural changes that take place to an expansive soil, due to addition of lime. Jawad et al. (2014) and Mishra (2012) presented an overview of studies of lime treated soil, its advantages and disadvantages are discussed here.

The present study involves experimental laboratory work to characterize soil and waste sand from EICL, and to study the effect of waste sand on compaction behavior, California Bearing ratio, shear strength parameters and swelling

characteristics to assess its usefulness for modifying the soil structure. Further improvement of the soil–waste mix is also carried out by the addition of lime to the mixture. The tests are performed in accordance with Indian Standard Specifications.

2 Properties of Soil

Soil used in this study was collected from Changanassery, Kerala. The soil sample was air-dried, pulverized, and passed through 425 μm sieve before carrying out the tests. The index properties and engineering properties of soil used are tabulated in Table 1. The waste sand obtained from EICL contained 95% sand and 5% silt and clay. Commercially available lime from local sources was used for treating the soil–sand mix.

3 Partial Replacement of Soil by Waste Sand

The soil used for the study is highly compressible and has plasticity index greater than 10%, so in their natural state the soil is highly unsuitable to be used as subgrade under the pavement. Since waste sand was available in abundance and to find a suitable use for them, the soil was treated with different percentages sand and their behavior was studied. The soil was replaced with different percentages of waste sand, i.e., 10, 20, 30, 40, and 50% to understand the changes in behavior of soil by conducting Atterberg limits tests, Standard Proctor tests, and CBR tests.

3.1 Atterberg Limit Test

With increase in the percentage of sand the liquid limit, plastic limit and the plasticity index decreased as shown in Table 2. This is due to the increase in

Table 1 Properties of soil

Property	Value
Sand (%)	2
Clay (%)	11
Silt (%)	87
Liquid limit (%)	57
Plastic limit (%)	44
Plasticity index (%)	13
Soil classification	MH
Unconfined compressive strength (kN/m^2)	286
Specific gravity	2.52
Maximum dry density (kN/m^3)	12.3
Optimum moisture content (%)	36.60

Table 2 Variation of Atterberg limits with increase in percentage of sand in soil–sand mix

% Sand in soil	Liquid limit (%)	Plastic limit (%)	Plasticity index (%)
0	57	44	13
10	50	36	13
20	44	33	11
30	40	31	9
40	35	28	7
50	33	27	6

particle size and the mix becoming coarser due to presence of sand. It was difficult to obtain plastic limit since the threads crumbled before reaching 3 mm due to lack of cohesion. Beyond 50% replacement it was unable to obtain Atterberg limit values.

3.2 Standard Proctor Compaction Test

Standard Proctor compaction tests were conducted for different percentages of sand replacing the soil. It can be seen from Fig. 1 that, with increase in the percentage of waste sand Maximum Dry Density (MDD) increased from 12.3 to 15.6 kN/m^3 and optimum moisture content (OMC) decreased from 36.6 to 22.4% for 50% replacement of soil by sand. This increase in the MDD and decrease in OMC can be attributed to the improvement in gradation of the mix thus resulting in a better packing of the soil–sand mixture. Also, with increase in sand content the surface area gets reduced and hence only less amount of water is required for attaining MDD.

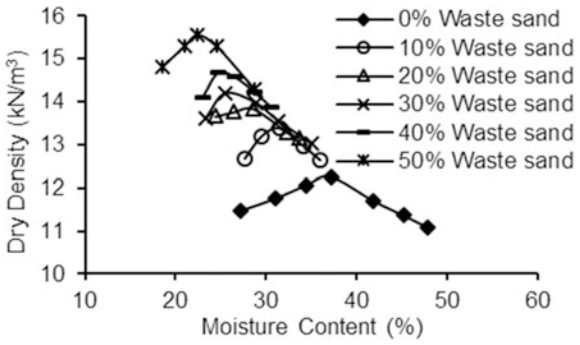

Fig. 1 Compaction curve for different percentages of waste sand in soil

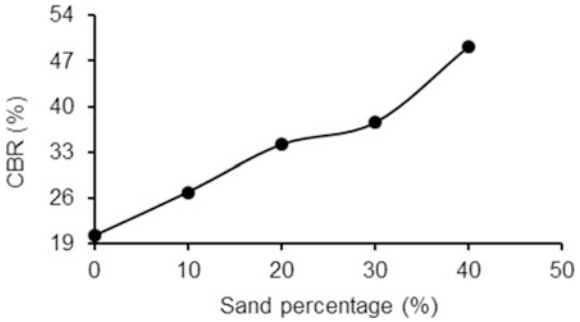

Fig. 2 Variation in CBR value with increasing sand content in the soil

3.3 California Bearing Ratio Test

Unsoaked CBR tests were conducted on different soil–sand mixtures and it was observed that the unsoaked CBR value increased with increasing percentage of waste sand in all cases. This may be because the soil became more uniformly graded making the mixture more mechanically stable. The value of unsoaked CBR increased from 20.17 to 49.3% for 50% replacement of soil by sand and the variation is plotted in Fig. 2.

From the compaction and CBR test results it can be concluded the optimum soil–sand mix for this soil is 50% sand and 50% soil.

4 Lime Stabilization of the Optimum Soil–Sand Mix

The use of easily and cheaply available waste sand helped in improving the soil so that it could be used as subgrade, but to improve its consistency limits and workability, lime treatment was also carried out. Eades and Grim pH test (ASTM-D 6276–99a, 1999) was carried out to obtain the Initial consumption of lime (ICL) of the soil–sand mix. The ICL is the percentage of lime corresponding to a pH of 12.45 and it can be observed from Fig. 3 that the pH of the lime soil mixture reached 12.45 at 4% lime. In the present study the effect of lime treatment below ICL is considered, i.e., at 1 and 2% lime.

4.1 Atterberg Limit

This optimum sand–soil mix was treated with lime so as to improve its properties further and the results are shown in Table 3. There was an increase in the liquid limit of the 50–50 soil–waste sand mix with increase of lime percentages from 0.5 to 2% in the mix. The addition of lime causes aggregation of the soil due to the

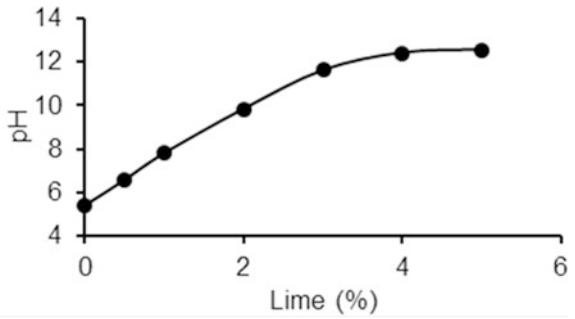

Fig. 3 Variation in pH value with lime content in soil

Table 3 Variation of Atterberg limits with increase in percentage of lime

% lime in mix	Liquid limit (%)	Plastic limit (%)	Plasticity index (%)
0	33	27	6
1	35	31	4
2	37	33	4

formation of cementitious compounds which in turn leads to higher imbibing of water and hence there is an increase in liquid limit with increase in lime content. The calcium ions in lime react with clay minerals and reduce the adsorbed layer thickness. This along with the formation of cementitious materials in the presence of water increases the plastic limit of the soil (Bhuvaneshwari et al. 2014).

4.2 Standard Proctor Compaction Test

Figure 4 shows the effect of lime treatment on the compaction behavior of the optimum soil–sand mix

The OMC increased and MDD decreased with increasing lime content. The increase in OMC is due to hydrophilic nature of lime and also due to flocculation of the mix on addition of lime. Hence additional moisture is required for hydration of calcium ions and its reaction with clay minerals. The decrease in the MDD with increase in lime percentage can be due to the fact that, because of cation exchange the flocculated and agglomerated soil particles occupy larger spaces, thus increasing the volume of voids and consequently reducing MDD.

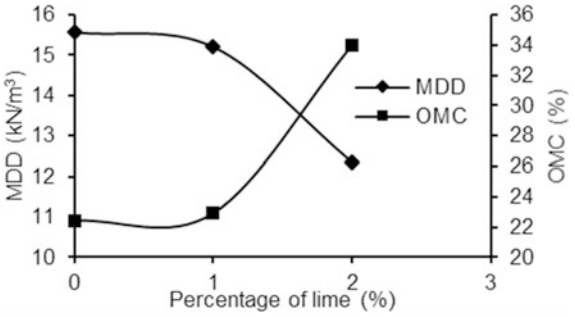

Fig. 4 Variation of MDD and OMC with lime in soil

4.3 Unconfined Compressive Strength (UCS)

It can be seen that in soil–sand mix at 50–50 proportion with 1% lime there is improvement in UCS of soil. There is a tremendous increase in the strength of soil–sand mix at 50–50 proportion with 1% lime after 7 days curing as can be seen in Fig. 5. The improvement in the UCS may be attributed to the binding property of lime. The compounds formed are at the gel stage initially, their solidification with respect to time imparts further strength to the soil–lime composites.

4.4 CBR Value

It can be observed from Fig. 6 that unsoaked CBR value of soil increased with addition of lime up to 1% and thereafter it decreased.

It was also seen that there was a remarkable improvement in the CBR value after 7 days due to formation of cementitious materials in soil–sand mix treated with lime.

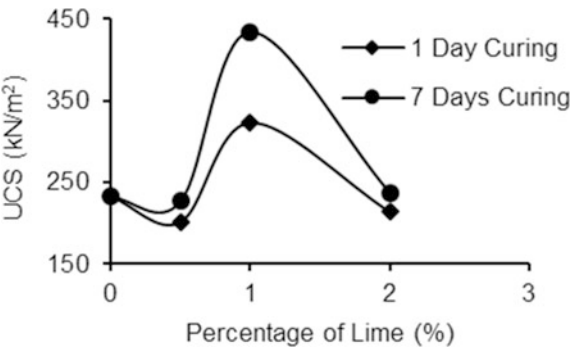

Fig. 5 Variation in UCS with lime in soil

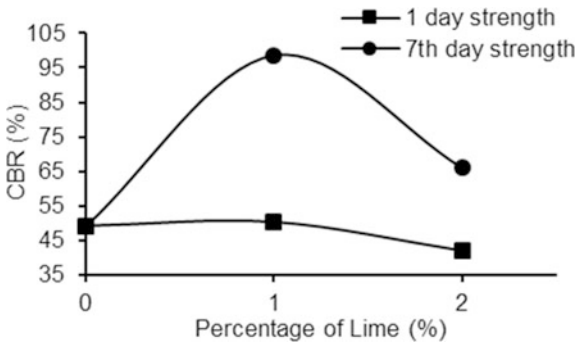

Fig. 6 Variation in CBR value with lime in soil

5 Conclusion

- The maximum dry density of soil–sand mix improved and OMC decreased with the replacement of soil by waste sand.
- The CBR value of soil–waste sand mix showed improvement.
- Hence the optimum soil–sand mix adopted for this soil is 50% sand and 50% soil taking into account the improvement in properties of the mix.
- Addition of 1% lime to soil–waste sand mix resulted in good MDD, gave highest UCS value and good CBR value.
- The UCS value and CBR value after 7 days curing showed remarkable improvement due to the pozzolanic action of lime.
- It can be concluded that the waste sand locally available in Kerala can be utilized in partially replacing the highly compressible soil found in that region.

References

ASTM, D 6276-99a. (1999). Standard test method for using pH to estimate the soil lime proportion requirement for soil stabilization. Annual Books of ASTM Standards, ASTM International, West Conshohocken.

Bhuvaneshwari, S., Robinson, R. G., & Gandhi, S. R. (2014). Behaviour of lime treated cured expansive soil composites. *Indian Geotechnical Journal, 44*(3), 278–293.

Brooks, R., Felix, F., & Takkalapelli, K. V. (2011). Geotechnical properties of problem soils stabilized with fly ash and limestone dust in Philadelphia. *Journal of Materials in Civil Engineering, 23*.

Jawad, I. T., Taha, M. R., Majeed, Z. H., & Khan, T. A. (2014). Soil stabilisation using lime: Advantages, disadvantages and proposing a potential alternative. *Research Journal of Applied Sciences, Engineering and Technology, 8*(4), 510–520.

Louafi, B., & Bahar, R. (2012). Sand: An additive for stabilization of swelling clay soils. *International Journal of Geosciences, 3*, 719–725.

Mishra, N. K. (2012). Strength characteristics of clayey subgrade soil stabilized with fly ash and lime for road works. *Indian Geotechnical Journal, 42*(3), 206–211.

Muktabhant, C., & Ongskul, S. (1969). Stabilization of lateritic soil with sand. In *Proceedings of the speciality session. Engineering properties of lateritic soils. VII ICSMFE*, Bangkok, pp. 153–64.

Shemy, S. B., Nair, S. M., Rohit, P. B., Soman, N., Kumar, M. M., & Hari, G. (2010). Improvement of clayey sub grade using waste sand form EICL. In *Proceedings of Indian Geotechnical conference*, Bombay, pp. 499–502.

Assessment of Vetiver Grass Root Reinforcement in Strengthening the Soil

Donal Nixon D'Souza, A. K. Choudhary, P. Basak and S. K. Shukla

Abstract Vegetation has been used globally for centuries to control soil erosion on slopes. It is widely recognized that vegetation contributes to slope stability, but to an unquantifiable degree. Vetiver grass (*Chrysopogon zizanioides*) is being utilized to reduce the soil erosion and strengthen the slopes. Vetiver roots are massive, fine-structured, and grow fast and deep. With an average tensile strength of 85 MPa, which approximates to one-sixth of that of mild steel, Vetiver root is compared to as 'living soil nail'. Roots of trees and other vegetation increase the shear strength of soil by root reinforcement. The difference between shear strength values of root-permeated soil and root-free soil sheared under the same conditions gives the shear strength increase caused by the roots. This paper presents the investigation on increase in shear strength of soil by Vetiver roots. Using a custom made large-scale in situ direct shear test apparatus, in situ direct shear tests were conducted at different depths on a soil plot with one-year-old Vetiver grass planted at 0.15 m spacing in an equilateral triangular pattern. The tests prove that the Vetiver grass roots increase the shear strength of soil by up to 139% at 0.15 m depth and up to 47% at 0.75 m depth.

Keywords Soil bioengineering · Vetiver grass · In situ direct shear test
Root reinforcement

D. N. D'Souza (✉) · A. K. Choudhary · P. Basak
Department of Civil Engineering, National Institute of Technology, Jamshedpur, India
e-mail: donalnixon@gmail.com

A. K. Choudhary
e-mail: drakchoudharycivil@gmail.com

P. Basak
e-mail: punyabratabasak@gmail.com

S. K. Shukla
Discipline of Civil and Environmental Engineering, Edith Cowan University, Joondalup, Perth, Australia
e-mail: s.shukla@ecu.edu.au

T. Thyagaraj (ed.), *Ground Improvement Techniques and Geosynthetics*, Lecture Notes in Civil Engineering 14, https://doi.org/10.1007/978-981-13-0559-7_15

1 Introduction

On July 30, 2014, a landslide occurred in the village of Malin in Maharashtra killing at least 151 people. Major cited cause for the landslide was excessive deforestation in that area. Deforestation not only removes trees but also the root structures that hold the soil. Slope failures affect and disrupt transportation routes, urban development, mining and timber harvesting operations. These activities are very often themselves a major cause for slope failures.

The use of vegetation as a bioengineering tool for erosion control and slope stabilization has been implemented for centuries and its popularity has increased remarkably in the past few decades. The cost-effectiveness and environment-friendliness of this bioengineering approach have greatly increased it cachet.

Vetiver grass has been used by Indian farmers for over 200 years mainly for soil and water conservation. However, its real impact on slope stabilization and soil erosion control started in the late 1980s following the promotion of Vetiver system by the World Bank.

The biological name of Vetiver grass is *Chrysopogon zizanioides*. Vetiver is most closely related to sorghum, but shares many morphological characteristics with other fragrant grasses, such as lemongrass, citronella and palmarosa. Vetiver is native to tropical and sub-tropical India. Vetiver plant can be grown over a very wide range of climatic and soil conditions, and if planted correctly can be used virtually anywhere under tropical, semi-tropical, and Mediterranean climates. Vetiver's physiological traits make it tolerant to extreme climatic variations such as prolonged drought, flood, submergence, fire, frost, and heat waves. It is also tolerant to a wide range of soil acidity, alkalinity, salinity, sodicity, agrochemicals and elevated levels of heavy metals in the soil.

Unlike most grasses which spread roots horizontally, Vetiver roots grow vertically downward up to 2–4 m in depth. Depending on the soil conditions, the roots can grow up to 3 m within the first year of planting. Vetiver roots possess very high tensile strength which varies between 40–180 MPa. The unique property of resilience along with deep and strong roots makes Vetiver an ideal plant for use in soil bioengineering applications.

The purpose of this investigation is to quantify the increase in shear strength of soil due to Vetiver roots. Accurate information about the quantitative effects of roots on soil strength is necessary to guide the design and management of Vetiver systems.

2 Literature Review

The role played by vegetation in enhancing soil stability is found in several publications (e.g., Greenway 1987; Gray and Leiser 1989; Coppin and Richards 1990; Gray and Sotir 1996). In a direct mechanical sense, vegetation increases the

strength and competence of the soil by root reinforcement. A root-permeated soil behaves as a composite material in which fibers of a relatively high tensile strength are embedded in a matrix of lower tensile strength. Some of the most promising studies of roots as soil reinforcement have been direct measurement with empirically applicable results, either on a qualitative or quantitative basis. These include laboratory shear tests of soils with roots (Waldron 1977), and in situ shear tests on soil blocks with roots (Nilaweera 1994). These studies produced data that show increase in shear strength due to soil-root interaction and describe functional relationships and characteristics that influence the reinforcement phenomenon.

Several researchers agree that the effect of roots is to provide an increase in the effective cohesion of the soil (Gray and Ohashi 1983; Sotir and Gray 1989). Coppin and Richards (1990) have stated that the magnitude of the mechanical reinforcing effect of plant roots is a function of density, tensile strength, tensile modulus, length/diameter ratio, surface roughness, alignment, and orientation.

Perhaps the most complete overview of soil reinforcement by roots and artificial fibers is provided by Gray and Sotir (1996). The basic process involves the transfer of shear stress within the soil to tensile resistance of the roots, which becomes a function of the interface friction along the root surface. The orientation of the fiber relative to the shear force, the skin friction of the root, the elongation behavior of the root, the fraction of the soil cross-section occupied by roots, and the tendency to break rather than pullout are all factors influencing the reinforcing effect. Direct shear tests have been conducted in laboratory as well as field settings to evaluate performance of mainly woody plants and various fibers designed to simulate roots.

Endo and Tsuruta (1969) and Ziemer (1981) conducted in situ direct shear tests on root-permeated soils. Their results show an approximately linear increase in the root cohesion with increasing root biomass. Laboratory tests conducted by Gray and Sotir (1996) in root-permeated soils show a similar relationship. Test results for hardwood trees obtained by Nilaweera (1994) show an increase in shear resistance values. Hengchaovanich and Nilaweera (1996) conducted soil block shear test on two year old Vetiver hedges and found increase in soil strength.

Experimental research data that quantitatively address the soil reinforcement contribution of Vetiver plants have been scarce to date. In addition, there is a wide range of soil strength data depending on sample size, spacing of planting, age of plant and condition of root.

3 Soil Properties

The study site is located in Hemavathi Estate in the village of Niduvale, of Mudigere Taluk in Chikmagalur District of Karnataka in India. The GPS coordinates of the site are 13° 10′ 28.7″N 75° 29′ 43.1″E. The site is 1047 m above the mean sea level. The soil properties of the study area are shown in Table 1.

Table 1 Soil properties at study area

Specific gravity	2.56
Gravel content (%)	11.2
Sand content (%)	50.8
Silt and clay content (%)	38.0
Liquid limit (%)	21
Plastic limit (%)	17
Soil type (as per indian soil classification system)	SM-SC
Saturated unit weight (kN/m^3)	18.6

4 Tests and Methodology

The reinforcing effect on the increase of shear strength of soil due to roots can be quantified by conducting in situ direct shear tests on root-permeated and root-free soils at the same location. The difference between shear strength values of root-permeated soil and root-free soil sheared under the same conditions gives the shear strength increase due to the roots. In order to determine the root reinforcement effect of Vetiver grass, large-scale in situ direct shear tests were performed on a soil vegetated with Vetiver. Locally sourced South Indian genotype Vetiver was planted at 0.15 m spacing in equilateral triangular pattern on a level ground. The tests were conducted after one year of planting. The tests were conducted with the shear plane at different depths. The tests were conducted on saturated soil by flooding the site for 96 h prior to testing. The average tensile strength of Vetiver roots was 85 MPa.

The principle of in situ shear testing is described in BS 5930 and IS 7746 (1991). However, this system has mainly been developed for in situ testing of rock but not for root-reinforced soil. A number of researchers have therefore devised and developed in situ shear testing apparatus for this purpose. The first reference to in situ testing of root-reinforced soil was Endo and Tsuruta (1969) who designed the apparatus to measure the contribution of small *Alnus glutinosa* roots to the strength of homogeneous nursery soil in Japan. O'Loughlin (1972) later used a slightly modified design for the study of old-growth forests of coastal British Columbia, Canada. Endo reused his shear apparatus in 1980 to measure the strength of *Betula japonica* and *Alnus japonica* tree roots.

In this study, a custom-made large-scale in situ direct shear test apparatus was developed to conduct in situ direct shear test. The apparatus comprised of 30 cm × 30 cm shear boxes along with a reaction frame, screw jack, proving ring and dial gauges. The height of the lower shear box was 15 cm and the height of the upper shear box was equal to the depth of shear plane from the ground level. The height of the upper shear box was varied depending on the depth of the shear plane. The lower shear box has a sharpened cutting edge. The two shear boxes were stacked up driven into the ground planted with Vetiver. A relatively undisturbed soil-root sample gets transferred into the shear box. The soil surrounding the shear box was removed. By using a reaction frame, the lower shear box was restrained against any lateral movement. The upper shear box was sheared horizontally under

strain controlled condition at a rate of 1 mm/min. The shear load and shear deformation were noted at every 30 s interval. A pair of guide rollers was used to prevent twisting and tilting of shear boxes. The guide rollers guide the shear box along the direction of shear load without twisting and tilting. After failure, the shear surface and the orientation of failed roots were examined carefully in order to study the failure pattern. The total cross-sectional root area on the shear plane was measured to determine the root area ratio. The same procedure was repeated to conduct tests by increasing the depth of shear plane. Tests were conducted at every 0.15 m interval up to a total depth of 1.20 m. For each depth level of shearing, a

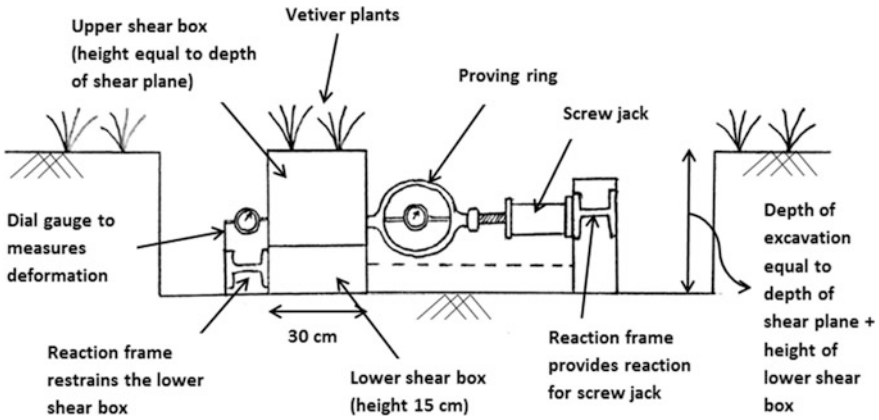

Fig. 1 Schematic diagram of in situ direct shear test apparatus

Fig. 2 In situ direct shear test being conducted on field with Vetiver planted at 0.15 m spacing

root-free soil profile adjacent to the root-permeated soil profile was also sheared under the same shearing conditions. Each soil block was sheared under its own self-weight as the normal load. A stress–strain variation with depth is plotted for both Vetiver-rooted and non-rooted soil.

Figure 1 shows the schematic diagram of the in situ test apparatus developed. Figure 2 shows the actual in situ direct shear test being conducted on field with Vetiver plants being planted at 0.15 m spacing.

5 Results and Discussion

The stress–strain plots of in situ direct shear tests conducted on non-rooted and Vetiver-rooted soils are shown in Figs. 3 and 4, respectively.

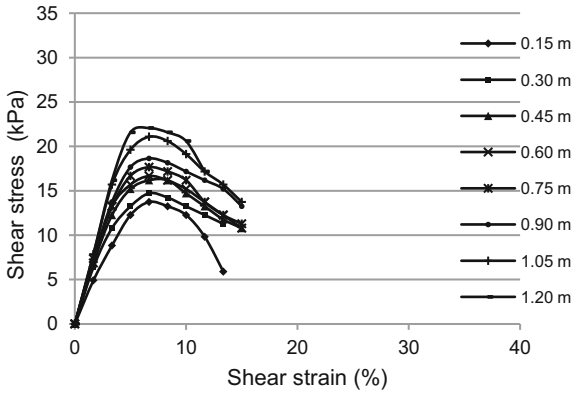

Fig. 3 Stress–strain plot of in situ direct shear test conducted at various depths on non-rooted soil

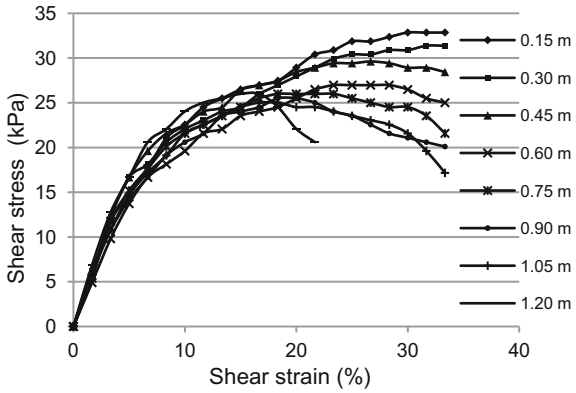

Fig. 4 Stress–strain plot of in situ direct shear test conducted at various depths on one-year-old Vetiver-rooted soil planted at 0.15 m spacing

Table 2 Variation of peak stress in in situ direct shear test

Depth of shear plane (m)	Peak stress (non-rooted) (kPa)	Root area ratio (RAR)	Peak stress (Vetiver-rooted) (kPa)	Percentage increase in peak stress
0.15	13.73	0.57	32.85	139.3
0.30	14.71	0.49	31.38	113.3
0.45	16.18	0.43	29.62	83.1
0.60	16.67	0.36	26.97	61.8
0.75	17.65	0.29	25.99	47.3
0.90	18.63	0.25	25.50	36.9
1.05	21.08	0.22	25.01	18.6
1.20	22.06	0.15	25.99	17.8

Figures 3 and 4 show that shear strength of Vetiver-rooted soil is higher than non-rooted soil. Compared to non-rooted soil, Vetiver-rooted soil exhibits very large strain prior to failure. Large strain leads to progressive failure which would provide sufficient warning before landslides.

Table 2 shows that the peak shear strength of Vetiver-rooted soil is higher than that of non-rooted soil. An increase of up to 139% can be observed at a depth of 0.15 m. The increase in shear strength is directly proportional to the root area ratio (RAR). The increase in strength is greatest at shallow depths due to high root area ratio and reduces when root area ratio reduces with depth. While conducting tests it was also observed that at shallow depth, the roots failed primarily by slippage. With increasing depths, the roots failed by root breakage.

6 Conclusions

The in situ direct shear tests show that the Vetiver roots increase the shear strength of soil by root reinforcement. The increase in strength is dependent on root area ratio, which depends on soil and climate conditions.

The increase in shear strength is limited by the depth of roots and thus the root reinforcement by Vetiver is useful only to shallow depths.

References

Coppin, N. J., & Richards, I. G. (1990). *Use of vegetation in civil engineering*. London: Butterworth.

Endo, T., & Tsuruta, T. (1969). The effect of tree roots upon the shearing strength of soil. *Annual Report of the Hokkaido Branch, Tokyo Forest Experimental Station, 18,* 168–179.

Gray, D. H., & Leiser, A. T. (1989). *Biotechnical slope protection and erosion control*. New York: Van Nostrand Reinhold.

Gray, D. H., & Ohashi, H. (1983). Mechanics of fiber reinforcement in sand. *Journal of Geotechnical Engineering, ASCE, 109*(3), 335–353.

Gray, D. H., & Sotir, R. B. (1996). *Biotechnical and soil bioengineering slope stabilization*. New York: Wiley.

Greenway, D. R. (1987). Vegetation and slope stability. In M. G. Anderson & K. S. Richards (Eds.), *Slope stability* (pp. 187–230). New York: Wiley.

Hengchaovanich, D., & Nilaweera, N. S. (1996). An assessment of strength properties of vetiver grass roots in relation to slope stabilization. In *Proceedings, First International Vetiver Conference* (pp. 153–158), Thailand.

Nilaweera, N. S. (1994). Effects of tree roots on slope stability: The case of Khao Luang Mountain area, southern Thailand. *Doctor of Technical Science Dissertation*. Thailand: Asian Institute of Technology.

O'Loughlin, C. L. (1972). An investigation of the stability of the steep land forest soils in the coast mountains, southwest British Columbia. *Ph.D. dissertation*. Canada: University of British Columbia.

Sotir, R. B., & Gray, C. H. (1989). Fill slope repair using soil bioengineering systems. In *Proceedings, 20th International Erosion Control Association Conference* (pp. 473–485), Vancouver, BC, February 15–18, 1989.

Waldron, L. J. (1977). The shear resistance of root permeated homogeneous and stratified soil. *Soil Science Society of America Journal, 41,* 843–849.

Ziemer, R. (1981). *Roots and shallow stability of forested slopes* (pp. 343–361). International Association of Hydrological Sciences, Publication No. 132.

Geotechnical Aspects of Various Constructions along the Canal Embankment using Rice Husk Ash as Stabilizer

T. Vamsi Nagaraju and P. V. V. Satyanarayana

Abstract This paper discusses the use and efficacy of rice husk ash (RHA) as a stabilizing additive to problematic expansive soils. RHA is an agricultural industrial waste. It is abundantly available and therefore needs to be effectively disposed. The paper presents experimental results obtained from tests conducted on RHA-clay blends. Liquid limit, plasticity index, free swell index (FSI), compaction characteristics, strength parameters, and CBR were determined on the expansive clay specimen to which RHA was added in different quantities such as 5, 10, 15, 20… 50% by dry weight of the soil. Test results indicated that FSI and PI decreased with increasing RHA content. Further, CBR and angle of internal friction increase while cohesion decrease.

Keywords Expansive soil · FSI · RHA · CBR

1 Introduction

Coastal areas of Andhra Pradesh are familiar with Black cotton soils. They present various challenges to engineers due to their characteristics of severe loss of strength, excessive swelling and shrinking with respect to changes in moisture regime (American Society of Civil Engineers 2012; Chen 1988). The primary problem that arises with regard to expansive soils is that deformations are significantly greater than elastic deformations and they cannot be predicted by classical elastic or plastic theory (Nelson and Miller 1992). The damages caused to the pavement by the movements of expansive soils are well documented worldwide. Expansive soils are capable of absorbing large volumes of water due to the presence of montmorillonite. Recently Indian government announced Visakhapatnam,

T. Vamsi Nagaraju (✉)
SRKR Engineering College, Bhimavaram, AP, India
e-mail: Varshith.varma@gmail.com

P. V. V. Satyanarayana
Department of Civil Engineering, Andhra University, Visakhapatnam, AP, India

T. Thyagaraj (ed.), *Ground Improvement Techniques and Geosynthetics*, Lecture Notes in Civil Engineering 14, https://doi.org/10.1007/978-981-13-0559-7_16

Kakinada, and Tirupati as smart cities which are located along the costal belt, and also newly bifurcated AP government has been giving prime importance to connect these cities. These cities require new roads due to scarcity of lands and not possible further widening of the existing roads in the delta regions, so roads along canals have been gaining more importance but causes of failures of roads along the canals are quite common mainly due to seasonal variation of moisture in sub grade. Roads running through expansive soil subgrade are subjected to severe unevenness with or without cracking, longitudinal cracking parallel to the pavement centre line, rutting of pavement surface and localized failure of the pavement associated with disintegration of the surface. The losses due to extensive damage to highways running over expansive sub-grades are estimated to be in billions of dollars all over the world. To protect and safeguard the structures from distress caused by the inherent peculiar volume change behaviour of expansive soils under varying moisture content is a challenging task. Therefore there is a need to go for alternative solution to rectify these problems. Hence research is focused on potentially cost effective materials, admixtures and waste products like fly ash, rice husk ash and marble dust that can improve the properties of Expansive soil (Haji Ali et al. 1992; Phanikumar and Sharma 2004). Rice Husk Ash (RHA) is an agricultural industrial waste which is major waste found abundantly in delta regions which is nearly 5.5 million tonne, requires huge quantities of land for its disposal. Presence of very high quantities of SiO_2 makes RHA a pozzolanic material. It high strength (Sharma et al. 2008; Sivapullaiah et al. 2004) and has attains coarse grained, non-plastic, porous and high volume. The use of RHA will reduce the importation of conventional materials like cement. The use of RHA in soil stabilization is therefore economic and environment friendly.

2 Materials

The expansive soil was collected at a depth of 0.6 m where road surface is frequently damaged at Yendagandi along the canal embankment of Major District road from Bhimavaram to Tadepalligudem. RHA was collected from Sesali, AP, India. The soil and the RHA were dried, pulverized into the required sizes and tested for properties like gradation, compaction and strength as per the relevant IS codes. The gradation curve of black cotton soil is shown in Fig. 1a. Typical scanning electron microscope image is shown in Fig. 1b. Table 1 shows the index properties and engineering properties of the expansive soil and the RHA.(b) Image of SEM analysis for RHA particles

Table 1 Geotechnical properties of soil and RHA

Property	Black cotton soil	RHA
Gravel (%)	0	0
Sand (%)	4	84
Silt (%)	50	16
Clay (%)	46	0
Liquid limit (%)	74	NP
Plastic limit (%)	29	NP
Plasticity index (IP)	45	–
IS classification	CH	SM
Optimum moisture content (%)	26	38
Maximum dry density (g/cc)	1.52	0.7
California bearing ratio (%)	1.22	8
Angle of shearing resistance (ϕ)	15	36
Cohesion (t/m^2)	10	–

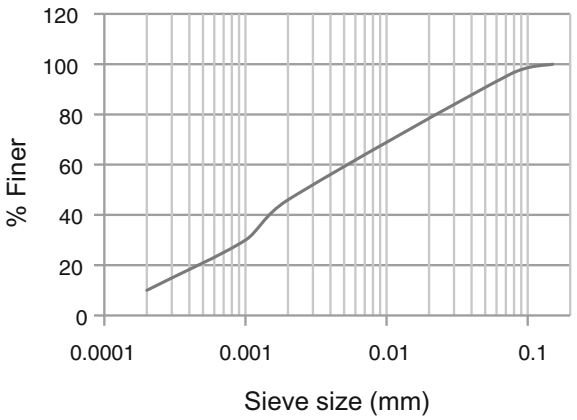

Fig. 1 (a) Gradation curve of black cotton soil

(b) Image of SEM analysis for RHA particles

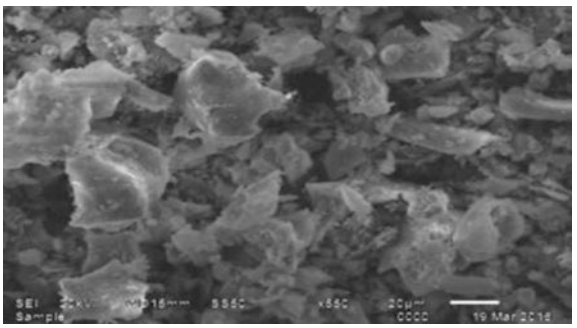

2.1 Expansive Soil

The soil contains 95% of fines in which 55% of silt and 46% of clay particles. The presence of fines contributed for high liquid limit (LL) of 74% and plasticity index of 45%. The soil classify as CH. It also exhibited high swelling characteristics with FSI as 115% and swell pressure as 90 kPa. Under soaking condition, the CBR was 1.22%.

2.2 Rice Husk Ash

Majority of RHA particles are under fine sand range and of angular shape with rough surface texture. It is non-plastic in nature and well graded with $C_u = 9.74$ and $C_c = 1.75$.

The OMC and MDD were found to be 38% and 0.7 g/cc. From the compaction curve it can be seen that Rice husk ash attained lower densities for wide variation in moisture contents. Regarding strength characteristics it has an angle of shearing resistance (ϕ) as 36° under un-drained condition and CBR of 8% and has good drainage characteristics with coefficient of permeability as 3.4×10^{-3} cm/sec. RHA attained low densities due to low specific gravity, porous nature and distribution of uniform size of particles.

Chemical analysis of RHA was carried out using Scanning Electron Microscope (SEM). SiO_2 is the major component (97%) and oxides of calcium, iron, potassium, sodium as minor compounds.

3 Results and Discussion

3.1 Performance of CBR with Seasonal Variation of Sub Grade Black Cotton Soil

Both soaked and unsoaked CBR was determined for samples collected in mid-May, mid-Aug, mid-Nov, mid-Feb, mid-Apr at natural moisture content (NMC), optimum moisture content (OMC). Tables 2, 3 and Fig. 2a, b show the test results.

Based on NMC variation, monsoon arrives in mid-Aug monsoons arrives and in mid-Apr (pre summer) canals over flow for summer storage purpose.

As NMC was found to be greater than OMC, CBR at NMC was observed to be less than that at OMC. However, CBR value in mid-May was high due to less moisture content.

Table 2 Seasonal variation of sub grade CBR at OMC

Bulk density ρ (g/cc) 2.016			
Dry density ρ_d (g/cc) 1.68			
Months	OMC (%)	CBR (%)	
		Soaked	Unsoaked
Mid-May	20	1.28	2.17
Mid-Aug	20	1.21	2.1
Mid-Dec	20	1.26	2.15
Mid-Feb	20	1.28	2.18
Mid-Apr	20	1.24	2.12

Table 3 Variation of CBR sub grade with NMC

Months	NMC	ρ (g/cc)	ρ_d (g/cc)	CBR (%)	
				Soaked	Unsoaked
Mid-May	5.8	1.63	1.54	1.22	18.56
Mid-Aug	28.4	1.72	1.33	1.26	1
Mid-Dec	12.86	1.92	1.65	1.23	12.9
Mid-Feb	17.79	1.96	1.66	1.28	5.4
Mid-Apr	24	1.95	1.57	1.25	1.02

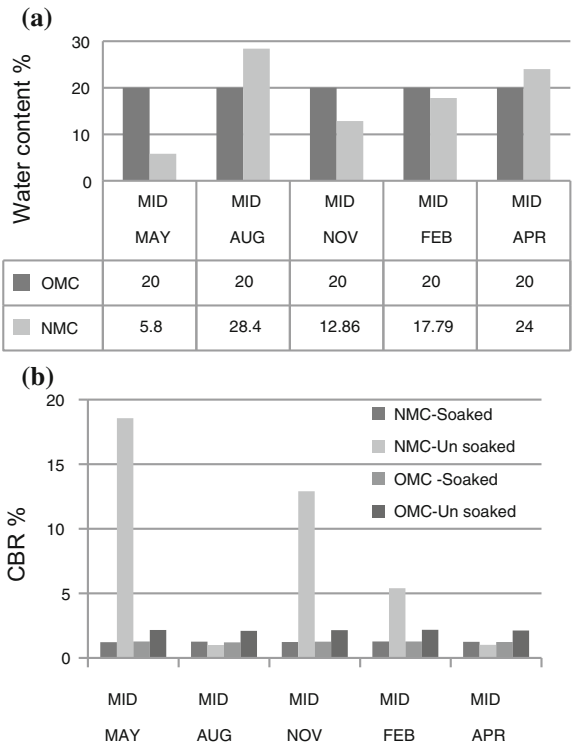

Fig. 2 **a** Comparison of moisture contents with seasons; **b** Variation of CBR values with moisture

3.2 Performances of RHA Soil Matrix

To study the effect of RHA on expansive soil, various amounts of RHA such as 5, 10… 50% by dry weight of soil were added, effectively mixed and tested for plasticity, compaction, strength, CBR and swell. Table 4 and Fig. 3a–g shows the results.

Consistency limits showed that liquid limit decreased, plastic limit values increased and plasticity index decreased with increasing percentage of RHA up to 25%. At higher RHA contents, the blends became non-plastic. The decrease in liquid limit is due to the decrease in diffused double layer by replacement of clay particles by RHA particles. Increase in plastic limit is due to development of shear resistance at inter-particle level, and the soil-RHA matrix requires high moisture content to roll.

Compaction test data showed that with increasing percentage of RHA, OMC increased and MDD decreased. At lower percentages of RHA this phenomenon is steady and at higher percentage, it is rapid. The increase in OMC is due to the development of flocculated structure which resists the compaction effort and requires more water to mobilize and offers low dry densities.

CBR test data showed that the increase in percentage of RHA increased the CBR values. The increased CBR values are due to the development of shear resistance generated against penetration.

Shear test data showed that with increasing percentages of RHA, cohesion decreased and angle of shearing resistance increased. The decreased cohesion and increased angle of shearing resistance are due to replacement of fines by RHA particles.

Table 4 Effect of RHA on properties of expansive soil

RHA %	Consistency limits			Compaction parameters		Strength parameters			Swell parameter
	W_L (%)	W_P (%)	I_P (%)	OMC (%)	MDD (g/cc)	CBR (%)	C' (t/m^2)	ϕ (°)	FSI
0	74	29	45	26	1.52	1	10	15	115
5	70	30	43	26.5	1.5	1.5	9	16	100
10	63	31	32	27.2	1.47	2.5	7.5	18	85
15	56	32	24	28	1.43	3.5	6	20	70
20	42	34	8	28.8	1.4	5	4	24	55
25	32	NP	NP	29.8	1.36	6	1.5	28	35
30	NP	NP	NP	30	1.32	7	0.5	30	20
40	NP	NP	NP	31.8	1.24	8.5	0	32.5	0
50	NP	NP	NP	33.2	1.15	9.5	0	34	0

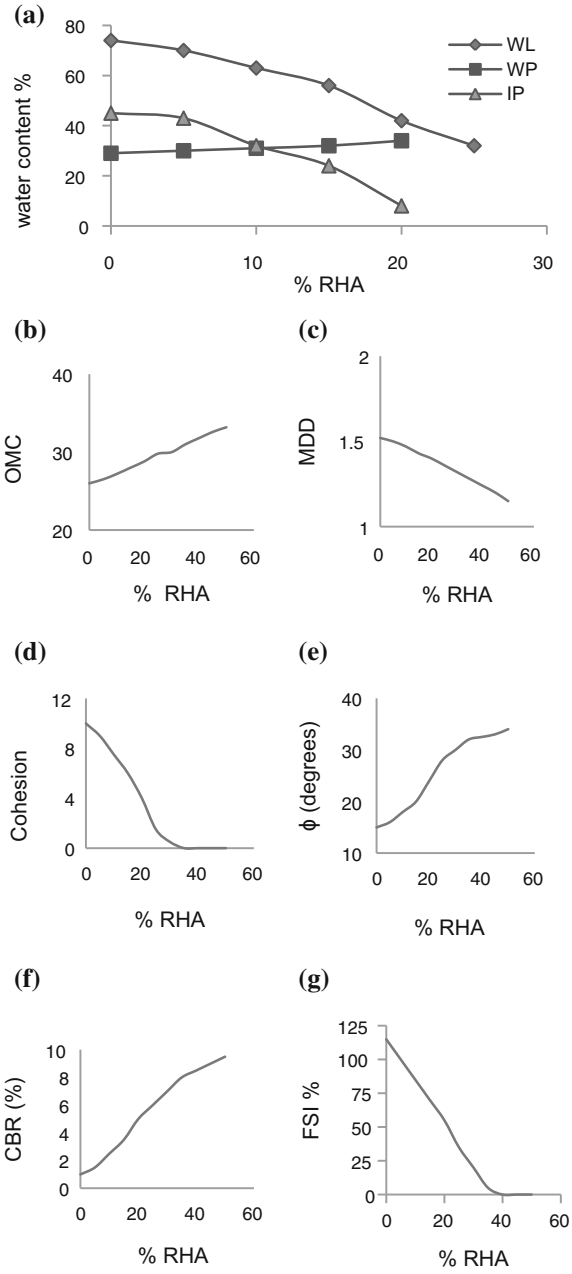

Fig. 3 **a** RHA% versus plasticity characteristics; **b** RHA% versus OMC; **c** RHA% versus MDD; **d** RHA% versus C; **e** RHA% versus ϕ; **f** RHA% versus CBR; **g** RHA% versus FSI%

4 Conclusions

Rice Husk Ash is an industrial agricultural waste of light weight porous and high volume material with high strength values can be individually used as subgrade, fill and embankment material.

It is also used as admixture with black cotton soil for a subgrade, fill and embankment material at a dosage of 30–40% by maintaining CBR values 8–10%, density 1.24–1.32 g/cc and ϕ values in the range of 32°–36°.

References

American Society of Civil Engineers (2012). *ASCE Proceedings, GeoCongress 2012 Geotechnical Engineering State of the Art and Practice: Keynote Lectures from GeoCongress 2012*, GeoCongress 2012, GSP 226.

Chen, F. H. (1988). *Foundations on expansive soils*. Amsterdam: Elsevier.

Haji Ali, F., Adnan, A., Choy, C. K. (1992). Geotechnical properties of a chemically stabilized soil from Malaysia with rice husk ash as an additive. *Geotechnical & Geological Engineering, 10* (2), 117–134 (Spinger).

Nelson, D. J., & Miller, J. D. (1992). *Expansive soils: Problems and practice in foundation and pavement engineering*. New York: Wiley.

Phanikumar, B. R., & Sharma, R. S. (2004). Effect of fly ash on engineering properties of expansive soils. *ASCE Journal of Geotechnical and Geoenvironmental Engineering, 130*(7), 764–767.

Sharma, R. S., Phani Kumar, B. R., & Rao, B. V. (2008). Engineering behaviour of a remoulded expansive clay blended with lime, calcium chloride and rice husk ash. *Journal of Materials in Civil Engineering, ACSE, 20*(8), 509–515.

Sivapullaiah, P. V., Subba Rao, K. S., & Gurumurthy, J. V. (2004). Stabilisation of rice husk ash for use as cushion below foundations on expansive soils. *Ground Improvement, 8*(4), 137–149.

Use of Jhama Columns as Replacement of Stone Columns

Siddhartha Kr. Karmakar, Parbin Sultana and Ashim Kanti Dey

Abstract Use of stone columns for ground improvement in clayey soil is a common practice. Due to the high cost and scarcity of stone in some areas, jhama (over burnt brickbats) are being used as an alternative to stones. It is intended in the present study to compare the load carrying capacity of stone columns with that of jhama columns through laboratory tests and to conclude whether the jhama columns can be an alternative to stone columns. Model tests were carried out on 50 mm diameter and 400 mm long columns embedded in soft clay in a tank of size 1 m × 1 m × 1 m. The load-settlement plots were studied to observe the difference in behaviour of a stone column and a jhama column in terms of bearing capacity and mode of failure. A numerical analysis using Plaxis-2D was also carried out to observe the load-settlement behavior of all the models. A good agreement of experimental and analytical results was observed.

Keywords Jhama columns · Stone columns · Load-settlement plots Numerical analysis

1 Introduction

Due to the growing demand of infrastructure and scarcity of good land, the sites with poor ground conditions like marshy low lands and soft clayey deposits are being used for construction. These soils have low shear strength and high compressibility, and thus require some ground improvement technique to achieve the

S. Kr. Karmakar · P. Sultana (✉) · A. K. Dey
Department of Civil Engineering, National Institute of Technology Silchar, Silchar 788010, India
e-mail: parbinsultana@rediffmail.com

S. Kr. Karmakar
e-mail: siddharthkarmakar91@gmail.com

A. K. Dey
e-mail: ashim_kanti@yahoo.co.in

T. Thyagaraj (ed.), *Ground Improvement Techniques and Geosynthetics*, Lecture Notes in Civil Engineering 14, https://doi.org/10.1007/978-981-13-0559-7_17

desired bearing capacity. Out of many methods, stone columns are successfully being used to enhance the performance of such soils in many areas. Stone columns are adopted as an economic alternative to develop poor soil sites (Schweiger and Pande 1986; Poorooshasb and Meyerhof 1997; Ambily and Gandhi 2007). But there is a scarcity of stone and its price is high in some parts of India like Tripura and Mizoram. In these areas jhama bricks are used as construction material instead of stone. Hence jhama can be used economically as column material instead of stone in such areas. The jhama are the broken pieces of over burnt bricks obtained abundantly in brick kilns. In this study, load tests were performed on stone columns and jhama columns in soft clayey soil. A numerical analysis was also carried out using Plaxis-2D. All the outcomes were compared to investigate the feasibility of jhama column as a replacement of stone column.

2 Materials Used

The soil used in the tests was soft clay with low shear strength. Locally available stone and jhama were used for construction of granular columns. The properties of these materials are given in Tables 1 and 2 respectively.

Table 1 Properties of clay

Property	Value
Specific gravity	2.63
Liquid limit (%)	53
Plastic limit (%)	25
Indian standard classification	CH
Optimum moisture content (%)	18
Maximum dry density (kN/m^3)	15.3
Undrained cohesion at test condition, C_u (kPa)	7.7

Table 2 Properties of granular column materials

Material	Property	Value
Stone	Size (mm)	2–6
	Angle of friction, ϕ (°)	45.60
	Cohesion, C (kPa)	0
Jhama	Size (mm)	2–6
	Angle of friction, ϕ (°)	43.25
	Cohesion, C (kPa)	0

3 Test Program

Three number of load tests were performed in this study among which one was on plain clay bed and the other two were on stone and jhama column reinforced clay beds. All the tests were performed in the laboratory using a steel tank of dimension 1 m × 1 m × 1 m.

3.1 Clay Bed Preparation

The clay bed was prepared in the tank to simulate field condition. At first, the inner face walls of the tank were covered with smooth polyethylene sheets (Yadu and Tripathi 2013) so that the friction between the clay and tank wall is minimum. The clay was placed in layers of thickness 50 mm. To obtain a soft consistency, the water content of the clay was maintained at around 50% for all the tests. The clay layers were laid up to a height of 900 mm from the bottom of the tank. After completion of the laying, the surface of the tank was sealed with a polyethylene sheet for 5 days to achieve uniform water content and self consolidation of the clayey soil mass.

3.2 Construction of Granular Column

For the granular column tests, 50 mm diameter and 400 mm long granular columns were constructed by the replacement method. An auger of diameter 50 mm was pushed into the clay bed up to a depth of 100 mm at a time and then pulled out slowly. This process was repeated till a cylindrical hole of depth 400 mm was formed. In this hole the granular material (stone or jhama) was filled in five layers of equal thickness. Each layer was compacted with a steel rammer of 3 cm diameter by giving 10–15 blows. Seven numbers of columns were constructed in triangular pattern as shown in Fig. 1 to observe the behavior of the central column as mentioned in IS: 15284 Part-1 (2003). Spacing of the columns was kept 3 times the column diameter, i.e., 150 mm.

3.3 Load Test Setup

The load tests were performed on a circular steel plate of diameter 100 mm and thickness 10 mm. The load was applied using a hydraulic jack and was measured by a load cell. Two LVDTs were placed diagonally opposite to each other and settlement was measured by taking average of the two LVDT readings. For granular

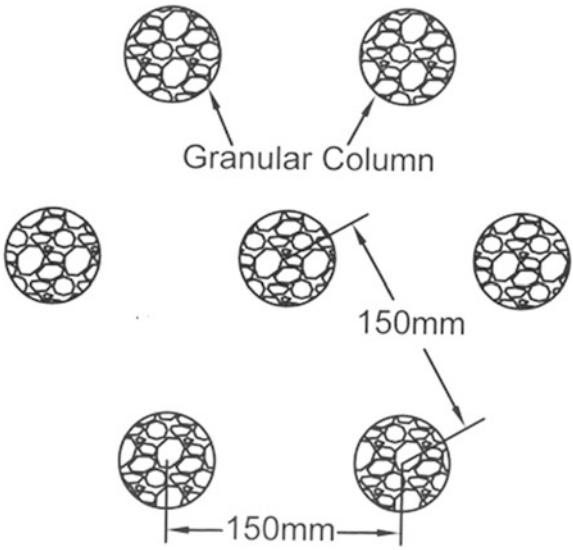

Fig. 1 Layout of granular columns in triangular pattern

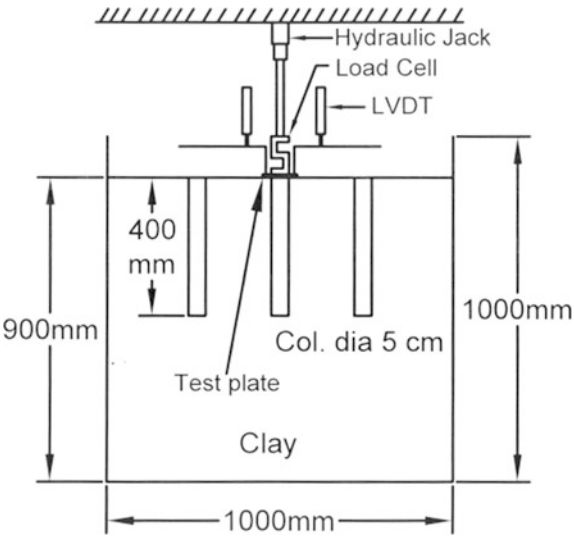

Fig. 2 Schematic diagram of the test set up

column tests, the test plate was placed centrally over the middle column as shown in Fig. 2. The length of column was kept more than the critical length (i.e., four times the column diameter) to avoid shear failure (Barksdale and Bachus 1983; IS: 15284 part 1 2003). In the present study, the length to diameter ratio (*L*/*D*) is 8 and hence columns are long columns. In the single column tests on long columns generally failure occur due to bulging of the central column up to a depth of *D* to 2*D* from the top of the column (Murugesan and Rajagopal 2007; Ghazavi and Afshar 2013).

4 Results of the Test Data

The failed soil surfaces after completion of load tests are shown in Figs. 3 and 4 for stone column and jhama column respectively. Cracks were observed at the soil surfaces due to shear failure. The central granular columns on which the load was applied are shown in Fig. 5 after completion of the tests. A slight bulging was observed up to a depth of 10 cm from the top. The load-settlement curves of the three load tests are shown in Fig. 6. It is observed that both stone columns and jhama columns improve the ultimate bearing capacity of the footing. However the improvement due to stone column is slightly more than that due to jhama column.

The improvement in performance of the clay bed due to installation of granular columns can be measured by a non dimensional improvement factor. Dash and Bora (2013) has defined the improvement factor as the ratio of the bearing pressure

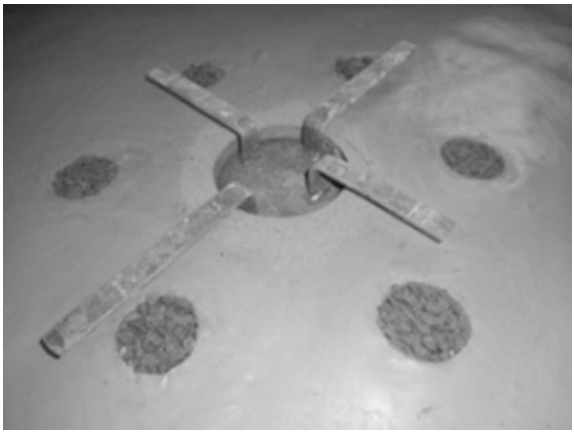

Fig. 3 Soil surface with stone column after the load test

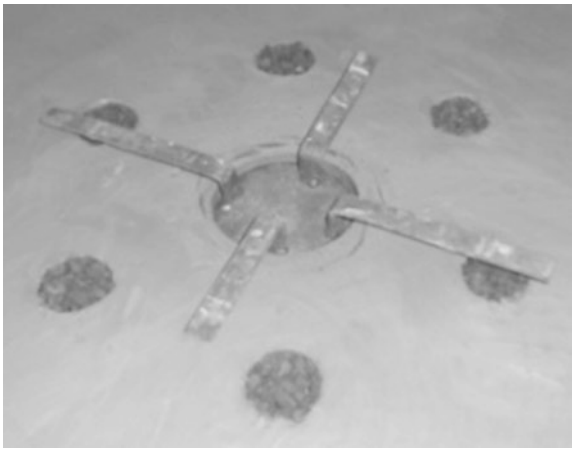

Fig. 4 Soil surface with jhama column after the load test

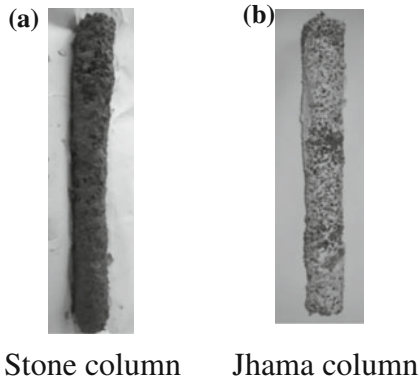

Fig. 5 The central granular columns after the load tests

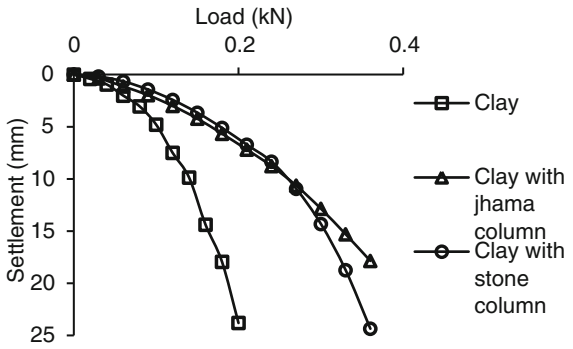

Fig. 6 Load-settlement plots for all load tests

on the granular column reinforced clay to the bearing pressure on the plain clay bed at constant normalized settlement. Normalized settlement is the settlement divided by diameter of test plate expressed in percentage. For the present study, the variation of improvement factors of stone column and jhama column reinforced soil at different normalized settlements are shown in Fig. 7. It is observed that the improvement factor of stone column is fluctuating within a narrow range of 1.7–1.9; but the improvement factor of jhama column is gradually increasing from 1.5 to 2.0.

5 Numerical Analysis

A two-dimensional finite element model is sufficient to develop the settlement of the circular footing. This model assumes that the displacement and strain in the direction of footing length are zero; however the normal stresses are taken into account.

To perform the finite element analysis, Plaxis-2D software was used (Abdi and Zandieh 2014). The model was divided into finite number of triangular elements. A 15-node, triangular element was used in the finite element mesh. They are

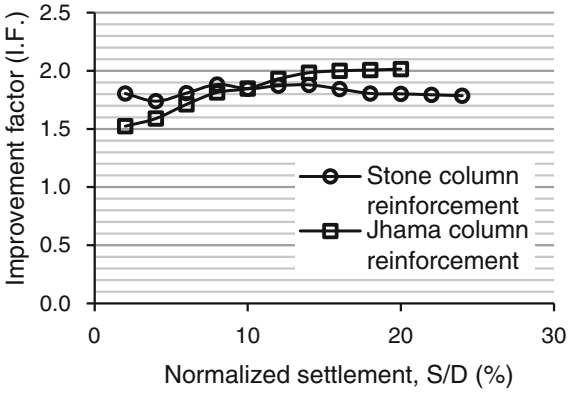

Fig. 7 Variation of improvement factor with normalized settlement

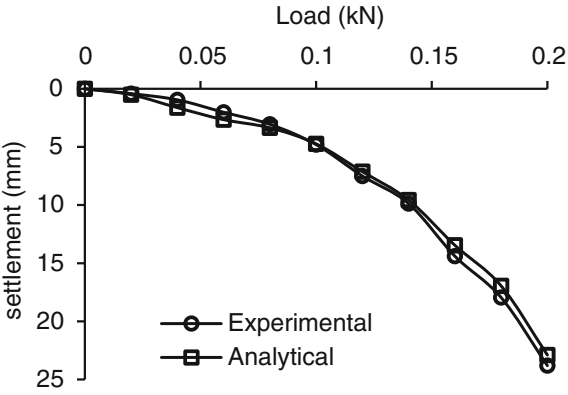

Fig. 8 Load-settlement curve of plain clay

accurate elements that have produced high stress results for the soil collapsing. The displacements are obtained by solving fourth-order interpolation function and stresses are obtained at 12 points through numerical integration. A medium mesh was generated along the footing of the soil interfaces and the horizontal surface adjacent to slope because the deformation of this area is relatively critical. The deformation of the footing was obtained from the deformed mesh.

The experimental and analytical load-settlement curves for plain clay, clay with stone column and clay with jhama column are shown in Figs. 8, 9, and 10 respectively. It is observed that experimental results match closely with the analytical results.

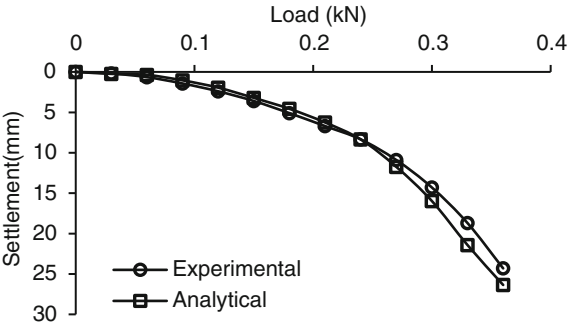

Fig. 9 Load-settlement curve of clay with stone column

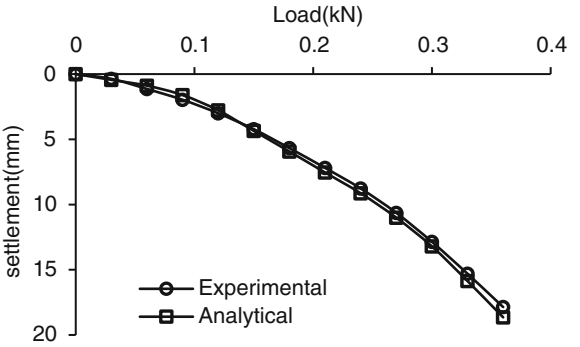

Fig. 10 Load-settlement curve of clay with jhama column

6 Summary and Conclusion

Stone columns improve the bearing capacity of soft clayey soils by introducing a good drainage path and bearing the load through friction. The hardness and porosity of compacted stones make it ideal as granular column material. Since jhama is cheaper, easily available and possess similar properties as stone, the utility of jhama as replacement of stone in granular columns is studied in this work. Following conclusions are drawn from this study:

- The load carrying capacity of foundation on soft clayey soil increases due to the introduction of stone column and jhama column.
- Initially stone column takes more load than jhama column up to a certain settlement. But later on, the settlement rate of stone column is very high and subsequently jhama column takes higher load than stone column.
- The load-settlement curve of stone column shows a clear failure load, whereas that of jhama column does not show a clear failure load. Hence it can be assumed that the load-settlement curve of stone column resembles a general shear failure and that of jhama column resembles a local shear failure.
- The ultimate load bearing capacity of soft soil is increased by 2.1 times by using stone column and 1.8 times by using jhama column.

- The improvement factor of stone column is almost constant ranging in between 1.7 and 1.9 at different normalized settlements. But the improvement factor of jhama column gradually increases from 1.5 to 2.0 for a normalized settlement range of 2–20%. The reason may be that initially the angular corners of the jhama chips get broken and hence the column takes lesser load. With increasing stress, the jhama chips get rearranged into a denser form and carry larger load than stone.
- The load-settlement curves obtained from numerical analysis are very close to experimental curves.
- As a bottom line it can be concluded that jhama is a fairly good substitute of stone for construction of granular columns in soft clay.

References

Abdi, M. R., & Zandieh, A. R. (2014). Experimental and numerical analysis of large scale pull out tests conducted on clays reinforced with geogrids encapsulated with coarse material. *Geotextiles and Geomembranes, 42*, 494–504.

Ambily, A. P., & Gandhi, S. R. (2007). Behavior of stone columns based on experimental and FEM analysis. *Journal of Geotechnical and Geoenvironmental Engineering, 133*(4), 405–415.

Barksdale, R. D., & Bachus, R. C. (1983). *Design and construction of stone columns vol. I* (Report No. FHWA/RD-83/026). US Department of Transportation, Federal Highway Administration.

Dash, S. K., & Bora, M. C. (2013). Improved performance of soft clay foundations using stone columns and geocell-sand mattress. *Geotextiles and Geomembranes, 41,* 26–35.

Ghazavi, M., & Afshar, J. N. (2013). Bearing capacity of geosynthetic encased stone columns. *Geotextiles and Geomembranes, 38,* 26–36.

IS: 15284 (Part 1) (2003). *Design and construction for ground improvement—guidelines*. Bureau of Indian Standards, New Delhi, India.

Murugesan, M., & Rajagopal, K. (2007). Model tests on geosynthetic-encased stone columns. *Geosynthetics International, 14*(60), 346–354.

Poorooshasb, H. B., & Meyerhof, G. G. (1997). Analysis of behavior of stone columns and lime columns. *Computers and Geotechnics, 20*(1), 47–70.

Schweiger, H. F., & Pande, G. N. (1986). Numerical analysis of stone column supported foundations. *Computers and Geotechnics, 2,* 347–372.

Yadu, L., & Tripathi, R. K. (2013). Effect of the length of geogrid layers in the bearing capacity ration of geogrid reinforced granular fill-soft subgrade soil system. *Procedia - Social and Behavioral Sciences, 104,* 225–234.

Laboratory Study on the Performance of Geosynthetic Reinforced Sand Bed

B. Ram Priya and M. Muttharam

Abstract Layout and configuration of reinforcement play a vital role in improvement of geosynthetic reinforced foundation soil. In the present study, laboratory performance of square footing resting on geosynthetic reinforced sand bed of given density is analyzed. The configuration of the reinforcement is altered by varying parameters such as number of reinforcing layers and vertical spacing of reinforcement. The concept of pressure bulb is used while designing the layout of reinforcement. By this method, breadth of the reinforcement varies with depth corresponding to the breadth of pressure bulb at the particular depth. The effect of breadth of reinforcement is compared in every case by providing uniform breadth of reinforcement. Aluminum angles are used as anchors in the reinforcement. Presence of anchors improves the foundation soil by the development of passive resistance. The rate of improvement is studied by varying the position and height of anchors. It is observed that, reinforcement increases the bearing capacity and reduces the settlement at a particular load. Providing reinforcement breadth with respect to pressure bulb gives comparable results with the reinforcement of uniform breadth. The influence of breadth of reinforcement is more pronounced in case of single layer of reinforcement. The improvement in bearing capacity is about 2.8 times with the inclusion of reinforcement and about 3.9 times with the inclusion of anchors. By the inclusion of anchors at various positions, a layer of reinforcement can be reduced.

Keywords Geosynthetics · Bearing capacity · Anchors

B. Ram Priya (✉) · M. Muttharam
Department of Civil Engineering, Anna University, Guindy, Chennai 600 025, India
e-mail: b.rampriya@gmail.com

M. Muttharam
e-mail: muttharam@annauniv.edu

T. Thyagaraj (ed.), *Ground Improvement Techniques and Geosynthetics*, Lecture Notes in Civil Engineering 14, https://doi.org/10.1007/978-981-13-0559-7_18

1 Introduction

Reinforcing the foundation soil is one of the popular methods of ground improvement. Many materials such as natural fibers, metallic strips and geosynthetics are used as reinforcing materials. Binquet and Lee (1975a, b) have done a pioneering study on the behavior of reinforced soil with length of reinforcement much larger than the footing width. Huang and Tatsuoka (1990) worked with reinforcement having length equal to the width of the footing and concluded that reinforcement beyond the footing width contribute secondarily to the improvement in the bearing capacity. Many researchers have studied the beneficial effects of geosynthetic reinforcements (Fragszy and Lawton 1984; Huang and Tatsouka 1990; Khing et al. 1993; Yetimoglu et al. 1994; Adams and Collin 1997; Huang and Menq 1997; Shin and Das 1999; Kumar and Saran 2003; Michalowski and Shi 2003; Kumar et al. 2007; Latha and Somwanshi 2009 and Dixit and Patil 2014; Panda and Ray 2014; Ronad 2014). The above studies revealed that layout and configuration of reinforcement plays an important role in the improvement apart from the tensile strength and density of foundation soil.

In this study an attempt has been made to reduce both the width and depth of excavation without compromising on the improvement. The experimental program is designed to achieve the above-mentioned objective. The concept of pressure bulb is used to arrive at the breadth of reinforcement. Anchors are introduced in the reinforcement for further increase in bearing capacity and reduction in settlement. Laboratory plate load tests are conducted on model square footing resting both on reinforced and unreinforced sand bed. The parameters varied in the program are number of reinforcing layers (N), vertical spacing of reinforcement (h), breadth of reinforcement (b), height of anchors (h_a) and spacing of anchors.

2 Tests on Model Footing

2.1 Test Equipment

Laboratory plate load test are conducted on 100 mm steel square plate placed on the surface of sand bed of relative density 65% filled in a cubical steel tank of size 740 mm. Load is applied through loading frame by means of hand operated hydraulic jack. Proving ring and two dial gauges placed along the diagonal are used for the measurement of load and settlement respectively. Desired unit weight of sand bed is achieved through controlled pouring and tamping technique.

2.2 Test Materials

The test medium in the study is of medium sand classified as poorly graded sand (SP) as per IS classification system. The angle of internal friction by means of direct

shear test is 37° conducted at a unit weight of 16.6 kN/m^3. Geonet CE-121 is used as reinforcing material having tensile stiffness of 300 kN/m. Aluminum angles are used as anchors and are attached to geonet with bolt and nut arrangement.

2.3 Test Program

All reinforcement layers used are square in shape. The location of top layer of reinforcement is kept constant as 0.3*B* from the bottom of the footing. The geometric parameters used in the study are shown in Fig. 1.

A model plate load test is done in unreinforced and four groups of tests are done in reinforced sand bed. Details of the experimental program are shown in Table 1.

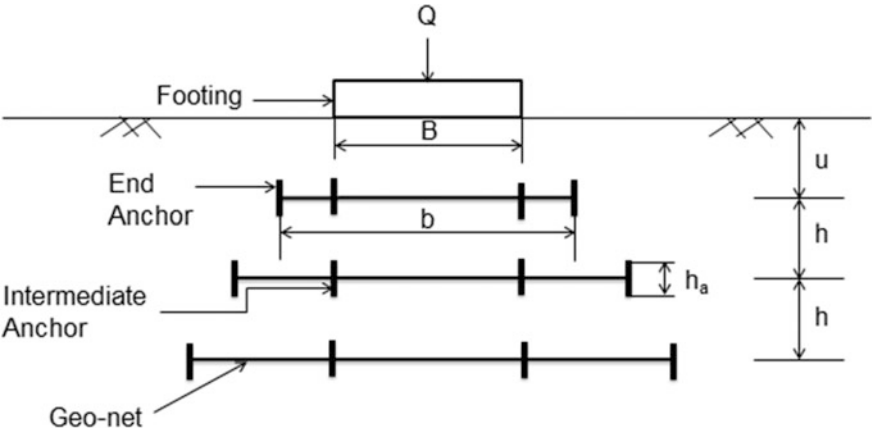

Fig. 1 Typical diagram defining various geometric parameters

Table 1 Details of experimental program

1	N = 1, 2, 3 h = 0.2B, 0.3B, 0.4B	2	N = 1, 2, 3 h = 0.2B, 0.3B, 0.4B
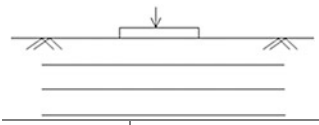		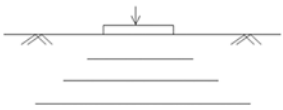	
3	N = 1, 2, 3 h = 0.3B h_a = 0.1B, 0.25B, 0.38B	4	N = 1, 2, 3 h = 0.3B h_a = 0.25B
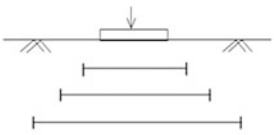		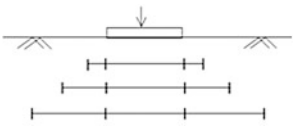	

3 Results of Tests

3.1 Effect of Breadth of Reinforcement (b)

To study the effect of breadth of reinforcement in the improvement of bearing capacity, the results from group 1 and 2 are compared. The ultimate bearing capacity is obtained from the load-settlement curve by tangent intersection method. The ultimate bearing capacity obtained for reinforced sand bed is divided by that obtained for unreinforced sand bed which is called the bearing capacity ratio (BCR). Figure 2 represents the load-settlement behavior of footing when the reinforcements provided are of varying breadth as per pressure bulb. In both groups, increase in BCR is observed with the increase in number of reinforcing layers. There is not much improvement observed in the BCR with respect to vertical spacing as proposed by Yetimoglu et al. (1994). However, a slight decrease in BCR is obtained with the increase in vertical spacing of reinforcement in case of three layered reinforcement. This may be due to the fact that, the volume of reinforcement present within the pressure bulb of influence reduces, which leads to the reduction in the resistance offered by the reinforcement which resulted in decrease in BCR.

Figure 3 shows the effect of breadth of reinforcement in BCR. The difference in BCR values for both groups where other parameters remains the same is around 35% for single-layered, 4% for double-layered, and 0% for three-layered reinforcement. It is clear that for multi-layered reinforcement, the influence of breadth of reinforcement in the bearing capacity is negligible. Except for single-layered reinforcement, breadth provided according to the pressure bulb is sufficient to cover the shear zone developed below the footing.

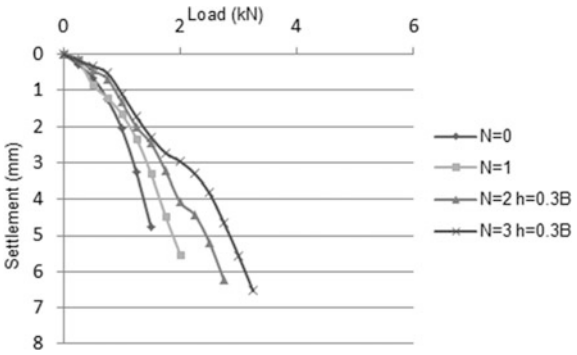

Fig. 2 Load-settlement plot for sand bed with reinforcing layers of vertical spacing 0.3*B*

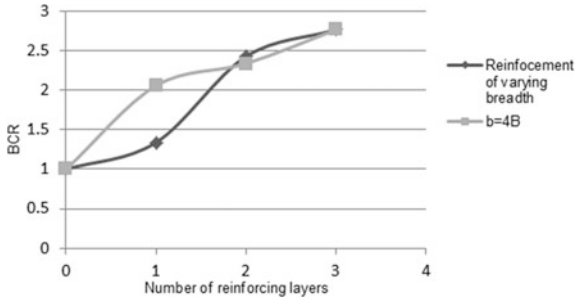

Fig. 3 Number of reinforcing layers–BCR plot for given breadth of reinforcement

3.2 *Effect of End Anchors*

In group 3, tests were conducted to study the effect of end anchors in reinforcement and the influence of their height (0.1*B*, 0.25*B* and 0.38*B*). Figure 4 represents the load-settlement behavior of footing when end anchors are provided in the reinforcement layers. The increase in BCR with anchored reinforcement ($h_a = 0.1B$) compared to unanchored reinforcement for three layered reinforcement is 3.5%. It is seen that anchors reduces the settlement at a particular load and overall settlement of the reinforced sand bed.

The height of anchors is increased to achieve further increase in BCR. Figure 5 shows the variation of BCR with the height of end anchors. The maximum increase

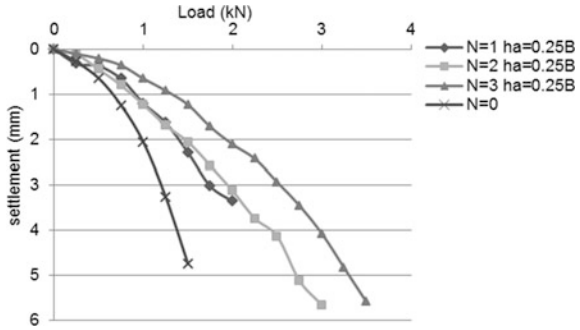

Fig. 4 Load-settlement plot for sand bed with reinforcing layers of vertical spacing of 0.3*B* and 0.25*B* anchor height

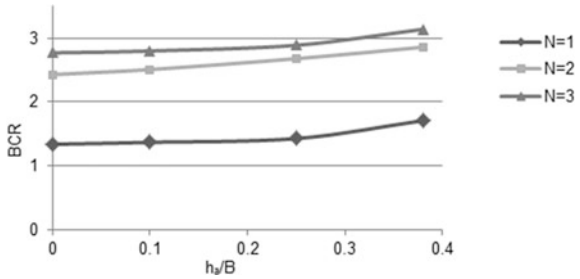

Fig. 5 h_a/B–BCR plot for given number of reinforcing layers

obtained is about 13.4%. Considering practically, 0.25*B* is taken as the optimum value of height of anchors. It is also observed that the effect of end anchors is increasing with the number of reinforcing layers.

3.3 *Effect of Intermediate Anchors*

Group 4 tests were done to learn behavior of intermediate anchors along with the end anchors. The improvement is further increased with the introduction of intermediate anchors. It seen that there is a linear relation between bearing capacity ratio and number of reinforcing layers when the anchors are introduced at the intermediate positions. The improvement due to intermediate anchors is more pronounced in case of three-layered reinforcement than in case of single and doubled-layered reinforcement as seen in Fig. 6. This is because of two facts. One is, more number of anchors means more soil involved in the development of passive resistance and the resistance is more. Also anchors act as metallic strips in sand which led to the improvement of reinforced soil.

Figure 7 compares the variation of bearing capacity ratio with the number of reinforcing layers for the case of reinforcement with uniform breadth and reinforcement with intermediate anchors. It is inferred from the graph that the improvement obtained with reinforcement of breadth 4*B* and three reinforcing

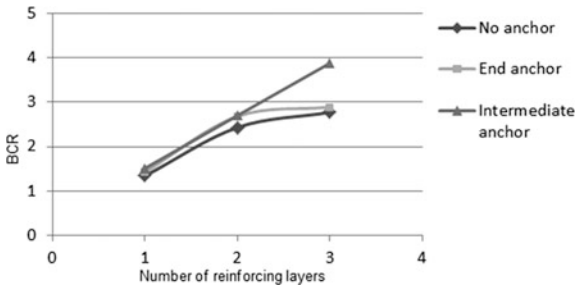

Fig. 6 Number of reinforcing layers–BCR plot for various anchor spacing

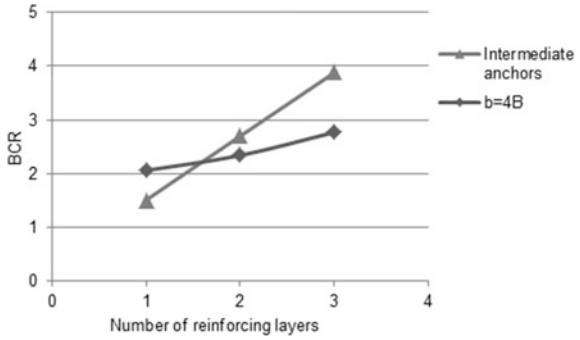

Fig. 7 Number of reinforcing layers–BCR plot for reinforcement of uniform breadth and reinforcement with intermediate anchors

layers can be obtained by using two layers of reinforcement with intermediate anchors. Thus the overall depth of reinforcement is reduced. Since the breadth of anchored reinforcements is provided as per pressure bulb, the improvement is less in case of single layer of reinforcement. Extend of failure surface will be large in horizontal direction below the footing. Hence, wider layer is needed in case of single-layered reinforcement.

4 Conclusion

The primary objective of the present investigation is to study the performance of square footing resting on sand bed with and without reinforcement. Accordingly, tests were conducted on model square footing resting on sand bed by varying the parameters like number of reinforcing layers, vertical spacing between reinforcing layers, breadth of reinforcement, height of anchors and spacing of anchors. The experimental results are discussed and the important conclusions drawn from the study are presented below.

Except for single layer of reinforcement, the reinforcement of uniform breadth and reinforcement of varying breadth as per pressure bulb gives comparable improvement in the bearing capacity. This implies that without compromising on bearing capacity, the breadth of reinforcement could be reduced if pressure bulb is considered for deciding the breadth of the reinforcement. Influence of vertical spacing of reinforcement on improvement of ultimate bearing capacity and settlement is marginal. Provision of end anchors provides good improvement in both the load carrying capacity and settlement, due to the development of passive resistance. The maximum BCR gained in case of reinforcement alone is 3.14 and that of reinforcement with end anchors is 3.88 where all other parameters remain the same. Higher the anchor height more the soil involved and hence better improvement. Addition of anchors at the intermediate positions outshines the performance of reinforcement with uniform breadth in both the load carrying capacity and settlement. A layer of reinforcement may be saved with the provision of intermediate anchors.

References

Adams, M. T., & Collin, J. C. (1997). Large model spread footing load tests on geosynthetic reinforced soil foundations. *Journal of Geotechnical and Geoenvironmental Engineering, 123* (1), 66–72.

Binquet, J., & Lee, K. L. (1975a). Bearing capacity tests on reinforced earth slabs. *Journal of the Geotechnical Engineering Division, 101*(12), 1241–1255.

Binquet, J., & Lee, K. L. (1975b). Bearing capacity analysis of reinforced earth slabs. *Journal of the Geotechnical Engineering Division, 101*(12), 1257–1276.

Dixit, M. S., & Patil, K. A. (2014). Effect of reinforcement on bearing capacity and settlement of sand. *Electronic Journal of Geotechnical Engineering, 19,* 1033–1046.

Fragszy, R. J., & Lawton, E. (1984). Bearing capacity tests of reinforced sand subgrades. *Journal of Geotechnical Engineering, 110*(10), 1500–1507.

Huang, C. C., & Menq, F. Y. (1997). Deep footing and wide slab effects in reinforced sandy ground. *Journal of Geotechnical and Geoenvironmental Engineering, 123*(1), 30–36.

Huang, C. C., & Tatsouka, F. (1990). Bearing capacity of reinforced horizontal sandy ground. *Geotextiles and Geomembranes, 9,* 51–82.

Khing, K. H., Das, B. M., Puri, V. K., Cook, E. E., & Yen, S. C. (1993). The bearing capacity of a strip foundation on geogrid-reinforced sand. *Geotextiles and Geomembranes, 12*(4), 351–361.

Kumar, A., & Saran, S. (2003). Closely spaced footings on geogrid reinforced sand. *Journal of Geotechnical and Environmental Engineering, 129,* 660–994.

Kumar, A., Ohri, M. L., & Bansal, R. K. (2007). Bearing capacity tests of strip footings on reinforced layered soil. *Geotechnical and Geological Engineering, 25,* 139–150.

Latha, G. M., & Somwanshi, A. (2009). Bearing capacity of square footings on geosynthetic reinforced sand. *Geotextiles and Geomembranes, 27,* 281–294.

Michalowski, R. L., & Shi, L. (2003). Deformation patterns of reinforced foundation sand at failure. *Journal of Geotechnical and Geoenvironmental Engineering, 129*(5), 439–449.

Panda, S., & Ray, N. H. S. (2014). A study on behavior of centrally loaded shallow foundation on sand bed reinforced with geogrid, failure and improvement. *International Journal of science, Engineering and Technology Research, 3*(7), 1896–1903.

Ronad, H. (2014). An experimental study of square footing resting on geogrid reinforced Sand. *International Journal of Research in Engineering and Technology, 3*(5), 177–181.

Shin, E. C., & Das, B. M. (1999). Bearing capacity of strip foundation on geogrid-reinforced sand. In *Proceedings of the XI Asian Regional Conference on Soil Mechanics and Geotechnical Engineering* (pp. 189–192), Seoul.

Yetimoglu, T., Wu, J. T. H., & Saglamer, A. (1994). Bearing capacity of rectangular footings on geogrid-reinforced sand. *Journal of Geotechnical Engineering, 120*(12), 2083–2099.

Repeated Load Response of Encapsulated Granular Trench Supported Footings on Embankments

Sony Sanjeev and N. Unnikrishnan

Abstract Geosynthetic encapsulated granular trenches (EGT) have found to improve the load carrying capacity of strip footings situated on weak soil under monotonic load. Granular trench is a two-dimensional plane strain variant of stone column. The EGT is formed by wrapping a geosynthetic around the granular trench. In the investigation reported herein, repeated load behaviour of EGT supported strip footings situated on earth embankments was studied. Repeated load tests were carried out on model strip footings resting on granular trenches with and without encapsulation. A cyclic hydraulic actuator with control and data acquisition facilities was used. River sand was used to prepare the embankment and 6 mm aggregate was used as the fill for the trench. Geogrid reinforcement was used for encapsulation. Non linear finite element simulations were carried out to arrive at the optimum dimensions of the EGT under monotonic loading. The optimum dimension thus obtained was used for repeated load studies. Influence of magnitude and frequency of repeated loading were investigated through experiments. Details of test setup, experimental programme, observations and results are discussed in the paper. It was found that the EGT system effectively improves the bearing capacity of footings situated on earth embankments under repeated loading.

Keywords Encapsulated granular trench · Repeated loading · Slope stability
Strip footings

S. Sanjeev · N. Unnikrishnan (✉)
Department of Civil Engineering, College of Engineering Trivandrum, Kerala, India
e-mail: unnikrishnan_n@yahoo.com

S. Sanjeev
e-mail: sonysanjeev@cet.ac.in

T. Thyagaraj (ed.), *Ground Improvement Techniques and Geosynthetics*, Lecture Notes in Civil Engineering 14, https://doi.org/10.1007/978-981-13-0559-7_19

1 Introduction

Strip footings on sloping surfaces or adjacent to a sloped crest are widely used in situations such as for bridge abutments. Railway tracks resting on ballasts can also be considered as footings on the crest of slopes. The estimation of the ultimate load capacity and the load-settlement behaviour of such foundations are important for their safe and efficient design. Granular Trench (GT) has been proved to be effective in resisting static as well as repetitive load (Madhav and Vitkar 1978). In the case of bridge structures, the positioning of an abutment in relation to the edge of an embankment fill has implications on the safety of the bridge abutment and also on the economic efficiency of the overall design of the bridge structure (Lee and Manjunath 2000). Granular trench is a two dimensional plane strain variant of stone column. An encapsulated granular trench is formed by wrapping a geosynthetic around the granular trench (Unnikrishnan et al. 2010). First of all the trench is excavated to the desired level. The geosynthetics are then spread on the surface of the trench with the edges unfolded over the ground surface. The trench is then filled with granular material to the desired level at the desired relative density. The granular trench is then wrapped in the geosynthetic by keeping the edges left over together. Over this the footing construction can be carried out (Unnikrishnan et al. 2011).

The conventional method of slope stability improvement is by the incorporation of soil reinforcing techniques to enhance the load carrying capacity and settlement behaviour (Selvadurai and Gnanendran 1989). The inclusion of encapsulated granular trenches under strip footing near slopes or on embankments is a new area of research although its application on level ground has been studied earlier (Mathai and Unnikrishnan 2015). The present investigation aims at the study of the behaviour of strip footings near sandy slopes supported on rectangular granular trenches under repeated loading condition. The comparison of performance with and without geosynthetic encapsulation has been made.

2 Materials Used

2.1 Bulk Soil

River sand at low relative density was used as the bulk soil resembling the weak slope fill. Relative density of the sand fill was controlled by sand raining (pluviation) technique. The physical properties of the river sand used to form the weak soil is listed in Table 1. The particle size distribution was determined using the dry sieving method and the results are shown in Fig. 1. Procedures in the relevant IS codes were followed in the determination of the properties.

Table 1 Properties of river sand and aggregate

Property	River sand	Aggregate
Effective particle size (D_{10}), mm	0.2	2
Uniformity coefficient (C_u)	2.15	3.6
Coefficient of curvature (C_c)	1.27	3.56
Cohesion (c) (kN/m^2)	0	0
Friction angle (φ) (°)	30	35
Maximum density (γ_{max}) (kN/m^3)	15.8	–
Minimum density (γ_{min}) (kN/m^3)	14.8	–
Bulk density (γ) (kN/m^3)	–	17.5
Specific gravity (G)	2.68	2.7

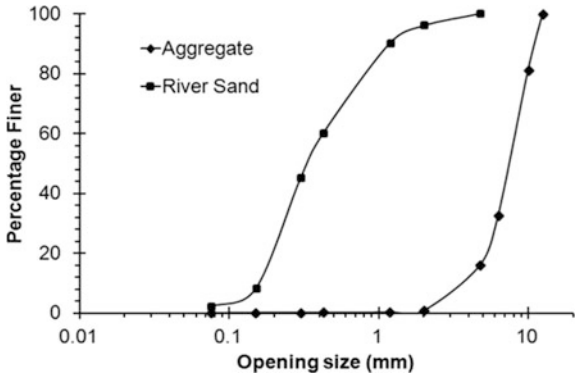

Fig. 1 Particle size distribution curve

2.2 Aggregates

Aggregates passing through 10 mm IS sieve were used as the replacement material within the excavated trench. The properties of aggregates determined are given in Table 1 and particle size distribution is shown in Fig. 1.

2.3 Geogrids

Two different types of geosynthetics were used to encase or wrap the granular trench, namely Grid-1 and Grid-2, the properties of which are given in Table 2. Grid-1 was used for separating the bulk soil and gravel, without getting mixed each other. Grid-2 was used as the structural support for EGT. Together it formed the encapsulation for the granular trenches.

Table 2 Properties of geogrids used

Property	Grid-1	Grid-2
Thickness (mm)	1	5 (at node)
Mass per unit area (g/m^2)	240	265
Opening size	Diamond, 2 mm × 2 mm	Square, 37 mm × 37 mm
Tensile strength (kN/m)	1.2	11.35
Strain at specified tensile strength (%)	80	25

3 Finite Element Analysis

The optimum size and position of the trench to be used below the strip footing was fixed by performing nonlinear finite element analysis. Initial configuration of rectangular granular trench was obtained from previous studies (Mathai and Unnikrishnan 2015).

Two-dimensional plane strain finite element analysis were carried out. Fifteen-noded triangular elements were selected to model the soil, the aggregate and the footing. Soil and aggregate were modelled using elastic-plastic Mohr–Coulomb model. The geosynthetic was modelled using the geogrid element in the PLAXIS element library, essentially a two dimensional linear bar element. Footing was modelled as linearly elastic material made of mild steel as in the experimental investigation. The properties of sand, gravel, geogrid, and footing to be used in the experimental programme were used in the numerical study. Table 3 shows the material parameters which were used in Mohr–Coulomb Model. Automatic mesh generation facility was used. Refinements were applied to the mesh and the optimum level of refinement was chosen based on analysis of model footings. Figure 2 shows a typical finite element mesh used for the analysis. The footings were assumed to be located on the ground surface. The effect of water table was not taken into consideration.

Footings supported on rectangular trenches of top widths 15, 30, 45, and 60 cm were analysed. The respective depths were 5, 10, 15, and 20 cm, maintaining a width to depth ratio of 3 throughout. Second configuration was found optimum by comparing with the experimental results conducted simultaneously in the laboratory under similar conditions.

Table 3 Material set and parameters used in the modelling

Property	River sand	Aggregate	Geogrid	Footing
E (kPa)	40,000	60,000	50,000	2.1×10^8
Cohesion (c) (kPa)	1	1	–	–
Friction Angle (φ) (°)	30	35	–	–
Unit weight (γ) (kN/m^3)	16	18	–	–
Poisson's Ratio (υ)	0.3	0.35	–	–

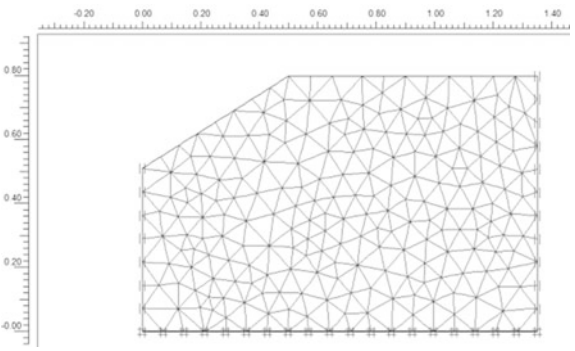

Fig. 2 Typical mesh used for the analysis

4 Experimental Investigation

A model strip footing, 0.135 m wide, 0.78 m long, and 0.05 m thick, made of steel was used for the load tests. Details of test tank are shown in Fig. 3. Loads were applied through an automated computer-controlled hydraulic cyclic loading equipment. The data acquisition system was also associated with the machine and the settlement values corresponding to time period were recorded automatically.

Soil bed was formed by sand pluviation method at 40% relative density. Two thin wooden planks were used to create the trench. The river sand bed was formed up to the bottom level of proposed trench. Then the wooden planks with desired spacing were kept in position. For EGT, the geosynthetic was placed below the frame. River sand was placed outside the trench. Aggregates were placed within the trench keeping the geosynthetic close to the timber planks. The frame was lifted in stages. On reaching the final height, the geosynthetic was overlapped and EGT is

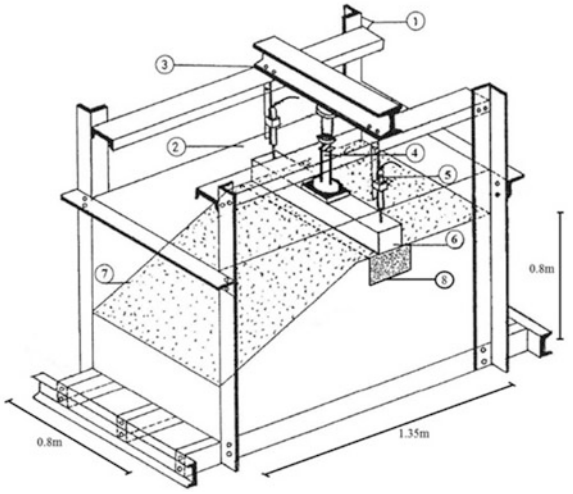

Fig. 3 Three dimensional view of the model test setup (not to scale). 1 loading frame; 2 test tank; 3 reaction frame; 4 loading piston; 5 LVDT; 6 model footing; 7 sand slope; 8 granular trench

completed along with a cover of about 2 cm. Then the slope was cut without disturbing the remaining portion. The footing was placed over the completed trench and finally the load was applied.

5 Results and Discussions

For the purpose of comparison of the performance of footings over various tests, three dimensionless parameters-Settlement Ratio (SR), Load Ratio (LR) and Percentage Reduction in Settlement (PRS) were used. SR is expressed as the ratio of the settlement of the model footing to the width of the footing. In the present investigation, width of the model footing was kept constant at 135 mm. The loads are expressed in terms of load ratio, which is obtained by taking the ratio of load values to the ultimate load (q_m). PRS is the difference between settlement ratios of granular trenches and encapsulated granular trenches expressed in percentage.

Figure 4 shows the variation of monotonic load with Settlement Ratio (SR) for a strip footing supported on bulk soil alone. This unreinforced test was the reference test for comparison with the upcoming repeated load tests on footings over granular trench with geosynthetic encapsulation. Load corresponding to 20% SR was considered to be the ultimate load. Accordingly, the ultimate load obtained was 5.67 kN/m, which corresponds to 452 kg of load applied through the cyclic hydraulic actuator. This ultimate monotonic load designated as q_m was used to obtain the load ratios in the following experiments.

The efficient configuration obtained from finite element analysis was adopted in all the trenches which followed. In order to study the influence of frequency, repeated loading tests were performed at frequencies of 1, 2, and 3 Hz and the load amplitude for repeated load test was kept constant at 60% of q_m. Further higher frequencies were not employed due to difficulties experienced with the test tank and

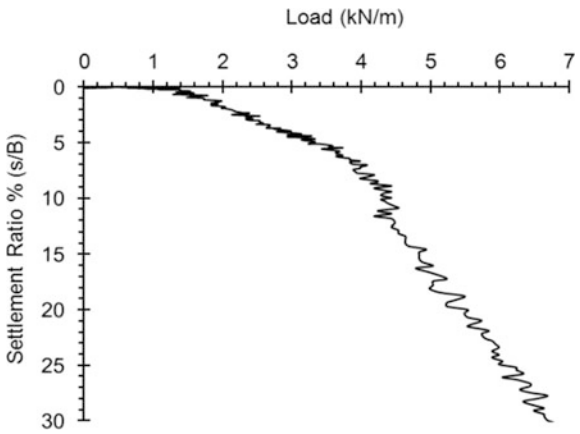

Fig. 4 Variation of load with SR for river sand alone

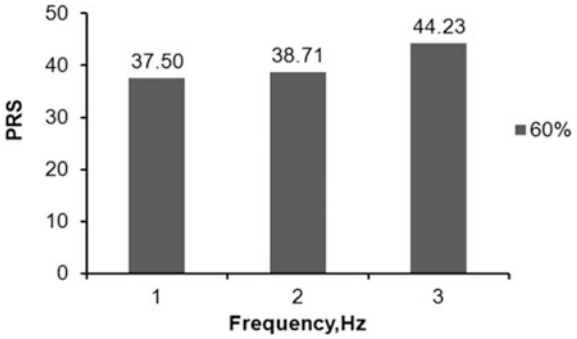

Fig. 5 Variation of PRS with frequency of loading

loading system. Tests were conducted on strip footings with encapsulation and without encapsulation separately. Figure 5 shows the variation of the percentage reduction in settlement for 1000 cycles with respect to frequency, due to the provision of encapsulation to GT. It can be observed that there is an increase in improvement due to encapsulation, and this is more at higher frequencies.

In order to study the influence of load amplitude, repeated loading tests were done at amplitudes of 60, 40, and 20% of q_m and the frequency for repeated load test was kept constant at 3 Hz, since maximum PRS was found to be at 3 Hz in the previous test series. Tests were conducted on strip footings with encapsulation and without encapsulation separately. Figure 6 shows the percentage reduction in settlement for 1000 cycles against the variation in amplitude. It was observed that the efficiency increases initially and then slightly decreases.

The load carrying capacity has improved considerably after repeated loading test. This may be accounted to the rearrangement of granular particles to a much better and closer configuration which gives increased load carrying capacity to the strip footing. Encapsulation of GT gives further improvement by preventing the lateral spreading of granular material into the weak soil. Failure was not observed anywhere throughout the test. This may be due to the lesser number of cycles for which the test was performed and the absence of water table during the tests.

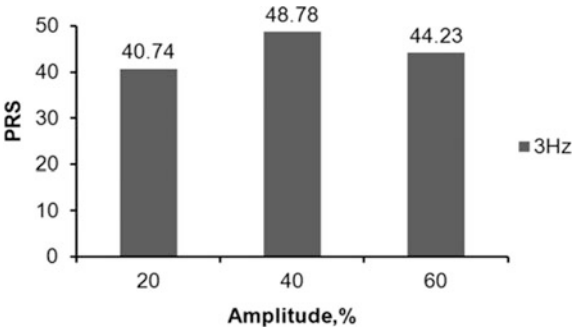

Fig. 6 Variation of PRS with amplitude of loading

The improved load carrying capacity can be accounted to the confinement provided by geogrid layer. The possible reason could be deep footing effect. When the restraining force exerted by EGT is imposed on soil particles, the reorientation of the associated strain characteristics occurs near the geogrid. A part of the reinforced zone where relatively large force has developed behaves like a part of the rigid footing and a major part of the footing load is transferred into a deeper zone, thereby reducing the settlement for a given repeated load amplitude.

6 Conclusions

The results of investigations showed that encapsulation with geogrid improve the load carrying capacity of granular trench under repeated loading. The general conclusions from the investigation are

- Provision of EGT reduced settlement of the model strip footing by 35% than GT under repeated loading condition.
- Efficiency of encapsulation was found to be more at higher frequencies due to the rearrangement of aggregates within the confinement of geosynthetics.
- Geosynthetic encapsulation improves efficiency with higher amplitudes of load. After reaching maximum efficiency it decreases slightly.

References

Lee, K. M., & Manjunath, V. R. (2000). Experimental and numerical studies of geosynthetic reinforced sand slopes loaded with a footing. *Canadian Geotechnical Journal, 37,* 828–842.

Madhav, M. R., & Vitkar, P. P. (1978). Strip footing on weak clay stabilized with a granular trench or pile. *Canadian Geotechnical Journal, 15*(4), 605–609.

Mathai, B., & Unnikrishnan, N. (2015). Repeated load behaviour of strip footings on encapsulated granular trenches. In *Proceedings of the National Conference on Technological Trends* (NCTT 2015), 14–16 Sept 2015, College of Engineering Trivandrum, pp. 201–206.

Selvadurai, A. P. S., & Gnanendran, C. T. (1989). An experimental study of a footing located on a sloped fill: Influence of a soil reinforcement layer. *Canadian Geotechnical Journal, 26*(3), 467–473.

Unnikrishnan, N., Rajan, S., & Johnson, A. S. (2010). Response of strip footings supported on granular trench. In *Proceedings of the Indian Geotechnical Conference* (IGC 2010), GeoTrendz, 16–18 Dec 2010, Indian Institute of Technology Bombay, pp. 525–528.

Unnikrishnan, N., Rajan, S., & Johnson, A. S. (2011). Bearing capacity of strip footings on encapsulated granular trenches. In *Proceedings of the Indian Geotechnical Conference*, (IGC 2011), Geochallenges, 15–17 Dec 2011, Kochi, pp. 191–194.

Re-Appraisal of the Physico-Mechanical Stability of Lime Treated Soils

C. Cherian and D. N. Arnepalli

Abstract The quantification of the kinetics of short-term clay–lime interactions is a key step for optimizing the parameters during lime stabilization of fine-grained soils, and also for predicting the long-term performance of lime treated soil matrix. The existing scientific literatures often believed that monitoring of consistency limits as well as compaction characteristics of lime treated soils yield significant amount of information regarding their physico-mechanical behaviour. However, apparently limited extent of works has been carried out to assess the role of clay mineralogy and pore fluid chemistry on inherent variations in plasticity and compaction characteristics. Further, no definite single conclusion could be drawn from the previous studies conducted to comprehend the plausible mechanisms of stabilization occurring in the lime treated soils during short-term and long-term interaction periods.In order to enhance the current understanding, this study primarily focused on the critical evaluation of plasticity properties and compaction characteristics variations of lime treated soils with respect to change in pore fluid chemistry (such as pH and concentration of lime). The study employed soils with quite diverse physico-chemical and mineralogical compositions so as to highlight the role played by the clay mineralogy in governing the extent of short-term improvement that can be mobilized by lime treatment. Based on the significant observations gathered from experimental works, attempts have been made to elucidate the possible short-term mechanisms of lime stabilization which also contribute to long-term strength and durability of lime treated soil.

Keywords Lime stabilization · Plasticity · Compaction · Mineralogy
Pore fluid chemistry

C. Cherian (✉) · D. N. Arnepalli
Department of Civil Engineering, Indian Institute of Technology Madras,
Chennai 600036, India
e-mail: chinchu0401@gmail.com

D. N. Arnepalli
e-mail: arnepalli@iitm.ac.in

T. Thyagaraj (ed.), *Ground Improvement Techniques and Geosynthetics*, Lecture Notes in Civil Engineering 14, https://doi.org/10.1007/978-981-13-0559-7_20

1 Introduction

In the present era of continuous and steadfast developments in industrial sector and expansion of urban areas, lime stabilization is an attractive proposition for upgrading workability and engineering performance of in situ problematic fine-grained clayey soils. In the course of lime stabilization, calcium (Ca^{2+}) and hydroxyl (OH^{-}) ions from lime, upon interaction with water, dissolves into the soil pore solution. The free Ca^{2+} ions are momentarily adsorbed on to negatively charged sites of clay minerals by cation exchange, and concurrently OH^{-} ions raises pH of pore solution. As a consequence, concentration of counter ions on charged clay surface increases, thereby resulting in contraction of diffused double layer and prompts flocculation-aggregation of soil particles.

The fundamental literatures state that instantaneous ion exchange reactions on charged surfaces of clay mineral platelets result in the drastic decline of soil plasticity (Marshall 1967). Further, pozzolanic reactions continue to occur between reactive clay minerals and free lime under appropriate conditions, leading to irreversible transformations of clay mineral phases and crystallization of new cementitious gels such as calcium-silicate and aluminate hydrates (Arabi and Wild 1986). Though, considerable amount of research has been devoted to evaluate the kinetics of soil–lime interactions. Yet, no definite conclusion could be arrived in order to comprehend the plausible effects of inherent clay mineralogy and pore fluid chemistry (pH and ionic strength) upon the consequent amendments occurring in lime treated soil matrix. In view of this, the primary objective of the present study is to critically evaluate the physico-mechanical modifications of lime treated soils in terms of plasticity and compaction properties variations with respect to change in pH and calcium ion concentration.

2 Material Characterization

The soils selected for the present study include commercially available kaolinite (designated as KT) and sodium bentonite (designated as NB). A commercial hydrated lime (calcium hydroxide, $Ca[OH]_2$), designated as HL, is used for the treatment of chosen soils. The selected soils are characterized by fairly different physical and geotechnical properties, as shown in Table 1.

In addition, the chemico-mineralogical properties are determined and presented in Table 2. The pH of virgin soils is determined as per BIS and ASTM standards; further, total SSA is measured by employing EGME adsorption technique (Arnepalli et al. 2008). The CEC of virgin soils is determined in accordance with standard guidelines, and buffer capacity is determined using nitric acid titration method (Yong et al. 1990).

Table 1 Physical and geotechnical properties

Properties	Soil type	
	KT	NB
Physical properties		
Specific gravity, G	2.64	2.73
Hygroscopic moisture content (%)	1.3	11.9
Consistency limits (%)		
Liquid limit	57	258
Plasticity index	38	226
Grain size distribution (% by weight)		
Gravel size	0	0
Sand size	32	0
Silt size	40	37
Clay size	28	63

Table 2 Chemico-mineralogical properties

Properties	Soil type	
	KT	NB
pH	5.4	10.2
Buffer capacity (cmols H^+/kg)	5.9	13.4
Specific surface area (m^2/g)	87.3	757.7
$CEC_{[Ca]}$ (meq./100 g)	42.3	88.6

3 Soil–Lime Compatibility Test

The compatibility of HL for successful stabilization of soils used in this study is evaluated in terms of optimal HL concentration required to achieve a highly alkaline pH equivalent to saturated lime pH of 12.4 (Eades and Grim 1966). For this purpose, batch tests are conducted by preparing samples of soil-lime suspensions (liquid-to-solid ratio of 10), blank lime suspensions (without soil) and control solutions (without lime) corresponding to different HL concentrations (i.e. 0–8% by dry weight of soil). These samples are homogeneously mixed using magnetic stirrer and conditioned using wrist-action shaker. Later, pH and electrical conductivity (EC) values are recorded at the end of one hour equilibration period using portable water quality analyser. The obtained results are presented in Fig. 1. Further, the test is continued for longer interaction periods for assessing the time-dependency of soil–lime reaction kinetics. It is noticed that both KT and NB show similar trends of pH and EC variation with time lapse; for the sake of brevity the results obtained for KT are presented in Fig. 2.

In Fig. 1, all samples show consistent increase in pH with HL addition, attributed to supply of free OH^- ions from lime dissolution. For blank lime solutions,

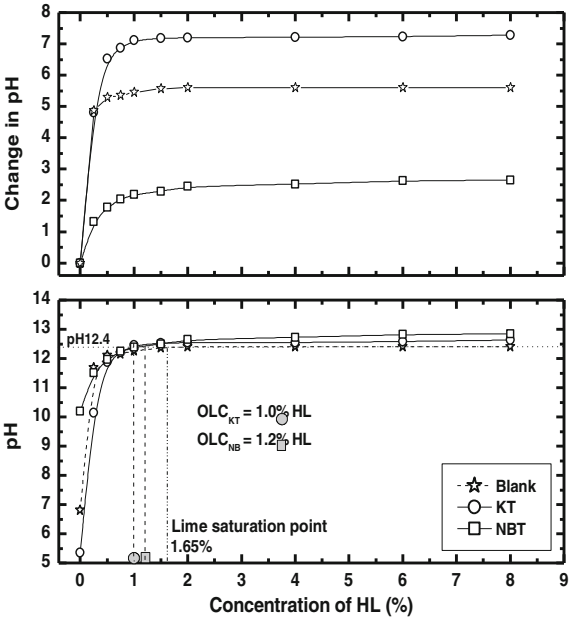

Fig. 1 pH versus HL concentration in batch experiment

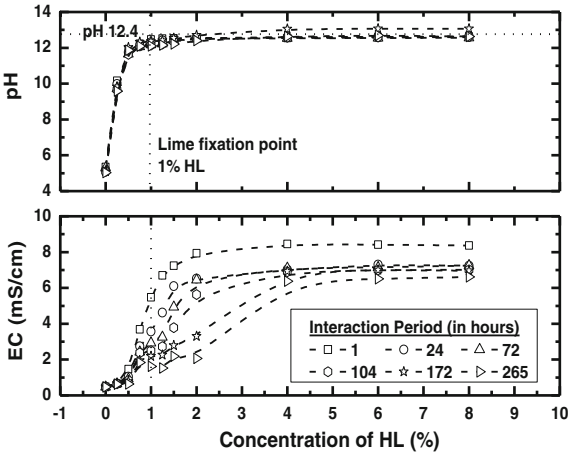

Fig. 2 Time-dependent variations of pH and EC for KT

maximum pH of 12.4 is obtained corresponding to 1.6% HL at 25 °C; this point is known as lime saturation. It is also observed that upon lime addition KT exhibits rise in pH by almost 7 units corresponding to 1% HL, whereas for NB pH raised by 2.5 units only, which is due to the higher pH buffering capacity of latter. Further,

the optimum lime content (OLC) corresponding to 12.4 pH is observed to be 1% for KT and 1.2% for NB (Eades and Grim 1966). It is worth to mention that soils with higher SSA and CEC values usually exhibit relatively higher OLC values as they demand more amount of lime to satisfy the affinity for nullifying their net charge deficiency However, in this study both KT and NB exhibit apparently similar OLC values although they have quite diverse chemico-mineralogical properties. This is hypothesized to be the combined masking effects of initial pH and buffer capacity values (Cherian and Arnepalli 2015).

Figure 2 presents time-dependent variations of pH and EC for KT; in general, both pH and EC attain maximum values at the end of one hour for both soils. With time elapse, pH exhibits a gradual decrement which might be owing to electrostatic attraction of OH^- ions by positively charged cations fixed on to clay platelet surface. Similarly, EC value decreases with elapsed time for both soils which can be attributed to continuous lowering of electrolyte concentrations as a result of ion exchange reactions (Bandipally et al. 2014). It is also worth to note that there is a shift in the rate of pH and EC variations when lime content reaches approximately 1% HL; this region marks lime fixation point with highest rates of cation exchange reactions. At this point, highly alkaline pH 12.4 of the medium induces maximum dissolution of reactive silica and alumina from clay minerals and initiates active pozzolanic reactions with excess free lime. As a result, new cementitious products are formed thereby reducing free ion concentration, and rate of change of pH and EC declines beyond lime fixation point.

4 Physico-Mechanical Properties of Lime Treated Soils

For assessing the short-term physico-mechanical stability of lime treated KT and NB soils, primarily the compaction characteristics of different soil-lime mixtures varying from 0 to 8% HL are determined by conducting standard proctor compaction tests as per ASTM guidelines (Fig. 3). It is clearly observed that addition of slightest amount of 2% HL causes drastic change in compaction characteristic curve, probably owing to cation exchange reactions (Al-Ne'aimi and Hussain 2010). Correspondingly, all soil–lime mixes show consistent relaxation of compaction curves characterized by relative decrement in maximum dry unit weight (MDW) and increment in optimum moisture content (OMC) with increasing lime content. This is more prominent in NB than KT indicating that the former becomes relatively less sensitive to moisture than the latter upon lime treatment.

The relative drop in MDW of soil–lime mixtures with increasing lime content is supposed to be partially attributed by the replacement of a specific proportion of soil by lime which has a rather low true density (2.2 g/cc) compared to virgin soil (2.6–2.8 g/cc). The other contributing factor might be the increase in total volume of voids in the compacted specimen owing to material bulking and textural changes as a result of flocculation-agglomeration phenomena. Further, the so formed coarser

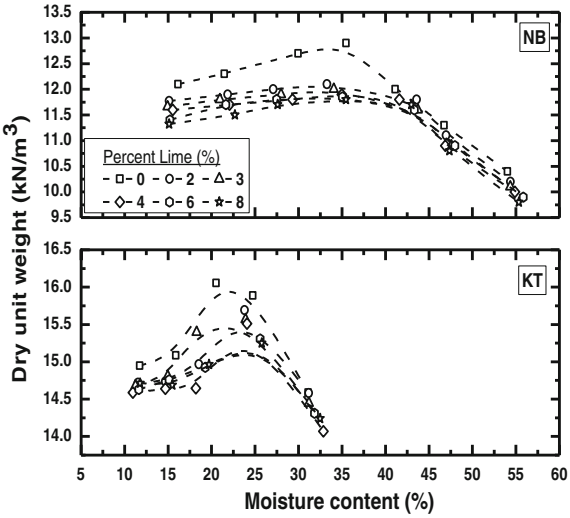

Fig. 3 Characteristic compaction curves of KT and NB

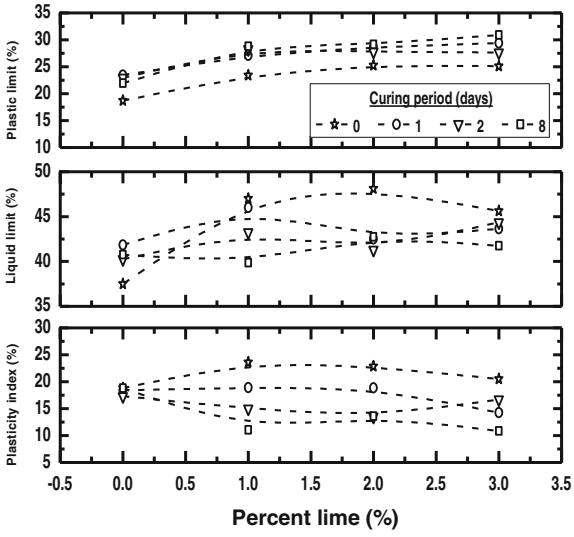

Fig. 4 Plasticity properties of lime treated KT

lumps occupy larger spaces and bind to form strong matrix which resist compaction and results in drop of MDW (Singh and Goswami 2012).

Similarly, rise in OMC upon lime treatment can be partially explained by higher water affinity of added lime particles. Yet another plausible reason might be high osmotic suction caused by increased cation concentration in soil-lime mixes, as well

as larger affinity for moisture to mobilize hydration of pozzolanic reaction products. Furthermore, the particle flocculation by cation exchange reduces total surface area of treated soil and raises water adsorption potential of clay particles, thereby enhancing the OMC value (Ramesh and Sivapullaiah 2011).

For further validation of short-term soil–lime reactions, variations of consistency limits with respect to lime content are evaluated, along with the effect of time elapse up to 8 days of curing. For the sake of brevity, Fig. 4 presents the results obtained for KT; NB also exhibits quite comparable results. In the case of uncured KT sample liquid limit increases instantaneously by almost 10% with addition of 1% HL, whereas cured samples did not show significant variations even up to 8 days. However, for NB liquid limit decreases with increasing HL content, which is attributed to diffused double layer contraction and deposition of cementitious reaction compounds (Saeed et al. 2015). Further, plastic limit for both soils increase with lime content up to 8 days; consequently, minimum plasticity index is obtained after 8 days which might be due to prolonged soil-lime interaction. Moreover, in both soils variation in liquid limit and plastic limit beyond 2% HL is negligible, as a result of completion of cation exchange activity up on charge neutralization with 1–2% HL (Marshall 1967).

5 Conclusions from the Study

The present study verifies that addition of lime causes momentous physico-chemical interactions and subsequent irreversible modifications in treated soils, primarily owing to short-term cation exchange phenomena. However, early pozzolanic reactions occurring between free lime and reactive clay minerals also play a less significant role. Therefore, it can be concluded that prior knowledge of intrinsic chemico-mineralogical composition of virgin soils (viz., soil pH, SSA, CEC, buffer capacity, etc.) will aid to predict the long-term efficacy of lime treatment.

References

Al-Ne'aimi, R. M. S., & Hussain, H. A. (2010). Some engineering characteristics of lime-treated soil Semeel region. *Al-Rafadain Engineering Journal, 19*(5), 12–27.

Arabi, M., & Wild, S. (1986). Micro structural development in cured soil-lime composites. *Journal of Material Science, 21,* 497–503.

Arnepalli, D. N., Shanthakumar, S., Rao, B. H., & Singh, D. N. (2008). Comparison of methods for determining specific-surface area of fine-grained soils. *Geotechnical and Geological Engineering, 26,* 121–132.

Bandipally, S., Cherian, C., Arnepalli, D. N., & Pooja, C. P. (2014). Influence of pH on long term performance of lime stabilized fine-grained soils. In *Proceedings of Indian Geotechnical Conference-2014*, Kakinada, India.

Cherian, C., & Arnepalli, D. N. (2015). A critical appraisal of the role of clay mineralogy in lime stabilization. *International Journal of Geosynthetics and Ground Engineering, 1*(8), 1–20.

Eades, J. L., & Grim, R. E. (1966). A quick test to determine lime requirements for soil stabilization. *Highway Research Record, 139,* 61–72.

Marshall, R. T. (1967). Factors influencing the plasticity and strength of lime-soil mixtures. *Engineering Experiment Station Bulletin, 492,* 1–19.

Ramesh, H. N. G., & Sivapullaiah, P. V. (2011). Role of moulding water content in lime stabilization of soil. *Ground Improvement, 164*(G11), 15–19.

Saeed, K. A. H., Kassim, K. A., Yunus, N. Z. M., & Nur, H. (2015). Physico-chemical characterization of lime stabilized tropical kaolin clay. *Jurnal Teknologi, 72*(3), 83–90.

Singh, B., & Goswami, R. K. (2012). Compaction characteristics of lateritic soil mixed with fly ash and lime. *International Journal of Geotechnical Engineering, 6,* 437–444.

Yong, R. N., Warkentin, B. P., Phadungchewit, Y., & Galvez, R. (1990). Buffer capacity and lead retention in some clay materials. *Water, Air, and Soil Pollution, 53,* 53–67.

Back Analyses of PVD Performance in Mumbai Port

M. Ashok Kumar, N. Kumar Pitchumani and Aminul Islam

Abstract This paper presents the instrumentation and back analyses conducted to assess the field performance of ground improvement works in one of the port development projects along Mumbai coast. Ground improvement using Prefabricated Vertical Drains (PVD) with Preloading in excess of 90 ha reclamation of land was carried out to improve the soft estuarine deposit below the seabed. The marine clay along the Mumbai coastline was found to be very soft with undrained shear strength less than 5–7 kPa at the top of the mud. Extensive geotechnical campaigns were carried out to comprehend the variations in the geotechnical properties of the clays. The PVD design was conducted based on various design parameters derived from the investigation data. As the coefficient of horizontal consolidation (c_h) values were found to be crucial in the estimation of rate of consolidation over time, various radial consolidation and cone dissipation tests were carried out. The c_h values from these tests were observed to be in the range of 1.8–5.2 m^2/yr, which yielded the design value of around 3 m^2/yr. Extensive instrumentation and monitoring were conducted using multilevel magnetic extensometers, settlement gauges and piezometers to back calculate the field c_h values. The back calculated field c_h values were in the range of 3.7–4.7 m^2/yr with smear diameter ratio of 2.5 and smear permeability ratio around 3–4. The back analyses helped to apply suitable corrections in the design parameters in the field, thereby accounting for the parametric variations in the field and also effectively mitigating the geotechnical risks.

M. Ashok Kumar (✉) · N. Kumar Pitchumani
AECOM India Pvt. Ltd, VBC Solitaire, 2nd Floor, Bazullah Road, T Nagar, Chennai 600017, India
e-mail: Ashok.kumarm@aecom.com

N. Kumar Pitchumani
e-mail: NKumar.Pitchumani@aecom.com

A. Islam
ITD Cementation India Limited, National Plastic Building, A-Subhash Road Vile Parle (East), Mumbai 400057, India
e-mail: Aminul.Islam@itdcem.co.in

T. Thyagaraj (ed.), *Ground Improvement Techniques and Geosynthetics*, Lecture Notes in Civil Engineering 14, https://doi.org/10.1007/978-981-13-0559-7_21

Keywords Soft soil improvement · PVD · Field monitoring · Back analyses c_h values

1 Introduction

Indian coastal regions primarily comprise of estuarine deposit of very soft marine clays which are known for their poor geotechnical properties such as high compressibility and very low bearing capacity. Lack of suitable ground improvement in this soft clay, will cause excessive settlement and adversely affect both the stability and durability of the port infrastructures built over these clays. Preloading with Prefabricated Vertical Drains (PVD), is one of the most commonly adopted ground improvement technique. In the ground improvement design using PVD, a reasonable estimation of both the magnitude and time of consolidation are indispensable for planning and execution of works within the project cost and time. These estimations depend on the assumption of a number of consolidation parameters. Although, these consolidation parameters are derived from large number of in situ field tests and sophisticated laboratory tests, it is practically difficult to accurately predict the magnitude and duration of consolidation for the given large scale of the reclamation works, especially due to smearing effects around PVD (Indraratna et al. 2003), uncertainties and variations associated with the ground condition and geotechnical parameters. Hence, a proper instrumentation and monitoring campaign is indispensable to assess the PVD performance in the field. The back analyses based on the observed field data can be used to address the parametric variations in the field and also to apply suitable corrections in the design during construction. This paper presents a case study of instrumentation and back analyses carried out in one of the ongoing ground improvement projects for port development in Mumbai.

2 Site and Soil Condition

The land reclamation of around 90 ha area is being carried out along the coastal region of Mumbai, for the extension and development of the proposed container yard adjacent to the existing port facilities. The average sea bed level and sea water level obtained through bathymetric survey were around 0.0 mCD and +2.51 mCD respectively (i.e. 0 mCD = −2.51 MSL). The geology of the site predominately comprises of 4–18 m thick soft clay underlain by a thin layer of sandy gravel and basaltic rock. An extensive geotechnical investigation campaign was conducted to comprehend the characteristics and engineering properties of the soft marine clay which were found to be very soft, sensitive and normally to over consolidated. The campaign included boreholes, cone penetration tests, dissipation tests, Field vane

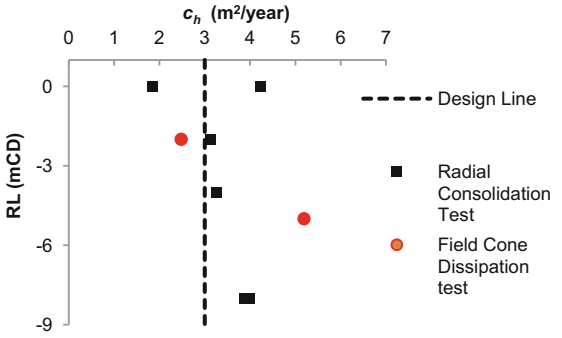

Fig. 1 Coefficient of horizontal consolidation (m^2/yr)

shear tests, oedometer tests, radial consolidation tests, drained and undrained triaxial compression tests to obtain the consolidation and stability design parameters. The plasticity index of the soft clay varied from 55 to 70 and the natural moisture content was almost close to the liquid limit. The ratios of horizontal to vertical coefficients of consolidation were observed to be in the range of 2.1–2.5. The clay was slightly to over consolidated with the over consolidation ratio of 1.5–3.4 decreasing with the depth. Radial consolidation tests and Cone dissipation tests showed the c_h value in the range of 2.0–5.2 m^2/yr as shown in Fig. 1. Table 1 shows the ranges of various geotechnical parameters interpreted from the investigation data.

The port development works involved the reclamation of two major functional zones such as rail corridor and container yard portions with their estimated future design loads of 30 and 50 kPa respectively over a design final formation level of around +7 mCD. As per design, the required thickness of preloading is estimated up to 10.5 and 12 m for rail and container yard portion respectively. The total consolidation settlement of around 0.5–1.5 m was envisaged.

Table 1 Geotechnical parameters for soft clay

Parameters	Ranges
Density, γ	15 kN/m^3
Thickness (m)	3.7–22.5
Plasticity index, *I*p	55–70
Compression index, C_c	0.5–0.95
Initial void ratio, e_o	1.4–2.5
Compression ratio CR	0.19–0.3
Coefficient of consolidation c_v (m^2/year)	0.8–1.7
Coefficient of radial consolidation c_h (m^2/year)	1.9–5.2
c_h/c_v	2.1–2.5
Secondary compression index, c_α	0.016– 0.034
c_α/C_c	0.023–0.055
OCR	1.5–3.4

3 Ground Improvement and Controlled Preloading

The initial platform up to +5.5 mCD was formed using conventional dumping method and the ground treatment using PVD was carried out. PVD were installed in triangular pattern at 1.0–1.2 m spacing which was followed by the preparation of filter blankets. The design was carried out as per IS 15284 Part 2 (2004). The preloading up to +10.5 mCD to +12 mCD was built up in three stage lifts with the waiting period allowed between each stage to allow for consolidation, thereby enhancing the compressibility of underlying soft clay and stabilising the reclamation slopes for the next uplift.

4 Field Instrumentation

Extensive instrumentation and monitoring were carried out all over the reclamation zone as shown in the snapshot presented in Fig. 2. Instrumentation included surface settlement markers, deep settlement markers, magnetic extensometers, open stand pipe, vibrating wire piezometers, and inclinometers. Instrument clusters were installed in regular grid patterns of size 25 m × 25 m as shown in Fig. 2 over the entire site to closely monitor the process of consolidation. Totally around 1000 numbers of instrument grids were proposed. The instruments were arranged in such a way that at every 100 m × 100 m size of ground improvement, there were at least 25 numbers of settlement markers/plates, five numbers of boreholes, four numbers of vibrating wire piezometers. Inclinometers were provided at every 100 m spacing along the reclamation boundary to monitor the lateral movement and stability of the preload.

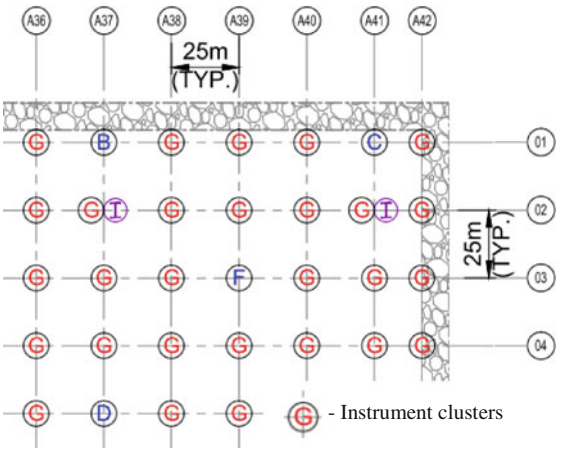

Fig. 2 Instrumentation layout plan

5 Back Analyses

Rigorous back analyses were performed based on the observed field data to theoretically back calculate various design parameters such as coefficient of consolidation, smear coefficients, OCR and compression ratio of the clay. Figures 3 and 4 show the back analyses prediction based on the multilevel Magnetic extensometers and settlement gauges respectively.

The back analyses calculations considered the multiple stage ramp preloading and the effect of submergence in surcharge due to settlement. The Compression Ratio (*CR*) and the horizontal coefficient of consolidation (c_h) were adjusted in the back calculation to match the theoretical predicted curve with various settlement data observed in the field both horizontally and vertically as shown in Fig. 3. The horizontal coefficient of consolidation c_h which gave similar settlement trend as observed in the field was around 3.75–4.0 m^2/yr with c_h/c_v ratio around 2.3. Similarly, smearing permeability ratio was also estimated to be in the range of 3–4 with smear diameter ratio of 2.5.

5.1 *Back Calculation of c_h from Piezometer*

The following relationship can be derived from the equation proposed by Hansbo (1979),

$$1 - \frac{\Delta u_t}{\Delta u_0} = 1 - e^{-\alpha t}, \tag{1}$$

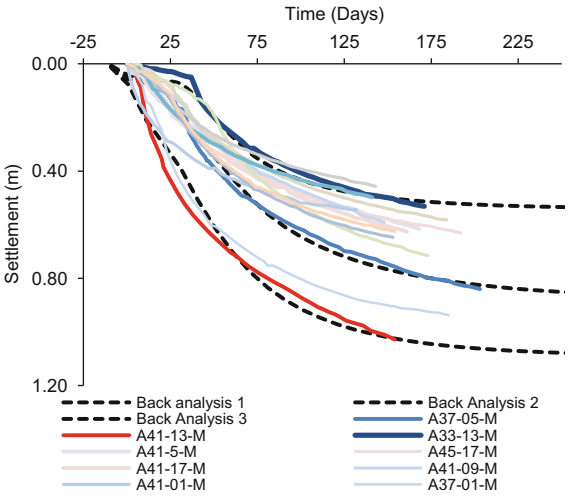

Fig. 3 Back analyses based on magnetic extensometer data

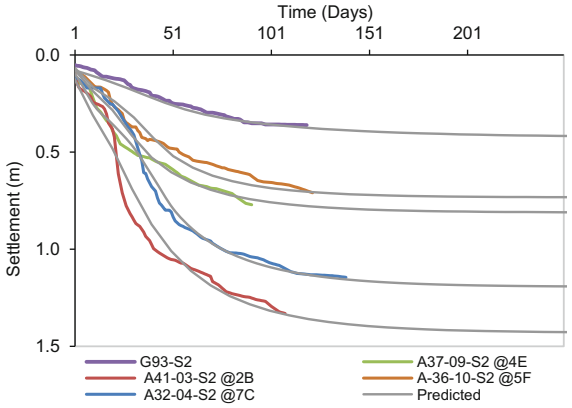

Fig. 4 Back analyses based on settlement data

where,

$$\alpha = \frac{8c_h}{D_e F}, \tag{2}$$

where u_0 is the excess pore pressure observed at time $t = 0$; u_t is the excess pore pressure at time t; D_e is the effective diameter of a unit cell of drain; and F is a resistance factor for the effects of spacing, smear, and well resistance. $F = \ln(n) - 0.75 + \ln(s)(k_h/k_s - 1)$. The Eq. (1) can be rewritten as,

$$\ln \frac{\Delta u_0}{\Delta u_t} = \propto t. \tag{3}$$

Hence, Eq. (3) shows a linear relationship with time, with α being the slope of the line, from which c_h can be back calculated directly from the piezometer data.

As shown in Fig. 5, for the slope of the line (a) around 0.008–0.02, the back analysed values of c_h were in the range of 1.8–4.7 m^2/yr including the smearing diameter ratio and permeability ratio of 2.5 and 4 as estimated from the back analyses results (Figs. 3 and 4). The c_h values found lower than 2.0 m^2/yr ($\alpha \sim 0.008$) were ignored, as the dissipation of excess pore pressure was observed to be improper in those piezometers due to clogging of the filter.

5.2 *Back Calculation of c_h from Magnetic Extensometer*

Equation (1) can be rewritten in terms of settlement as Eq. (4) and can be rearranged as (5)

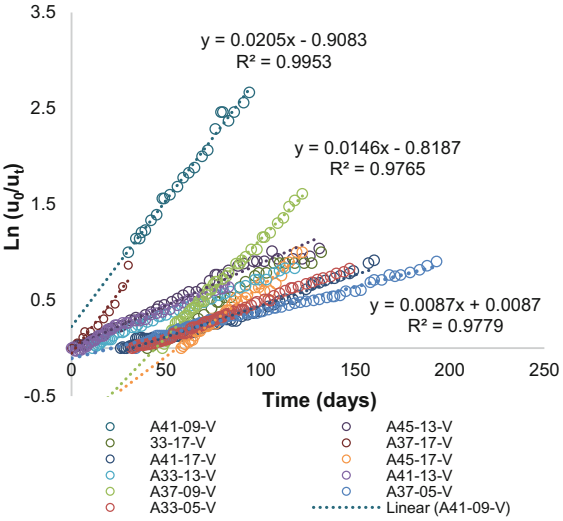

Fig. 5 Estimation of field horizontal consolidation coefficient c_h from piezometer data

$$\frac{S_t}{S_f} = 1 - e^{-\alpha t} \tag{4}$$

$$\ln \frac{S_f}{S_f - S_t} = \alpha t, \tag{5}$$

where S_f is the final settlement and S_t is the settlement at any time t. The linear relationship of this function can be used to estimate the slope α from the field settlement data.

As shown in the Fig. 6, for the value of $\alpha = 0.0185$ estimated from the settlement data, the back calculated c_h was around 3.7 m^2/yr for the adjusted smearing diameter ratio and permeability ratio of 2.5 and 3 respectively.

5.3 *Back Calculation of c_h from Settlement Gauges*

The back calculation carried out based on the settlement gauges data installed at +5.5 mCD, yielded α around 0.033 and corresponding c_h value of about 4.7 m^2/yr as shown in Fig. 7. Based on various methods as discussed above, the c_h values were estimated to be around 2–5.2 m^2/yr as shown in Table 2.

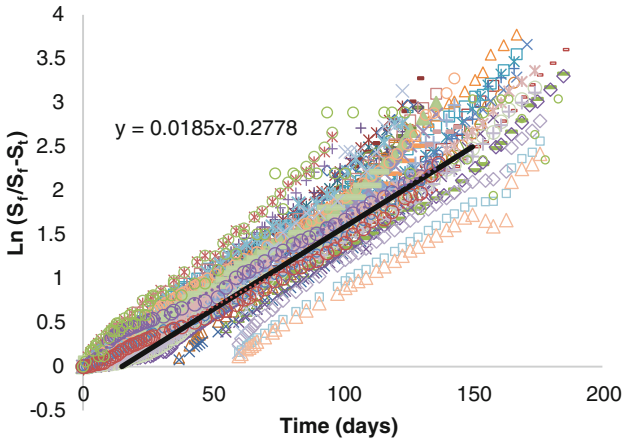

Fig. 6 Estimation of field horizontal consolidation coefficient c_h from Magnetic extensometer data

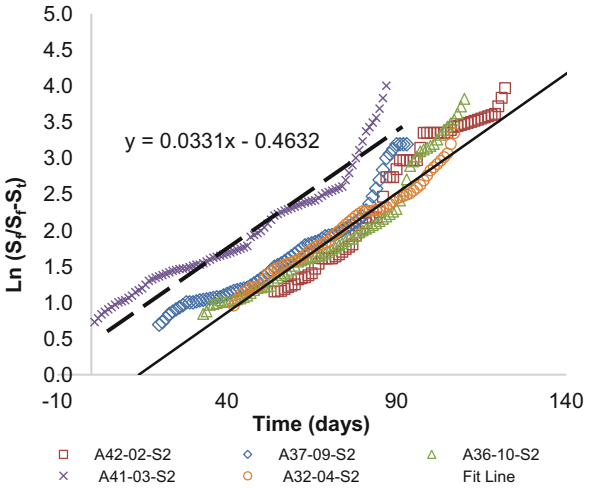

Fig. 7 Estimation of field horizontal consolidation coefficient c_h from settlement data

Table 2 Summary of estimated c_h values

S. No.	Methods	Estimated c_h value (m^2/yr)
1.	Radial consolidation tests in laboratory	2–4.2
2.	Field cone dissipation tests	2.5–5.2
3.	Back analyses based on Field Settlement data	3.75–4.0
4.	Back calculation from α value	3.42–4.7

6 Conclusions

The port development along the mumbai coast required extensive reclamation and ground improvement works for over 90 ha area in the soft marine deposit. The geotechnical investigation campaign carried out for the design of ground improvement works showed wide variations in the design parameters especially the c_h values. The laboratory and field dissipation tests showed the c_h value in the range of 1.8–5.2 m^2/yr. The back analyses carried out based on various instrument data observed in the field showed the c_h values in the range of 3.75–4.7 m^2/yr with smear diameter ratio of 2.5 and smear permeability ratio around 3–4. The back calculated c_h values obtained from the theoretical back calculation based on settlement curves were found to be reasonably matching with the back calculated c_h value from α values.

References

Hansbo, S. (1979). Consolidation of clay by band-shaped prefabricated drains. *Ground Engineering, 12*(5), 16–25.

IS 15284 Part 2. (2004). *Design and construction for ground improvementGuidelines*.

Indraratna, B., Bamunawita, C., Redana, I. W., & McIntosh, G. (2003). Modelling of prefabricated vertical drains in soft clay and evaluation of their effectiveness in practice. *Ground Improvement, 7*(3), 127–137.

Discharge and Absorption Capacity Tests on Composite Prefabricated Vertical Drains

P. Sishma, P. K. Jayasree and K. Balan

Abstract This paper deals with the discharge and absorption capacity tests conducted in the laboratory on newly developed and fabricated four different types of prefabricated vertical drains (PVDs) made from combination of both natural and polymer geotextiles, commercially available polymer-based PVD and natural PVD. The newly developed PVDs are made from single-layer nonwoven polyester sheath as filter wrapped around a core of coir ropes or coir mats and single-layer nonwoven jute sheath as filter wrapped around a core of cardboard or corrugated polyester, designated as composite prefabricated vertical drains (PC–PVD, PN–PVD, JC–PVD, and JP–PVD). The natural PVD is made from single-layer nonwoven jute wrapped around a core of coir ropes. The rubber membrane-confined short term discharge capacity tests were conducted at different compressive stresses and hydraulic gradients. The test results of the composite PVDs are compared and discussed, with the results from polymer-based PVD and natural PVD.

Keywords Geosynthetics · Composite prefabricated vertical drains
Discharge capacity · Absorption capacity

1 Introduction

Soft soil stabilization using prefabricated vertical drains (PVDs) are applied worldwide. The use of PVDs along with pre-compression accelerates the primary consolidation of soft soil. The commercially available synthetic PVDs have both

P. Sishma (✉) · P. K. Jayasree · K. Balan
Department of Civil Engineering, College of Engineering Trivandrum, Trivandrum 695016, India
e-mail: sishmap@gmail.com

P. K. Jayasree
e-mail: jayasreepk@cet.ac.in

K. Balan
e-mail: drkbalan@gmail.com

T. Thyagaraj (ed.), *Ground Improvement Techniques and Geosynthetics*, Lecture Notes in Civil Engineering 14, https://doi.org/10.1007/978-981-13-0559-7_22

filter and core made with polymer materials and is not biodegradable. The increasing environmental awareness and sustainability, and the high cost of petroleum products, are lead to the utilization of substitutes made from natural products (Balan 1995; Banerjee and Sampath Kumar 2000; Beena and Babu 2007; Asha and Mandal 2012, 2014). Natural materials like jute and coir are biodegradable in nature having high water absorption capacity, filtration capacity and low cost (Banerjee and Sampath Kumar 2000; Asha and Mandal 2012, 2014). But natural PVDs have less discharge capacity than commercially available PVDs (Balan 1995; Banerjee and Sampath Kumar 2000; Beena and Babu 2007; Asha and Mandal 2012, 2014). For commercially available PVDs, the filter materials exhibit small opening size and less absorption capacity but are almost free from clogging, and core structure will not flatten during the consolidation process. So it has high vertical discharge capacity hence exhibit high efficiency (Banerjee and Sampath Kumar 2000; Asha and Mandal 2012, 2014). The use of natural and synthetic geotextiles together in the development of PVDs can combine the advantage of both, are named as composite PVDs. In the present paper, the discharge and absorption capacity of four different types of newly developed and fabricated composite PVDs were studied and compared with commercially available PVD and natural PVD in detail.

2 Composite Prefabricated Vertical Drains

The newly developed and fabricated four different types of composite prefabricated vertical drains are shown in Fig. 1, and these composite PVDs are compared with a natural PVD and a commercially available polymer PVD. The physical properties of all the PVDs are given in Table 1.

Among four composite PVDs, two of them had nonwoven needle punched adhesive bonded polyester as filter sheath and the other two had nonwoven jute as filter sheath. First composite PVD is made from single-layer nonwoven polyester as filter sheath wrapped around a core of coir strands of five numbers and each coir strand was separated by longitudinal stitches designated as PC–PVD. Second composite PVD is made from single-layer nonwoven polyester as filter sheath wrapped around a core of nonwoven coir designated as PN–PVD. Third composite PVD is made from single-layer nonwoven jute as filter sheath wrapped around a core of corrugated cardboard designated as JC–PVD. The fourth composite PVD is made from single-layer nonwoven jute as filter sheath wrapped around a core of corrugated polyester designated as JP–PVD. The natural PVD is fabricated from single-layer nonwoven jute as filter sheath wrapped around a core of coir strands of five numbers and each coir strand was separated by longitudinal stitches designated as NPVD. The commercially available synthetic polymer PVD had nonwoven polyester filter sheath and corrugated polyester core structure designated as PPVD.

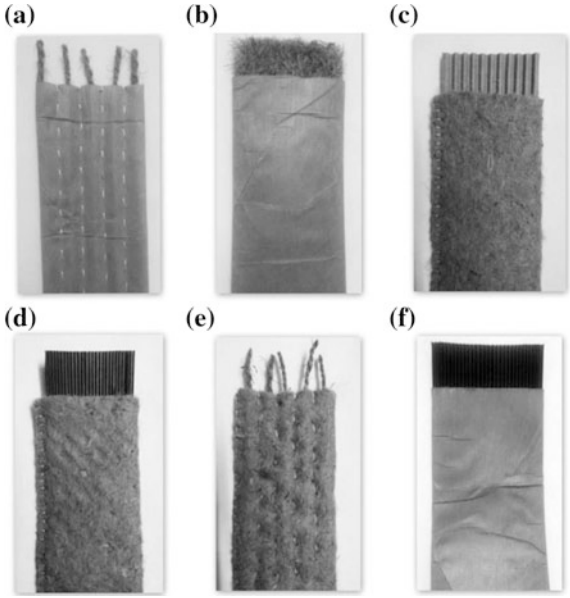

Fig. 1 Prefabricated vertical drains: **a** PC–PVD, **b** PN–PVD, **c** JC–PVD, **d** JP–PVD, **e** NPVD and **f** PPVD

Table 1 Physical properties of PVDs

Property (Unit)	Type of PVD					
	PC–PVD	PN–PVD	JC–PVD	JP–PVD	NPVD	PPVD
Width (mm)	100	100	100	100	100	100
Mass per unit length (g/m)	48	62	219	227	215	102
Thickness at 20 kPa (mm)	4	7.5	10	9.5	17	5

3 Discharge Capacity Tests

Discharge capacity of all the PVDs confined in a rubber membrane were conducted in the laboratory in discharge capacity test apparatus fabricated by the guidelines provided in ASTM D 4716 and Asha and Mandal 2012. The apparatus is a rectangular steel configuration consisting of bottom unit, top unit and a loading plate. The internal dimensions of bottom unit is 200 mm × 100 mm and an internal dip of 25 mm. Bottom unit consist of small inlet and outlet weirs for the entire width and the inlet weir is connected to a constant head water tank. The internal depth of the top unit is 25 mm. A rectangular loading plate of 150 mm × 100 mm × 25 mm is inserted into the top unit and the units are held together by screw connections. The test set-up is shown in Fig. 2.

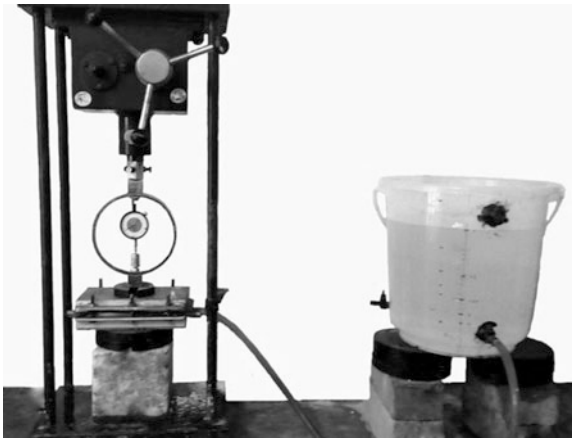

Fig. 2 Discharge capacity test set-up

200 mm long sample is soaked in water for 24 h and the rubber membrane wrapped sample is placed at the weir top level of bottom unit. The gap between the sample and the base of the bottom unit is sealed using thick rubber sheets. Another rubber membrane is placed at the bottom of top unit and the loading plate is placed, then the screws are tightened. The test is conducted at normal compressive pressures of 10, 50, 100, and 250 kPa with varying hydraulic gradients 1, 0.5, 0.25 and 0.1. A constant head water tank is used for passing water through the sample and water is collected at outlet using a measuring jar. The time required to collect water is noted and the discharge capacity is calculated by dividing the quantity of water collected in the measuring jar per unit time by the hydraulic gradient.

4 Absorption Capacity Tests

The water absorption capacity of the composite PVDs, PPVD, and NPVD were determined according to ASTM D 1117 and Asha and Mandal 2012. The test method is designed to determine the water absorption capacity of PVDs with time. 200 mm long PVD specimen is used for the test. The dry weight of all PVD specimens are noted. Then all the PVD specimens immersed in a plastic container of 100 mm deep, containing water at 85 mm deep. The PVD specimens removed from water and wet weight is noted after soaking periods of 2, 4, 8, 16, 24, or 32 h. The specimens are allowed to drain in vertical position for 10 min before taking the wet weights. The specimens immersed in water are shown in Fig. 3. The water absorption capacity of PVD specimen is calculated by dividing the difference between the wet and dry weight of PVD by the dry weight of PVD. The absorption capacity of all PVDs were found and reported as percentage of dry weight.

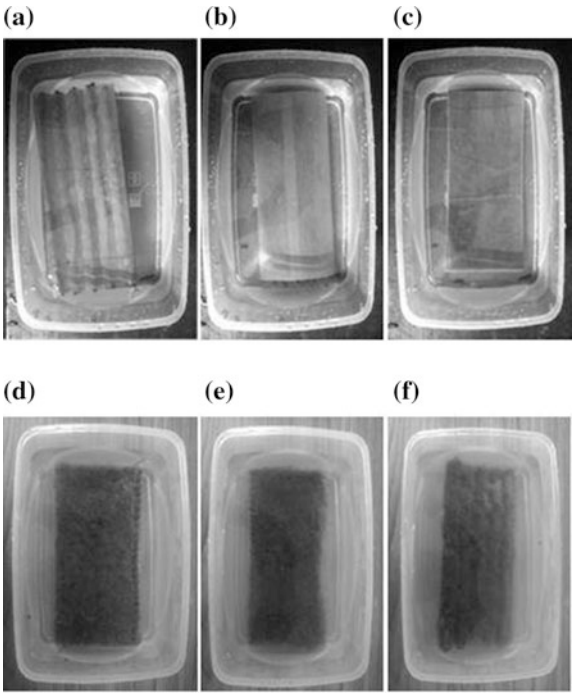

Fig. 3 PVD specimens immersed in water: **a** PC–PVD, **b** PN–PVD, **c** PPVD, **d** JP–PVD, **e** JC–PVD and **f** NPVD

5 Test Results and Discussion

5.1 Discharge Capacity Tests

The discharge capacity of Composite PVDs, NPVD, and PPVD against normal compressive pressure at different hydraulic gradients 1, 0.5, 0.25 and 0.1 is shown in Fig. 4. The discharge capacity of all the PVDs decreases with the increase in compressive pressure at all hydraulic gradients. The discharge capacity increases with decreasing hydraulic gradient for composite PVDs, NPVD, and PPVD.

The discharge capacity of PPVD is almost same under different compressive pressure at constant hydraulic gradient due to stiff core structure, and increases with decreasing hydraulic gradient. The discharge capacity of PC–PVD is almost similar or greater than the discharge capacity of PPVD at 10 kPa, but decreases with increasing pressure. The higher discharge capacity of PC–PVD at lower pressure is due to the gaps present around the coir strands. Among composite PVDs, lowest discharge capacity was observed for JC–PVD, which is lower than NPVD. Beyond 200 kPa, the discharge capacity of JC–PVD was almost negligible. The discharge capacity of PC–PVD and JP–PVD is higher than NPVD but lesser than PPVD. The discharge capacity of JP–PVD is almost same under different compressive pressure

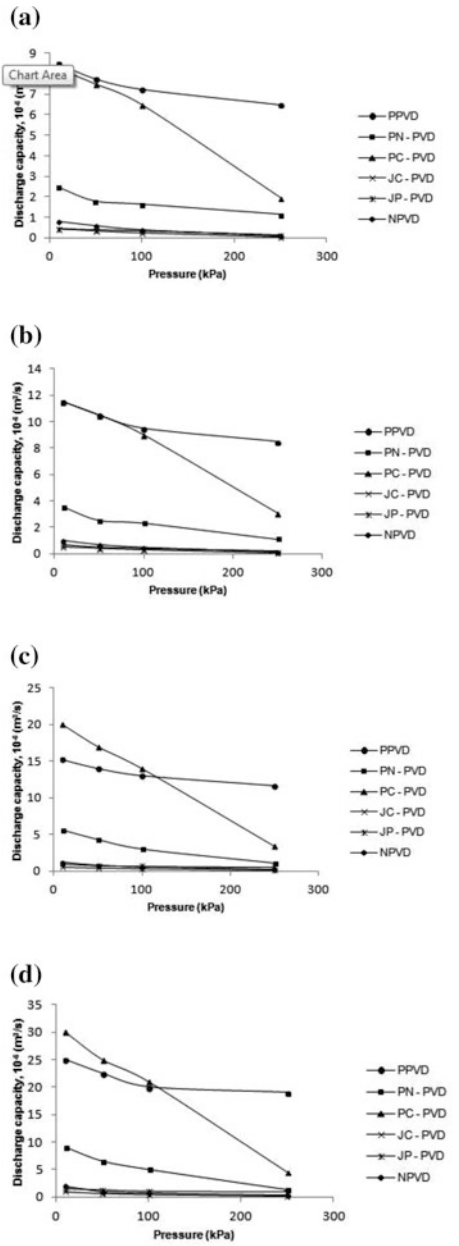

Fig. 4 **a** Discharge capacity of composite PVDs, NPVD and PPVD with pressure at hydraulic gradient = 1. **b** Discharge capacity of composite PVDs, NPVD and PPVD with pressure at hydraulic gradient = 0.5. **c** Discharge capacity of composite PVDs, NPVD and PPVD with pressure at hydraulic gradient = 0.25. **d** Discharge capacity of composite PVDs, NPVD and PPVD with pressure at hydraulic gradient = 0.1

similar to PPVD, because both PVDs have same core structure. The discharge capacity of PN–PVD decreases with increasing compressive pressure. The discharge capacity of PC–PVD, NPVD, PN–PVD, and JC–PVD decreases with increasing compressive pressure, because the corresponding core structures such as coir core, nonwoven coir and cardboard are compressed as the compressive pressure increases

The variation in discharge capacity with increasing compressive pressure is almost the same in the composite PVDs, NPVD and PPVD at all hydraulic gradients. Except PC–PVD, the reduction in discharge capacity of all other PVDs is gradual with increasing compressive pressure.

5.2 *Absorption Capacity Tests*

The absorption capacity of Composite PVDs, NPVD, and PPVD against time are shown in Fig. 5. JC–PVD and NPVD have maximum absorption capacity. JC–PVD has maximum absorption capacity of 7.16% of its dry weight at 24 h and NPVD has maximum absorption capacity of 6.64% of its dry weight at 24 h. This is due to the hygroscopic nature of nonwoven jute sheath. The absorption capacity of JP–PVD was 4.29%, PC–PVD was 3.93% and PN–PVD was 3.7% of its dry weight at 24 h. PPVD has lowest absorption capacity of 1.8% of its dry weight at 24 h. Among NPVD, JC–PVD and JP–PVD, the lowest absorption capacity was found for JP–PVD due to the corrugated polyester core structure. For PC–PVD and PN–PVD, absorption capacity was almost same, and is due to the absorption capacity of coir core structure. After 2 h of soaking period in water, all the PVDs reached their maximum absorption capacity, and after that the increase in absorption capacity was negligible. Therefore a minimum 2 h of soaking in water is sufficient to saturate the composite PVDs, NPVD, and PPVD.

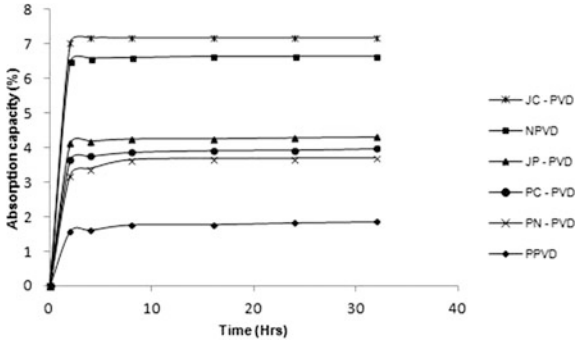

Fig. 5 Absorption capacity of composite PVDs, NPVD and PPVD against time

6 Conclusions

Four composite PVDs and one natural PVD newly developed and fabricated were tested for discharge and absorption capacity with increasing normal compressive pressure and compared with commercially available polymer PVD.

- The Discharge capacity is maximum for PPVD than all composite PVDs and NPVD. Except PPVD and JP–PVD, the rate of reduction in discharge capacity is greater for all other PVDs. For PPVD and JP–PVD, the discharge capacity is almost same with increase in compressive pressure due to stiff core structure.
- The lowest discharge capacity was observed for JC–PVD, and the rate of reduction in discharge capacity is more, and beyond 200 kPa the discharge capacity was almost negligible.
- The rate of reduction in discharge capacity is maximum for PC–PVD due to the gaps present around the coir strands.
- The variation in discharge capacity with increasing compressive pressure is almost the same in the composite PVDs, NPVD, and PPVD at all hydraulic gradients.
- The absorption capacity is maximum for JC–PVD and NPVD, due to hygroscopic nature of jute sheath. PPVD has minimum absorption capacity. After 2 h of soaking period in water, all the PVDs reached their maximum absorption capacity, and after that the increase in absorption capacity is negligible. Therefore a minimum 2 h of soaking in water is sufficient to saturate all the PVDs.

References

Asha, B. S., & Mandal, J. N. (2012). Absorption and discharge capacity tests on natural prefabricated vertical drains. *Geosynthetics International*, *19*(4).

Asha, B. S., & Mandal, J. N. (2014). Laboratory performance tests on natural prefabricated vertical drains in marine clay. *Proceedings of the Institution of Civil Engineers-Ground Improvement*, paper 1300001.

Balan, K. (1995). *Studies on engineering bahaviour and uses of geotextile with natural fibres (Ph. D. thesis)*, Indian Institute of Technology, Delhi.

Banerjee, P. K., & Sampath Kumar, J. P. (2000). Production method and characteristics of braided PVD. *Indian Journal of Fibre & Textile Research, 25,* 182–194.

Beena, K. S., & Babu, K. K. (2007). Testing coir geotextile drains for soft ground improvement. *Proceedings of Institution of Civil Engineers*, G11, 43–49.

Stabilization of Clay at Sunnam Cheruvu Area in Nadergul, Hyderabad Using Organic Waste

R. Sandhya Rani, P. Pradeep Kumar, K. V. Krishna Reddy and S. Praveen

Abstract Clay soils inherit certain problems due to its properties such as plasticity, volume change, low strength, etc. To overcome these problems an attempt has been made in the present study to determine the utility of organic waste in stabilization of clay which has been obtained from Sunnam Cheruvu area of Nadergul, Hyderabad. Organic wastes have been considered due to their economical and environmental advantage. Ash of sugarcane pulp, wood, and coconut shell have been considered to investigate their potential in stabilizing the clay soil in pursuit of obtaining a cheaper and effective stabilizer. Laboratory experimentation was done to evaluate the differential free swell and unconfined compressive strength (UCC) for various percentages of ash contents. Curing of stabilized soil samples for 7 and 28 days were considered. Stabilization also required addition of lime to control swell. The results show that the swell and strength properties of samples were improved with the addition of various ash contents and also with curing period. Therefore it is concluded that sugar cane pulp ash, wood ash and coconut shell ash have a good potential in improving the properties of clay soil.

Keywords Sugarcane pulp ash · Wood ash · Coconut shell ash
Clay soil · UCC

R. S. Rani (✉) · P. P. Kumar · K. V. K. Reddy · S. Praveen
Department of Civil Engineering, MVSR Engineering College, Hyderabad 501510
e-mail: sandhyaupendar@gmail.com

P. P. Kumar
e-mail: ppkumar1985@gmail.com

K. V. K. Reddy
e-mail: kvkr2004@rediffmail.com

S. Praveen
e-mail: praveensgari@gmail.com

T. Thyagaraj (ed.), *Ground Improvement Techniques and Geosynthetics*, Lecture Notes in Civil Engineering 14, https://doi.org/10.1007/978-981-13-0559-7_23

1 Introduction

As the growing world population and increased human need leads to increase in industrial and agricultural wastes, construction industry opens a window to the use of such wastes. Millions of tons of waste are produced every year, which not only pose a serious problem to disposal issues but also contaminate the environment in different ways, Therefore it results in increased health risk. Further this motivates to find solution to dispose/utilize the waste produced. Clay soils exhibit certain problems such as low shear strength, bearing capacity, low permeability and high volume change due to presence of montmorillonite in its mineralogical content and these properties make the clay soils unfit for construction (Bowles 1979; Das 1998). Stabilization is the process of blending and mixing materials with a soil to improve certain properties of the soil. The process may include the blending of soils to achieve a desired gradation or the mixing of commercially available additives that may alter the gradation, texture, or plasticity, or act as a binder for cementation of the soil. Therefore usage of agricultural waste in improving soil properties has been an important area of study.

Many researchers have suggested the use of fly ash in stabilizing the soils (Kolias et al. 2005; Rama Rao et al. 2008). Fly ash is also used in combination with lime and bentonite to dispose of industrial wastes (Edil et al. 1987). Baggase ash can also be used as stabilization material for expansive soils (Kharade et al. 2014). Monovalent cations such as Sodium and Potassium are commonly found in expansive clay soil and these cations can be exchanged with cations of higher valencies such as calcium which are found in lime and agricultural waste ash. The most common improvements achieved through stabilization are therefore to improve the soil strength, to improve the bearing capacity and durability under adverse moisture and stress condition, and to improve the volume stability of a soil mass (Amu et al. 2011).

Waste materials have proved both efficiency and acceptance due to their economical and environmental aspects. The present work undertakes use of agricultural waste in stabilizing clay soil that summarizes the performance of lime along with ashes of Sugar cane pulp, wood, and coconut shell.

1.1 Materials

The materials used in the present study are Clay, Lime, Sugarcane pulp ash, Wood ash, and Coconut shell ash. Various laboratory experiments were carried out on soil specimens with different proportions of admixtures to examine the effect on strength properties.

The clay has been excavated from Sunnam Cheruvu, Nadergul, Hyderabad at an average depth of 1.5 m to obtain true representative samples. The disturbed soil was then taken to the laboratory and spread on different matting to facilitate air drying.

Table 1 Chemical composition of various ashes

Constituent	% Composition		
	Sugar cane pulp ash	Wood ash	Coconut shell ash
SiO_2	63.38	41.06	4.64
MgO	1.85	1.12	1.32
CaO	14.54	45.34	9.26
Na_2O	1.15	1.52	15.42
K_2O	3.56	3.39	54.01
Fe_2O_3	5.56	5.39	4.39
Al_2O_3	8.6	1.46	
P_2O_5	0.01	0.02	4.64
SO_3	1.28		5.75

All the lumps in the sample were broken down and well pulverized. Then it was sieved through a required IS sieve for performing several tests.

Lime is an excellent choice for short term modification of soil properties. Lime can modify almost all fine-grained soils, but the most dramatic improvement occurs in clay soils of moderate to high plasticity. It imparts much strength through the soil by pozzolanic reaction. The key to pozzolonic reactivity and stabilization is a reactive soil, a good mix design protocol, and reliable construction practices (Dallas 2001). Modification occurs because cations supplied by the hydrated lime replace the cations normally present on the surface of the clay minerals, promoted by the high pH environment of the lime-water system. Lime was bought from the locally available market.

The ashes of Sugarcane pulp, Wood, and Coconut shell used in the study have been obtained locally by subjecting the dried material to open air burning in separate metal drums. The chemical composition of ashes obtained from Sugarcane pulp, Wood, and Coconut shell have been shown in Table 1.

2 Experimental Investigation

Preliminary tests (Specific gravity, Particle size analysis and Atterberg's limits) were performed on soil sample for classification and identification purposes. Engineering property tests (Compaction and UCC) were also performed on the sample and presented in Table 2.

Free swell index is calculated for various percentages of ash (5, 10, and 15%) and lime (1, 3, and 5%) separately for all three ash types added to clay. The value of Free swell index was less than 20 at 3% lime for all ash types. **Initially lime was used to control swelling of soil. As lime also imparts strength to soil initial test have been conducted with only lime and only ash but however the combination**

Table 2 Properties of clay

S. No.	Property of soil	Value
1.	Specific gravity	2.8
2.	Liquid limit	40%
3.	Plastic limit	18%
4.	Plasticity index	22%
5.	Free swell index	28%
6.	Maximum dry density	1.59 gm/cc
7.	Optimum moisture content	18.6%
8.	Unconfined compressive strength	0.24 x 10^3 kPa
9.	IS classification	CI

of both organic waste and lime imparts 15% more strength as compared to individual strengths and also reduces the requirement of lime.

Nine different blends are prepared for each type of ash (1, 3 and 5% of lime; 5, 10 and 15% of ash) and a total of 27 blends for all three ash types. **Compaction characteristics have been determined for different ash and lime combinations and UCS samples have been prepared at respective OMC and MDDs**. The samples were cured for 7 and 28 days. The effect of Lime and ash as stabilizing agent on the samples have been determined by conducting Unconfined compression tests on each sample before and after curing. The procedure for various tests were carried out in accordance with that stipulated in IS code.

3 Results and Discussion

The variation of UCC with curing period for the same has been presented in Fig. 1. The UCC of soil has been found to be increase with no of days of curing. It has been observed the improvement of strength from 0 to 28 days for wood ash, sugar cane pulp ash, and coconut shell ash was found to be 39, 43, and 65% respectively. Significant improvement in strength 26, 28, and 50% has been observed during 0–7 days of curing as compared to 10, 10 and 11% from 7 to 28 days for wood ash, sugarcane pulp ash and coconut shell ash respectively. However UCC test have been conducted for 1, 3, and 5 wood ash gives the maximum strength as compared to sugar cane pulp ash and coconut shell ash.

Percentage mix of lime with different admixture ashes. Therefore the variation of UCC and percentage of lime for 28 days curing has been shown in Fig. 2. It has been found that at 3% lime content maximum UCC was obtained. The maximum increase in strength was found to be 24% between coconut shell ash and wood ash.

From Figs. 1 and 2 It has been observed that UCC was found to be maximum at 28 days and 3% lime therefore the variation UCC for different percentages of ash for 28 days curing and 3% lime has been presented in Fig. 3. It has been observed

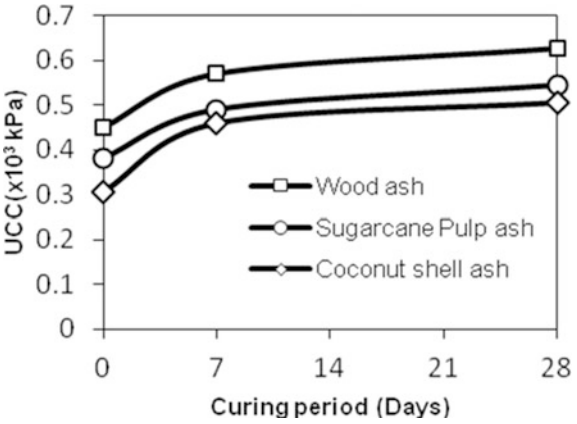

Fig. 1 UCC versus curing period for 3% lime and 10% Ash

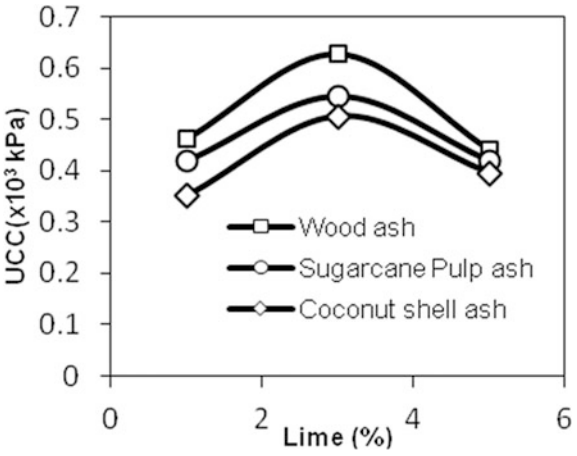

Fig. 2 UCC versus lime content for 10% Ash and 28 days curing

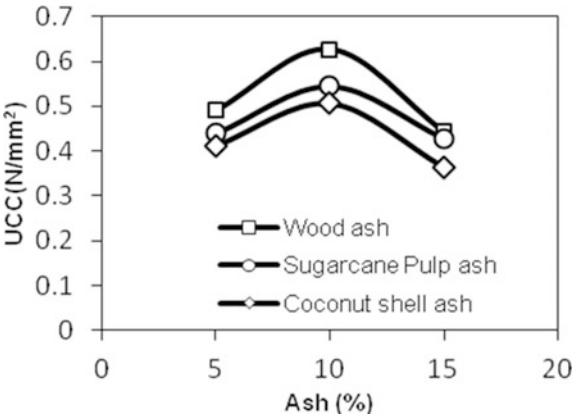

Fig. 3 UCC versus ash content for 3% lime and 28 days curing

that maximum strength was found to be at 10% of ash. UCC has been found to be maximum for wood ash. The difference between UCC of coconut shell ash and sugarcane pulp ash, wood ash and sugarcane pulp ash was found to be 7 and 15% respectively. Increased Unconfined compressive strength values could be attributed to ion exchange at the surface of clay particles as the Ca^{2+} in the ash reacted with the lower valence metallic ions in the clay microstructure which resulted in agglomeration and flocculation of the clay particles (Ijimdiya et al. 2012).

The Unconfined compressive strength increase slowly with increase of percentage of ash, maximum strength obtained for 10% of ash content. The strength then decrease with increase of percentage of ash. The increase recorded was marginal at 7 days curing period.

4 Conclusions

From the present study the following conclusions are made:

- The strength increases with increase in curing period.
- The effective percentage replacements of all three ash types were found to be 10%.
- The compressive strength of soil increases with increase in lime content up to 3% and then decreases.
- The strength achieved was high in case of wood ash compared to the other two because of high lime content.
- Soil stabilization can be done using different additives but use of Sugarcane pulp, Wood and Coconut shell ash which are waste materials, at the same time difficult to dispose will be much significant.
- The swelling index reduced with the addition of various percentages of ash and lime content, indicating a reduction in swelling potential and hence an increase in strength.

Therefore it is concluded that sugar cane pulp ash, wood ash and coconut shell ash have a good potential in improving the strength properties of clay soil. Its benefits include greatly reducing the cost of stabilization and reducing the adverse environmental impact.

References

Amu, O. O., Owokade, O. S., & Shitan, O. I. (2011). Potentials of coconut shell and husk ash on the geotechnical properties of lateritic soil for road works. *International Journal of Engineering and Technology, 3*(2), 87–94.

Bowles, J. E. (1979). *Physical and geotechnical properties of soil* (4th ed.). London: Publish division of international Thomas publishing.

Dallas, N. L. (2001). *Evaluation of structural properties of lime stabilized soils and aggregates* (Vol. 3), Mixture design and testing protocol of lime stabilized soils. Texas A&M University.

Das, B. M. (1998). *Principles of geotechnical engineering* (4th ed.). London: PWS publish division of international Thomas publishing.

Edil, T. B., Berthouex, P. M., & Vesperman, K. D. (1987). Fly ash as a potential waste liner. In *Proceedings of the Conference on Geotech Practice for Waste Disposal*, Vol. 13. Geotech Special publication, ASCE, pp. 447–461.

Ijimdiya, T. S., Ashimiyu, A. L., & Abubakar, D. K. (2012). Stabilization of black cotton soil using groundnut shell ash. *EJGE, 17,* 3645–3652.

Kharade, A. S., Suryavanshi, V. V., Gujar, B. S., & Deshmukh, R. R. (2014). Waste product bagasse ash from sugar industry can be used as stabilizing material for expansive soils. *International Journal of Research in Engineering and Technology (IJRET), 3*(3), 506–512.

Kolias, S., Kasselouri-Rigopoulou, V., & Karahalios, A. (2005). Stabilization of clay soils with high calcium and cement. *Cement & Concrete Composites, 27,* 301–313.

Rama Rao, M., Sreerama Rao, A., & Dayakara Babu, R. (2008). Efficacy of cement-stabilized fly ash cushion in arresting heave of expansive soils. *Geotechnical Geological Engineering, 26,* 189–197.

The Tensile Strength Behavior of Lime-Stabilized Soft Soil with Inclusion of Plastic Fiber

Dhar Subhradeep and Hussain Monowar

Abstract In this paper an experimental investigation was conducted to study the effects of lime and plastic fiber on split-tensile strength and toughness properties of a soft soil. The specimens were prepared and tested at three different percentages of lime (i.e. 3, 5 and 9% by weight of the dry soil) and four different percentages of fiber content (i.e., 0.5, 1, 1.5, and 2% by weight of the dry soil). It was found that lime content, curing duration and fiber content has a significant influence on the split-tensile strength and toughness of the lime-stabilized-fiber-reinforced soil. The test results indicated that lime amendment enhanced the split-tensile strength up to 5% of lime beyond that it shows an adverse effect. Moreover, the inclusion of discrete plastic fiber with lime-stabilized soil further enhanced the spilt-tensile strength and toughness of the treated soil. This improvement is up to 1.5% of fiber beyond that effectiveness of the reinforcement reduced. Therefore, 5% lime with the inclusion of 1.5% plastic fiber is the optimum combination to improve the soft soil. With this combination of lime and fiber at 28 days curing, the split-tensile strength shows an increase of 20 times compared to parent soil. This improvement of the treated soil enhanced the pavement life and stability of the other geotechnical structures.

Keywords Soft soil · Lime stabilization · Fiber reinforcement
Split-tensile strength

D. Subhradeep · H. Monowar (✉)
Department of Civil Engineering, National Institute of Technology Silchar,
Silchar 788010, Assam, India
e-mail: monowarhussain@gmail.com

D. Subhradeep
e-mail: subhradeep24@gmail.com

T. Thyagaraj (ed.), *Ground Improvement Techniques and Geosynthetics*, Lecture Notes in Civil Engineering 14, https://doi.org/10.1007/978-981-13-0559-7_24

1 Introduction

In slope, earth dams, embankment, highway and airfield pavements tensile cracks are common and their stability depends on the tensile strength of soil. But soil has weak in tensile strength and as a result, tensile cracks are often observed. The tensile strength can be improved by using chemical binders and reinforcement. Among all chemical stabilizer, lime stabilization is widely used because of its overall economy and ease of construction (Bell 1996; Cai et al. 2006; Dash and Hussain 2012). The advantageous effect of lime is that when lime is added to soft soil it generates long-term strength gain through pozzolanic reaction. Due to this reaction promotes stable calcium silicate hydrates (CSH) and calcium aluminates hydrates (CAH) forms which coat the soil particles and subsequently crystallize to bond them. However, lime treatment contributed to the brittle failure characteristics of soils which led to a rapid and great loss in strength when a failure occurs. Discrete fibers can be mixed randomly into soils to improve the strength and stiffness of the treated soil (Maher and Ho 1994). Fiber-reinforced soil exhibits greater toughness and ductility and a smaller loss of post-peak strength as compared to the unreinforced soil (Cai et al. 2006). The improvement of tensile stress is essential in pavement because during traffic loads its layer is subjected to repeated tensile stresses, and failure is initiated due to the formation and propagation of tensile cracks. Therefore, knowledge of tensile strength is of primary interest for design engineers. This paper highlights the results of an experimental investigation on the tensile strength and toughness behavior of lime-stabilized soft soil with the inclusion of plastic fiber.

2 Materials

2.1 Soil

The soil used in this study is locally available soft soil. It has predominantly fine-grained consisting of 72% silt and clay, of which the silt is predominant (67.10%). The specific gravity, liquid limit and plastic limit of soil are 2.6, 43.4 and 22.4% respectively. As per Unified Soil Classification System (USCS) the soil is classified as clay with low plasticity (CL).

2.2 Lime

Laboratory reagent grade quick lime (CaO) is used in this investigation. Its molecular weight and minimum assay are found to be 56.08 and 95% respectively.

2.3 Plastic Fiber

The fiber used in this study is commercially available synthetic plastic fiber. The characteristics of plastic fibers used as reinforcement are given in Table 1.

3 Experimental Program

The split-tensile strength test was performed to evaluate the improvement of tensile strength due to the soil-lime-fiber reaction. The specimens were statically compacted at optimum water content and maximum dry density in a split mould of size 38 mm in diameter and 76 mm in length. An additional amount of water equal to 32% of the mass of lime was added to take into account for slacking of lime and loss due to evaporation (Greaves 1996). The compacted specimens were then extracted from the mould and stored in desiccators. The prepared specimens were placed horizontally between the bearing blocks of the compression testing machine adjusted for a strain rate of 1.2 mm/min. A strips of mild steel of 5 mm thick, 5 mm wide, and 50 mm long curved at the contact surface were placed on the upper and lower bearing elements of the cylinder to ensure uniform bearing pressure. A photographic view of a specimen for the split-tensile test is shown in Fig. 1. The split-tensile strength (σ_t) is obtained by the following equation:

$$\sigma_t = \frac{2p}{\pi td}, \tag{1}$$

where p = load at failure; t = thickness or length of the specimen; d = diameter of the specimen.

Table 1 Physical and engineering properties of fiber used

Property	Value
Type	Plastic (synthetic)
Average length (mm)	15
Average diameter (mm)	0.17
Aspect ratio (L/d)	88.24
Color	White
Breaking tensile strength	355.05 MPa
Modulus of elasticity	1836.11 MPa
Toughness index	138.19 MPa
Tensile elongation (%)	77.84

Fig. 1 Photographic view of split-tensile test

4 Results and Discussion

4.1 Tensile Strength of Lime-Stabilized Soft Soil

Split-tensile strength is performed to understand the tensile strength behavior of the lime-stabilized soil. Figure 2 shows the variation of split-tensile strength with the percent of lime content at different curing period. The split-tensile strength of lime-stabilized soil increases with increase in lime content up to 5% of lime beyond that it decreases with increase in lime content, meanwhile, the tensile strength value of lime-stabilized soil further increased with increase in the curing period. With 5% lime at 28 days curing the maximum split-tensile strength obtained is 65.94 kPa which represented an increase of nearly 9 times that of untreated soil. It is also observed that for all curing period the split-tensile strength attains maximum value at 5% of lime content. Therefore 5% lime is the optimum lime content. The addition of lime to the soil, in a strongly basic environment (pH $\geq$ 12), progressively dissolves the silica and alumina that form the cementations compound like CSH and CAH (Bell 1996; Dash and Hussain 2012). These cementations compounds bind the particles leading to increase in tensile strength and make the material more

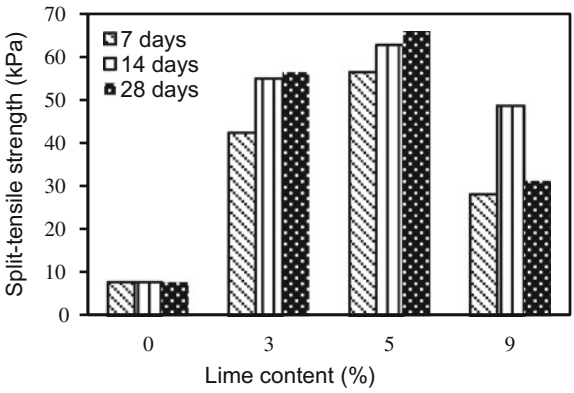

Fig. 2 Split-tensile strength of lime stabilized soil at different curing period

brittle. However, at higher lime content, a reduction in strength takes place due to excessive formation of cementations gel materials which counteract the strength gain.

4.2 Tensile Strength of Fiber-Reinforced Soft Soil

Figure 3 represents the variation of split-tensile strength with percentage of fiber content. It was observed that split-tensile strength increases with the increase in fiber content up to 1.5% and beyond that it was decreased with further addition of fiber. Similar behavior was observed by Maher and Ho (1994). With this optimum fiber content (i.e., 1.5%), fiber-reinforced soil developed a split-tensile strength of 28.52 kPa which represents an increase of 3.63-folds compared with that of unreinforced soil. The increase in the split-tensile strength is due to the friction between the fiber and soil particles, which make difficult for soil particles that surround fibers to change in position from one point to another and thereby improves the bonding force between soil particles (Jiang et al. 2010). However, with fiber content higher than 1.5%, the relative volume occupied by fibers increases and fiber-to-fiber interaction dominated compared to soil to fiber interactions. Hence, the degree of interlocking and friction mobilized in the sample reduced and hence decreases the tensile strength (Anggraini et al. 2015).

4.3 Tensile Strength of Lime-Stabilized-Fiber-Reinforced Soft Soil

Variation of split-tensile strength with fiber and lime content for lime-stabilized-fiber-reinforced soil at 28 days curing is depicts in Fig. 4. Result shows that fiber plays a major role in lime treated soil and its influence on normal

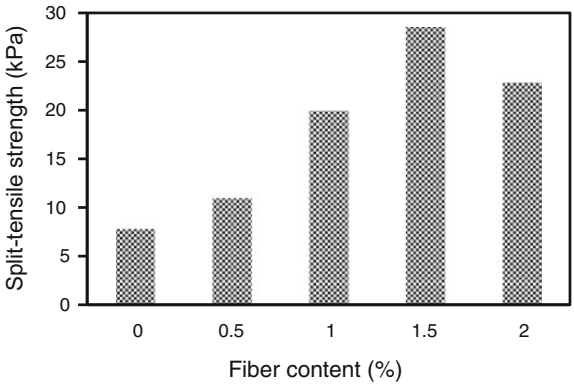

Fig. 3 Variation of Split-tensile strength with percentage of fiber content

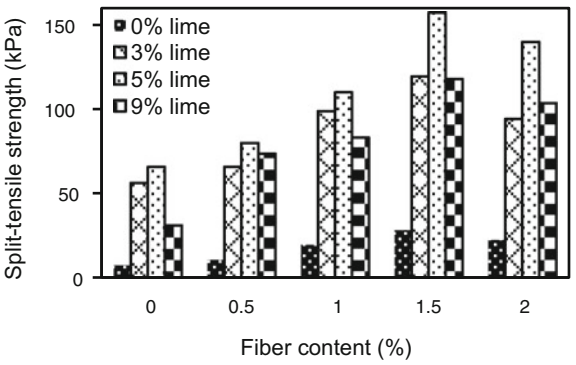

Fig. 4 Variation of split-tensile strength with fiber and lime content at 28 days curing

soil is not significant. Due to the smaller pores in the lime-stabilized soil than that of untreated soil, the effective contact area of a fiber with soil particles in the lime-fiber treated soil is greater than that in the pure fiber soil. Thus, the total effective friction between fiber and soil particles in the fiber–lime treated soil is greater, which causes more effective fiber reinforcement (Cai et al. 2006). It is also observed that for any fiber content, the axial stress increases with increase in lime content up to 5% and beyond that it declines. Similar behavior is observed for 7 and 14 days curing period. Dash and Hussain (2012) reported that lime produces cementations gel that has a substantial volume of pores upon reacting with soil. Therefore, with increased lime content, the soil structure tends to be increasingly porous and amorphous structure which counteracts the strength gain attributable to cementation. Further, this amorphous structure of lime treated soil reduced the effective friction and interlocking bonding between fiber and treated soil.

Figure 5 shows the variation of split-tensile strength with curing period (i.e., 7, 14, and 28 days) for lime-stabilized-fiber-reinforced specimen at optimum lime content (i.e., 5%). It is observed that strength increases while increasing the length of curing. The increase in strength with the curing period is attributed to the

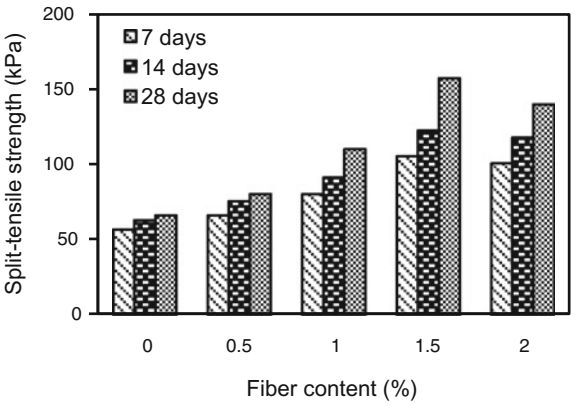

Fig. 5 Variation of split-tensile strength with varying percentage of fiber and curing period at 5% lime content

long-term pozzolanic reactions of lime with the soil leading to an increase in strength (Rao and Rajasekaran 1996). Similar behavior is observed at lime content 3 and 9%.

The maximum split-tensile strength of the treated soil is obtained for the combination of 5% lime (i.e., optimum lime) with 1.5% fiber (i.e., optimum fiber) at 28 days curing period is 157.09 kPa. This represents an increase of 20 times compared to the untreated soil. The inclusion of randomly oriented fibers to stabilized soil ensures that instead of a catastrophic brittle failure, a structure is still able to bear load, sometimes increasing load after the first crack. This enhances the service life of a pavement structure.

4.4 Toughness Characteristics

Toughness is the ability of a material to absorb energy without fracturing. It is measured from the area under the load-deflection curve up to failure (Onyejekwe and Ghataora 2014). Increased toughness may bring about improved resistance to fatigue failure which is extremely beneficial for pavement applications. Figure 6 shows the variation of toughness with fiber and lime content at 28 days curing period. It is clear that for a particular lime content toughness increases with increase in fiber content up to 1.5% fiber and beyond that it generally decreases. Meanwhile, the toughness also increases with increasing in the curing period. The rate of absorbed energy increases on increasing fiber content because of a larger probability of intersecting weak zones by fibers and also because of absorbed energy by fibers that are already in tension (Mirzababaei et al. 2013). The improved toughness and ductility of fiber-reinforced soil has led to its use in pothole repairs (Balamu 1998).

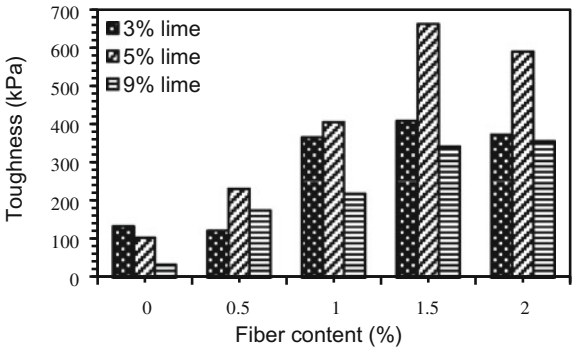

Fig. 6 Variation of toughness with fiber and lime content at 28 days curing period

5 Conclusions

- Amendments of lime enhanced split-tensile strength up to 5% of lime beyond that its shows adverse effect. The increase in tensile strength is about ninefold in comparison to parent soil. The gain in strength due to long-term pozzolanic reaction between lime and soil.
- Addition of discrete fiber increases the Split-tensile strength of soil up to 1.5% of fiber content and beyond that it decreases due to too much fiber added adhere to each other to form lumps.
- The inclusion of fiber reinforcement within lime-stabilized soil caused an increase in the tensile strength. Fiber plays a major role in lime treated soil than normal soil. The maximum split-tensile strength is obtained for the combination of 5% lime and 1.5% fiber at 28 days curing and its value is 157.09 kPa, which is 20 times that of the untreated soil.
- Inclusion of plastic fiber in lime-stabilized soil improved the toughness and ductility of the treated soil. This improvement of the treated soil enhanced the pavement life and stability of the other geotechnical structures.

References

Anggraini, V., Asadi, A., Huat, B. B. K., & Nahazanan, H. (2015). Effects of coir fibers on tensile and compressive strength of lime treated soft soil. *Measurement, 59,* 372–381.

Balamu, P. B. (1998). *Reinforcement of soils with natural fibre sisal (M.Sc. thesis, Dept. of Civil Engineering)*, University of Birmingham, Edgbaston, Birmingham, UK.

Bell, F. G. (1996). Lime stabilization of clay minerals and soils. *Engineering Geology, 42*(4), 223–237.

Cai, Y, Shi, B., Ng, C. W. W., Tang, C. (2006). Effect of polypropylene fibre and lime admixture on engineering properties of clayey soil. *Journal of Engineering Geology, 87*, 230–240.

Dash, S. K., & Hussain, M. (2012). Lime stabilization of soils: Reappraisal. *Journal of Materials in Civil Engineering, 22,* 533–538.

Greaves, H. M. (1996). An introduction to lime stabilization. In *Proceedings of Seminar on Lime Stabilization* (pp. 5–12), *Loughborough University*, London.

Jiang, H., Cai, Y., & Liu, J. (2010). Engineering properties of soils reinforced by short discrete polypropylene fiber. *Journal of Material Civil Engineering, 22,* 1315–1322.

Maher, M. H., & Ho, Y. C. (1994). Mechanical properties of kaolinite/fiber soil composite. *Journal of Geotechnical Engineering, 120,* 1381–1393.

Mirzababaei, M., Miraftab, M., Mohamed, M., & McMahon, P. (2013). Unconfined compression strength of reinforced clays with carpet waste fibers. *Journal of Geotechnical and Geoenvironmental Engineering, 139*(3), 483–493.

Onyejekwe, S., & Ghataora, G. S. (2014). Effect of fiber inclusions on flexural strength of soils treated with nontraditional additives. *Journal of Material in Civil Engineering, 26*.

Rao, S. N., & Rajasekaran, G. (1996). Reaction products formed in lime-stabilized marine clays. *Journal of Geotechnica Engineering, 122,* 329–336.

Pullout Behaviour of Geosynthetics—A Review of Laboratory Testing Techniques

Riya Bhowmik, Manoj Datta and J. T. Shahu

Abstract Stability of anchored geosynthetics in landfill covers and liners depends on the efficiency of anchorage of reinforcement at berms and top of landfills. Pull-out tests can give an insight into the anchorage behaviour of geosynthetics. A review of literature for horizontal and inclined pull-out apparatus has been done and reported in this paper. A large number of pull-out apparatus have been developed for horizontally embedded geosynthetics. However none of these are suitable for the study of geosynthetics embedded in anchor trenches. For inclined pull-out apparatus, only two studies have been reported so far. Both the apparatus facilitate modelling of anchor trenches, but both of them had limitations. From the comparative study, it is concluded that there is a need to develop a universal pull-out system for study of behaviour of geosynthetics embedded in anchor trenches. An optimal solution could be obtained from a hybrid design of the two inclined pull-out apparatus and ASTM recommendations.

Keywords Geosynthetics · Anchor Trench · Inclined pull out

1 Introduction

In applications such as liners and covers of landfills, the stability of the geosynthetic reinforcement depends on the efficiency of the anchorage system. The most common types of anchors are simple run-out anchors or anchors embedded in a trench along the berm. In order to study the behaviour of anchor trenches, pull-out model tests are needed to be carried out on anchored geosynthetics.

R. Bhowmik (✉) · M. Datta · J. T. Shahu
Department of Civil Engineering, IIT Delhi, New Delhi 110016, India
e-mail: riyabhowmik89@gmail.com

M. Datta
e-mail: mdatta@civil.iitd.ac.in

J. T. Shahu
e-mail: shahu@civil.iitd.ac.in

T. Thyagaraj (ed.), *Ground Improvement Techniques and Geosynthetics*, Lecture Notes in Civil Engineering 14, https://doi.org/10.1007/978-981-13-0559-7_25

2 Objective and Methodology

The present study focuses on identifying the most suitable pull-out set-up for study of the behaviour of geosynthetics buried in anchor trenches, when pulled horizontally as well as in inclined direction along the slope of landfill.

The methodology adopted comprises of review of literature and comparison of the equipment details relating to dimensions of laboratory apparatus, direction of pull, conditions at top wall, conditions at front and side walls, effect of sleeves and clamps and modelling of anchor trench.

3 Horizontal Pull-Out Test Apparatus

Table 1 summarises the primary features of the existing test apparatus for horizontal pull out, as well as inclined pull out, as reported in literature. The table also highlights whether the apparatus facilitates modelling of anchor trench. It can be noticed from Table 1, that the design of the apparatus is influenced by the need to minimise the effect of the boundary conditions.

3.1 Boundary Conditions

3.1.1 Dimensions of Pull-Out Box

Palmeira and Milligan (1989) found that the development of lateral stresses on the front wall during pull out of geosynthetics is lower for large pull-out boxes. Large boxes also enable longer embedded length of the reinforcement. As the embedded length and normal stress increases, the stress–strain behaviour changes from strain-softening to strain-hardening (Moraci and Recalcati 2006). The largest pull-out box was set up by Lajevardi et al. (2014) while the smallest pull-out box was set up by Palmeira and Milligan (1989) (refer Table 1).

3.1.2 Conditions at Top Wall

The vertical stress on the testing area is applied either by a rigid plate (refer Table 1) or by flexible water or air pressurised rubber bags. Researchers found that use of a flexible system allows even distribution of the normal stress on the entire surface of the reinforcement (Farrag et al. 1993), while use of a rigid load application system results in concave pressure distribution (Hsieh and Hsieh 2003). Some researchers used higher sample height over the reinforcement to reduce the influence of the rigidity of the top plate (Palmeira and Milligan 1989; Farrag et al. 1993; Lopes and Ladeira 1996).

Table 1 Summary of horizontal and inclined pullout test apparatus

Reference [Lab] [Horizontal Pull (H)/Inclined Pull (I)]	Dimensions (mm)	Front wall condn. Sleeves (S)—Yes/No Clamps (C)—In/Out	Side wall condn.	Top load	Anchor Trench (Y/N)
Palmeira and Milligan (1989) [Univ. of Oxford, UK] [H]	1000 × 1000 × 1000 253 × 150 × 200	Varies S—No C—Out	Perspex Sheets	Water Bag	N
Farrag et al. (1993) [LSU., USA] [H]	1520 × 900 × 760	S—Yes C—In	Steel Plates	Air Bag	N
Wilson Fahmy et al. 1994 [Drexel Univ., USA] [H]	1900 × 910 × 1100	S—Yes C—In	Steel Plates	Air Bag	N
Alfaro et al. (1995a, b) [Saga Univ., Japan] [H]	1600 × 600 × 500	S—Yes C—In	Lubricated Rubber Membranes	Air Bag	N
Raju. (1995) [The University of British Columbia, Canada] [H]	1300 × 640 × 600	Aluminium S—No C—Out	Hard Glass Sheet glued with Plexi Glass Sheet	Water & Air Bag	N
Lopes and Ladeira (1996) [Univ. of Porto, Portugal] [H]	1530 × 1000 × 800	S—Yes C—Out	Thick Neoprene sheet	Cylindrical masses	N
Voottipruex et al. (2000) [AIT, Thailand] [H]	1270 × 760 × 508	S—Yes C—Out	Steel Plates	Air Bag	N
Sugimoto et al. (2001) [Nagaoka Univ. of Tech., Japan] [H]	680 × 300 × 625	Rigid and flexible cond. S—No C—Out	Acrylic Plates glued with Hard Glass Plates	Air Bag	N
Moraci and Recalcati (2006) [Univ. of Reggio Calabria, Italy] [H]	1700 × 600 × 680	S—Yes C—In	Smooth Teflon films	Air Bag	N

(continued)

Table 1 (continued)

Reference [Lab] [Horizontal Pull (H)/Inclined Pull (I)]	Dimensions (mm)	Front wall condn. Sleeves (S)—Yes/No Clamps (C)—In/Out	Side wall condn.	Top load	Anchor Trench (Y/N)
Teixeira et al. (2007) [Univ. of Sao Paulo, Brazil] [H]	1500 × 700 × 480	S—Yes C—Out	Lubricated PE membranes	Air Bag	N
Abdi and Arjomand (2011) [KNT Univ, Iran] [H]	300 × 300 × 200	S—Yes C—Out	Steel Plate	Rigid Plate	N
Abdi and Zandieh (2014) [KNT Univ, Iran] [H]	1000 × 600 × 600	Geofoam S—No C—Out	PE Sheet and Grease-lubrication	Air Bag	N
Lajevardi et al. (2014) [CNAM Paris, France] [H]	2000 × 1100 × 1100	S—Yes C—In	Steel Plate	Air Bag	N
Prasad and Ramana (2016a, b) [CRRI, India] [H]	1540 × 1100 × 1000	S—Yes C—In	Steel Plate	Rigid Plate	N
ASTM D6706-01 (2001) [H]	610 × 460 × 305	S—Yes C—In	HDPE/PE/lubricant/150 mm dist.	Air Bag	N
Koerner and Wayne (1991) [Drexel Univ., USA] [I]	1890 × 910 × 1070	Wood S—No C—Out	Wooden walls	Air Bag	Y
Chareyre et al. (2002) [Cemagref, France] [I]	1200 × 1000 × 1500	No front wall S—No C—Out	PP Geomembrane	–	Y

3.1.3 Effect of Front Wall

The influence of this boundary condition has been widely studied by many researchers. It was found that as the pull-out test progresses, the pressure at front wall increases (Raju 1995). This increment can be attributed to increment in the relative density of the soil in the vicinity of the rigid wall as a consequence of non-uniform displacement in the reinforcement at the time of pull out. This local increment in relative density causes local upsurge in the vertical stresses on the geogrid. Palmeira and Milligan (1989) showed that the increment in vertical stress is directly related to the interface friction angle (δ) between the infill soil and the front wall. Thus, the friction along the front walls is reduced by using low-friction materials (Teflon, Polyethylene sheets, Geofoam, oil/grease), flexible air bags, sleeves and clamping inside the box (refer Table 1).

3.1.4 Effect of Side Wall

The friction developed against the side walls can reduce the effective normal stress on the reinforcement. This is the reason that pull-out resistance increases when reinforcement width decreases (Farrag et al. 1993). To overcome this frictional effect, researchers have used low-friction materials glued to the wall (refer Table 1).

3.2 ASTM Guidelines

ASTM has drafted a standard (D6706-01) with recommendations to minimise the influences of the boundary conditions (refer Table 1 and Fig. 1).

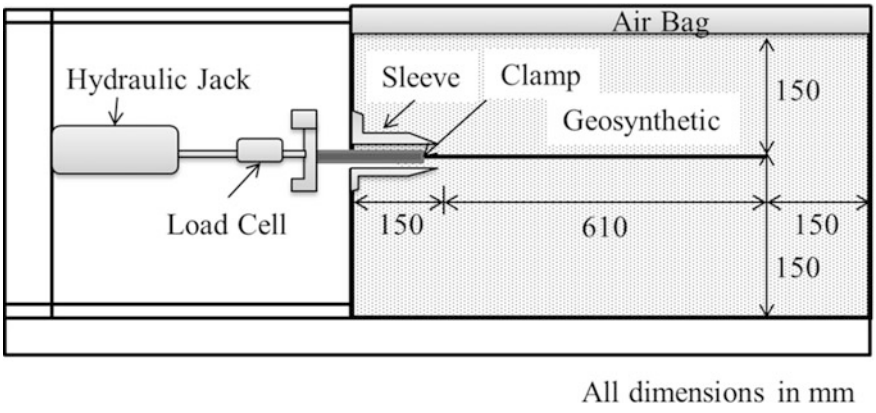

Fig. 1 Schematic diagram of experimental set-up recommended by ASTM D6706-01

It recommends the minimum reinforcement length to be greater of 610 mm and 5 times the aperture size of the geosynthetic. The minimum width is recommended to be greater of 460 mm and 20 times the D_{85} of soil, for smooth lateral walls; or 760 mm for rough lateral walls. The height of soil sample above and below the reinforcement is recommended to be 150 mm and at least 6 times D_{85} of soil or 3 times the maximum soil particle size.

3.3 Inclined Pull-Out Test Apparatus

On reinforced cover of landfills, the pull induced on the anchored geosynthetics is in inclined direction. To simulate the inclined pull on anchored geosynthetics, Koerner and Wayne (1991) developed a pull-out apparatus where a jacking system could pull the anchored geosynthetic in inclined direction, while the vertical stress was provided by air bag (Fig. 2). The front wall of the test box was rigid and this rigidity shadowed the influence of the inclination on the pull-out capacity.

Chareyre et al. (2002) developed an inclined pull-out device, consisting of an anchorage bench and a traction system. The anchorage bench did not have any front wall and the vertical stress on the reinforcement was provided by overburden only. No system for external application of vertical stress was provided. The traction system consisted of a winch and a pulley that enabled tensile forces to be applied at inclined angles (Fig. 3).

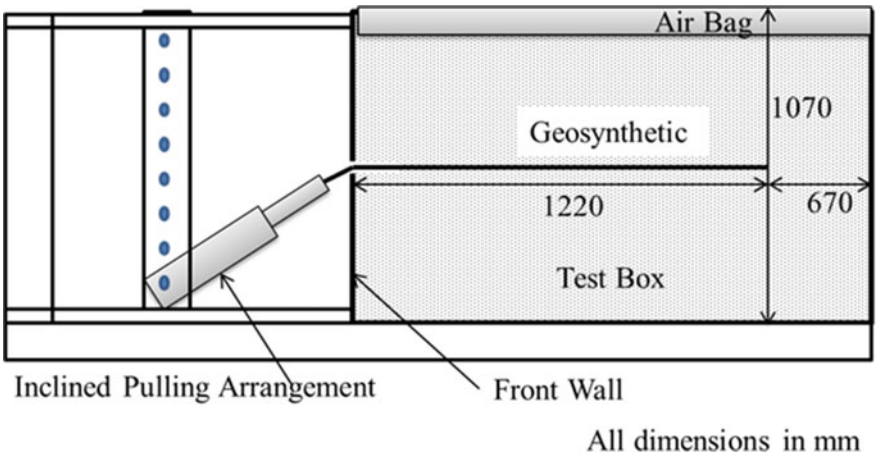

Fig. 2 Schematic diagram of experimental set-up developed by Koerner and Wayne (1991)

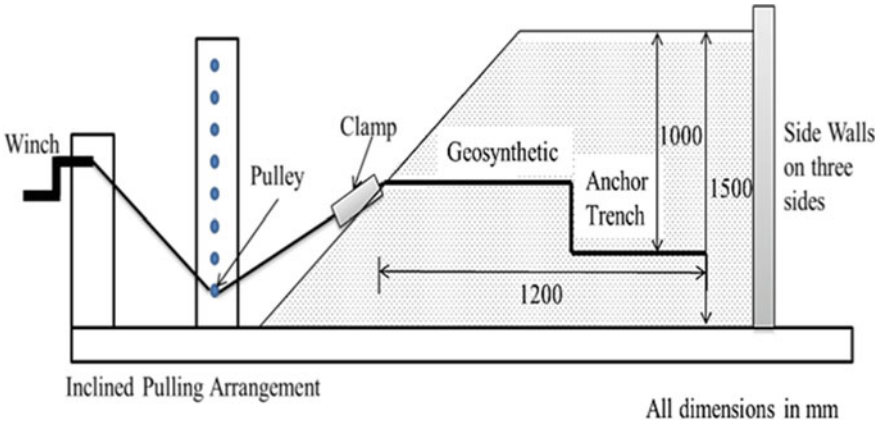

Fig. 3 Schematic diagram of experimental set-up developed by Chareyre et al. (2002)

The pull-out capacity was reported to be increasing with inclination of pull. However, the system cannot be used for applying medium to high normal stresses.

Although these apparatuses facilitated inclined pull on geosynthetics, but none of them satisfied the conditions provided by ASTM D6706-01.

4 Conclusions

- Horizontal pull-out apparatus have been developed by many researchers and standardised by ASTM for study of pull-out behaviour of horizontally embedded geosynthetics in RE walls. However, these apparatus do not have provision for modelling anchor trenches.
- Two studies have been reported for inclined pull-out apparatus with provision of anchor trenches. Both the apparatus have limitations; the apparatus by Koerner and Wayne (1991) is subjected to rigid front wall effect and the apparatus by Chareyre et al. (2002) has no system for external application of vertical load.
- A hybrid of the apparatus developed by Koerner and Wayne (1991) with sleeve arrangement, and Chareyre et al. (2002) with surcharge arrangement would be an optimal solution. Such an apparatus should also satisfy the conditions provided by ASTM D6706-01.

References

Abdi, M. R., & Arjomand, M. A. (2011). Pullout tests conducted on clay reinforced with geogrid encapsulated in thin layers of sand. *Geotextiles and Geomembranes, 29*, 588–595. https://doi.org/10.1016/j.geotexmem.2011.04.004.

Abdi, M. R., & Zandieh, A. R. (2014). Experimental and numerical analysis of large scale pull out tests conducted on clays reinforced with geogrids encapsulated with coarse material. *Geotextiles and Geomembranes, 42,* 494–504. https://doi.org/10.1016/j.geotexmem.2014.07.008.

Alagiyawanna, A. M. N., Sugimoto, M., Sato, S., & Toyota, H. (2001). Influence of longitudinal and transverse members on geogrid pullout behavior during deformation. *Geotextiles and Geomembranes, 19,* 483–507. https://doi.org/10.1016/S0266-1144(01)00020-6.

Alfaro, M. C., Hayashi, S., Miura, N., & Watanabe, K. (1995a). Pullout interaction mechanism of geogrid strip reinforcement. *Geosynthetics International, 2,* 679–698.

Alfaro, M. C., Miura, N., & Bergado, D. T. (1995b). Soil–geogrid reinforcement interaction by pullout and direct shear tests. *Geotechnical Testing Journal, 18,* 157–167.

ASTM D6706-01. (2001). *Standard test method for measuring geosynthetic pullout resistance in soil*. Philadelphia: ASTM.

Bergado, D. T., Youwai, S., Teerawattanasuk, C., & Visudmedanukul, P. (2003). The interaction mechanism and behavior of hexagonal wire mesh reinforced embankment with silty sand backfill on soft clay. *Computers and Geotechnics, 30,* 517–534. https://doi.org/10.1016/S0266-352X(03)00054-5.

Chareyre, B., Briançon, L., & Villard, P. (2002). Theoretical versus experimental modeling of the anchorage capacity of geotextiles in trenches. *Geosynthetics International, 9,* 97–123. https://doi.org/10.1680/gein.9.0212.

Farrag, K., Acar, Y. B., & Juran, I. (1993). Pull-out resistance of geogrid reinforcements. *Geotextiles and Geomembranes, 12,* 133–159.

Hayashi, S., Shahu, J., & Watanabe, K. (1999). Changes in interface stresses during pullout tests on geogrid strip reinforcement. *Geotechnical Testing Journal, 22*(1), 32–38. http://dx.doi.org/10.1520/GTJ11314J. ISSN 0149-6115.

Hsieh, C., & Hsieh, M. W. (2003). Load plate rigidity and scale effects on the frictional behavior of sand/geomembrane interfaces. *Geotextiles and Geomembranes, 21,* 25–47. https://doi.org/10.1016/S0266-1144(02)00034-1.

Koerner, R. M., & Wayne, M. H. (1991). Mechanical and hydraulic testing of geomembranes. In A. Rollin & J. M. Rigo (Eds.), *Geomembrane identification and performance testing, RILEM report 4* (pp. 204–218). London: Chapman and Hall.

Lajevardi, S. H., Briançon, L., & Dias, D. (2014). Experimental studies of the geosynthetic anchorage—Effect of geometric parameters and efficiency of anchorages. *Geotextiles and Geomembranes, 42,* 505–514. https://doi.org/10.1016/j.geotexmem.2014.07.010.

Lajevardi, S. H., Dias, D., & Racinais, J. (2013). Analysis of soil-welded steel mesh reinforcement interface interaction by pull-out tests. *Geotextiles and Geomembranes, 40,* 48–57. https://doi.org/10.1016/j.geotexmem.2013.08.002.

Lajevardi, S. H., Silvani, C., Dias, D., Briançon, L., & Villard, P. (2015). Geosynthetics anchorage with wrap around: Experimental and numerical studies. *Geosynthetics International, 22,* 273–287. https://doi.org/10.1680/gein.15.00010.

Lopes, M. L., & Ladeira, M. (1996). Role of specimen geometry, soil height and sleeve length on the pull-out behaviour of geogrids. *Geosynthetics International, 3*(6), 701–719.

Moraci, N., & Recalcati, P. (2006). Factors affecting the pullout behaviour of extruded geogrids embedded in a compacted granular soil. *Geotextiles and Geomembranes, 24,* 220–242. https://doi.org/10.1016/j.geotexmem.2006.03.001.

Palmeira, E. M., & Milligan, G. W. E. (1989). Scale and other factors affecting the results of pull-out tests of grids buried in sand. *Geotechnique, 39,* 511–524.

Prasad, P. S., & Ramana, G. V. (2016a). Imperial smelting furnace (zinc) slag as a structural fill in reinforced soil structures. *Geotextiles and Geomembranes, 44,* 406–428.

Prasad, P. S., & Ramana, G. V. (2016b). Feasibility study of copper slag as a structural fill in reinforced soil structures. *Geotextiles and Geomembranes, 44,* 623–640. https://doi.org/10.1016/j.geotexmem.2016.01.009.

Raju, D. M. (1995). *Monotonic and cyclic pullout resistance of geosynthetic* (Ph.D. thesis). The University of British Columbia, Vancouver, Canada.

Sugimoto, M., Alagiyawanna, A. M. N., & Kadoguchi, K. (2001). Influence of rigid and flexible face on geogrid pullout tests. *Geotextiles and Geomembranes, 19,* 257–277.

Teixeira, S. H. C., Bueno, B. S., & Zornberg, J. G. (2007). Pullout resistance of individual longitudinal and transverse geogrid ribs. *Journal of Geotechnical and Geoenvironmental Engineering, 133,* 37–50.

Voottipruex, P., Bergado, D. T., & Ounjaichon, P. (2000). Pullout and direct shear resistance of hexagonal wire mesh reinforcement in weathered Bangkok clay. *Geotechnical Engineering Journal, 31*(1), 43–62.

Wilson-Fahmy, R. F., Koerner, R., & Sansone, L. (1994). Experimental behavior of polymeric geogrids in pullout. *Journal of Geotechnical Engineering, 120,* 661–677.

Model Study on Cyclic Loading Responses of Flexible Pavement System Laid on Expansive Subgrade

G. Radhakrishnan, M. Anjan Kumar and G. V. R. Prasada Raju

Abstract Flexible pavement system laid on the expansive soil subgrades show signs of continuous distress in the form of cracking, unevenness, rutting, etc., during its service period. Extensive laboratory, model, and field studies have been carried out by various researchers have shown promising results with the utilization of industrial by-products, i.e., quarry dust, rice husk ash, blast furnace slag, flyash, etc., for the stabilization of expansive subgrade. These materials offer two folded advantage of effective utilization and solution for their safe disposal. In this present work, an attempt has been made to study the efficacy of flyash in stabilizing the expansive soil subgrade. Laboratory experimentation was conducted for finding the optimum content of flyash required for treating the expansive soil. Model flexible pavement systems are prepared in circular tanks with different untreated and flyash treated subgrade layers. Tests are conducted to study their cyclic load responses. The experimental results show that model flexible pavement with 10% flyash treated subgrade is showing low heaving and low settlement to the applied cyclic loading. The coefficient of elastic uniform compression, representing variation of elastic rebound of the model pavements is assessed for model pavements.

Keywords Model flexible pavement system · Expansive subgrade
Cyclic loading

G. Radhakrishnan (✉)
Research Scholar Department of Civil Engineering,
JNT University Kakinada, Kakinada 533003, India
e-mail: radhakrishnan.gunupudi@gmail.com

M. Anjan Kumar
BVC College of Engineering, Palacharla 533104, India
e-mail: anjan_mantri@yahoo.com

G. V. R. P. Raju
Professor of Civil Engineering & Registrar, JNT University Kakinada,
Kakinada 533003, India
e-mail: gvrp_raju@yahoo.com

T. Thyagaraj (ed.), *Ground Improvement Techniques and Geosynthetics*, Lecture Notes in Civil Engineering 14, https://doi.org/10.1007/978-981-13-0559-7_26

1 Introduction

Many countries all over the world have huge accumulations of industrial byproduct like flyash. Flyash is an ash produced during the combustion of coal. In many countries the flyash quantity has been accumulating day by day, causing severe problem for its disposal at the cost of environmental sustainability. The production of flyash in India is around 175 million tons (Kaniraj and Gayathri 2003). The best solution for this problem is its utilization as a construction material, which may give a two-folded advantage. In India, a developing country, an extensive road network is under construction. Waste materials like flyash could be used in the road projects, particularly when the flexible pavements are laid on the expansive subgrade soils. Flyash is effective because of its pozzolanic reactivity with soil and also its silty character. Expansive soil exists in a typical state and its behavior is sensitive to changes in their moisture content. The swell pressures associated with changes in moisture content is responsible for the undesirable heave movements, which will contribute to significant damages to light weight civil engineering structures like light weight buildings, flexible pavements, pipelines, canal linings, etc. The financial loss due to these damages will generally exceed the loss due to natural hazards (Jones and Holtz 1973). Practicing engineers are using different stabilization techniques to reduce these losses associated with expansive soils (Puppala et al. 2006). There was an appreciable increase in CBR and resilient modulus values of the soil with the addition of flyash (Edil et al. 2006). It was suggested to use flyash for the stabilization of native expansive soils of Oklahoma as addition of flyash content reduced the linear shrinkage of the expansive soil (Buhler and Cerato 2007). A stabilized flyash layer was used in the pavement design to provide more stiffness to the conventional pavements (Bin-Shafique et al. 2004). Stabilization of the subgrade soil using flyash may enhance the dynamic properties of the pavement constructed on it. Model tests were conducted on square footings supported on sand beds and the variation of relative density of soil with coefficient of elastic uniform compression was reported (Moghaddas et al. 2008). In this present work an attempt is made to examine the effect of flyash as an additive in the stabilization of expansive subgrade soil. Model flexible pavements have been prepared with untreated and flyash treated subgrade layers and evaluated their cyclic load responses.

2 Materials Used

2.1 Expansive Soil

The high swelling soil sample used in the study was procured near Amalapuram town, East Godavari District, Andhra Pradesh, India. Soil was collected from a depth of 1.5 m below ground level. Soil was found to be fine grained and black in

Table 1 Basic Geotechnical properties of soil

Property	Value
Liquid limit (%)	85
Plastic limit (%)	29
Plasticity index (%)	56
Shrinkage limit (%)	12
Differential free swell (%)	140
Swell pressure (kPa)	295
Max dry density (kN/m^3)	15.2
OMC (%)	25
UCS (kPa)	94
California bearing ratio (%)	2.12

color. Soil grading showed that it contains silt and clay content of 23 and 65% respectively. This soil got classified as inorganic clay of high compressibility (CH) as per ISC System. The geotechnical properties of the soil are presented in Table 1.

2.2 Flyash

The flyash used in the study was collected from Vijayawada Thermal Power Station of Andhra Pradesh, India. It has a specific gravity of 1.95 and liquid limit of 25%. The maximum dry unit weight (MDD) and optimum moisture content (OMC) were found to be 13.25 kN/m^3 and 24% respectively. The chemical composition of fly ash was SiO_2 = 61.00%; Al_2O_4 = 21.6%; Fe_2O_3 = 3.09%; CaO = 1.02%; MgO = 0.50% and loss on ignition is around 0.2%. The fly ash is class F type and it was abundant.

2.3 Murrum

Murrum was used as a subbase material for preparing the model flexible pavements. The material is meeting the prescribed physical requirements. It contains gravel and fine sand contents of 62 and 27% respectively. The MDD and OMC were found to be 18.15 kN/m^3 and 18% respectively.

2.4 Aggregates

The coarse aggregate used is a crushable type aggregate of laterite having standard specification.

3 Experimental Work

3.1 Test Setup

Model tests are conducted using the test setup shown in Fig. 1, which consists of GI tank containing different layers of flexible pavement, reaction beam, hydraulic jack, proving ring, and dial gauges. The dimensions are chosen so that the families of isobars formed under a uniformly loaded circular area placed on top of the model pavement are confined within the model system. The vertical load was applied on the pavement system by means of hydraulic jack placed centrally on a circular metal bearing plate of 100 mm diameter and 25 mm thickness as shown in Fig. 1. Proving ring of 50 kN capacity was used to record the applied load and the settlement of the plate is measured with dial gauges of 0.01 mm sensitivity.

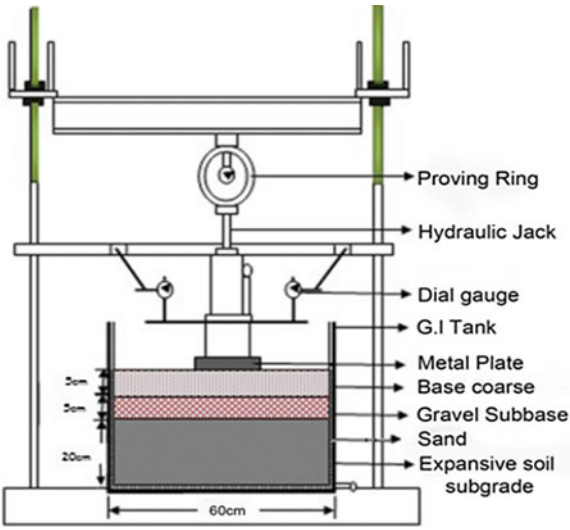

Fig. 1 Schematic diagram of test setup

3.2 Preparation of Subgrade, Subbase, and Base courses

Air dried expansive soil passing 4.75 mm sieve is used for preparing the subgrade. For treated subgrade, optimum percentage of flyash content obtained from laboratory experimentation has been mixed to form a homogeneous mixture. Water is added to the mix at optimum moisture content (OMC) of the natural soil and prepared a wet mix. Before laying the subgrade, a sand bed of 1 cm thickness was laid in the tank to serve as a drainage bed. Similarly this drainage has been provided all round the subgrade, by filling the annular ring between the perforated metal grid and GI tank with sand. This mix was placed in GI tank, compacted in layers of 2.5 cm thick to a final thickness of 20 cm. Each layer was compacted to MDD & OMC of natural soil. On top of the prepared subgrade, subbase and base courses have been laid with murrum and course aggregate for a thickness of 5 cm each and were well compacted.

3.3 Saturation and Heave Measurement

The prepared model flexible pavement systems have been connected to a water tank for saturation. Water enters from all sides, making the subgrade to swell, thus heaving up of the pavement system. The heaving of the system has been recorded at regular time intervals with the help of dial gauges fixed on top of the base course as shown in Fig. 2. Recording were continued until the heaving ceased.

Fig. 2 Heave measurement of pavement

Fig. 3 Cyclic plate load test setup

3.4 Cyclic Load Testing

As shown in Fig. 3 the prepared model pavement system is subjected to model cyclic plate load testing. The pavement was placed on the pedestal of a compression testing machine and a jack was centrally placed between the bearing plate and the proving ring.

Cyclic plate load test is carried out corresponding to different pressure increments such that the ultimate load is reached in five to six increments. In this testing pressure intensities ranging from 0 to 1200 kPa were applied. Load was applied at a rate of 1 mm per minute. At each applied pressure the total settlement of the plate has been recorded which is incidentally followed by measurement of elastic rebound on unloading. The cycles of incremental loading, unloading and reloading were continued until the bearing capacity failure of the model pavement occurs.

4 Experimental Results and Discussion

4.1 Effect of Flyash on Different Parameters

The summary of results of laboratory testing on the soil samples treated with different percentages of flyash contents are shown in Table 2. With the increase in flyash content liquid limit was found to decrease while plastic limit increases,

Table 2 Summary of the results of testing

Sample	PI (%)	DFS (%)	MDD kN/m^3	CBR (%)	UCS (kPa)
Untreated soil	56	140	15.2	2.12	94
Soil + 5% FA	51	110	17.1	4.23	140
Soil + 10% FA	48	100	17.5	6.14	195
Soil + 15% FA	44	90	17.0	6.65	160
Soil + 20% FA	37	80	16.6	6.72	155

causing a net reduction in plasticity index (PI). The differential free swell (DFS) value decreased with increase in flyash content. The increase in the Maximum dry density (MDD) and California bearing ratio (CBR) and unconfined compressive strength (UCS) is significant up to the addition of 10% flyash content and it became nominal afterwards. Considering an optimum amount of 10%, the CBR and UCS values have got increased by thrice and twice their original value respectively.

4.2 *Heaving of Model Pavement*

Heaving of the model pavements measured during the subgrade saturation period is shown in Fig. 4.

Significant reduction in heaving has taken place for the pavement containing treated subgrade. The percentage reduction in heaving at the end of saturation period has been found to be close to 40% of that of the heaving of model pavement with untreated subgrade.

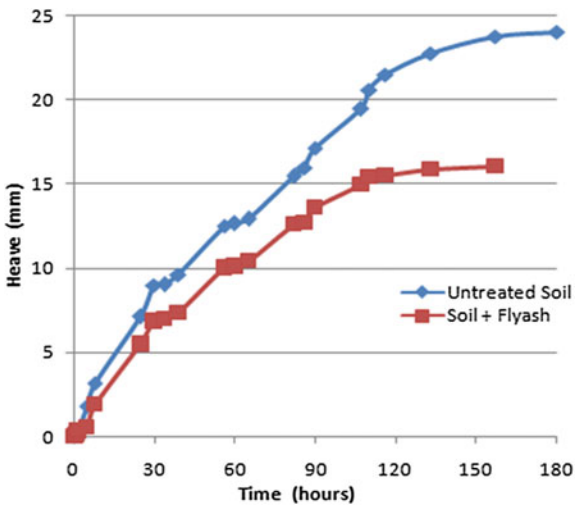

Fig. 4 Variation of heaving of the pavement

4.3 Results of Cyclic Load Testing

The variation of the total settlement versus the applied pressure for untreated and flyash treated subgrades of model pavements is shown in Fig. 5. It is evident that the total settlement reduces for model pavement containing flyash treated subgrade.

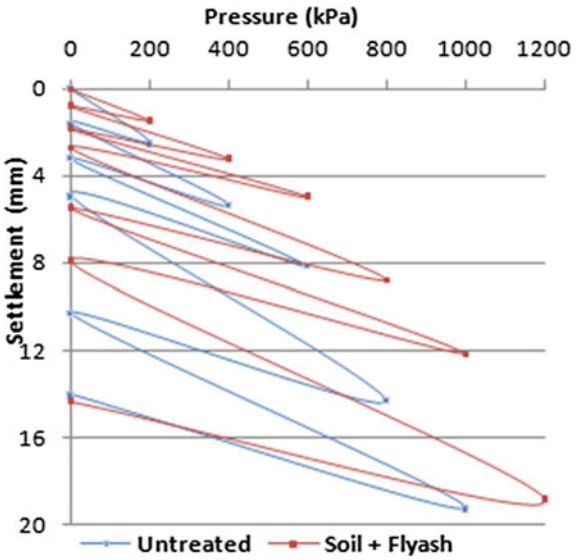

Fig. 5 Pressure-settlement curve for both loading and unloading phases

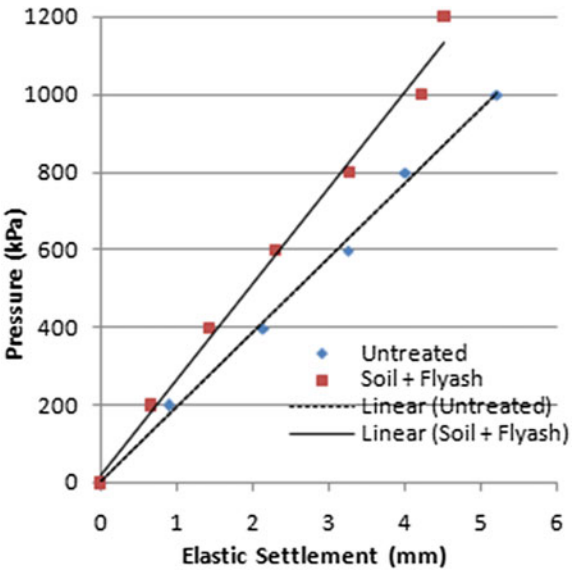

Fig. 6 Variation of elastic settlement with pressure

The elastic rebound of the model pavements with corresponding pressure intensity is as shown in Fig. 6. It is seen from the figure the slope of elastic line increased for subgrade soil treated with flyash. Slope of the elastic line, representing coefficient of elastic uniform compression (C_u) (IS: 5249-1992), was found to be more (0.19 N/mm^3 for untreated and 0.26 N/mm^3 for soil treated with flyash) for model pavement system provided with flyash treated subgrade. The coefficient C_u is found to be in close relation with the elastic and shear modulus of soil (Barkan D. D 1962). Increase in the value of C_u obviously enhances the elastic properties of the pavement.

5 Conclusions

Addition of flyash to the soil caused a reduction in plasticity index and differential free swell, while dry density and California bearing ratio and unconfined compressive strength of the soil have got increased. Considering an optimum amount of 10% flyash content, the dry density increased from 15.2 kN/m^2 (Original value) to 17.5 kN/m^2 (After addition of flyash). Similarly, the CBR and UCS values increased to thrice and twice their original value respectively. Model flexible pavement systems have shown significant reduction in heaving of the model pavement provided with flyash treated subgrade. A constant C_u used to define the elastic properties of the pavement and has been found to be greater for the model pavement with treated subgrade.

References

Barkan, D. D. (1962). *Dynamics of bases and Foundations*. New York: McGraw Hill.

Buhler, R. L., & Cerato, A. B. (2007). Stabilization of Oklahoma expansive soils using lime and class C Flyash. In *Problematic soils and Rocks and in-situ characterization* (pp. 1–10), GSP 162, ASCE.

Bin-Shafique, S., et al. (2004). Incorporating a fly-ash stabilized layer into pavement design. *Proceedings of the ICE-Geotechnical Engineering, 157*(4), 239–249.

Edil, T., Acosta, H., & Benson, C. (2006). Stabilizing soft fine-grained soils with fly ash. *Stabilization of Geomedia Using Cementitious Materials, ASCE, 18*(2), 283–294.

IS:5249 (1992), *Determination of dynamic properties of soil*. New Delhi, India: Bureau of Indian Standards.

Jones, D. E., & Holtz, W. G. (1973). Expansive soils-Hidden disaster. *Civil Engineering, 43*(8), 4951.

Kaniraj, S. R., & Gayathri, V. (2003). Geotechnical behaviour of fly ash mixed with randomly oriented fiber inclusions. *Geotextiles and Geomembranes, 21*(3), 123–149.

Puppala, A. J., et al. (2006). Soil-water characteristic curves (SWCC) of stabilized expansive soils. *Journal of Geotechnical Engineering and Geo-environmental Engineering, 132*(6), 736–751.

Moghaddas Tafreshi, S. N., Zarei, S. E., & Soltanpour, Y. (2008). Cyclic loading on foundation to evaluate the coefficient of elastic uniform compression of sand. In *14th World Conference on Earthquake Engineering*, Beijing, China.

Evaluating the Strength Characteristics of Lime and Metakaolin Stabilized Expansive Soil

Venkateswarlu Dumpa, Rajesh Vipparty, Anjan Kumar Mantripragada and G. V. R. Prasada Raju

Abstract Expansive soils, such as black cotton soils, are a worldwide problem. Construction on this soil has been drawing the attention of practicing engineers and researchers for many years. With changes in moisture regime, expansive soils are subjected to erratic changes in volume. In monsoon, predominantly they take up water and swell but in summer, they tend to shrink on evaporation of water, thus posing the problem of alternate cycles of swelling and shrinkage. This behavior of expansive soils is attributed to the presence of mineral-montmorillonite, which has an expanding lattice. Many researches, all over the world, are working to evolve more effective and practical treatment methods, to mitigate the problems posed to the construction of pavements on expansive soil sub grade. Stabilization is one of the effective methods adopted to improve the characteristics of expansive soils. Of late, good stabilizing agents like lime, cement and metakaolin are employed extensively in soil stabilization for building foundations or pavement sub-grades. Keeping in view the research findings outlined above, in the present work, experimentation was carried out to investigate the efficacy of different additives, Viz., Lime, Metakaolin and Lime + Metakaolin combination, in stabilizing the expansive soil sub grade, thereby, improving the strength and reducing swelling potential of stabilized soil.

V. Dumpa (✉)
Department of Civil Engineering, GIET, Rajahmundry 533296, India
e-mail: dumpa.venkateswarlu@gmail.com

R. Vipparty
Graduate Student, Department of Civil Engineering, BVC Odalarevu, Rajahmundry, India
e-mail: rajesh.nani571@gmail.com

A. K. Mantripragada
Principal, BVC College of Engineering, Palacharla, Rajahmundry 533104, India
e-mail: anjan_mantri@yahoo.com

G. V. R. P. Raju
Registrar & Professor of Civil Engineering, JNT University Kakinada, Kakinada 533003, India
e-mail: gvrp_raju@yahoo.com

T. Thyagaraj (ed.), *Ground Improvement Techniques and Geosynthetics*, Lecture Notes in Civil Engineering 14, https://doi.org/10.1007/978-981-13-0559-7_27

Keywords Flexible pavements · Expansive soil sub-grade · Lime Metakaolin

1 Introduction

Expansive soils are found in the states of Andhra Pradesh, Gujarat, Karnataka, Madhya Pradesh, Maharastra, and TamilNadu. Cracking and break-up of pavements, railway and highway embankments, roadways, building foundations, slab-on-grade members, irrigation systems, water lines, sewer lines, canal and reservoir linings can be identified as the threats posed by expansive soils (Gromko 1974; Wayne et al. 1984; Mowafy and Yousry 1985; Kehew 1995). Unfortunately the limitations of these soils stand as an obstacle to their adaptability in all conditions. So work is being done all over the world, for a more evolved and effective practical treatment methods, to control the problems caused to any structures laid on expansive soil strata. Many innovative foundation techniques have been devised as solutions to the problems posed by Expansive soils.

The technology of road construction is subjected to problems arising due to varied weather conditions, changing vehicular pattern, construction materials, and sub-grade condition. Majority of the pavement failures can be attributed to the presence of poor sub grade conditions and expansive soils sub grade is one such problematic situation. It has been found that the beneficial properties of metakaolin may be used in improving the mechanical properties of soils and can be used as a structural material (Kolovos et al. 2013). The properties of lateritic soil can be improved by adding metakaolin for barrier system for the containment of municipal solid waste (Umar et al. 2015).

2 Materials Used

2.1 Expansive Soil

The soil used for sub-grade was a typical black cotton soil collected form "Godi Lanka" near Amalapuram, in East Godavari District, Andhra Pradesh State, India. The properties of the soil are Specific gravity—2.70, **Grain size distribution** (Sand—2%, Silt—42%, Clay—56%), **Compaction Parameters** (Maximum Dry Density—15 Kn/m^3, O.M.C.—27.6%), **Atterberg's limits** (Liquid limit—87%, Plastic limit—34%, Plasticity index—53%, Shrinkage Limit—11.5%, IS classification—CH, Differential Free Swell—146%, CBR-soaked—1.8%, Permeability—1.50×10^{-7} cm/s.

2.2 Murrum

The murrum soil was used as a sub-base material in this investigation. It was collected from Dwarapudi, East Godavari district, A.P. The properties obtained from the laboratory tests are Specific gravity—2.7, **Grain size distribution** (Sand —28%, Silt & Clay—11%, Gravel—61%), **Compaction Parameters** (Maximum Dry Density—19 Kn/m^3, O.M.C.—19%), **Atterberg's limits** (Liquid limit—26%, Plastic limit—20%, Plasticity index—6%, CBR-soaked—17%, Permeability—1.2×10^{-4} cm/s.

Above all the tests were carried out as per relevant IS codes.

2.3 Road Metal

Road metal of size 20 mm were used for the preparation of base course for this study.

Additives Used

2.4 Lime (L)

Commercial grade lime mainly consisting of 62% CaO and 8% silica was used in this study.

2.5 Metakaolin (MK)

Metakaolin (MK) is a thermally activated aluminosilicate material, white in color with a dull luster, obtained by calcining kaolin clay within the temperature range 650–800 °C. In the present investigation, Metakaolin marketed by Jeetmull Jaichandlall Pvt. Ltd. Chennai, TamilNadu was used. The physical and chemical characteristics furnished by the manufacturer are moisture content of 0.18%, specific gravity of 2.65, bulk density of 710 kg/m^3 and pH of 7.0. Metakaolin consists majorly of SiO_2, Al_2O_3, and Fe_2O_3 contributing 53.7, 39.2, 3.84%, of the total. The next most abundant component is titanium oxide, TiO_2 (5.97%). According to ASTM standard specification (C 618-2012), the sum of SiO_2, Al_2O_3, Fe_2O_3 be $\geq 70\%$ for any material to be used as a pozzolana.

3 Laboratory Study

Various tests were conducted in the laboratory to investigate the index and other important properties of the materials used during the study following standard procedures recommended in the respective I.S. codes of practice. The details of various tests on the expansive soil treated with different combinations of additives and the optimum dosages corresponding to soaked CBR value required for sub-grade material (8% CBR) as per IRC: 37-2012 are presented in Table 1.

3.1 Construction of Model Flexible Pavements in the Test Tank

In the present investigation four model flexible pavements were prepared in the laboratory by using 60 cm diameter mild steel tank and the details are given in Table 1. Out of four model flexible pavements one with expansive soil sub-grade, one with lime treated expansive soil, one with metakaolin treated expansive soil and the other with lime + metakaoline treated expansive soil sub-grade were considered in this study. Above all the four alternative sub-grades murrum mixed with water at OMC was laid in two layers each of 2.5 cm compacted thickness to a total thickness of 5 cm as subbase course were laid uniformly. On the prepared subbase course two layers of WBM-III each of 2.5 cm compacted thickness, were laid to a total thickness of 5.0 cm. The details of construction procedures followed in the construction of model flexible pavements in the test tank are given below.

3.2 Preparation of Untreated and Treated Expansive Soil Sub-grade

Sand bed of 1.0 cm thick was placed before laying the sub-grade soil in the tank. The expansive soil was allowed to dry and then pulverized and sieved through

Table 1 Different percentages of additives and their optimum dosages of Lime, Metakaolin and Lime + Metakaolin mixtures corresponding to 8% soaked CBR as per IRC specifications

S. No.	Type of sub grade material	Admixtures	Different percentages of stabilizing alternatives (% by weight)	Optimum percentage of stabilizing alternatives (% by weight)
1	Expansive soil	Lime	0, 2, 4, 6, 8, 10	10
2	Expansive soil	Metakaolin	0, 3, 6, 9, 12, 15	12
3	Expansive soil	Lime + Metakaolin	0 + 0, 1 + 2, 2 + 1, 2 + 4, 4 + 2, 3 + 6, 6 + 3	6L + 3M

Plate 1 Saturation of model tank

4.75 mm sieve. Then it was compacted to 4.0 cm thickness in 5 layers to a total thickness of 20 cm to its optimum moisture content and maximum dry density in the selected mild steel test tank model flexible pavement S. No. 1. Vertical drains were provided by means of 6 perforated vertical PVC pipes of 1.27 cm diameter from bottom of the sub-grade to top of the base course for attaining full saturation. In the similar procedure explained above the treated expansive soil sub-grade was prepared by mixing the virgin expansive soil with 10% lime, 12% metakaoline and 6% lime + 3% metakaoline model flexible pavement S. No. 2, 3, and 4 respectively (optimum contents obtained from the laboratory investigation). Vertical drains were provided as explained above. A typical model test tank can be seen in Plate 1.

3.3 Experimental Setup and Procedure

The laboratory plate load tests were carried out at OMC and at FSC on flexible pavement systems in a circular mild steel tank, loading was done through a circular metal plate of 10 cm diameter laid on the model flexible pavement system. The steel tank was placed on the pedestal of the compression testing machine. A 50 kN capacity proving ring connected to the loading frame and the extension rod welded to the circular plate was brought in contact with proving ring.

Two dial gauges of least count 0.01 mm were placed on the metal flats welded to the vertical rod to measure the vertical displacements of the loading plate. The load was applied, cyclically, until there was insignificant increase in the settlement of the plate between successive cycles. The deformations attained equilibrium after six

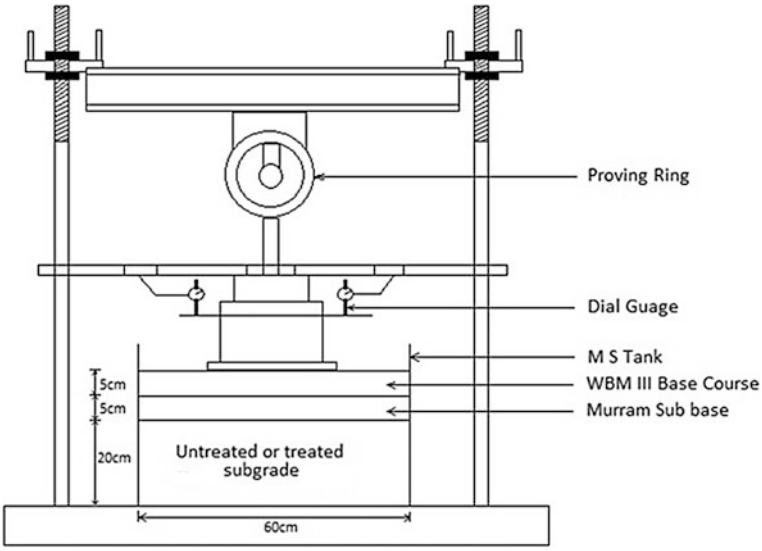

Fig. 1 Laboratory experimental setup for conduct of cyclic load

cycles of loading and unloading for all the pressure increments tried during the study. The testing was further continued till the occurrences of failure to record the ultimate loads. The entire setup was shown in Fig. 1.

4 Results and Discussion

Cyclic plate load tests were conducted on untreated expansive soil and treated expansive soil as sub-grade with murrum as subbase and WBM-III as base course in the model flexible pavement under pressures, viz 500, 560, 630, 700, 1000 and 1200 kPa.

The tests were conducted until the failure of untreated expansive soil, treated expansive soil at OMC and at FSC (Full Saturation Condition) and the results were given in the Figs. 2, 3, 4 and 5 and Tables 2 and 3.

From Figs. 2, 3, 4 and 5 it can be inferred that, by treating weak expansive soil sub-grade, the pavement performance was enhanced and there by evolved a better alternate pavement system particularly if these weak deposits are encountered in the road alignment. Hence the authors effectively initiated the research in improving weak expansive soil deposits to cater the pavement requirements and successfully arrived with a suitable solution.

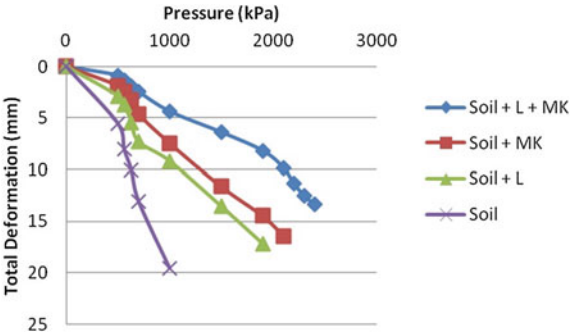

Fig. 2 Variation of pressure versus total deformation for soil treated with different additives at OMC

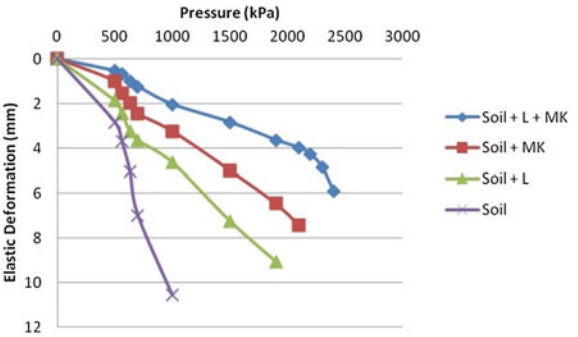

Fig. 3 Variation of pressure versus elastic deformation for soil treated with different additives at OMC

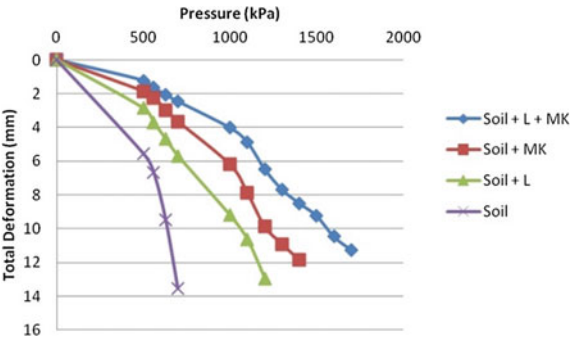

Fig. 4 Variation of pressure versus total deformation for soil treated with different additives at FSC

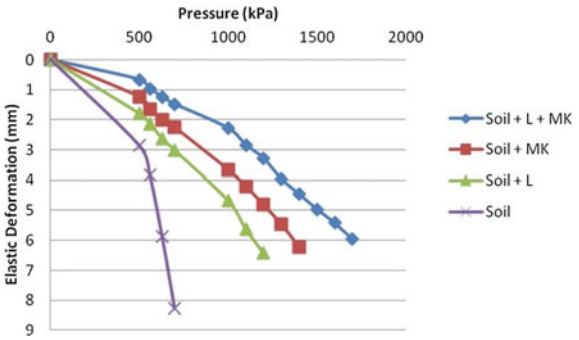

Fig. 5 Variation of pressure versus elastic deformation for soil treated with different additives at FSC

Table 2 Variation of pressure—deformation for soil treated with different combinations tested at OMC

Pressure (kPa)	Soil + Lime + Metakaolin		Soil + Metakaolin		Soil + Lime		Untreated soil	
	TD (mm)	ED (mm)	TD (mm)	ED (mm)	TD (mm)	ED (mm)	TD (mm)	ED (mm)
0	0	0	0	0	0	0	0	0
500	0.86	0.54	1.86	1	2.86	1.89	5.54	2.84
560	1.36	0.66	2.42	1.54	3.68	2.46	8.02	3.68
630	1.92	1	3.29	2	5.42	3.24	10.06	5.02
700	2.46	1.24	4.63	2.46	7.32	3.66	13.04	6.98
1000	4.38	2.04	7.46	3.24	9.2	4.64	19.54	10.56
1500	6.40	2.84	11.64	4.98	13.56	7.24		
1900	8.2	3.64	14.48	6.46	17.2	9.06		
2100	9.86	3.98	16.42	7.42				
2200	11.36	4.28						
2300	12.54	4.86						
2400	13.36	5.92						

Table 3 Variation of pressure—deformation for soil treated with different combinations tested at full saturation condition (FSC)

Pressure (kPa)	Soil + Lime + Metakaolin		Soil + Metakaolin		Soil + Lime		Untreated soil	
	TD (mm)	ED (mm)	TD (mm)	ED (mm)	TD (mm)	ED (mm)	TD (mm)	ED (mm)
0	0	0	0	0	0	0	0	0
500	1.22	0.66	1.86	1.24	2.86	1.80	5.54	2.86
560	1.64	0.96	2.24	1.64	3.70	2.14	6.64	3.84
630	2.08	1.24	2.96	2.0	4.69	2.64	9.48	5.88
700	2.46	1.48	3.64	2.26	5.68	3.02	13.54	8.26
1000	4.02	2.28	6.2	3.66	9.20	4.68		
1100	4.86	2.84	7.86	4.2	10.63	5.62		
1200	6.46	3.28	9.86	4.82	12.94	6.42		
1300	7.67	3.96	10.90	5.46				
1400	8.48	4.46	11.85	6.22				
1500	9.23	4.96						
1600	10.46	5.42						
1700	11.24	5.96						

5 Conclusions

The following conclusions are drawn based on the results of the laboratory testing.

The untreated and treated sub-grade options were tested with murrum subbase with WBM-III as base course

1. When the virgin soil is treated with (10%L) lime the percentage improvement in soaked CBR is 79% and treated with (12% MK) metakaolin the percentage improvement was further increased to 78% and also the combination of both lime + metakaolin i.e., (6L + 3 MK) the percentage improvement is 82%.
2. The optimum content for all the three alternative additives are found to be 10% L, 12%MK, 6%L + 3%MK, for Lime, Metakaolin and Lime + Metakaolin respectively for both compaction, penetration characteristics.
3. It was noticed from the laboratory investigations of the cyclic plate load test results that, the ultimate load carrying capacity of the untreated expansive soil sub-grade model flexible pavement has increased from 1000 to 1900 kPa when the expansive soil was treated with lime at OMC and 700–1200 kPa at FSC.
4. It was noticed from the laboratory investigations of the cyclic plate load test results that, the ultimate load carrying capacity of the untreated expansive soil sub-grade model flexible pavement has increased from 1000 to 2100 kPa when the expansive soil was treated with metakaolin at OMC and 700–1400 kPa at FSC.

5. It was noticed from the laboratory investigations of the cyclic plate load test results that, the ultimate load carrying capacity of the untreated expansive soil sub-grade model flexible pavement has increased from 1000 to 2400 kPa when the expansive soil was treated with metakaolin + lime at OMC and 700–1600 kPa at FSC.
6. The final conclusion of the present study is that there is an improvement in the ultimate load carrying capacity of the treated expansive soil sub-grade.

References

Gromko, G. J. (1974). Review of Expansive soils. *Jr. of Geotechnical Engineering Division, 100* (6), 667–687.

Wayne, A. C., Mohamed, A. O., & El-Faith, M. A. (1984). Construction on expansive soils in Sudan. *Jr. of Construction Engineering and Management, 110,* 359–374.

Mowafy, M., & Yousry, M. (1985). *Treatmetn of expansive soils: A laboratory study, TRR-1032* (pp. 34–39). Washington: TRB.

Kehew, E. A. (1995). *Geology for engineers and environmental scientists* (2nd ed., pp. 295–302). New Jersey: Prentice Hall Englewood Cliffs.

Kolovos, K. G., Asteris, P. G., Cotsovos, D. M., & Tsivilis S. (2013). Mechanical properties of Soilcrete mixtures modified with metakaolin. *Construction and Building Materials 47*, 1026–1036.

Umar, S. Y., Elinwa1, A. U., & Matawal, D. S. (2015). Hydraulic conductivity of compacted lateritic soil partially replaced with metakaolin. *Journal of Environment and Earth Science, 5* (4).

IRC: 37-2012. Guidelines for the design of flexible pavements. New Delhi.

Ground Improvement Using Sand Columns to Mitigate Liquefaction—A Case Study

Minu Ann George, J. Jasmine Nisha and Ghan Sandeep Mangal

Abstract Soil strata is highly varying in nature and it is a challenging task for Geotechnical engineers to come up with the most suitable foundation system that is safe during static and dynamic loadings. In this paper, a case study on ground improvement using sand columns at Puri in Odisha is discussed. The strata at site comprised mostly fine sands of low SPT-N values with some intermittent clay seams at intermediate depths. The water table was also encountered at very shallow depths at the location. The geotechnical profile of the boreholes was analyzed on the guidelines of Seeds and Idris and it was observed that the liquefaction potential of the soil layers is prominent and ground improvement is inevitable up to a depth of 10.5 m below existing ground level in view of stability of structures. The selective methods like vibro compaction, dynamic compaction were considered to be the suitable methods for the ground improvement. However, as the liquefiable layer is 10–11 m deep from ground level, provision of sand column is found to be the best alternative to reach those depths. In this method, the natural sand is densified with displacement method so that the relative density of the sand will be enhanced to avert the liquefaction risk. It was proposed to use Raft foundation with supporting ground improvement. Field tests such as sand column test, Pre and post DPTs, SPTs tests were carried out at site for assessing the extent of improvement and the results for the same are briefed in this paper.

Keywords Liquefaction · Sand column · DPT

M. A. George · J. Jasmine Nisha (✉) · G. S. Mangal
L&T Construction, Chennai 600089, India
e-mail: jasminenisha@lntecc.com

M. A. George
e-mail: minuann@lntecc.com

G. S. Mangal
e-mail: Sandeep-ghan@lntecc.com

T. Thyagaraj (ed.), *Ground Improvement Techniques and Geosynthetics*, Lecture Notes in Civil Engineering 14, https://doi.org/10.1007/978-981-13-0559-7_28

1 Introduction

This paper presents a case study of ground improvement work executed by M/s. L&T Construction in one of its project site at Puri in the state of Odisha. The site under discussion falls in seismic zone 3 as per IS 1893 and lies in close proximity to the sea. The site stratigraphy comprises mostly of fine sand layer with minor intermittent clay seams. Water table lies at 0.5 m depth below Natural ground Level (NGL) and during monsoon season, the water table is almost at natural ground level. The SPT-N values of the soil layer are indicated in Fig. 1 which are showing very low values in the depths of 4.50–10.50 m below ground level. As indicated above, the liquefaction check of the site was verified based on standard design practice and suitable remedial measures are applied. The same is discussed here with in this paper.

2 Sub-soil Profile

The soil exploration of the present site was done in the form of seven boreholes terminated at 40 m depth below NGL. As already stated earlier, the site comprised mostly of fine sand with some silt content and some clay seams were encountered at shallow depths. The generalized profile considered for design and analysis is shown

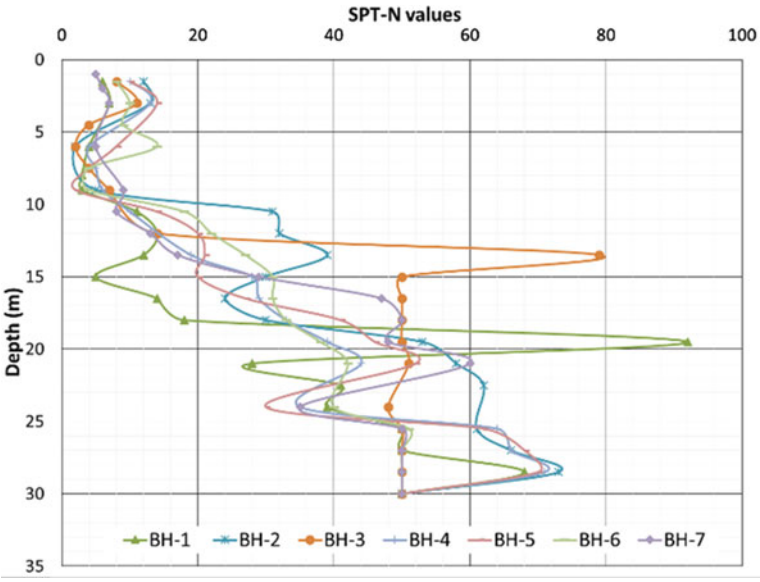

Fig. 1 SPT-N versus depth

Table 1 Generalized profile

S. No.	Depth range below NGL (m)	Soil description
1	0–4.5	Silty Sand (SP-SM)
2	4.5–7.0	Clayey Silt (ML-CL)
3	7.0–22.5	Silty Sand (SP-SM)
6	22.5–25.5	Silty Clay (CI)
7	25.5–40.0	Silty Sand (SP-SM)

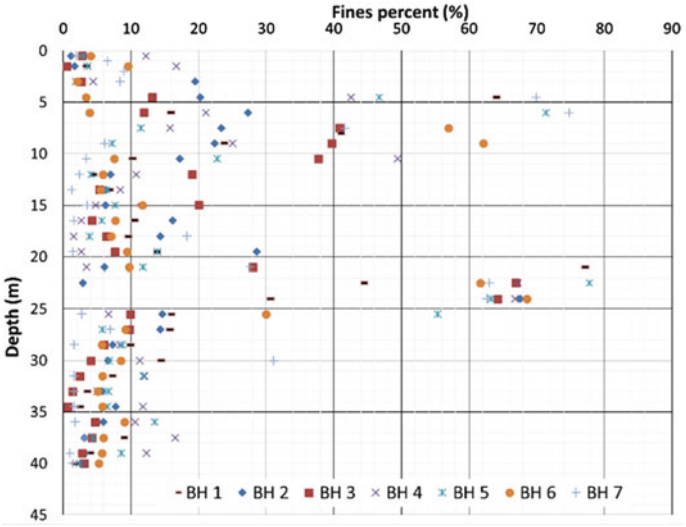

Fig. 2 Percentage of fines versus depth

in Table 1. The variation in SPT-N values and percentage of fines passing 75 μm with depth are presented in Figs. 1 and 2 respectively.

As seen from Fig. 1, it is evident that the field SPT-N values ranges from 2 to 5 especially in the depth range of 4.5–10.5 m. This indicates the loose nature of soil. In Fig. 2, the percentage of fines variation with depth is shown and the fines (%) is falling within 20% except in location where clayey silt strata is encountered.

3 Liquefaction Assessment

Due to the presence of water table almost at ground level and loose fine silty sand layers till 10.5 m depth, the susceptibility of in situ soil for liquefaction was checked using Seed and Idriss method (Youd and Idriss 2001).

Puri site falls in seismic zone 3 as per IS 1893-2002. Hence an earthquake magnitude of 6 and peak ground acceleration of 0.16 g was used in the analysis based on the earthquake histories and as recommended by IS 1893.

The calculated cyclic stress ratio (CSR) and cyclic resistance ratios (CRR) values were in the range 0.24–0.25 and 0.12–0.13 respectively. The factor of safety values were in the range of 0.81–0.94.

As the factor of safety values obtained as a result of Seed and Idriss analysis were less than 1, the need for densifying the loose sand deposits were felt by the designers. The number of options for improving the ground was discussed and finally, after checking the site constraints and material availability, it was decided to use sand columns.

The diameter and spacing of sand column required to mitigate liquefaction potential was verified using Priebe's method detailed in (Priebe 1998). Sand columns of 900 mm diameter with 2 m center to center spacing were required to mitigate the liquefaction potential of present site and thereby factor of safety against liquefaction values enhanced to the range of 1.23–1.42.

4 Ground Improvement Scheme

The ground improvement scheme for the site discussed here comprised of 900 mm diameter vibro-sand columns. The columns were arranged in a square pattern at 2 m center to center spacing. A sand blanket layer of 500 mm compacted sand was provided over the installed sand columns which acted as a drainage layer. The blanket layer was compacted to 75–80% of relative density. A sketch of sand column arrangement is shown in Fig. 3.

The properties of column material considered for design and further analysis are given below.

Sand column design parameters

- Unit weight of column material—18 kN/m^3
- Angle of internal friction—34°.

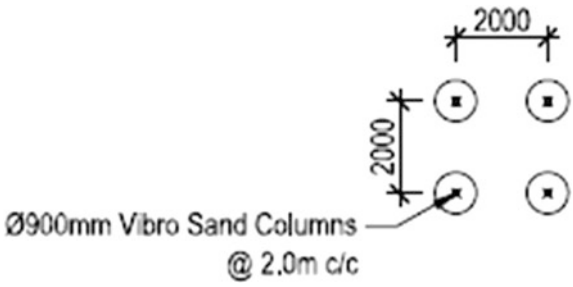

Fig. 3 Square pattern arrangement of Sand columns

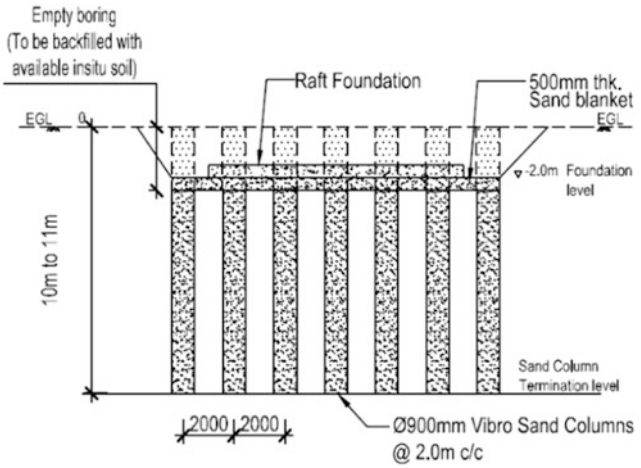

Fig. 4 Sketch showing the typical arrangement of sand column below Raft

A sketch showing the typical arrangement of sand columns below the proposed raft foundation is shown in Fig. 4.

The column installation was done using a dry vibro-displacement method, hence the formation and disposal of muck which was common in vibro-replacement method of sand column installation was eliminated. Throughout the installation process, the site remained fairly clean.

The sand columns were terminated at depth 10–11 m below the natural ground level depending on the penetration resistance achieved (60–70 A at termination level). Raft foundation was proposed for the main structures and isolated footings were proposed for ancillary-/single-storied structures. One to two additional rows of sand columns were provided outside the raft foot print area to provide confinement for the different structures of this site. A total of 5266 sand columns were proposed for the footprint area of 15,044 m^2.

5 Field Testing and Improvements

Sand column load tests, dynamic penetration tests and SPTs were conducted at the site for checking the extent of improvement.

Dynamic penetration tests (DPT) which employs a light weight penetrometer for finding out the resistance offered by in situ soils in terms of no. of blows for every 10 cm penetration. This DPT was carried out at site instead of SPT as the testing was simpler in the former case whereas the latter requires a borehole. Due to the

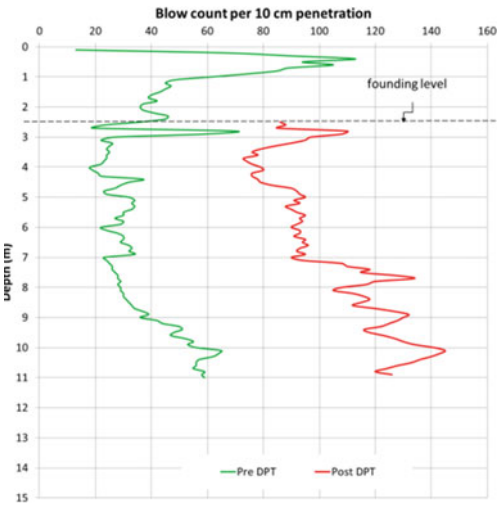

Fig. 5 Pre and post dynamic penetration test plot

ease in carrying out DPT, a total of 29 pre-DPTs and 14 post DPTs where conducted at site. That is, the DPTs were carried out at site before and after the installation of sand columns covering the entire project site.

A correlation between SPT (7 no. of boreholes) and DPT (29 nos. pre DPT) values prior to treatment was established for the entire site. This correlation was used to arrive at the post SPT values from DPT values after treatment. A typical DPT test result details with respect to the treatment depth before and after improvement is shown in Fig. 5.

From the post SPT values, the static cone penetration resistance values are obtained as per Ramaswamy et al. (1982) and the relative density enhancement was arrived using Schmertmann's method (Schmertmann 1978). The static cone penetration resistance and relative density enhancement graphs are shown in Figs. 6 and 7 respectively.

Theoretical capacity of sand column is estimated as per IS 15284: Part 1: (2003) and SBC recommended for foundation design was 15 t/m^2. Sand column load test was carried out to verify the SBC of treated ground. The load-settlement graph of the test is shown in Fig. 8.

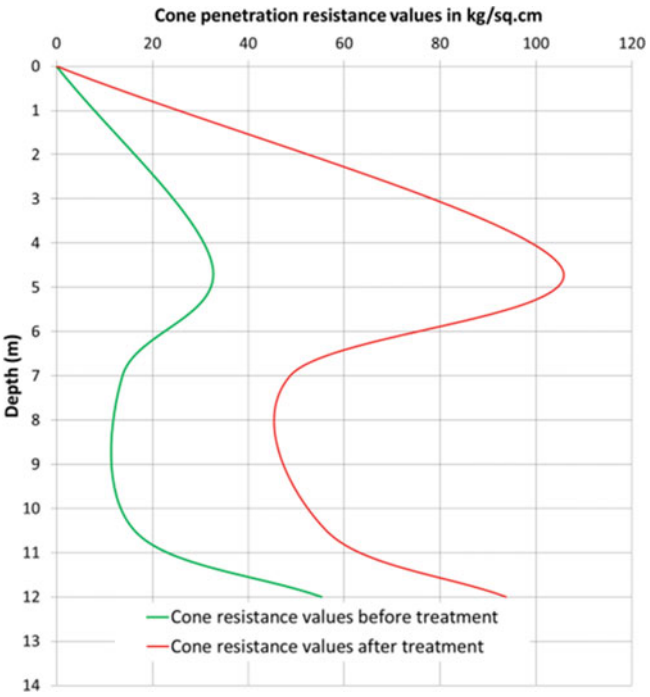

Fig. 6 Cone penetration resistance values before and after treatment

From Fig. 8, it is evident that the recommended bearing capacity of 15 t/m^2 is safe. The settlement was less than 8 mm, within acceptable limits as per IS 15284 (part 1).

In addition to the DPTs and sand column load test detailed above, 4 nos. of boreholes (2 in treated ground and 2 in untreated ground) were taken at site as part of verification of ground improvement. The SPT-N versus depth and the CRR improvement for this is presented in Figs. 9 and 10 for comparison purposes.

From the field testing and further after interpreting the test data, it is concluded that the desired improvement was achieved due to the ground improvement works.

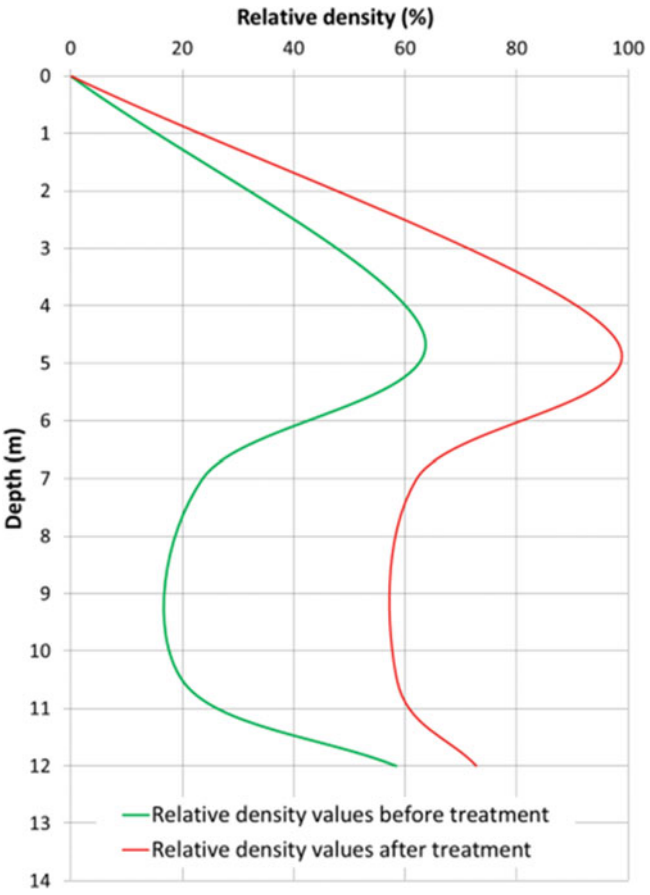

Fig. 7 Relative density plot before and after treatment

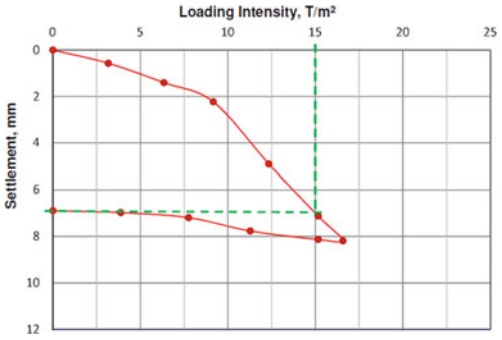

Fig. 8 Load–settlement curve of sand column load test

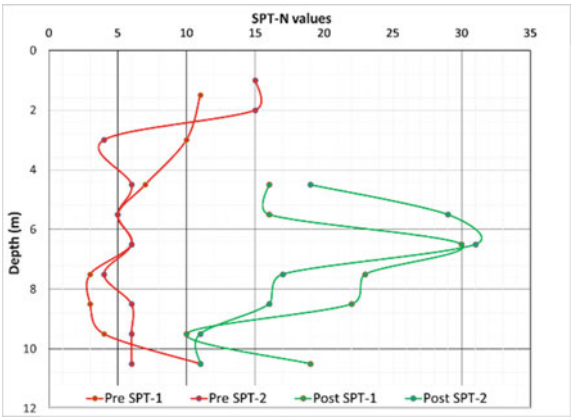

Fig. 9 SPT plot before and after treatment

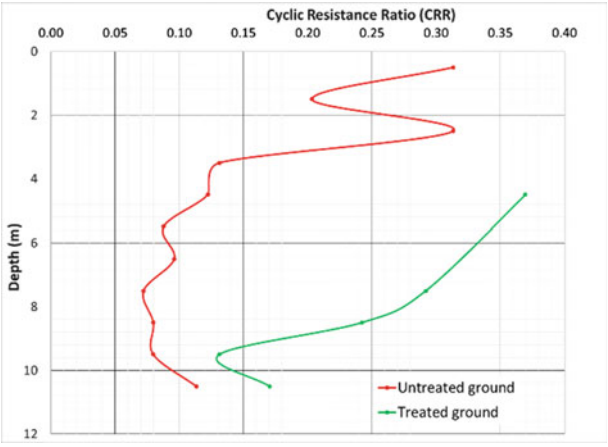

Fig. 10 Variation in cyclic resistance ratios (as per Youd and Idriss 2001) before and after treatment

6 Conclusion

In the study detailed in this paper, the designers recommend the use of ground improvement technique using sand columns as an effective method for mitigating the liquefaction potential of saturated fine sandy soils. For the same project site, the suitability of pile foundation was also checked but discarded as no lateral resistance would be offered by piles considering liquefaction prone layers at shallow depths and extending up to 10.50 m.

Acknowledgements The authors acknowledge the help rendered by the geotechnical team of M/s. Keller for the successful completion of Sand columns and testing.

References

Youd, T. L., & Idriss, I. M. (2001). Liquefaction resistance of soils: Summary report from the 1996 NCEER and 1998 NCEER/ NSF workshops on evaluation of liquefaction resistance of soils. *Journal of Geotechnical and Geo-environmental Engineering, 127*.

IS 1893: part I: (2002). Criteria for earthquake resistant design of structures.

Priebe, H. J. (1998). Vibro replacement to prevent earthquake induced liquefaction. In *Proceedings of the geotechnique-colloquium at darmstadt,* Germany, Technical paper 12-57E.

Ramaswamy, S. D. et al. (1982). Pressuremeter correlations with standard penetration and cone penetration tests. In *2nd ESOPT,* Vol. 1, pp. 137–142.

Schmertmann, J. H. (1978). Study of feasibility of using Wissa-type piezometer probe to identify liquefaction potential of saturated fine sands, Technical report S-78-2.

IS 15284: Part 1: (2003). Design and construction for ground improvement—guidelines—stone columns.

Stabilization of Expansive Soil with Red Mud and Lime

G. Sridevi, Sanjeet Sahoo and Subhrajeet Sen

Abstract Expansive soils lack the required engineering properties for use in pavement subgrades, and as a foundation supporting layer under buildings. In the present study red mud, a byproduct of bauxite industry is stabilized with lime and in turn is used to stabilize the expansive soil. Compaction studies and unconfined compressive strength studies were conducted in order to see the efficacy of these materials in improving the strength of the soil. Red mud is stabilized with 4% lime and lime-stabilized red mud is added to the expansive soil in different percentages varying from 10 to 50% in increments of 10%. Tests are also conducted on soils stabilized with lime-stabilized red mud and flyash, adding them in equal quantities along with 4% lime. The results show that red mud as well as red mud–flyash improves the geotechnical properties of the soil.

Keywords Expansive soil · Red mud · Flyash · Lime · UCS

1 Introduction

Red mud is a byproduct of the Bayer process, which is used for the production of alumina from bauxite. In India, about 4.71 million tons of red mud is produced every year which is 6.25% of world's total generation (Paramguru et al. 2005;

G. Sridevi
BVRIT, Narasapur, Telengana, India
e-mail: gudasridevi@yahoo.co.in

S. Sahoo (✉)
CVRCE, Bhubaneswar, Odisha, India
e-mail: sanjeet476@gmail.com

S. Sen
AEE, Government of Odisha, Cuttack, Odisha, India
e-mail: Subhrajit.igit@gmail.com

T. Thyagaraj (ed.), *Ground Improvement Techniques and Geosynthetics*, Lecture Notes in Civil Engineering 14, https://doi.org/10.1007/978-981-13-0559-7_29

Parlikar et al. 2011). Red mud is differentiated into two grades: fine-grained "red mud" and coarse "red sand." Typical red mud grading show up to 20–30% clay-sized, with the majority of particles in the silt range (Miners 1973; Somogyi and Gray 1977). Vick (1981) observed that red mud exhibits low plasticity with liquid limit (LL) of 45% and plasticity index (PI) of 10% with relatively high specific gravity (G_S) of 2.8–3.3.

Red mud creates a lot of health hazards to the ecology, if it is disposed without necessary precautions. Red mud is highly alkaline (pH = 11–13) material (Li 1998; Sundaram and Gupta 2010) and mineral components include hematite, goethite, gibbsite, calcite and complex silicates. Red mud is found to have greater than 50% of the particles less than 2 μm size in some cases. The cation exchange capacities of red mud are comparable with kaolin or illite. Kalkan (2006) studied efficacy of red mud for the preparation of clay liners and found that the compacted clay samples containing red mud and cement–red mud additives have a high compressive strength and low hydraulic conductivity as compared to natural clay samples. Newson et al. (2006) carried out investigations on physiochemical and mechanical properties of red mud and established that the compression behaviour found to be similar to clayey soils, but frictional behaviour closer to sandy soils. Rout et al. (2012) observed that the maximum dry density (MDD), specific gravity and angle of internal friction are very high compared to local soil. Kusum Deelwal et al. (2014) studied geotechnical properties such as Specific gravity, Particle size distribution, Atterberg limits, OMC and MDD. The performance of stabilized mixes depends upon the compaction or densification of the fill.

2 Objectives of the Work

The aim of present work is to ensure the suitability and utilization of red mud as a stabilizing agent to the soil. The work is carried in three stages. In the first stage the material characterization of expansive soil, flyash and red mud are done. In the second stage red mud is added to expansive soil from 10 to 50% in increments of 10% along with 4% lime and geotechnical properties of red mud-lime–soil mixes are studied. In the third stage both red mud and flyash are added together in equal quantities varying from 10 to 50% in increments of 10% along with 4% lime. In the present study effort is made to study the geotechnical properties like Atterberg limits, compaction characteristics, unconfined compressive strength and shear parameter. The development of alternate low-cost and environment suitable building materials from industrial wastes in an economic way will help to conserve the natural resources.

3 Materials and Methods

3.1 Expansive Soil

The soil used in the present study is obtained from Banapur block of Khurda District, Odisha state. The soil properties of soil are given in Table 1. Soil is classified s CH (Highly plastic clay).

3.2 Lime

The lime (L) used was a commercially available lime from Birla cements.

3.3 Red Mud

The red mud used in the present study is collected from NALCO, Damanjodi, Koraput in state of Odisha, India The geotechnical properties of red mud are given in Table 1 and chemical properties are given in Table 2.

Table 1 Geotechnical properties of soil, fly ash and red mud

Grain-size distribution	Soil	Fly ash	Red mud
Sand (%)	29	85	17
Silt (%) and Clay (%)	50 and 21	15	83
Liquid limit (%)	59	–	–
Plastic limit (%)	23	–	–
Plasticity index (%)	32	-NP-	-NP-
Shrinkage limit (%)	18	–	–
IS classification	CH	–	–
Specific gravity	2.67	2.1	3.2
OMC (%)	23	20.7	31
Maximum dry density (Mg/cum)	1.52	1.35	1.61
Free swell index (%)	80	Nil	Nil
CBR (%) (soaked)	3.1	3.15	5.2
Undrained cohesion (kPa)	18	12	15
Angle of internal friction (°)	12	31	28

Table 2 Chemical properties of fly ash and red mud

	Fly ash	Red mud
Al_2O_3	30.63	18
Fe_2O_3	4.79	51
TiO_2		4.6
SiO_2	60.43	9.8
Na_2O	0.1	5.3
CaO	0.28	1.8
P_2O_5		0.15
Loss on ignition	0.5	9.05

3.4 Flyash

Flyash is collected from Nalco (CPP) Anugul, India. The geotechnical properties are summarized in Table 1. The chemical composition of the flyash used in the study is given in Table 2, comes under category of Class F (ASTM C618).

4 Preparation of the Samples for Testing

Tests are conducted with soil alone as well as soil-red mud mixes containing different percentages of red mud. Red mud is stabilized with 4% lime and lime-stabilized red mud is added to the oven dried soil in desired quantities varying from 10 to 50% in increments of 10%. Water is added to the mixture and mixed until it becomes homogenous. The laboratory tests carried out on the natural soil include particle size distribution as per IS: 2720-1985 Part IV, Specific Gravity as per IS: 2720 Part III section 1-1980, Atterberg limits test as per IS: 2720 part V 1985, Compaction test as per IS: 2720 part VII-1980, Unconfined compressive strength test as per IS: 2720 part X. Unconfined compression tests are conducted on soil and red mud mixes compacted at their respective maximum dry density (MDD) and optimum moisture content (OMC). For preparing compacted specimen, first the required amount of dried soil and lime-stabilized red mud were weighed and mixed together in dry state, then, optimum moisture content was added to the mixture. The mixture was then kept for moisture equilibration for 30 min in sealed polythene covers. In the entire laboratory tests, three specimens were tested to obtain average results and to check reproducibility. Tests were also conducted with soil stabilized with lime-red mud and flyash.

5 Results and Discussion

5.1 *Effect of Red Mud and Red Mud–Flyash on Atterberg Limits*

Variation of liquid limit, Plastic limit with the admixture content is shown in Fig. 1. It is found that both liquid limit and plastic limit decrease as the lime-stabilized red mud content is increased. The addition of both flyash and red mud also resulted in the reduction in both liquid limit and plastic limit. The reduction in Atterberg limits is slightly higher in the case of stabilization with red mud alone. It is known that the addition of flyash causes flocculation of clay particles and improves the gradation (Sivapullaiah et al. 1996). The immediate and long-term effects together contribute to the beneficial changes in the plasticity characteristics in terms of decrease in Liquid Limit, plastic limit and Plasticity index (Ip).

Liquid limit and plastic limit both decreases with increase in stabilizer percentages. Addition of 40% lime-stabilized red mud reduced the liquid limit of untreated expansive soil by 24% and Plastic limit by 42%.

Addition of 40% lime-stabilized red mud and flyash together reduces the liquid limit by 33% and plastic limit by 50% when compared with the untreated expansive soil.

5.2 *Effect of Lime-Stabilized Red Mud and Lime-Stabilized Red Mud—Flyash on Compaction Characteristics*

The geotechnical properties of soil such as swell potential, compressive strength, CBR, permeability, and compressibility are dependent on the moisture and density at which the soil is compacted. Compaction of soil enhances the geotechnical properties of the soil to meet specified or desired properties of soil. The standard proctor test is conducted on natural soil as well as on mixes of soil treated with

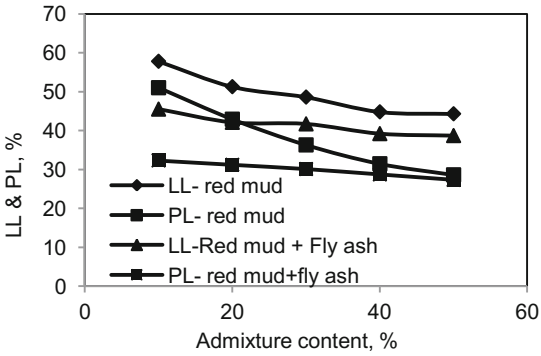

Fig. 1 Atterberg limits

different percentages of red mud to determine the optimum moisture content and maximum dry density. Figure 2 shows the variation of the Maximum Dry Density (MDD) and Optimum Moisture Content (OMC) with red mud content. The maximum Dry density of natural soil sample was 15.2 kN/m^3. The MDD for a soil sample with 50% red mud content is 16.3 kN/m^3 which implies that the MDD increases with the increase in red mud content and an increase in OMC is also observed from 23 to 28%. The increase in density may be due to the flocculation and agglomeration of clay particles facilitating better compatibility thus reducing void spaces leading to a corresponding increase in dry density. The increase in OMC may be due to increase in the fineness of red mud when compared with the soil.

Figure 2 shows the effect of the addition of Flyash and Red mud on the compaction characteristics of the expansive soil. The trend was similar to that of red mud alone. The increase in density may be related to the flocculated and agglomerated clay particles leading to better gradation and corresponding increase in dry density. The addition flyash and red mud to the soil increases OMC because of the coarse grain size of flyash compared to that of natural soil, which causes an increased void ratio in soil mixtures. The increase in MDD with the addition of red mud alone is little higher when compared with flyash and red mud addition, which may be due to comparatively low specific gravity value of flyash than that of replaced red mud and also simultaneous flocculation and agglomeration of clay particles.

5.3 *Effect of Lime-Stabilized Red Mud and Lime-Stabilized Red Mud Flyash on Unconfined Compressive Strength (UCS)*

The tests are performed on expansive soil stabilized with red mud and lime mixes compacted at OMC to their respective MDD. It can be seen from Fig. 3 that the unconfined compressive strength of the soil increases with addition of

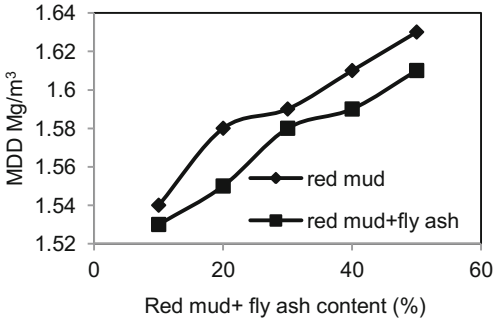

Fig. 2 Compaction characteristics

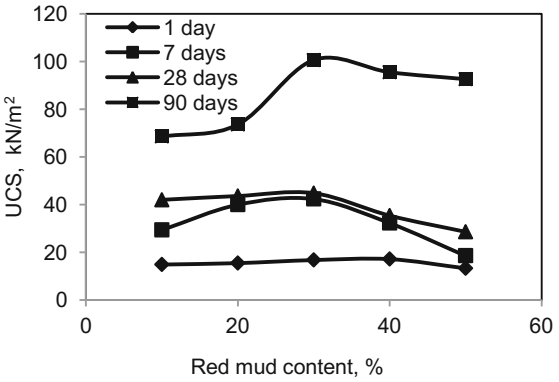

Fig. 3 Variation of UCS with curing time

lime-stabilized red mud up to 30% and there is a slight reduction beyond 30%. The increase in the UCS with addition of red mud may be attributed to the formation of cementitious compounds between the soil and the lime-stabilized red mud. Curing of the mixes showed a significant improvement in the UCS values. A marked increase of UCS is observed for 90 days curing. With the addition of lime-stabilized red mud, the UCS value increased from 14.9 to 16.8 kN/m^2. Considerable improvement was observed at 30% lime-stabilized red mud content in the soil. The UCS value increased from 16.8 to 100.6 kN/m^2 upon curing for 90 days.

The test results of unconfined compressive strength of lime-stabilized red mud–flyash treated soil are shown in Fig. 4. This figure illustrates the UCS of red mud and flyash treated soil with different admixture contents for different curing periods. The failure plane of specimens indicated that all the specimens are showing shear failure. There is a slight increase in unconfined compressive strength from 16.8 to 19.3 kN/m^2 with the addition of 30% lime-stabilized red mud and flyash. Curing contributed to significant improvement in UCS. The unconfined compressive strength of soil at 50% of flyash and lime-stabilized red mud content increased from 19.3 to73.27 kN/m^2 upon curing for 90 days. The reason for this improvement may

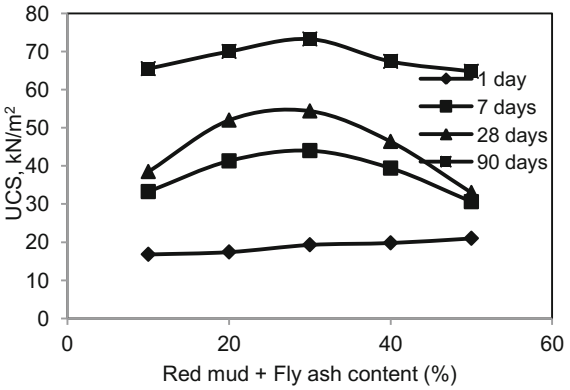

Fig. 4 Variation of UCS with curing time

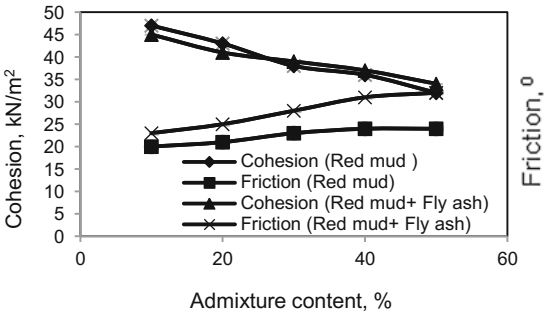

Fig. 5 Variation of shear parameters with the admixture content

be due to the immediate and long-term pozzolanic reactions of red mud, flyash and lime with soil. As the curing period is increased, the unconfined compressive strength increases both in the case of red mud addition as well as red mud and flyash addition. This is due to both pozollanic reaction between soil and flyash and red mud as well as due to improvement in friction.

5.4 Effect of Red Mud as Well as Red Mud and Flyash on Shear Parameters

Mostly, two mechanisms control the undrained strength in clays, namely cohesion or undrained strength is due to the net attractive forces and the mode of particle arrangement as governed by the interparticle forces, or cohesion is due to the viscous shear resistance of the double layer water (Sridharan et al. 2002).

In general fine-grained soils consist of different clay minerals with different exchangeable cations and varying ion concentration in the pore water and varying non clay size fraction. In imparting shear strength to clay both can function simultaneously or one of the mechanisms dominates. The effect of red mud and red mud–flyash content on shear parameters is shown in Fig. 5. From the figure it is evident that the cohesion decreases and friction increases with the increase in admixture content.

6 Conclusions

Addition of red mud as well as red mud–flyash decreases the liquid limit and plasticity index.

The admixtures impacts moisture-density relation of expansive soils—optimum moisture content increases and maximum dry density increases with the increase in admixture content. Dry density of compacted specimens is found to increase from 15.2 to 16.3 kN/m^3 with the addition of red mud by 50% by weight of dry soil.

With the addition of lime-stabilized red mud–flyash, 50% by weight of soil, MDD increased to 16.1 kN/m^3.

Addition of lime-stabilized red mud and lime-stabilized red mud–flyash cause significant changes in Shear parameters. With the addition of red mud 50% by weight Cohesion decreases from 47 to 32 kN/m^2 and friction increases from 20° to 24°.

With the addition of lime-stabilized red mud and flyash in equal quantities, 50% by weight, Cohesion decreases from 45 to 34 kN/m^2 and friction increases from 23° to 32°.

The UCS value is found to increase with the addition of lime-stabilized red mud and lime-stabilized red mud–flyash.

The effect of curing time on UCS was evaluated using soil and the two admixtures, lime-stabilized red mud alone and lime-stabilized red mud along with flyash. Between 7 and 28 days, the UCS increased modestly and steady increase was found up to 90 days of curing.

Expansive soil mixed with 30% red mud by weight of dry soil along with 4% lime is optimum content at which significant improvement in compaction characteristics and considerable increase in UCS is achieved.

Expansive soil mixed with 15% flyash and 15% red mud by weight of dry soil along with 4% lime exhibits improved geotechnical properties in terms of UCS and compaction characteristics.

References

Kalkan, E. (2006). Utilization of red mud as a stabilization material for the preparation of clay liners. *Engineering Geology, 87*(3), 220–229.

IS: 2720 (Part IV). (1985). Methods of test for soils—Part IV: Grain size analysis. New Delhi, India: BIS.

IS: 2720 (Part V). (1970). Methods of test for soils—Part V: Determination of liquid and plastic limit. New Delhi, India: BIS.

IS: 2720 (Part VII). (1980). Methods of test for soils—Part VII: Determination of water content—Dry density relation using light compaction. New Delhi, India: BIS (reaffirmed in 1987).

IS: 2720 (Part X). (1973). Determination of unconfined compressive strength. New Delhi: BIS.

IS: 2720 (Part XIII). (1986). Methods of test for soil: Direct shear test. New Delhi: BIS.

Deelwal, K., Dharavath, K., & Kulshreshtha, M. (2014). Evaluation of characteristic properties of red mud for possible use as a geotechnical material in civil construction. *International Journal of Advances in Engineering & Technology, 7*(3), 1053–1059.

Li, L. Y. (1998). Properties of red mud tailings produced under varying process conditions. *Journal of Environmental Engineering, 124*(3), 254–264.

Miners, K. (1973). Alcan's experience of the disposal of red mud from the Bayer ore process. In *Proceedings of 1st International Tailings Symposium* (pp. 553–562). San Francisco: Miller Freeman.

Newson, T., Dyer, T., Adam, C., & Sharp, S. (2006). Effect of structure on the geotechnical properties of bauxite residue. *Journal of Geotechnical & Geoenvironmental Engineering, 132* (2), 143–151.

Paramguru, R. K., Rath, P. C., & Misra, V. N. (2005). Trends in red mud utilization—A review. *Mineral Processing and Extractive Metallurgy Review, 26*(1), 1–29.

Parlikar, U. V., Saka, P. K., & Khadilkar, S. A. (2011). Technological options for effective utilization of bauxite residue (Red mud)—A review. In *International Seminar on Bauxite Residue (RED MUD)*. Goa, India.

Rout, S., Sahoo, T., & Das, S. K. (2012). Utility of red mud as an embankment material. *International Journal of Earth Sciences and Engineering 6*, 1645–1651.

Sivapullaiah, P. V., Prashanth, J. P., & Sridharan, A. (1996). Effect of fly ash on the index properties of black cotton soil. *Soils and Foundations, 36*(1), 97–103.

Somogyi, F., & Gray, D. (1977). Engineering properties affecting disposal of red mud. In *Proceedings of Conferance on Geotechnical Practice for Disposal of Solid Waste Materials*, ASCE, pp. 1–22.

Sridharan, A., El-Shafei, A., & Miura, N. (2002). Mechanisms controlling the undrained strength behavior of remolded Ariake marine clays. *Marine Georesources and Geotechnology, 20*(1), 21–50.

Sundaram, R., & Gupta, S. (2010). Constructing foundations on red mud. In *6th International Congress on Environmental Geotechnics*, pp. 1172–1175, New Delhi, India.

Vick, S. G. (1981). Planning, design and analysis of tailing dams. New York: Wiley, p. 369.

California Bearing Ratio and Permeability Behaviour of Fly Ash Reinforced with Geotextiles

Binata Debbarma and Sujit Kumar Pal

Abstract Two different laboratory tests, i.e., California bearing ratio (CBR) and permeability have been conducted on fly ash both in unreinforced and reinforced with nonwoven geotextiles. CBR test is conducted on fly ash and the values are 11.23 and 16.27% at 2.5 and 5 mm respectively. After reinforcement provided in three different layers, i.e., two layers in middle with fly ash layer in between, one layer each in middle and bottom, and one layer each in top, middle and bottom, the CBR values increases within the ranges between 11.72–17.58% at 2.5 mm and 17.5–22.46% at 5 mm penetration. However, the most improved (i.e., increased) values are observed when reinforcement is provided in three layers at equal interval. The permeability (k) value of well compacted fly ash is 3.30×10^{-7} m/s. The permeability value decreases after reinforcement has been provided in different layers and within the ranges 8.14×10^{-8} to 9.8×10^{-8} m/s and the most improved (i.e., decreased) values are observed in three layers reinforcement at equal interval. The modified permeability value minimizes the seepage of water through a fly ash embankment. So the fly ash and reinforced fly ash can be used as a structural fill and embankment materials.

Keywords California bearing ratio · Permeability · Fly ash · Nonwoven geotextiles · Reinforcement

B. Debbarma (✉)
Department of Civil Engineering, National Institute of Technology, Langol, Manipur, India
e-mail: betsdebbarma@gmail.com

S. K. Pal
Department of Civil Engineering, National Institute of Technology, Agartala 799046, India
e-mail: skpal1963@gmail.com

T. Thyagaraj (ed.), *Ground Improvement Techniques and Geosynthetics*, Lecture Notes in Civil Engineering 14, https://doi.org/10.1007/978-981-13-0559-7_30

1 Introduction

The disposal operation of fly ash is made either in dry condition or in wet condition, but in both the ways it consumes large area of land and also hampers the environment. Thus it has become very important to overcome the disposal problem of fly ash before it could cause more destruction to the environment. To increase the use of fly ash as a construction material, it is very essential to boost its properties since raw fly ash cannot be utilized as earth material, it will have to be used in conjunction with other materials.

Many researchers had worked on the index and engineering properties of fly ash and geotextiles in order to find out their inventive use in the field of construction. Iryo and Rowe (2003) studied the permeability behaviour of unsaturated nonwoven geotextiles in conjunction with soil and concluded that the geotextile can change from a pervious to an effectively impervious material as the water characteristic curve and permeability function for the geotextiles studied were steeper as compared to sand and also the air and water entry values of geotextiles were very small. Pickles and Zornberg (2012) studied the permeability behaviour of unsaturated nonwoven geotextiles in order to use it as capillary barriers and concluded that the interface of the two materials may create a capillary break which had the capability of preventing flow of moisture until the soil adjoining to the geotextile was nearly saturated. Prasad et al. (2014) in their investigation found that inclusion of geotextiles in soil as reinforcement increased the California bearing ratio (CBR) values and with increase in number of layers of reinforcement, CBR values also increased. In the present paper an effort has been made to evaluate the properties of fly ash using nonwoven geotextile as reinforcing material.

Many researchers have been studied on soil-geotextile combination and soil–fly ash-geotextile combination but there is paucity of data on fly ash-geotextile combination. Most of the study was made using geotextile as a fibre mixed with soil or fly ash or with both, but very less study has been conducted on fly ash using geotextile sheet as reinforcing material. The present study highlights the properties of fly ash using nonwoven geotextiles as reinforcing layer.

2 Materials and Methods

2.1 Materials Used

Fly ash used in the present study has been collected from the Thermal Power Station situated in Kolaghat, West Bengal, India. The fly ash used in the present study belongs to Class F fly ash.

In the present investigation, the geotextile used is a polypropylene needle punched nonwoven geotextile with 400 g/m^2 mass per unit area and thickness of

3.5 mm having a tensile strength of 24.5 kN/m. The materials used in the present study have been represented as shown below:

FA: Fly ash;
NW: Nonwoven geotextile;
MB: FA + NW + FA + NW (middle and bottom);
M: FA + NW + FA + NW + FA (only middle); and
3L: NW + FA + NW + FA + NW (top, middle and bottom).

2.2 Sample Preparations

The samples used in the present investigation are arranged at its optimum moisture content (OMC) and maximum dry density (MDD) obtained from standard Proctor compaction test as per ASTM D 698-07. The geotextiles reinforcement used in different layers is shown in Fig. 1.

2.3 Experimental Procedure

Different experiments have been carried out as per ASTM standards on fly ash with and without reinforcement for determining its physical and engineering properties.

Grain size analysis has been carried out on fly ash by hydrometer as per ASTM D 422-63. The grain size distribution curve of unreinforced fly ash is shown in Fig. 2. From the curve the sand size (4.75–0.075 mm), silt size (0.075–0.002 mm) and clay size (<0.002) of fly ash is found as 14.17, 77.33 and 8.5%. The coefficient of uniformity (C_u) and coefficient of curvature (C_c) for fly ash found as 3.889 and 0.917 respectively. The specific gravity of fly ash is 2.13 which is lower than the conventional earth material. The MDD corresponding to OMC is 11.98 kN/m^3, as per standard Proctor compaction. A plot showing dry density versus water content is shown in Fig. 3. From figure, the OMC is obtained as 26.8%.

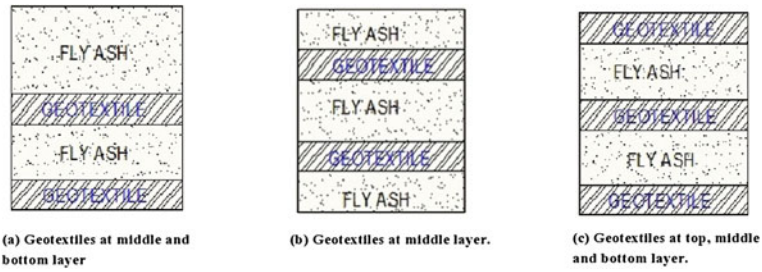

Fig. 1 Reinforcement used in different layers

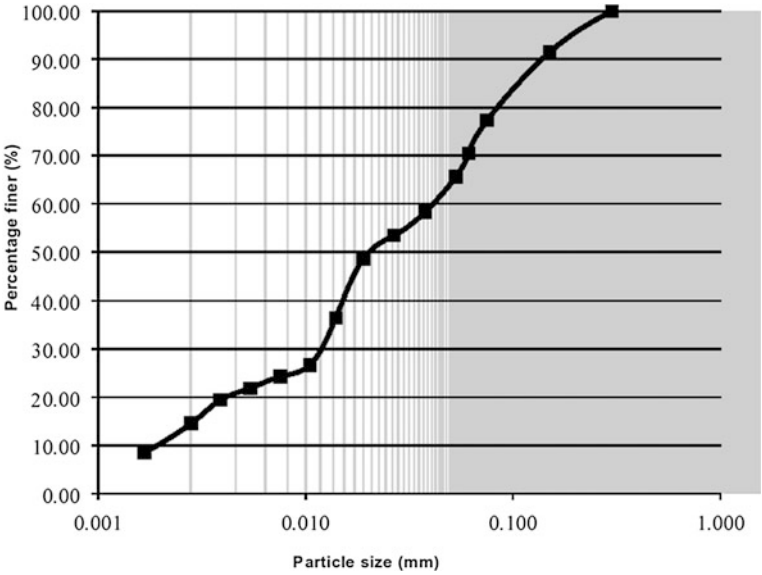

Fig. 2 Grain size distribution curve of fly ash

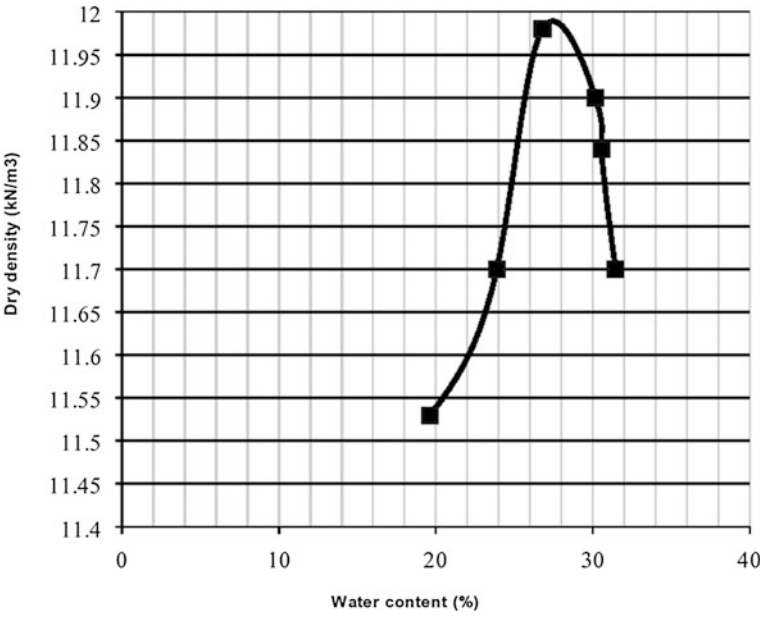

Fig. 3 Dry density versus water content curve of fly ash

3 Results and Discussions

The main aim of the present study is to bring out the effect of fly ash reinforced with nonwoven geotextile on CBR and permeability respectively. Accordingly, detailed discussions have been made in the subsequent sections.

3.1 Effect of Geotextiles on California Bearing Ratio (CBR) of Fly Ash

To analyse the effect of geotextile on CBR value of fly ash, un-soaked CBR test as per ASTM D1883 has been carried out on fly ash. The relevant plot and CBR values of fly ash with and without reinforcement are presented in Fig. 4 and Table 1. From relevant figure, it is exposed that when the geotextile is used in the form of reinforcement, it gives a very positive result in terms of bearing capacity. The CBR value of unreinforced fly ash is found 11.23 and 16.27% at 2.5 and 5 mm penetration respectively, whereas the CBR value of fly ash reinforced with non-woven geotextile in different layers ranges from 11.72 to 17.58% at 2.5 mm and 17.57 to 22.46% at 5 mm penetration respectively. So it can be seen that there is an improvement in CBR value when reinforced with nonwoven geotextile in different layers. However, the maximum improvement in CBR value is observed when

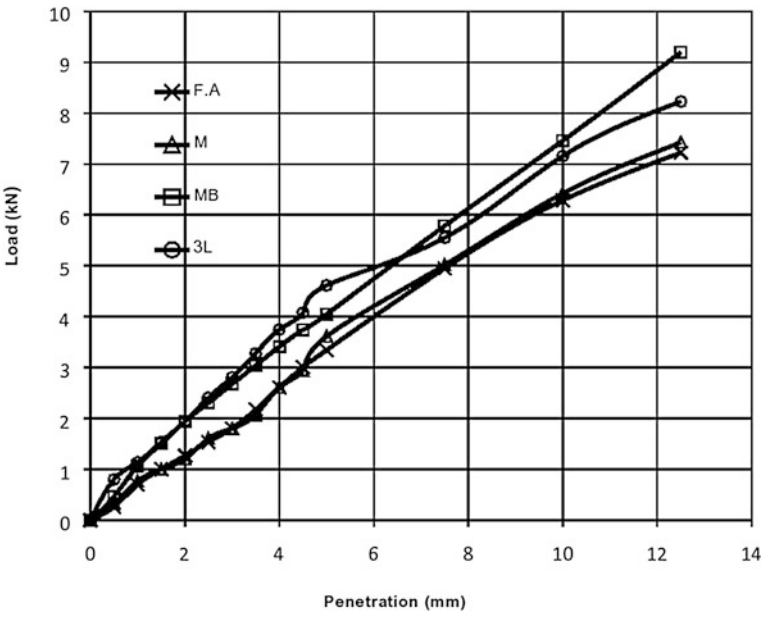

Fig. 4 Load versus penetration curve of fly ash with and without reinforcement

reinforcement is provided in three layers and the value was found to be 22.46% at 5 mm penetration. So this type of material, i.e., FA + NW can be used in highway construction. Prasad et al. (2014) observed similar trend in increase in overall CBR strength after reinforcement of geotextile had been provided. The increase in CBR value may be because geotextiles has interlocking property and have good tensile strength as compared to the fly ash. According to Singh (2013), the main function of the interlock was to transfer the overall stress from the fly ash to the reinforcing materials and as a result of which tensile strain decreased, and load carrying capacity of reinforced fly ash increased.

3.2 *Effect of Geotextiles on Permeability (*k*) of Fly Ash*

In order to study the outcome of geotextile on permeability behaviour on fly ash, falling head permeability tests as per ASTM D5856-95 are performed on both unreinforced and reinforced fly ash. Relevant plot is presented in Fig. 5. The variations in k values of fly ash with and without reinforcement are highlighted in Table 1. Figure 5 highlights the hydraulic conductivity behaviour vs. flow period which shows that with increase in flow period, the coefficient of permeability (k) decreases for fly ash with and without reinforcement. Similar trend had been observed by Pal and Ghosh (2011). The decrease in hydraulic conductivity (k) value with increase in flow period may be because of the rearrangement of fly ash particles. The k value of fly ash is found 3.30×10^{-7} m/s. Fly ash is highly permeable in nature as it contains large amount of voids. But after providing nonwoven geotextile as reinforcement in different layers, the k value decreases and value ranges from 8.14×10^{-8} to 9.8×10^{-8} m/s. However, the most decreased value is observed in 3 layers of reinforcement at equal interval (i.e., NW + FA + NW + FA + NW). The decrease in k values may be because of the material being used as reinforcement which is spongy in nature and as per Iryo and Rowe (2003), the decreasing trend in k values may be because the air and water entry values of geotextiles were very small which implied that geotextile can change from a permeable to an impermeable material. Pickles and Zornberg (2012) also observed that nonwoven geotextile imparts least hydraulic conductivity.

Table 1 Values of CBR and permeability (k) of unreinforced and reinforced fly ash

Specimen	California bearing ratio (%)		Percentage variation in CBR value w.r.t FA (%)		Hydraulic conductivity, k (m/s)
	2.5 mm	5 mm	2.5 mm	5 mm	
FA	11.23	16.27	–	–	3.30×10^{-7}
NW-M	11.72	17.57	4.36	7.99	9.80×10^{-8}
NW-MB	11.73	17.58	4.45	8.10	9.86×10^{-8}
NW-3L	17.58	22.46	56.54	38.04	8.14×10^{-8}

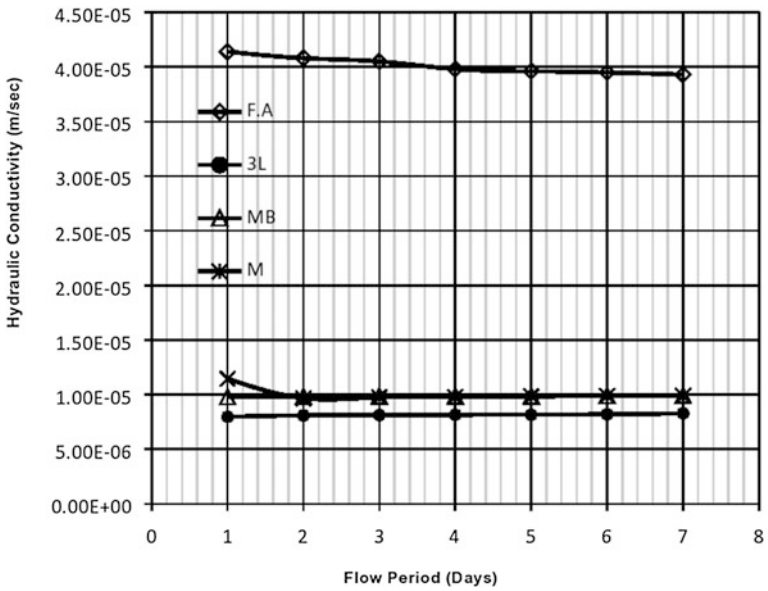

Fig. 5 Hydraulic conductivity versus flow period of fly ash with and without reinforcement

4 Conclusions

As per the results and discussions made above, the following conclusions may be drawn:

- Due to relatively low unit weight, i.e., 11.98 kN/m^3 of fly ash, the fly ash makes well suited for placement over low bearing strength of soil.
- The maximum improvement of CBR for fly ash reinforced with nonwoven geotextiles over fly ash without reinforcement is observed 38.05 and 56.54% at 5 and 2.5 mm penetration respectively.
- The hydraulic conductivity value decreases for fly ash reinforced with nonwoven geotextile and the values are found in the range of 8.14×10^{-8} to 9.8×10^{-8} m/s and the most decreased value is observed when reinforcement has been provided in three consecutive layers.
- Due to the provision of geotextiles to the fly ash, it modifies the behaviour of fly ash. So, from this point of view, the reinforced material can be used in highway construction and as structural fill materials.

5 Notations

The following symbols are used in this paper:

FA	Fly ash
NW	Nonwoven geotextile
C_u	Coefficient of uniformity
C_c	Coefficient of curvature
MDD	Maximum dry density
OMC	Optimum moisture content
CBR	California bearing ratio
k	Hydraulic conductivity

References

Iryo, T., & Rowe, R. K. (2003). On the hydraulic behaviour of unsaturated nonwoven geotextiles. *Geotextiles and Geomembranes, 21*(2003), 381–404.

Pal, S. K., & Ghosh, A. (2011). Compaction and hydraulic conductivity characteristics of Indian fly ashes. In *Proceedings of Indian Geotechnical Conference*, No. L-326, December 2011, Kochi, India.

Pickles, C. B., & Zornberg, J. G. (2012). Hydraulic classification of unsaturated nonwoven geotextiles for use in capillary barriers. In *Proceedings of GeoAmericas 2012, the second Pan-American Geosynthetics Conference*, 1–4 May 2012, Lima, Peru, pp. 408–420.

Prasad, S. S. G., Ch, S. K., & Surisetty, R. (2014). Stabilization of pavement subgrade by using fly ash reinforced with geotextile. *International Journal of Research in Engineering and Technology, 3*(08), 255–259.

Singh, H. P. (2013). Strength and stiffness of soil reinforced with jute geotextile. *International Journal of Current Engineering and Technology, 3*(03), 2277–4106.

Influence of Granulated Blast Furnace Slag Contents on California Bearing Ratio Value of Clay GBFS Mixture

Ashis Kumar Bera, Ashoke Das and Souvik Patra

Abstract Nowadays it is common practices to strengthening the soft subgrade by using waste materials. Granulated blast furnace slag (GBFS), an industrial waste may be used to stabilize soft clay sub-grade. In the present study, an attempt has been made to evaluate the effect of GBFS contents on California bearing ratio (CBR) value of clayey soil GBFS mixture. Three types of clayey soil and one types of GBFS has been used in the present investigation. Soaked CBR test has been performed with varying GBFS content (0–50%) for above three types of soil. From the experimental outcomes it has been found that with increase in GBFS content the soaked CBR values increases and reaches a maximum value at certain GBFS content after that it decreases. The optimum value of GBFS content is 30% irrespective of types of soil when it has been compacted at OMC and MDD of the respective mixture. Based on the experimental data a nonlinear power model has been developed to predict the CBR value of soil GBFS mixture in terms of GBFS content and CBR value of the respective soil alone.

Keywords GBFS · CBR · Soaked · Clay · Regression

1 Introduction

Nowadays due to rapid economic growth and industrialization a huge quantity of waste materials are produced as industrial by-product such as fly ash, bottom ash, blast furnace slag, etc., creating a tremendous threat to public health and ecology

A. K. Bera (✉) · A. Das · S. Patra
Department of Civil Engineering, Indian Institute of Engineering Science and Technology, Shibpur, Howrah 711103, India
e-mail: ashis@civil.iiests.ac.in

A. Das
e-mail: akaashnulkolkata@gmail.com

S. Patra
e-mail: souvik4rmjgec@gmail.com

T. Thyagaraj (ed.), *Ground Improvement Techniques and Geosynthetics*, Lecture Notes in Civil Engineering 14, https://doi.org/10.1007/978-981-13-0559-7_31

and also it requires a huge area for disposal. Consequently, there is a need for proper and wise disposal of such industrial waste materials. Use of such wastes for the purpose of soil stabilization for construction of road not only improves the engineering properties of soil but also reduces the cost of construction. Impact of industrial by-products on soil is of particular interest to many researchers. Akinmasuru (1991) studied the potential uses of steel slag wastes for civil engineering purposes. The author evaluates different engineering properties on steel slag wastes stabilized soil, obtained the optimum slag content 10% for maximum California bearing ratio (CBR) value of blast furnace slag stabilized soil. Wild et al. (1998) studied the effects of partial substitution of lime with ground granulated blast furnace slag (GGBS) on the physical, chemical, and mechanical properties of lime-stabilized sulphate bearing clay, with application of varying percentages of gypsum. Yadu and Tripathi (2013) studied the effect of blast furnace slag in the engineering behaviour of stabilized soft soil. Mircea et al. (2014) studied the use of GGBS to stabilization of expansive soil. Authors have also reported that GGBS reduces the soil expansion and improves the mechanical properties of GGBS to expansive soil mixture. From the literature it is found that a little has been documented on CBR of granulated blast furnace slag (GBFS) stabilized clay for road subgrade. In the present investigation an attempt has been made to study the GBFS stabilized soil in details. An attempt also has been made to develop an empirical relationship of CBR of clay GBFS mixture in terms of CBR of clay alone and GBFS contents.

2 Materials

In the present paper three types of clay and one type of GBFS have been used. Among three types of clays one natural clay procure from Agarpara, West Bengal, India and other two viz., kaolinite and yellow types (Commercial bentonite) artificial clay collected from Burrabazar, Kolkata, West Bengal, India. The above three types of clay may be designated as Soil 1, Soil 2, and Soil 3 for Agarpara soil, kaolinite and yellow types clay, respectively. Engineering properties viz., grain size distribution, specific gravity, liquid limit, plastic limit of the above three types of clay and GBFS has been performed in the geotechnical engineering laboratory, IIEST, Shibpur, India. Fine content (particle passing 0.075 mm sieve) of the soil 1, soil 2, soil 3 and GBFS are 97.30, 93.85, 86.18, and 15.00% respectively. Specific gravity of soil 1, soil 2, soil 3 and GBFS are 2.69, 2.65, 2.76, and 2.90, respectively. The plasticity index is 15.5, 15.8, and 16.6 for soil 1, soil 2, and soil 3, respectively. Based on the USCS the above soil may be classified as ML, CL, and ML, respectively for soil 1, soil 2, and soil 3. Standard proctor compaction tests for soil and individual mixed has been performed in accordance with ASTM D698 (1992). The values of OMC of soil 1, soil 2 and soil 3 are 22.55, 28.00 and 16.50%

respectively. Whereas the MDD of the respective soils (soil 1, soil 2, and soil 3) are 15.21, 14.20, and 17.50 kN/m^3 respectively. The values of OMC and MDD of respective soil GBFS mixture are presented elsewhere (Das 2016).

3 California Bearing Ratio Tests (CBR)

CBR is one of the important parameter for design of any types of roads viz., rural road, state highway, national highway, etc. CBR value depends on a number of factors such as density of soil, percent of admixture, plasticity index, etc. To know the effect of GBFS content on different types of soil a series of CBR tests on soil alone and also soil GBFS mixture has been performed. Table 1 presents the plan of CBR tests. In the present investigation soaked CBR test has been performed in accordance with IS: 2720 (Part 16) (1987). Data obtained from soaked CBR tests are presented in graphical from. Figure 1 shows the typical load versus penetration curve for soil 1 (GBFS = 30%) compacted at OMC and MDD of respective Soil 1 GBFS mixture. CBR value versus GBFS content curve with varying soil types

Table 1 Plan of CBR tests

Series	Types of soil	Moisture content and dry density	GBFS content (%)
A	Soil 1 soil 2 soil 3	MDD and OMC of the respective soil GBFS mixture	0, 10, 20, 30, 40, 50
B	Soil 1	MDD and OMC of the Soil 1 alone	0, 10, 20, 30, 40, 50

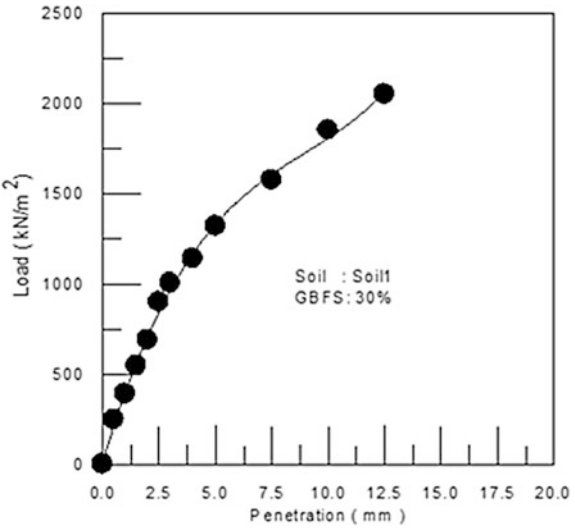

Fig. 1 Typical load versus penetration curve for soil 1 compacted at OMC and MDD of respective Soil 1 GBFS mixture

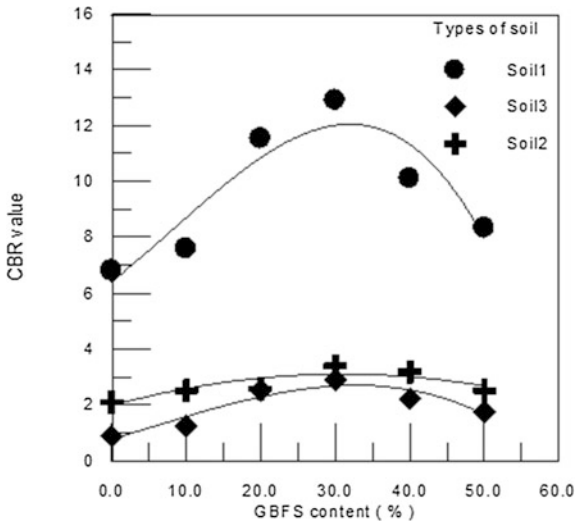

Fig. 2 CBR value versus GBFS content curve with varying soil types compacted at respective MDD and OMC

compacted at respective MDD and OMC are shown in Fig. 2. From Fig. 2 it has been observed that with increase in GBFS content the values of soaked CBR increases and reaches a peak value at certain GBFS content and after that the soaked CBR value decreases. The maximum value of soaked CBR has been obtained at GBFS content of 30% for all types of soil under the present study. It is may be due to that with increase in GBFS content (up to 30%) the values of WPI (weighted plasticity index) decreases. Figure 3 shows the comparison of CBR value obtained based on NCHRP (2001) and present in the present investigation. From Fig. 3 it has been seen that with increase in GBFS content (up to 30%) CBR value obtained based on NCHRP (2001) and present investigation increases. Above 30% of GBFS content the effect of WPI is insignificant as a result CBR value decreases. Pathak et al. (2014) also reported the similar types of results with increase in GGBS content (up to 25%) the values of CBR increases. Figure 4 shows the CBR value versus GBFS content curve soil 1 obtained due to compaction of MDD and OMC of soil alone and also compacted at respected MDD and OMC. From the curve presented in Fig. 4, it has been found that both peak value of CBR and optimum value of GBFS content higher in case of CBR compacted at respective MDD and OMC. It may be due to that for respective MDD are much higher than the MDD of soil alone.

4 Regression Model

Based on the present experimental data point and performing the multiple regression analysis a nonlinear power model has been developed as follows:

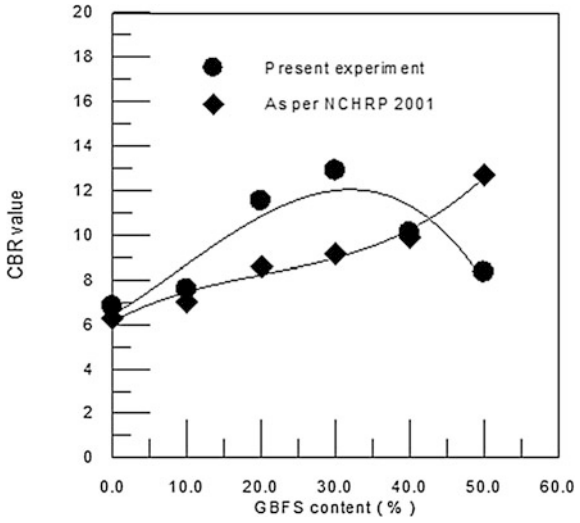

Fig. 3 Comparison of CBR value obtained from equation (NCHRP 2001) and present experimental data versus GBFS content for soil 1

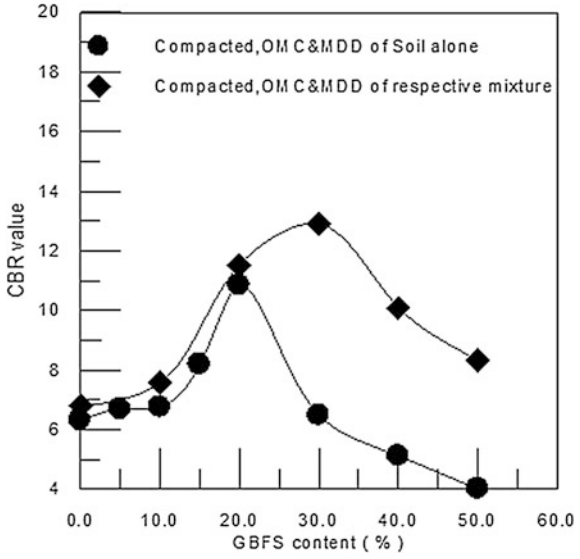

Fig. 4 Typical CBR value versus GBFS content curve soil 1

$$\mathrm{CBR_{mix}} = (\mathrm{CBR_{soil}})^{1.007399} \times (1.015071)^{(\mathrm{GC})} \quad (1)$$

where

$\mathrm{CBR_{mix}}$ CBR value for soil GBFS mixture,
$\mathrm{CBR_{soil}}$ CBR value for soil,
GC GBFS content (%).

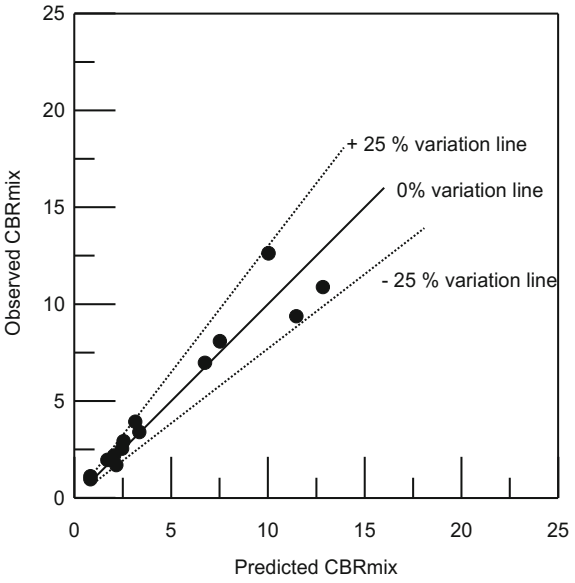

Fig. 5 Observed CBR_{mix} value versus predicted CBR_{mix} value curve

Significance of the model as a whole and partial has been checked by using *F*-statistics and *t*-statistics. Value of R^2 of the model is 0.995. Figure 5 shows the Observed CBR_{mix} value versus predicted CBR_{mix} value curve. From the curve it has been illustrated that all the CBR values are within ±25% error. Figure 6 presents the CBR_{mix} value versus GBFS content curve for Pathak et al. (2014) and predicted CBR_{mix} obtained from Eq. 1. From Fig. 6 it has been observed that the values CBR_{mix} obtained based on Eq. 1 and Pathak et al. (2014) are very close to each other. The above model may be useful within the range of GC and CBR_{soil}, $0\% < GC \leq 30\%$ and $0.89\% \leq CBR_{soil} \leq 6.8\%$. Beyond this range the CBR value need to be checked with at least one set of additional data.

5 Conclusion

Based on the experimental results presented and discussion made in the previous sections following conclusions may be drawn:

- With increase in GBFS content in GBFS soil mixture the CBR value of GBFS soil mixture increases and reaches a peak value at certain GBFS content (%) after that it is decreases.
- CBR value of soil GBFS mixture much more prominent when it is compacted at OMC and MDD of the respective mixture. In case of CBR_{mix} compacted at respective MDD and OMC the optimum value of GBFS content around 30%.

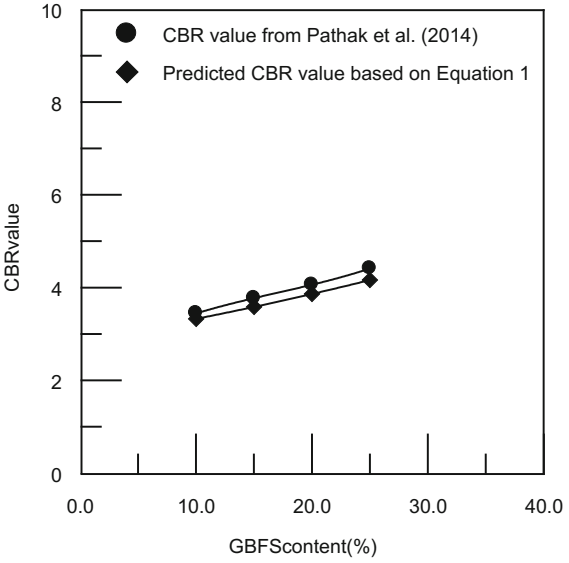

Fig. 6 CBR_{mix} value versus GBFS content curve

Whereas in case of CBR_{mix} compacted at MDD and OMC of soil alone the optimum value of GBFS content around 20%.

- A nonlinear power model has been developed for CBR_{mix} in terms of CBR_{soil} and GC. The model may be useful within the range of GC and CBR_{soil}, $0\% < GC \leq 30\%$ and $0.89\% \leq CBR_{soil} \leq 6.8\%$ respectively. Beyond this range the CBR_{mix} value need to be checked with at least one set of additional data.
- Clay GBFS mixture may be used effectively as subgrade material for roads.

References

Akinmasuru, J. O. (1991). Potential beneficial use of steel slag wastes for civil engineering purposes. *Journal of Resource Recycling Conservation, 5,* 73–80.

ASTM D698. (1992). *Test method for laboratory compaction characteristics of soil using standard effort*. Philadelphia: American Society of Testing Materials.

Das, A. (2016). *Influence of blast furnace slag on CBR value of soft clay road subgrade (M.E. thesis)*. Department of Civil Engineering, Indian Institute of Engineering Science and Technology, Shibpur, India, p. 65.

IS: 2720 (Part 16). (1987). *Methods of tests for soils: Laboratory determination of CBR*. New Delhi: Bureau of Indian Standards.

Mircea, A., Irina, L., & Anghel, S. (2014). Effects of eco-cement (GGBS) on the expansive soil strength. *Journal of Civil Engineering and Sciences, 3*(1), 74–80.

NCHRP. (2001). *Correlation of CBR values with soil index properties*. Illinois: MEPDG.

Pathak, A. K., Pandey, V., Murari, K., & Singh, J. P. (2014). Soil stabilization using ground granulated blast furnace slag. *International Journal of Engineering Research and Applications, 4*(5), 164–171.

Wild, S., Kinuthia, J. M., Jones, G. I., & Higgins, D. D. (1998). Effects of partial substitution of lime with ground granulated blast furnace slag (GGBS) on the strength properties of lime-stabilised sulphate-bearing clay soils. *Journal of Engineering Geology, 51*(1), 37–53.

Yadu, L., & Tripathi, R. K. (2013). Effects of granulated blast furnace slag in the engineering behaviour of stabilized soft soil. In *3rd International Conference on Tracks of Chemical, Civil and Mechanical Engineering* (NUiCONE2012), 6–8 December 2012, Nirma University, India.

Geocell Reinforced Dense Sand Bases Overlying Weak Sand Sub-grades Under Repeated Loading

Vijay Kumar Rayabharapu and Sireesh Saride

Abstract In this paper, results obtained from a series of large-scale repeated load model tests are presented. Repeated load tests were conducted on geocell reinforced and unreinforced dense sand layers overlying weak sub-grades to understand the general behavior of reinforced unpaved roads. The height of the weak sub-grade was always maintained and the height of the dense sand layer was varied according to the heights of the geocell mattress used. The relative densities of the weak sub-grade and dense sand were maintained at 30 and 75% respectively. The loading was applied through a circular steel plate which replicates the traffic loading applied through a sophisticated double acting linear dynamic actuator attached to a 3.5 m high reaction frame. Results from each case are presented, and different views on the results are discussed with the experimental tests. It was inferred that the rutting on the pavement surface can be reduced to about 35% by providing nominal size of the geocell mattress in base layers over weak sub-grades. The results are also quantified through a non-dimensional factor, called traffic benefit ratio (TBR), defined as a ratio of number of load cycles applied on reinforced section to the number of load cycles applied on unreinforced section at the same settlement. It was found that the TBR can be increased as high as 15 with geocell reinforcement at a settlement ratio of 5%.

Keywords Geocell · Weak sub-grades · Repeated loadings

V. K. Rayabharapu (✉)
Department of Civil Engineering, B. V. Raju Institute of Technology, Narsapur, 502313, India
e-mail: vkraya@gmail.com

S. Saride
Department of Civil Engineering,
Indian Institute of Technology Hyderabad, Kandi, 502285, India
e-mail: sireesh@iith.ac.in

T. Thyagaraj (ed.), *Ground Improvement Techniques and Geosynthetics*, Lecture Notes in Civil Engineering 14, https://doi.org/10.1007/978-981-13-0559-7_32

1 Introduction

As the sub-grade conditions vary from site to site and location to location in a given road network, the performance of the pavements alter dramatically from section to section depends on the sub-grade condition. To quantify the effectiveness of the geocell reinforcement, weak sub-grades are considered. As part of this, weak sand sub-grades, prepared at a relative density around 30%, are considered in this paper. To prepare the base course layers, a dense sand base layer is considered with and without geocell confinement. Hence, the pavement geometry comprises of weak sand sub-grades overlain be dense sand bases with geocell reinforcement. The considered test configuration is then subjected to cyclic and repeated loadings equivalent to a tire pressure of about 550 kPa. The influence of various parameters such as width of reinforcement layers (b), height of the reinforcement (h) are studied to understand the efficacy of the geocell material to achieve the optimum geometry of the geocell. Improvement is presented in terms of the performance indicators.

2 Background

Since the reinforcement forms ever used, many different kinds of geosynthetics have been used and the recent reinforcement type which has become popular nowadays is geocell reinforcement.

The studies on cyclic loading are not that extensively done and the available literature observed the higher performance of geocell reinforcement with dense infill on a good sub-grade Mhaiskar and Mandal (1994). Pokharel et al. (2011) studied the effects of geocell reinforced bases under cyclic loading proving the reinforced sections yielding less cumulative permanent deformations and sustaining for more cycles compared to the unreinforced. Yang et al. (2010), Zhang et al. (2010) studied the numerical analysis of geocell reinforced granular soils to prove that the geocell reinforcement increased with the increase of the modulus (or tensile stiffness) of the geocell and both the type of infill material and the resilient modulus of sub-grade significantly influenced the rut depth of the unpaved road and the benefit of geocell reinforcement in reducing rutting depends on the quality of base course materials.

Recently Pokharel et al. (2011) observed that the geocells have improved the strength, increased the percentage of elastic deformation and life of the unpaved road sections over weak sub-grade. The inclusion of the geocell layers reduces the vertical stress transferred down through the foundation bed by distributing the load over a wider area compared with the stress in the unreinforced bed (Moghaddas Tafreshi and Dawson 2012).

It is understand from the literature study that there is a research knowledge gap in understanding the mechanisms of geocell reinforced bases under repeated traffic

loading. In this study, an attempt has been made to understand the repeated loading behavior of geocell reinforced sand bases overlying weak sub-grades under traffic loading conditions which can be preferably used in increasing the life cycle of the unpaved roads.

3 Materials and Methods

The sand used in this investigation was dry sand. The particle size distribution of the sand was determined by dry sieve analysis as per IS 2720. The particle size distribution of the sand is shown in Fig. 1. The sand is classified as poorly graded sand with letter symbol SP. High density poly propylene (HDPE) geocell mattress obtained from M/s Strata Geosystems (I) Pvt. Ltd, with a weld spacing of 350 and a minimum seam strength of 1050 N are used in the study.

4 Test Setup

The soil beds with 70% relative density were prepared in a test tank with dimensions of 1 m × 1 m × 1 m (length × width × height). A rigid steel plate of 150 mm diameter (*D*) and 30 mm thickness was used to apply the traffic loading. The size of the plate was chosen such a way that the area of the plate resembles the area of tire pressure. Loading to the plate was given by graphical user interfaced MTS MPT software with the help of hydraulic power unit (HPU), hydraulic service

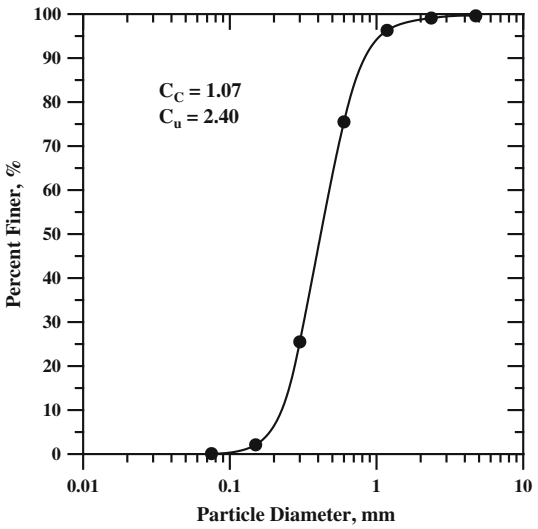

Fig. 1 Particle size distribution curve

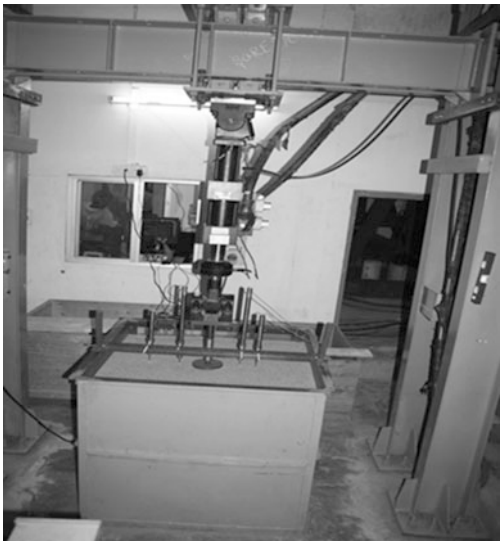

Fig. 2 Test setup

manifold (HSM) and sophisticated double acting linear dynamic 100 kN actuator which is attached to a 3.5 m high reaction frame shown in Fig. 2.

5 Testing Procedure

Test procedure can be explained under three sub-topics

(a) Preparation of relative density calibration chart
(b) Preparation of sand bed
(c) Cyclic load tests

6 Relative Density Calibration

To determine the density with which sand is to be poured in the tank, a special technique called sand raining technique is used. It is also called as sand pluviating technique. To achieve this, a special device is designed. It consists of long steel pipe with a cone fixed at the bottom. Apex of the cone is pointed up with Cone apex angle of 60°. This pipe is fitted with a movable scale to arrange different heights shown in Fig. 3.

Relative density calibration chart was obtained by conducting series of tests with different heights of fall. Natural densities were measured physically by collecting samples in small containers whose weights and volumes were known. With the

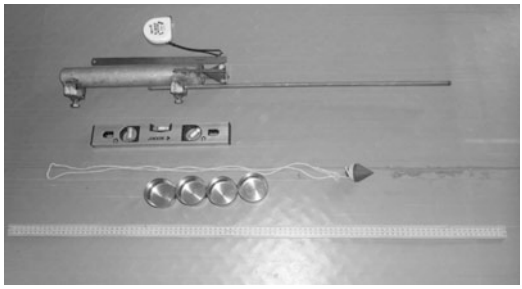

Fig. 3 Devices used in the preparation of test beds

known values of the minimum and maximum void ratios of sand taken in the investigation, a calibration chart was prepared for the height of fall against the corresponding relative density. For any required relative density corresponding height of fall can be read from calibration chart.

7 Sand Bed Preparation

The sand was placed in the test tank using a raining technique. This device has a hopper with a pipe welded to its bottom and a 400 mm long pipe with an inverted cone welded at its bottom. The sand passes through the 30 mm internal diameter pipe and disperses at bottom by a 60° inverted cone. The height of fall to achieve the desired relative density was determined by performing a series of trials with different heights of fall earlier. In each trial, the densities were monitored by collecting samples in small cups of known volume placed at different locations in the test tank. With the known values of the minimum and maximum void ratios of sand in the study, a calibration chart was prepared for the height of fall against the corresponding relative density. The height of fall can directly read from the graph corresponding to the required relative density. In all tests, relative density of sand was kept constant at 75%.

8 Cyclic Load Tests

The procedure adopted for all the tests were in accordance with the Indian Standard code IS 1880: 1982 (reaffirmed 1998). Upon filling the test tank up to the desired height, the fill surface was leveled and the footing was placed on a predetermined alignment such that the loads from the actuator applied would be transferred concentrically to the footing. A recess was made into the footing plate at its center to accommodate a ball bearing through which vertical loads were applied to the footing.

The cyclic load was applied to a loading plate using a computer-controlled servo hydraulic actuator, with a maximum load of 9.7 kN and a minimum on 0.97 kN equivalent to 550 and 55 kPa pressure which is the tire pressure. A 10% of load (0.97 kN) was constantly applied on the plate to make the cycle a closed loop. The load form was applied at a frequency of 1.0 Hz. Multi-Purpose Test Ware (MPT) software was set up to control and acquire the applied load data as well as the deformation data.

A series of repeated load tests were conducted to verify the efficiency of the geocell reinforcement in the sub-grade.

9 Results and Discussion

Figure 4 presents a typical pressure–settlement response for an unreinforced sub-grade. All the tests were conducted until about 20% of the plate diameter. The plot shows the cyclic behavior under repeated loads as specified. It can be noticed that the plastic settlements are higher during initial load cycles. Figure 4 presents the variation of settlement ratios with the number of loading cycles.

Settlement ratio is defined as the ratio of settlement to the plate width expressed in percentage. Initially, at low number of loading cycles ($N < 10$), the total settlement ratios are higher and get attenuated with increase in the number of loading cycles. As expected, the unreinforced sub-grade shows excess settlement ratios than the reinforced sub-grades. It is also observed that the settlement ratios have come down with increase in the amount of geocell reinforcement. To quantify the reduction in settlement ratios and the efficacy of geocell, cumulative permanent deformations (CPD) were calculated from the test data. Similar trends are also obtained from Saride et al. (2015).

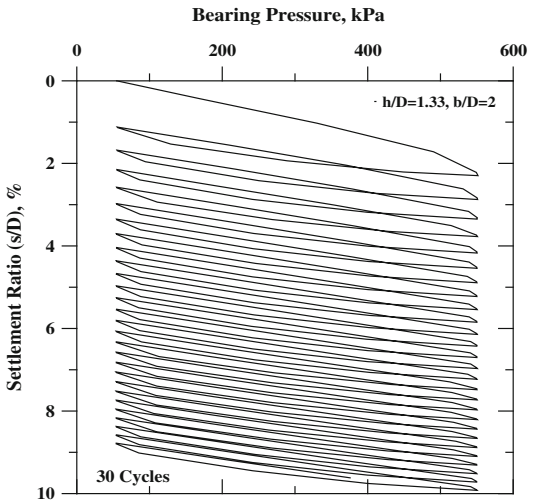

Fig. 4 Typical bearing pressure–settlement ratio pattern from repeated loading

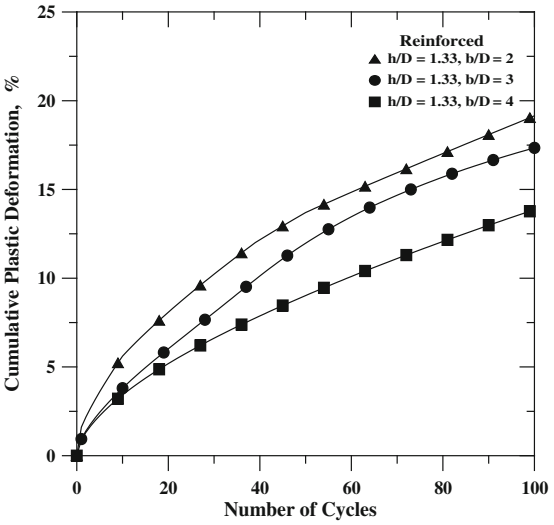

Fig. 5 Variation of settlement ratio with number of loading cycles—width series

The variation of CPD's with number of cycles is seen in Fig. 5 The highest CPD of about 20% is obtained in the case of least reinforced i.e. h/D = 1.33, b/D = 2. The lowest CPD of about 13% obtained in the case of highest reinforced i.e. h/D = 1.33, b/D = 4 geocell case.

CPD's with number of load cycles has reduced in the case of b/D = 4. This is attributed to the reduction in permanent deformations due to densification of sub-grade soil and cumulative resilient behavior of geocell reinforcement with the increase in number of load cycles. Based on the above discussion from the present study, the optimum width ratio (b/D) of the geocell mattress may be considered as 4 for dense sands overlying weak sands.

Figure 6 presents the cumulative permanent deformations of geocell reinforced beds with number of cycles for increased geocell heights. The CPD's are reduced with the increase in the height of the geocell. The highest and lowest CPD of about 20 and 13% is obtained in the case of least reinforced i.e. b/D = 4, h/D = 0.5 and in the case of highest reinforced, i.e. b/D = 4, h/D = 1.33 geocell.

The variation of TBR with settlement ratio, s/D is presented in Fig. 7. The TBR increases with increase in the s/D ratio and width ratio of geocell mattress (b/D). The TBR at s/D = 5% are observed to be 9, 10 and 15 for b/D = 2, 3 and 4 respectively. It can be inferred from Fig. 5 that to obtain higher structural support for the pavement layers, the geocell width should be adequate enough to provide the resilient response.

The higher permanent deformations, in this case, can be attributed to the least flexural stiffness of the geocell mattress available compared to the other cases. Lower permanent deformations observed in the other cases are due to the provision of enough structural support extended by the geocell mattress of heights, $h/$

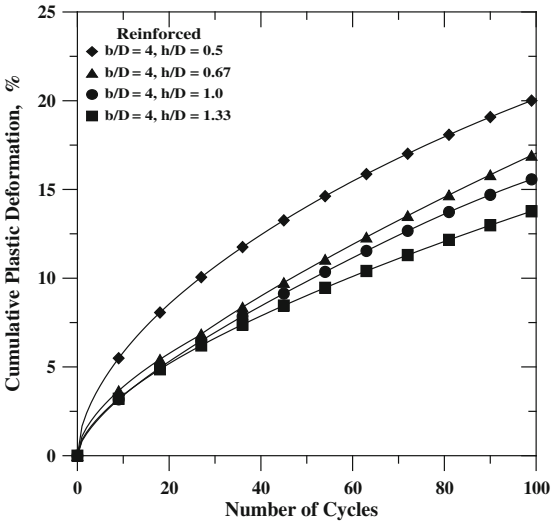

Fig. 6 Variation of settlement ratio with number of loading cycles—height series

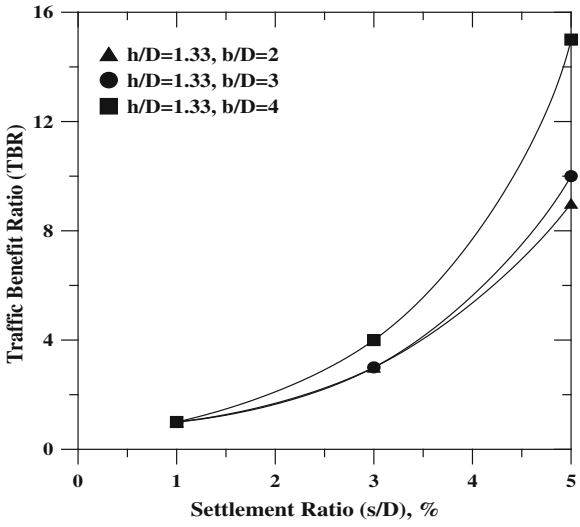

Fig. 7 Variation of TBR with settlement ratio—widths

D = 1.33 and 1.0 by virtue of encapsulating all the potential failure surfaces within the reinforced sub-grade zone.

The TBRs at 5% settlement ratio are observed to be 6, 10, 14, and 15 respectively for h/D = 0.5, 0.67, 1.0, and 1.33. It can also be inferred from Fig. 8 that for obtaining higher structural support for the pavement layers, the geocell height should be adequate enough to provide resilient behavior.

Further study is required to perform in understanding the optimum benefits from the geocell material.

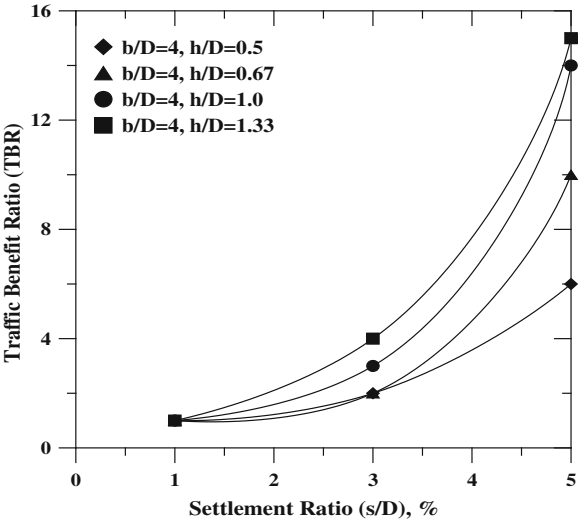

Fig. 8 Variation of TBR with settlement ratio—heights

10 Conclusions

From the tests conducted on geocell reinforced bases, following conclusions can be drawn

1. Geocells can be effectively used as a reinforcement system in pavement bases to increase the stiffness and resilient behavior of the sub-grades.
2. Geocell reinforcement cuts down the plastic settlements on the pavement surface. The plastic settlements can be referred as rutting.
3. A reduction in cumulative permanent deformations of 32% in case of $h/D = 1.33$, $b/D = 4$ against $h/D = 1.33$, $b/D = 2$ and 35% in case of $b/D = 4$, $h/D = 1.33$ against $b/D = 4$, $h/D = 0.5$.
4. Traffic benefit ratio (TBR) calculated at 5% of loading plate settlement has increased with increase in the geometry of the geocell. A TBR of as high as 15 was observed for $h/D = 1.33$ and $b/D = 4$.
5. Hence, the geocell of size $h/D = 1.33$ and $b/D = 4$ providing highest resilient behavior during the repeated traffic loading is considered as optimum size of geocell mattress for sand sub-grades in this study.

References

Mhaiskar, S. Y., & Mandal, J. N. (1994). Three dimensional geocell structure: Performance under repetitive loads. In *Proceedings of the 5th International Conference on Geotextiles, Geomembranes, and Related Products*, Singapore (pp. 155–158).

Moghaddas Tafreshi, S. N., Dawson, A. R. (2012, June). A comparison of static and cyclic loading responses of foundations on geocell-reinforced sand. *Geotextiles and Geomembranes, 32*, 55–68.

Pokharel S. K., Jie Han, Chandra Manandhar, Xiaoming Yang, Dov Leshchinsky, Izhar Halahmi, Robert L. Parsons (2011). Accelerated pavement testing of geocell-reinforced unpaved roads over weak subgrade. *Transportation Research Record, 2204,* 67–75.

Saride, S., Rayabharapu, V. K.,Vedpathak, S (2015). Evaluation of rutting behavior of geocell reinforced sand subgrades under cyclic loading. *Indian Geotechnical Journal, 45*(4), 378–388.

Yang, X., Han, J., Parsons, R. L., & Leshchinsky, D. (2010). Three-dimensional numerical modeling of single geocell-reinforced sand. *Frontiers of Architecture and Civil Engineering in China, 4*(2), 233–240.

Zhang, L., Zhao, M., Shi, C., & Zhao, H. (2010). Bearing capacity of geocell reinforcement in embankment engineering. *Geotextiles and Geomembranes, 28*(5), 475–482.

Load–Settlement Behavior of Granular Pile on Cochin Marine Clay Using Recycled Aggregate

T. G. Shilpa and T. G. Santhoshkumar

Abstract Cochin marine clay is usually associated with substantial difficulties, since these soils are sensitive to deformation and possess very small shear strength, which may lead to structural damages during the execution and throughout the lifetime of any structure. The foundations require strengthening of soil to carry the loads imposed over soft strata. Out of several techniques available for improving the load carrying capacity of soft clay strata, stone columns are ideally suited for structures with widespread loads with higher permissible settlements. Cementing agents are used in the pores of granular piles to improve the load-carrying capacity of soft soils. This paper presents the results of studies made on the influence of cementing agents such as cement, lime, flyash, and their combinations on load carrying capacity of soft soils.

Keywords Stone column · Recycled aggregate · Cementing agents

1 Introduction

The constructional activities in Cochin areas often demand deep foundations because of the poor engineering properties of Cochin marine clay. Construction in marine clays thus presents a geotechnical engineering challenge. Due to the changes in climatic conditions on the construction site, the pavement constructed on the marine clay will have less durability and require lot of maintenance cost. Some simple precautions, however, can be taken to reduce the hazard significantly. For the construction of high-rise buildings and other structures, pile foundation is most suitable ground improving technique. But for low-rise buildings and flexible structures like railroad embankments, oil storage tanks, factories, etc., stone column

T. G. Shilpa (✉) · T. G. Santhoshkumar
Department of Civil Engineering, Jai Bharath College of Management & Engineering Technology, Perumbavoor, Ernakulam 683556, India
e-mail: shilparaj74@gmail.com

T. G. Santhoshkumar
e-mail: santhoshkumartg65@gmail.com

T. Thyagaraj (ed.), *Ground Improvement Techniques and Geosynthetics*, Lecture Notes in Civil Engineering 14, https://doi.org/10.1007/978-981-13-0559-7_33

is one of the most suited techniques. The beneficial effects of stone column installation in weak deposits are manifested in the form of increased load carrying capacity, significant reduction in total and differential settlements, accelerating process of consolidation, reduction on liquefaction risks, improving the slope stability of embankments and natural slopes.

Kundan and Jain (2015) conducted a study on the swelling behavior of expansive soil using granular pile technique. The results shows that, the application of granular pile technique improves the performance of foundation on expansive soil. The swelling and shrinkage aspect is equally important and swelling aspect of expansive soil reinforced with granular piles reduces swelling and swelling pressure. Addition of cementing agents in granular piles shows significant improvement in load carrying capacity of soft soils. The addition of 4% cement/lime increases the value by 15 times that of normal granular pile (Harikrishnan and Airaj 2014). Pranav et al. (2012) studied the influence on cementing agents, and lime on load carrying capacity shows that 4% lime was found optimum for stabilization for soft soil. Narasimha and Gerald (2010) suggested for preventing formation of ettringite, an expansive mineral calcium sulfate is required in stabilizing soft marine clays.

2 Materials Used

Cochin marine clay was collected from a site at Vytila, Ernakulum which is in the greater Cochin area on the western coast of India. The properties of marine clay are given in Table 1.

Natural aggregates used in the study were collected from a quarry in Perumbhavoor of size between 6 and 12 mm whereas the recycled aggregate was collected locally in the form of structural demolished waste sieved into the same fraction. The properties of aggregates are shown in Table 2. Various cementing agents such as cement, lime, and flyash were used in the present study. Cement

Table 1 Properties of Cochin marine clay

Properties	Observed value
Initial water content (%)	62
Specific gravity	2.65
Free swell index	5.25
Liquid limit (%)	84
Plastic limit (%)	42.85
Plasticity index (%)	41.15
Shrinkage limit (%)	12.45
Optimum moisture content (%)	28
Maximum dry density (g/cc)	1.55
IS soil classification	CH
Grain sieve analysis (%)	Clay—68 Silt—22

Table 2 Properties of natural and recycled aggregates

Properties	Natural aggregate	Recycled aggregate
Specific gravity	2.7	2.63
Bulk unit Wt (kN/m^3), dense state	1.53	1.47
Bulk unit Wt (kN/m^3), loose state	1.46	1.4
Aggregate crushing value (%)	23.88	33.8
Impact value test (%)	20.55	28.5
Fineness modulus (%)	4.64	4.7
Los Angles abrasion value (%)	25.96	32.8

Table 3 Properties of cement

Properties	Observed value
Standard consistency	32%
Initial setting time	41 min
Final setting time	600 min
Compressive strength (28 days)	53 N/mm^2
Fineness modulus	2%

Table 4 Properties of flyash

Properties	Observed value
Specific gravity	2.03
Liquid limit	66
Plastic limit	Nonplastic

used is 53 grade Ordinary Portland cement, and the properties of cement are shown in Table 3. Lime used in the study was from specially selected uniform shells. The shells were burnt to remove CO_2 completely when they change to brittle white shells of calcium oxide which were preserved in airtight, multilayer polythene bags. The required amount of water alone was sprinkled over the lone shells taken from these bags on each day from the lime-treated samples, till all the shells crumble to fine powder, which was then sieved through IS 425 μm sieve. Flyash used in the study was purchased from Hindustan Newsprint Limit, Kottayam, and the properties of Flyash are shown in Table 4.

3 Experimental Procedure

In the present study, laboratory tests were conducted to determine the load carrying capacity of granular piles installed in soft soils using recycled aggregate in place of natural aggregate. To study the influence of cementing agents on load carrying capacity of granular piles, cementing agents such as cement, lime, and fly ash were added to the granular pile material.

The load tests were conducted in C.B.R mould. The mould was a rigid metal cylinder with inside diameter 15 cm and a height of 23 cm. According to IS: 2720 (Part 16)-1987, a representative sample of the soil weighing approximately 5 kg shall be taken. The mould is cleaned and oil is applied. Then fill one-fifth of the mould with soil. That layer is compacted by giving 56 evenly distributed blows using a hammer of 4.89 kg weight. After the fifth layer is compacted, excess soil is stroke off and leveled with trowel. The granular piles were installed by displacement method. An open pipe of 5 cm diameter, smeared with petroleum jelly, with a closed bottom was inserted into the soft clay up to a depth equal to length of granular pile. Stone aggregates with cementing agents were charged into the pipe and compacted with a hammer to maintain uniform density of granular pile. Aggregate with cementing agents was prepared by adding 4% of cementing agents (by weight of aggregate) to the aggregate and a uniform mixture was obtained by thoroughly mixed with a trowel. Then the pipe was slowly raised. This was continued till the granular pile is formed. The specimen was kept in room temperature for 24 h and thereafter cured in curing tanks for 7 and 28 days before testing. Figure 1 shows the test setup for loading.

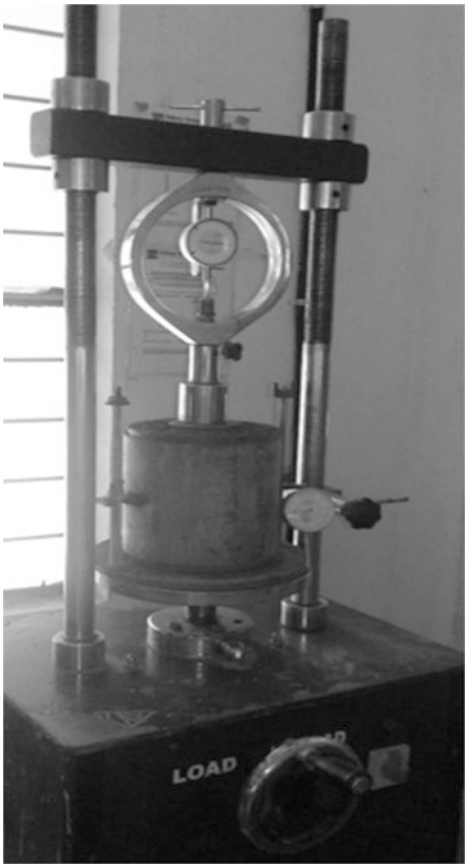

Fig. 1 Test setup for loading

Load shall be applied through the plunger into the soil at the rate of 1.25 mm per minute. Reading of the load taken at penetrations of 0.5, 1.0, 1.5, 2.0, 2.5, 4.0, 5.0 mm are noted. In the present study, tests were also conducted to determine the influence of combination of cementing agents (2% cement, 1% lime, 1% flyash) on the granular pile in order to assess the improvement in the load carrying capacity of soil.

4 Results and Discussions

Load tests were conducted on samples to determine the load–settlement characteristics of soils. Figure 2 shows the variation of the load–settlement curve of marine clay using granular piles of natural and recycled aggregates. It can be seen from the figure that the load-carrying capacity increases by the installation of granular pile in marine clay. Granular pile using natural aggregate shows more improvement in load carrying capacity than recycled aggregate.

To study on the effect of cementing agents on load carrying capacity of granular piles, cement, lime, and flyash were used as cementing agents. Figure 3 shows the load–settlement curve of marine clay using granular piles after 7 days curing in natural aggregate. The test results show that addition of cementing agents increased the load carrying capacity as compared to granular pile along with the aggregates. It can be seen in the figure that load-carrying capacity of soil is improved by the addition of cementing agents. Combination cementing agents improve the load carrying capacity than individual cementing agents.

Figure 4 shows load–settlement curve of marine clay using granular piles in recycled aggregate. In this case, it can be seen that addition of combination of cementing agents increased the load carrying capacity as compared to granular pile with cementing agents alone. Figure 5 shows the load–settlement curve of marine clay using granular piles in natural aggregate after curing period of 28 days. The

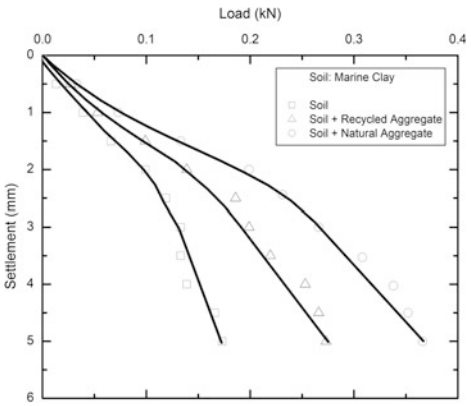

Fig. 2 Load–settlement curve of marine clay using granular pile

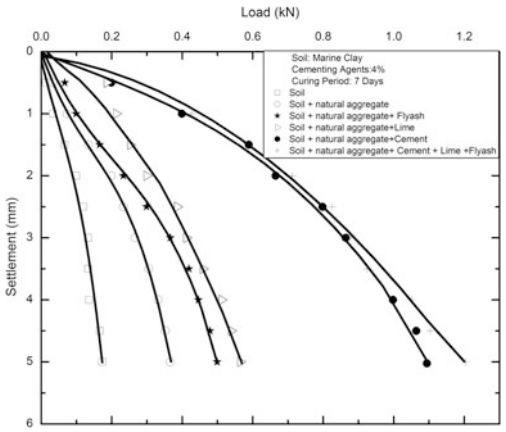

Fig. 3 Load–settlement curve of marine clay using granular pile (natural aggregate) with cementing agents cured for 7 days

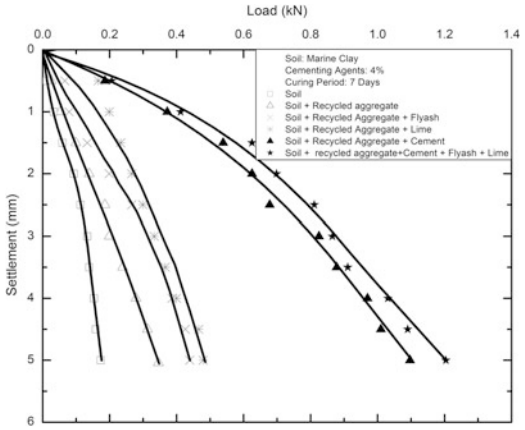

Fig. 4 Load–settlement curve of marine clay using granular pile (Recycled aggregate) with cementing agents cured for 7 days

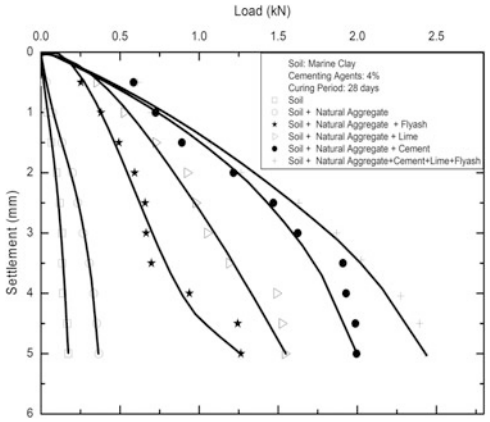

Fig. 5 Load–settlement curve of marine clay using granular pile (natural aggregate) with cementing agents cured for 28 days

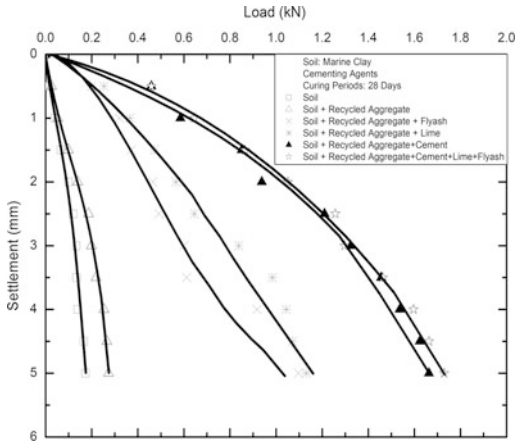

Fig. 6 Load–settlement curve of marine clay using granular pile (recycled aggregate) with cementing agents cured for 28 days

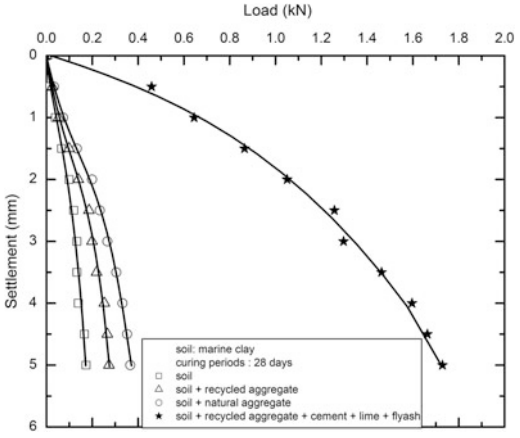

Fig. 7 Load–settlement curve of marine clay using granular pile with combination of cementing agents

test results show that the addition of cementing agents increased the load carrying capacity as compared to granular pile.

Figure 6 shows the load–settlement curve of marine clay using granular piles of recycled aggregate after curing period of 28 days. In this case, also the test results show that the addition of combination of cementing agents in granular pile increases the load carrying capacity of soil compared to granular pile with cementing agents alone.

Figure 7 shows the variation of load–settlement of granular pile with combination of 4% combination of cementing agents in natural and recycled aggregates for a period of 28 days curing in natural and recycled aggregate. From the figure, it is clear that the load carrying capacity of granular pile had been increased after the addition of combination of cementing agents compared to the granular pile alone. It can be seen that the granular pile with combination of 4% cementing agents in

recycled aggregate after 28 days of curing gives much significant increase in the load carrying capacity of soil.

5 Conclusions

Based on the test results, the following conclusions are drawn:

The load carrying capacity of Cochin marine clay is considerably increased by the usage of granular pile using natural and recycled aggregates. Settlement is remarkably reduced by the installation of granular pile using both natural and recycled aggregates. It can be seen that the load carrying capacity of the granular pile with natural aggregate is much higher than recycled aggregate. Addition of cementing agents increases the load carrying capacity considerably in case of both natural and recycled aggregate. Additional combination of 4% cementing agents considerably increases the load carrying capacity as compared with individual cementing agents. Curing period also enhances load carrying capacity considerably in natural and recycled aggregate.

References

Harikrishnan, P., & Airaj, A. K. (2014). A study on load carrying capacity of soft clays provided with granular piles of different materials. In *Indian Geotechnical Conference IGC-2014*.

IS 2720 (Part 16). (1987). *Methods of test for soils: Laboratory determination of CBR.* New Delhi, India: Bureau of Indian Standards.

Kundan, M., & Jain, P. K. (2015). Strength and settlement studies of black cotton soil reinforced with granular pile. *International Journal of Engineering Sciences & Research Technology*. ISSN: 2277-9655.

Narasimha, S. R., & Gerald, M. G. (2010). Degradation in cemented marine clay subjected to cyclic compressive loading. *Marine Georesources and Geotechnology, 21*, 37–62 (2003).

Pranav, P. R. T., Koteswara, R., & Venkatesh, G. (2012). A laboratory study on the lime and sawdust treated marine clay sub grade flexible pavement under cyclic pressure. *International Journal of Engineering and Innovative Technology (IJEIT), 2*(4).

Transmissivity of Coir Latex Composite

C. G. Anand, P. K. Jayasree and K. Balan

Abstract This paper deals with transmissivity test conducted in laboratory on newly developed coir latex composite to be used as separator in flexible pavement. The coir latex composite is developed by treating coir fibre of varying fibre length, woven coir geotextile and nonwoven coir geotextile with optimum latex content (50%). Transmissivity of the composite is measured under varying hydraulic gradient and normal pressure using a specifically designed apparatus to simulate field condition. Transmissivity of the coir latex composite seems to decrease with increase in hydraulic gradient as well as with increase in normal pressure. The results are compared under test conditions without using the composite as well as with coir geotextiles without latex treatment.

Keywords Transmissivity · Composite · Latex · Hydraulic gradient

1 Introduction

Proper drainage system plays a significant role in the life of a roadway. Inadequate subsurface drainage causes the failure of pavements much earlier than its expected life. For the proper subsurface drainage of water and reinforcement in pavements geosynthetics and composite geosynthetic separator layers are widely used. Even though geosynthetics have excellent drainage properties and increase the stability of pavements as a reinforcement they have a negative impact on the environment as they are non biodegradable in nature. Geotextiles made from natural coir fibres are

C. G. Anand · P. K. Jayasree (✉) · K. Balan
Department of Civil Engineering, College of Engineering
Trivandrum, Trivandrum 695016, India
e-mail: jayasreepk@cet.ac.in

C. G. Anand
e-mail: anand.cg20@gmail.com

K. Balan
e-mail: drkbalan@gmail.com

T. Thyagaraj (ed.), *Ground Improvement Techniques and Geosynthetics*, Lecture Notes in Civil Engineering 14, https://doi.org/10.1007/978-981-13-0559-7_34

eco-friendly and have superior mechanical and drainage properties. Coir fibre-polymer composites are hybrid materials which combine the properties of natural fibres and polymer which can be used as replacement for geosynthetic composite. Drainage properties of different coir latex composites are determined by conducting a series of transmissivity tests by using the composite as separator layer between a clay sub-grade and aggregate base. Transmissivity of the composites are determined under varying hydraulic gradient as well as normal pressure.

Tan et al. (2001) analysed the drainage behaviour of geosynthetics products embedded in poorly draining residual soil which showed that the rate of pore pressure dissipation was faster with the placement of permeable geosynthetics materials. Palmeira and Gardoni (2002), observed that confinement of the geotextile can significantly increase its retention capacity depending on the stress level and type of geotextile. Han et al. (2003) analysed that transmissivity of smart geotextiles and geonets decrease with increase in compressive stress. The transmissivity seems to vary with intrusion under compressive stress. Pak and Zahmatkesh (2010) observed that transmissivity decreases exponentially with increase in normal pressure which is significant for normal stresses up to 100 kPa. Sumesh (2015), investigated the influence of coir fibre length and latex content on the strength of coir fibre-latex composite. Optimum latex content was found to be 50%.

2 Materials and Tests

2.1 Materials Used

Coir is a natural fibre extracted from the husk of coconut and is found between the hard, internal shell and the outer coat of coconut. Coir is an easily available material and is found to be stronger and durable in nature. The coir fibre used for the development of composite is collected from a small scale industry in Chirayankeezhu, Trivandrum. The coir fibres are dried properly before latex treatment. Chemically treated rubber latex used was collected from Kairali coir mattress, Chirayankeezhu, Trivandrum. Woven and nonwoven geotextile used for the test are obtained from Coir craft, Statue, Trivandrum.

Commercially available kaolinite clay is used as subgrade material. Kaolinite clay is obtained from Coromandel clay, Kochuveli, Trivandrum. The properties of kaolinite clay collected are shown in Table 1. Locally available aggregate of size scaling down from 22.5 mm were used for base course.

Table 1 Properties of clay

Properties of clay	Value
Liquid limit (%)	55
Plastic limit (%)	30
Plasticity index (%)	25
Specific gravity	2.25
Maximum dry density (g/cm^3)	1.5
Optimum moisture content (%)	25
% of silt	11
% of clay	71

2.2 Development of Composites

The composites were developed at Kairali coir mattress, Chirayankeezhu, Triavandrum. For the development coir latex composite coir fibres which were manually cut to specified length, i.e., 5, 10, and 15 cm were uniformly spread on platform. Chemically treated rubber latex was manually sprayed uniformly on to the surface of the prepared coir fibre bed. 50% latex content is considered as optimum for the composite. The latex sprayed coir fibre bed is weighed in order to make sure optimum latex content is reached. The coir fibre bed is then heated at 1200 °C for 15 min. Same procedure is followed for the latex treatment of woven coir and nonwoven coir geotextile. Table 2 shows the representation and properties of the composites. Figure 1 shows different composites and geotextiles used as separator.

2.3 Test Procedure

The test section to determine transmissivity consists of three layer. The bottom subgrade layer consists of kaolinite clay filled in liquid limit in order to represent worst case scenario for subgrade. The composite layer is placed above the subgrade.

Table 2 Properties of separators

Composite	Representation	Latex content (%)
Woven coir	WC	–
Woven coir + latex	WCL	50
5 cm coir fibre + latex	CL5	50
10 cm coir fibre + latex	CL10	50
15 cm coir fibre + latex	CL15	50
Nonwoven coir	NWC	–
Nonwoven coir + latex	NWCL	50

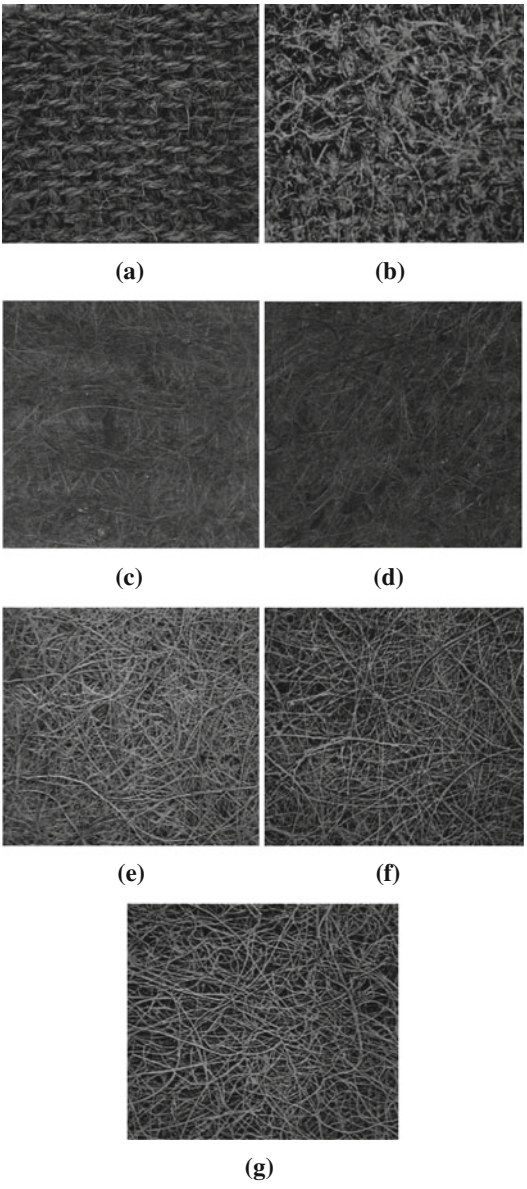

Fig. 1 Separators used: **a** WC, **b** WCL, **c** NWC, **d** NWCL, **e** CL 5, **f** CL 10 and **g** CL 15

The base layer at top consist of aggregates of size scaling down from 22.5 mm. A porous stone is placed at the top of the base layer followed by perforated base plate and loading plate.

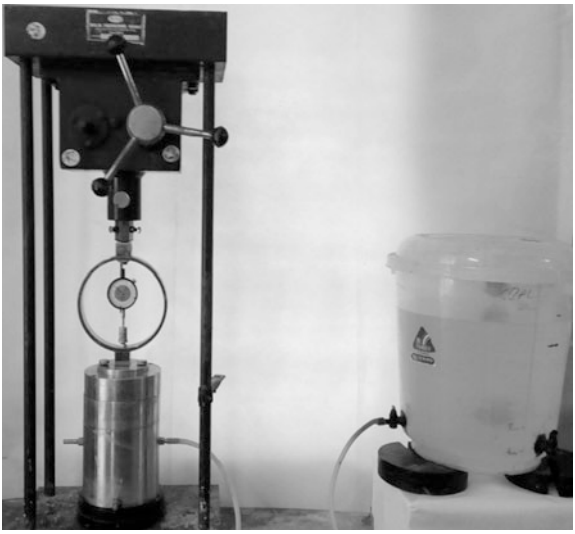

Fig. 2 Transmissivity test apparatus

Transmissivity of the composites are determined using a constant head transmissivity test. Figure 2 shows the test set up for the constant head test. The test section is placed at unit hydraulic gradient for 24 h by keeping the bottom outlet open. Transmissivity of different composites and geotextiles are determined by varying the hydraulic gradient and normal pressure. Transmissivity is determined using Eq. (1) according to ASTM D 4716.

$$\theta = \frac{q}{iw}, \tag{1}$$

where θ is transmissivity in cm^2/s, q is discharge per unit time in cm^3/s, i is hydraulic gradient and w is width of specimen in cm.

3 Results and Discussion

3.1 Transmissivity Under Varying Load and Hydraulic Gradient

Transmissivity of different composites and geotextiles were determined by varying the hydraulic gradient and normal pressure. Figure 3 shows transmissivity of coir fibre-latex composites having different fibre length. Transmissivity decreases with increase in hydraulic gradient and normal pressure. Transmissivity decreases with increase in fibre length. When fibre length decreases the pore space with in the

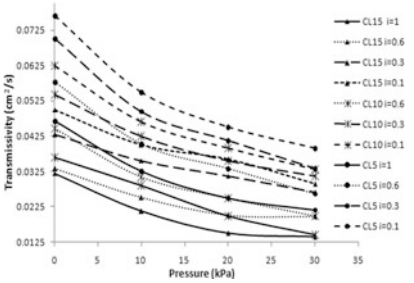

Fig. 3 Variation of transmissivity with pressure for coir latex composites under varying hydraulic gradient

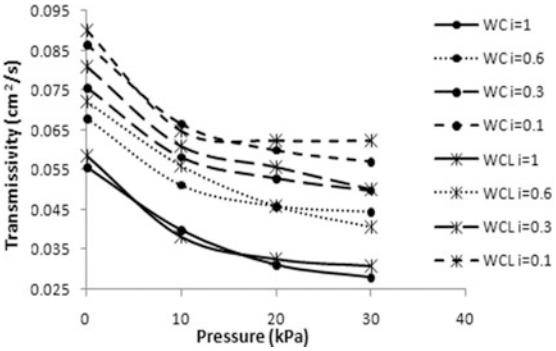

Fig. 4 Variation of transmissivity with pressure for WC and WCL under varying hydraulic gradient

composite decreases making it more tightly packed thus preventing the latex from seeping much into the composite. In this case more latex will adhere to the surface which will stop the clay from seeping into the composite and improve the transmissivity.

For minimum hydraulic gradient and maximum normal pressure CL5 have 15% more transmissivity than CL10 and 25% more transmissivity than CL15.

Figure 4 shows transmissivity of WC and WCL with variation in hydraulic gradient and normal pressure. Transmissivity curve shows similar trend as in the previous case. Woven geotextile has apparent opening size of 5 mm × 5 mm. There is no significant change in transmissivity with latex treatment because of the large opening size.

Figure 5 shows the transmissivity of NWC and NWCL. There was a significant improvement in transmissivity for nonwoven with latex treatment. With latex treatment the nonwoven geotextile becomes more sturdy and the surface pores are partially closed which inturn reduces the seepage of clay into the composite. At

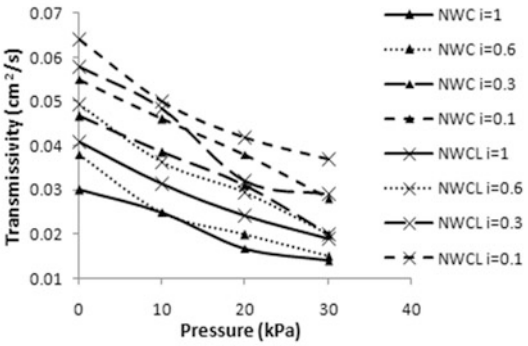

Fig. 5 Variation of transmissivity with pressure for NWC and NWCL under varying hydraulic gradient

maximum normal pressure for $i = 0.1$ NCWL exhibits 25% increase in transmissivity when compared to NCW.

3.2 Transmissivity for i = *0.1*

Figure 6 shows the variation of transmissivity of composites under varying normal pressure for $i = 0.1$. Maximum transmissibility is exhibited by WC and WCL. This may be due to the fact that the base aggregates enter the openings of the geotextile increasing the flow path. But they are not suitable in terms of drainage since they have very highly cross plane permeability. It can be concluded that placing a separator layer improves the drainage behaviour of the test section compared to the test section with out any separator.

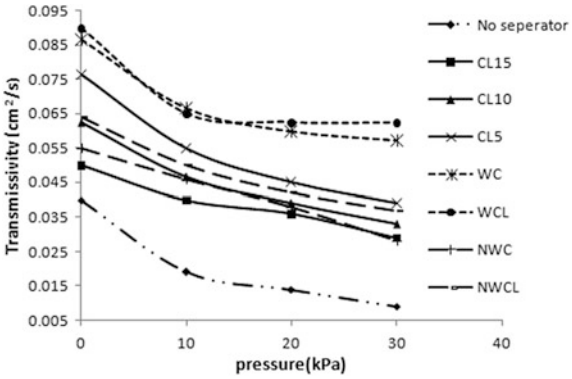

Fig. 6 Variation of transmissivity with pressure for different separators

4 Conclusions

Transmissivity of different composites used as separator between clay subgrade and base material were determined under varying hydraulic gradient and normal pressure. Following conclusions were drawn from the study:

- Transmissivity decreases with increase in normal pressure and hydraulic gradient
- Transmissivity increases with decrease in fibre length. CL5 exhibit 15 and 25% increase in transmissivity when compared to CL10 and CL15 respectively under maximum normal pressure
- Woven geotextile WC and WCL have almost similar transmissivity characteristics. Because of its large opening size latex treatment have no significant effect on WC
- Transmissivity of nonwoven geotextile NWC shows significant improvement in its drainage properties with latex treatment. NWCL exhibits 25% increase in transmissivity when compared to NWC under maximum normal pressure and minimum hydraulic gradient
- Placing a separator layer definitely improves the drainage in test section

References

Han, Y. J., Seong, H. K., Youn, I. C., Yeong, M. P., & Chin, G. C. (2003). Analysis of the drainage performance of geotextile composites under confined loads. *Polymer Testing, 23,* 239–244.

Pak, A., & Zahmatkesh, Z. (2010). Experimental study of geotextile's drainage and filtration properties under different hydraulic gradients and confining pressures. *International Journal of Civil Engineering, 9*(2), 97–102.

Palmeira, E. M., & Gardoni, M. G. (2002). Drainage and filtration properties of non-woven geotextiles under confinement using different experimental techniques. *Geotextiles and Geomembranes, 20,* 97–115.

Sumesh, C. (2015). *Development of a coir-fibre latex composite for use as a separator in flexible pavements*. M.Tech. thesis report (unpublished), College of Engineering Trivandrum, University of Kerala, Kerala, India.

Tan, S. A., Chew, S. H., Ng, C. C., Loh, S. L., Karunaratne, G. P., Delmas, Ph, et al. (2001). Large-scale drainage behaviour of composite geotextile and geogrid in residual soil. *Geotextiles and Geomembranes, 19,* 163–176.

Influence of Combined Vertical and Horizontal Reinforcement on Granular Piles in Soft Clays

M. Hasan and N. K. Samadhiya

Abstract Geosynthetic reinforced granular piles are commonly used in engineering practice to enhance the bearing capacity, reduce settlements and to increase the rate of consolidation of very soft clays. In the present paper, laboratory model tests have been carried out on vertical–horizontal combined reinforced floating granular piles installed in soft clay. A 75 mm diameter and 375 mm length single granular pile was formed by simulating unit cell concept. Geotextile and geogrid were used over the full length of granular piles as vertical encasement and horizontal strips respectively. Geogrid strips of 65 mm diameters were placed at three different centre to centre spacing of 25, 50, and 70 mm. Vertical load–settlement relationship of untreated clay bed, unreinforced and reinforced granular pile treated ground were obtained under short-term loading. The influence of reinforcement was examined in term of ultimate load intensity of granular piles compared to untreated ground. Model tests indicated significant improvement in the load carrying capacity of granular piles due to the incorporation of geosynthetic.

Keywords Stone columns · Geotextile · Geogrid · Ground improvement

1 Introduction

In very soft soils, granular piles (also known as stone columns) do not achieve significant load carrying capacity due to poor lateral confinement from surrounding soil. Geosynthetic reinforced granular piles are widely adopted throughout the world to provide additional confinement from geosynthetic in the form of either as vertical encasing or in horizontal layers. Vertical encased granular piles (VEGP)

M. Hasan (✉) · N. K. Samadhiya
Department of Civil Engineering, Indian Institute of Technology Roorkee, Roorkee 247667, India
e-mail: murtazadce@gmail.com

N. K. Samadhiya
e-mail: nksamfce@iitr.ac.in

T. Thyagaraj (ed.), *Ground Improvement Techniques and Geosynthetics*, Lecture Notes in Civil Engineering 14, https://doi.org/10.1007/978-981-13-0559-7_35

improve load carrying capacity and reduce bulging by mobilisation of hoop stress in reinforced material. Various researchers have conducted analytical, laboratory and in situ tests, and numerical analysis on VEGP in very soft soils (Murugesan and Rajagopal 2006, 2007, 2010; Gniel and Bouazza 2009; Pulko et al. 2011; Yoo and Lee 2012; Dash and Bora 2013; Ghazavi and Afshar 2013; Almeida et al. 2014; Zhang and Zhao 2015; Hasan and Samadhiya 2016). Murugesan and Rajagopal (2007) performed laboratory model tests on single encased granular piles by simulating unit cell concept. They indicated a clear improvement in the load capacity of the granular piles due to encasement, whereas effect of encasement decreases with increase in the diameter of the granular piles. Ghazavi and Afshar (2013) conducted large body laboratory tests on vertical geotextile encased granular piles. They found that the bearing capacity of granular piles increases by using vertical reinforcing material and further increases with the increase in the length and strength of reinforcement. The granular piles reinforced with horizontal strips placed at regular interval improve load carrying capacity and control bulging by mobilising frictional resistance between strips and stone aggregates. Large and small scale laboratory tests and numerical analysis have carried out by many researchers in the past (Madhav 1982; Sharma et al. 2004; Ayadat et al. 2008; Ali et al. 2012; Hong and Wu 2013). Sharma et al. (2004) performed a series of experimental results to investigate the effect of horizontal geogrid layers on bulging and load carrying capacity of granular piles in a soft clay bed. They revealed an increase in the load carrying capacity of reinforced granular piles with an increase in the number of strips and a decrease in the spacing between them. Ali et al. (2012) carried out laboratory model tests on short, floating, and fully penetrating single granular pile with and without reinforcement to evaluate the relative improvement in the failure stress of the composite ground due to different types of reinforcement. They conducted tests on both types of reinforced granular pile (encased as well as horizontal stripped) and the optimum configuration for each type was evaluated.

Past studies deal with only one type of reinforcement as in the form encasement or horizontal strips. Literature is not available on combined vertical encased-horizontal stripped granular piles for relative assessment of the load carrying capacity of treated ground. Limited experimental work has been reported on granular piles not resting on firm stratum but have their tips embedded in clayey soil layer. In the present study, combined reinforced granular piles (CRGP) have been installed in very soft clay to investigate the improvement in the ultimate load intensity of floating granular piles as compared to untreated ground.

2 Experimental Programme

In the present study, unit cell idealisation has been adopted to simplify the design of the apparatus needed to assess the behaviour of an interior granular pile in a large group of piles. This concept was described in detail by Barksdale and Bachus (1983). Ambily and Gandhi (2007) concluded that single granular pile with unit cell

concept simulates the field behaviour for an interior pile when a large number of piles are simultaneously loaded. In the present investigation, seven model tests have been performed in the laboratory. The laboratory model tests were carried out on clay bed, unreinforced granular piles (URGP), VEGP, Granular pile with horizontal strips (GPHS), and CRGP in soft clay. A 75 mm diameter and 375 mm (5d) length single floating granular pile was installed in the centre of 200 mm diameter and 525 mm height cylindrical tank. Clay bed of 525 mm height and having undrained shear strength close to 5 kPa was prepared for all experiments. The desired undrained shear strength of clay was determined by hit and trial method from laboratory unconfined compression tests. Water content for the required undrained shear strength of 5 kPa was found to be 34% and corresponding dry unit weight was 13.85 kN/m^3. A granular pile was constructed on 70% relative density by using replacement method in all tests. Ghazavi and Afshar (2013) revealed that bearing capacity of vertical encased granular piles increases with the increase in the length of reinforcement. Therefore in the present study, reinforcement has been provided throughout the length of granular piles. Geotextile and geogrid were used for vertical encasement and horizontal strips respectively. Circular geogrid strips of 65 mm diameters were used over the entire length of granular piles. These strips were placed at three different centre to centre spacing (S) of 25, 50 and 70 mm. First geogrid strip in each case was placed 25 mm below the loading plate. Fresh clay and aggregates were used for each laboratory test for better results.

2.1 Materials Properties

In the present study, clay, crushed stone aggregates and geogrid were used and collected from locally available sites and tested in the Geotechnical Engg. Lab, IIT Roorkee. The physical properties of clay are specific gravity = 2.73, optimum moisture content = 17.56%, maximum dry unit weight = 17.22 kN/m^3, liquid limit = 48%, Plastic limit = 18% and Plasticity index = 30%. The dry unit weight and undrained shear strength corresponding to 34% water content were 13.85 kN/m^3 and close to 5 kPa respectively. It has been classified as CI as per IS: 1498 (2000). The crushed stone aggregates were made of granite and were in the range of 2–6.3 mm in size. The maximum and minimum dry unit weights of the aggregate are 15.04 and 13.41 kN/m^3 respectively. The dry unit weight and angle of internal friction of stone aggregates at 70% relative density were 14.51 kN/m^3 and 43° respectively. The Particle size distribution curves for clay and stone aggregates are shown in Fig. 1.

Nonwoven geotextile and biaxial geogrid of thickness 2 and 1.5 mm respectively were used in this study. The ultimate tensile strength of geosynthetic materials was determined from standard wide-width tension tests (ASTM D4595, 1986). The ultimate tensile strength of geotextile and geogrid were found to be 4.41 kN/m (@ 54.62% strain) and 7.96 kN/m (@ 20.21% strain) respectively. The tensile stress–strain behaviour for geotextile and geogrid are shown in Fig. 2.

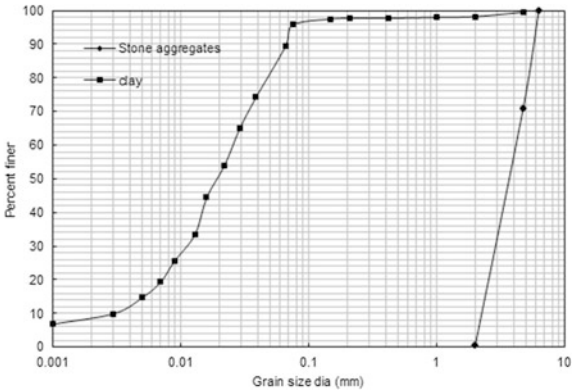

Fig. 1 Particle size distribution curves for clay and stone aggregates

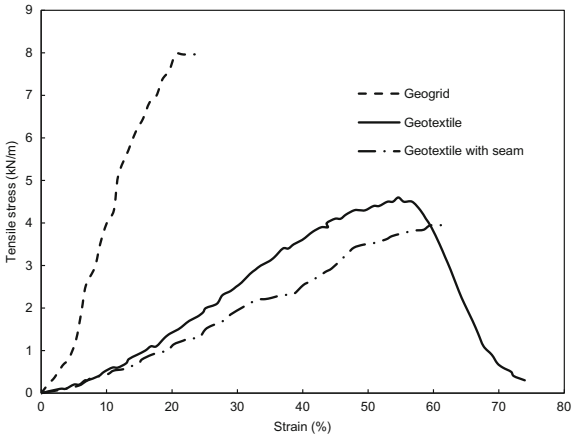

Fig. 2 Tensile stress–strain plots of geosynthetic

2.2 Test Set Up and Procedure

A typical schematic view of test setup for laboratory model tests is presented in Fig. 3. Vertical load was applied and measured by proving ring only over the cross sectional area of granular pile. The load was applied at a constant displacement rate of 1.2 mm/min. Settlement of loading plate was measured by dial gauge. Load was applied (up to 35 mm settlement) through a loading plate of 15 mm thickness and diameter equal to granular pile. Loading period is kept short to ensure undrained loading condition which simulates loading during construction. Vertical load–settlement relationship was studied for relatively assessment of performance of the granular piles.

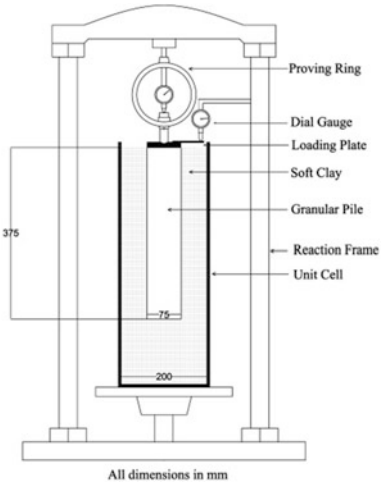

Fig. 3 Schematic view of test setup

3 Results and Discussion

Experimental investigations have been carried out to estimate the ultimate load intensity of floating granular piles. The results in terms of vertical load–settlement behaviour of clay bed, URGP, VEGP, and GPHS (50 mm c/c spacing) are presented in Fig. 4. The results have been summarised in Table 1. Perusal of Fig. 4 shows that the ultimate load intensity of treated ground improved due to installation of granular piles. It further improved due to inclusion of geotextile and geogrid strips in the granular piles. The ultimate load intensity for URGP, VEGP, and GPHS were found to increase by 195, 440, and 396% respectively as compared to clay bed. However the increase in ultimate load intensity for VEGP and GPHS were 83 and 68% respectively with respect to URGP.

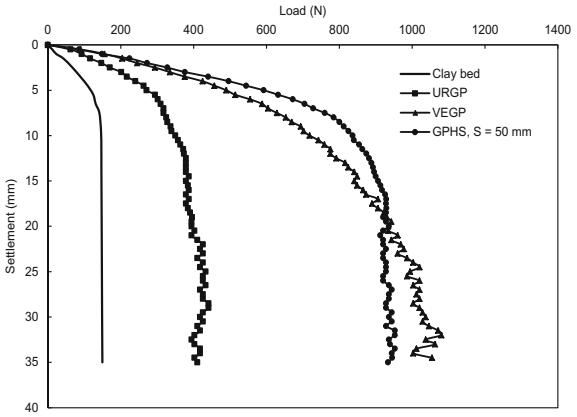

Fig. 4 Vertical load–settlement behaviour of granular piles

Table 1 Results of laboratory model tests

Test description	Strip spacing (mm)	Undrained shear strength (kPa)	Ultimate load intensity (kPa)
Clay bed	–	5.12	33.85
URGP	–	5.01	99.88
VEGP	–	5.21	182.87
GPHS	50	5.17	167.90
CRGP	25	5.32	198.27
	50	5.28	180.25
	75	5.15	178.76

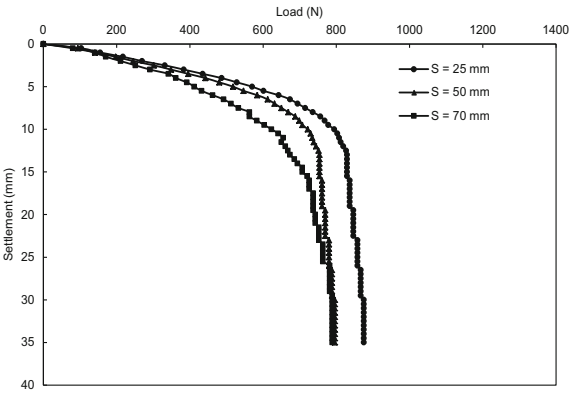

Fig. 5 Vertical load–settlement behaviour of CRGP

The combined effect of vertical encasing as well as horizontal strips on reinforced floating granular pile was also studied in present investigation. Figure 5 shows vertical load–settlement behaviour for CRGP from laboratory investigation. The ultimate load intensity of CRGP treated ground was found to improve with respect to that of GPHS treated ground. It was observed that the ultimate load intensity of 25, 50, and 70 mm centre to centre spaced CRGP increased by 485, 432, and 428% as compared to clay bed. However the horizontal spacing of geogrid strips has negligible effect on ultimate load intensity in case of CRGP. The ultimate load intensity of 50 mm spaced horizontal striped CRGP was found to increase by 8% as compared to GPHS @ 50 mm c/c. It may be noted that the floating granular piles with combined reinforcement start penetrating into soft clay rather than bulging.

4 Conclusions

Laboratory model tests were carried out on 75 mm diameter floating granular piles in the present investigation. The vertical load–settlement plots of granular piles from tests were compared with that obtained from untreated ground. The following conclusions can be drawn:

(1) The ultimate load intensity of treated ground improves due to installation of granular piles. It further improves due to inclusion of geosynthetic in form of vertical encasement and horizontal strips in the granular piles.
(2) The ultimate load intensity for URGP, VEGP, and GPHS increase by 195, 440, and 396% respectively as compared to untreated ground.
(3) The spacing of geogrid strips has negligible effect on the ultimate load intensity of the combined reinforced floating granular piles.
(4) The ultimate load intensity of 25, 50, and 70 mm @ c/c CRGP increase by 485, 432, and 428% as compared to untreated ground.

References

Ali, K., Shahu, J. T., & Sharma, K. G. (2012). Model tests on geosynthetic-reinforced stone columns: A comparative study. *Geosynthetics International, 19*(4), 292–305.

Almeida, M., Hosseinpour, I., Ricci, M., & Alexiew, D. (2014). Behavior of geotextile-encased granular columns supporting test embankment on soft deposit. *Journal of Geotechnical and Geoenvironmental Engineering ASCE*, 1943-5606.0001256, 04014116.

Ambily, A. P., & Gandhi, S. R. (2007). Behavior of stone columns based on experimental and FEM analysis. *Journal of Geotechnical and Geoenvironmental Engineering, ASCE, 133*(4), 405–415.

ASTM D4595. (1986). *Standard test method for tensile properties of geotextiles by the wide-width strip method*. West Conshohocken: ASTM International.

Ayadat, T., Hanna, A. M., & Hamitouche, A. (2008). Soil improvement by internally reinforced stone column. *Ground Improvement, 161*(2), 55–63.

Barksdale, R. D., & Bachus, R. C. (1983). *Design and construction of stone columns* (Vol. 1). Report no. FHWA/RD-83/026, National technical information service, Springfield, Virginia.

Dash, S. K., & Bora, M. C. (2013). Influence of geosynthetic encasement on the performance of stone columns floating in soft clay. *Canadian Geotechnical Journal, 50*(7), 754–765.

Ghazavi, M., & Afshar, J. N. (2013). Bearing capacity of geosynthetic encased stone columns. *Geotextiles and Geomembranes, 38,* 26–36.

Gniel, J., & Bouazza, A. (2009). Improvement of soft soils using geogrid encased granular columns. *Geotextiles and Geomembranes, 27*(3), 167–175.

Hasan, M., & Samadhiya, N. K. (2016). Experimental and numerical analysis of geosynthetic-reinforced floating granular piles in soft clays. *International Journal of Geosynthetics and Ground Engineering, 2,* 22. https://doi.org/10.1007/s40891-016-0062-6.

Hong, Y. S., & Wu, C. S. (2013). The performance of a sand column internally reinforced with horizontal reinforcement layers. *Geotextiles and Geomembranes, 41,* 36–49.

IS: 1498. (2000). *Classification and identification of soils for general engineering purposes*. New Delhi: Indian Standards Institution.

Madhav, M. R. (1982). Recent development in the use and analysis of granular piles. In *Proceedings of Symposium on Recent Development in Ground Improvement Techniques* (pp. 117–129), Bangkok.

Murugesan, S., & Rajagopal, K. (2006). Geosynthetic-encased stone columns: Numerical evaluation. *Geotextiles and Geomembranes, 24,* 349–358.

Murugesan, S., & Rajagopal, K. (2007). Model tests on geosynthetic encased stone columns. *Geosynthetics International Journal, 24*(6), 346–354.

Murugesan, M., & Rajagopal, K. (2010). Studies on the behaviour of single and group of geosynthetic encased stone columns. *Journal of Geotechnical and Geo environmental Engineering, ASCE, 136*(1), 129–139.

Pulko, B., Majes, B., & Logar, J. (2011). Geosynthetic-encased stone columns: Analytical calculation model. *Geotextiles and Geomembranes, 29*(1), 29–39.

Sharma, R. S., Kumar, B. R. P., & Nagendra, G. (2004). Compressive load response of granular piles reinforced with geogrids. *Canadian Geotechnical Journal, 41*(1), 187–192.

Yoo, C., & Lee, D. (2012). Performance of geogrid-encased stone columns in soft ground: Full-scale load tests. *Geosynthetics International, 19*(6), 480–490.

Zhang, L., & Zhao, M. (2015). Deformation analysis of geotextile-encased stone columns. *International Journal of Geomechanics, ASCE*, GM.1943-5622.0000389, 04014053.

Effect of GGBS and Lime on the Strength Characteristics of Black Cotton Soil

Rahul R. Pai and Satyajit Patel

Abstract In agriculture-based country like India road network plays a major role. The life and maintenance of roads mainly depend on the strength of both sub-base and subgrade of soil and traffic intensity. In India about 20% of the total area is covered by Black cotton soil. Because of the high swelling and shrinkage characteristics under varying water contents Black cotton soil poses problems in road construction and maintenance. This paper presents experimental results illustrating the behavior of Black cotton soil stabilized with Ground Granulated Blast furnace Slag (GGBS) and GGBS-lime mix. In order to estimate the strength of the stabilized soil, tests such as Unconfined Compressive Strength (UCS) and California Bearing Ratio (CBR) tests were performed. Tests were conducted on soil-GGBS mix for GGBS dosages 3, 6, 9, and 12% by weight of dry soil and soil-GGBS-Lime mix with 2 part GGBS and 1 part Lime for dosages 3, 6, 9, and 12% by weight of dry soil. Tests were conducted on both unsoaked and soaked samples, unsoaked samples were cured for 7 and 28 days whereas soaked samples were cured for 3 days and soaked for 4 days. The effect of binder content, curing period and soaking on the UCS and Elastic modulus were studied and subsequently the effect of binder content on CBR values were also studied. With the increase in binder content and curing period the strength of the treated soil was found to be enhanced. Soaking resulted in the decrement of the strength of the stabilized soil. From the experimental results it is clear that GGBS-lime mix is a superior binder content than GGBS for the improvement of black cotton soil, when used as a sub-base material in flexible pavement.

Keywords GGBS · Lime · Stabilize · Sub-base · UCS · CBR
Elastic modulus

R. R. Pai (✉)
Department of Civil Engineering, AISAT, Kalamassery, Kochi 682022, Kerala, India
e-mail: rahul.r@aisat.ac.in

S. Patel
Department of Applied Mechanics, SVNIT Surat, Surat 395007, Gujarat, India
e-mail: spatel@amd.svnit.ac.in

T. Thyagaraj (ed.), *Ground Improvement Techniques and Geosynthetics*, Lecture Notes in Civil Engineering 14, https://doi.org/10.1007/978-981-13-0559-7_36

1 Introduction

Road network plays a vital role in the overall development of a country. The life and maintenance of roads depend on the strength of both sub-base and subgrade of soil and traffic intensity. If the soil has CBR value less than 2%, it must be replaced by good quality material. Highway construction on clayey soils has been a confront to engineers and designers because of its high swelling and shrinkage behavior due to presence of inorganic clays of medium to high compressibility, which results in cracks in the pavement structure. To mitigate the failure of asphalt pavement laid on expansive subgrade, chemical stabilization techniques are often used to improve the engineering properties of expansive soils. This work is mainly focused on the strength enhancement of chemically stabilized expansive soil, the stabilizers being used are GGBS and lime.

Bahman et al. (2011) found that, addition of acrylic polymer to soft clay resulted in the improvement of UCS values. Islam et al. (2013) investigated the effect of curing environment on the UCS value and modal mineralogy of lime-GGBS treated Acid Sulfate Soil (ASS). The UCS test results of treated samples were found to be higher than that of untreated samples. Joseph and Muthukkumaran (2014) observed a five times increase in the UCS value of montmorillonite rich expansive soil stabilized with phosphogypsum and bottom ash. Patil and Patil (2013) studied combined effect of fly ash and RBI Grade 81 on clayey soil. There was appreciable increase in the maximum dry density of the treated soil. Yadu and Tripathi (2013) observed considerable increase in both the UCS and CBR values of the soft soil stabilized with GGBS. Gupta and Tare (2014) found a considerable increment in the CBR value of black cotton soil stabilized with fly ash and nylon fiber. Liska et al. (2014) studied the use of GGBS and reactive magnesia (MgO) mixes for soil stabilization, comparing them with GGBS-lime mixes and Portland cement (PC) for better geotechnical performance. Soil stabilized with GGBS-MgO showed greater early strength when compared to the soil stabilized with GGBS-Lime and Portland cement.

The objective of this study is to find the effect of binder content, soaking and curing period on the geotechnical properties such as UCS, Elastic modulus and CBR of chemically stabilized soil.

2 Experimental Program

2.1 Materials Used

Black cotton soil for the investigation was collected from SVNIT Campus, Surat. GGBS was obtained from a local cement manufacturer in Gujarat and lime was procured from local market. Table 1 shows the properties of Black cotton soil selected for the study.

Table 1 Properties of black cotton soil

Sl No.	Property	Value
1.	Specific gravity	2.57
2.	Grain size distribution (%)	
	Gravel	0
	Sand	22
	Silt	43
	Clay	35
3.	Consistency limits (%)	
	Liquid limit	58
	Plastic limit	21
	Plasticity index	37
4.	IS heavy compaction	
	OMC (%)	19
	MDD (g/cc)	1.77
5.	UCS (kPa)	517
6.	CBR (%) (soaked)	1.8
7.	IS Classification	CH

2.2 Mix Proportion

Black cotton soil was mixed with different dosages of additives. The different mix proportions adopted for the study are

- GGBS at dosages of 3, 6, 9, and 12% by weight of dry soil.
- GGBS and Lime at dosages of 2% GGBS + 1% Lime, 4% GGBS + 2% Lime, 6% GGBS + 3% Lime and 8% GGBS + 4% Lime by weight of dry soil.

2.3 Unconfined Compressive Strength Test

For the determination of unconfined compressive strength of various soil-GGBS and soil-GGBS-lime mixes, UCS test was carried out on samples of 50 mm diameter and 100 mm height. The test was conducted as per IS:2720, Part X (1991). For soil-GGBS mix and soil-GGBS-lime mix, soil and additives were mixed in dry state manually then water corresponding to OMC was added and mixed thoroughly. Next, cylindrical specimens of 50 mm diameter and 100 mm height were compacted in three layers by static press to achieve the MDD of the mix obtained from the modified proctor test. Samples were extruded by using hydraulic ejector and sealed in a polythene cover and kept for curing in a closed chamber. To determine the unsoaked UCS value soil-GGBS specimens and soil-GGBS-lime specimens were cured for 7 and 28 days. In order to determine the soaked UCS values of soil-GGBS and soil-GGBS-lime mixes the treated samples were cured for 3 days

and soaked for 4 days and then tested. Compressive strength of the specimens was determined using a compression testing machine at a strain rate of 1.2 mm/min.

2.4 California Bearing Ratio Test

In order to determine the CBR values of different soil-GGBS and soil-GGBS-lime mixes, CBR test was conducted in accordance with IS:2720, Part XIV (1987). The samples were cured for 3 days and soaked for 4 days. After the specified curing was over, the CBR moulds were taken out for test.

3 Results and Discussions

3.1 Unconfined Compressive Strength

3.1.1 Effect of GGBS Content

There was a sharp increase in the UCS value with the addition of GGBS when compared with the UCS of natural soil. The successive increase in the UCS value is attributed to the formation of cementitious compound (CSH-calcium silicate hydrates) resulting from the pozzolanic reaction among the excess SiO present in the slag, CaOH formed by the hydration of silicates and water. The variation of UCS value with GGBS content is shown in Fig. 1. From the figure it can be observed that there is a considerable increase in the UCS value with the increase in the binder content. For the maximum dosage of 12% the UCS value of 7 days cured

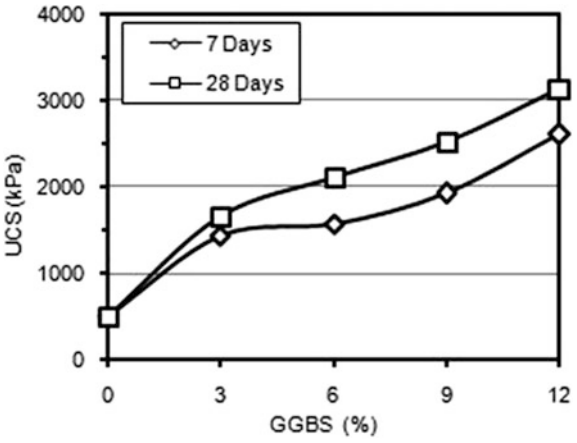

Fig. 1 Variation of UCS value with GGBS content

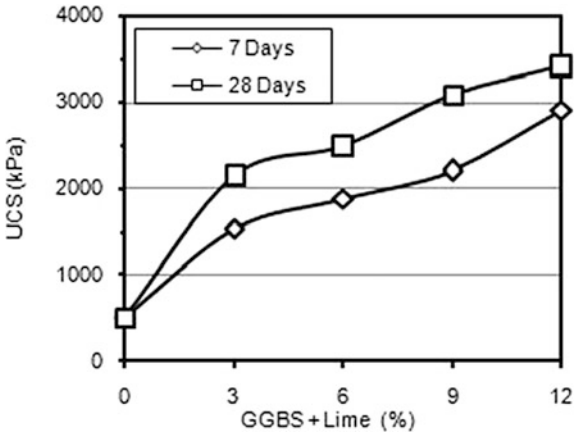

Fig. 2 Variation of UCS with binder (GGBS + lime) content

soil-GGBS mix was obtained as 2,610 kPa and that of 28 days cured mix was obtained as 3,147 kPa, the UCS value of untreated sample being 517 kPa.

3.1.2 Effect of GGBS-Lime Content

The variation of UCS value with GGBS-lime content is shown in Fig. 2. From the figure it can be observed that there is a considerable increase in the UCS value with the increase in the binder content. For the maximum dosage of 12% the UCS value of 7 days cured soil-GGBS-lime mix was obtained as 2,903 kPa and that of 28 days cured mix was obtained as 3,417 kPa, the UCS value of untreated sample being 517 kPa.

3.1.3 Effect of Curing Period

From both Figs. 1 and 2 it is clearly visible that, with the increase in curing period the UCS values showed a remarkable increment. For soil-GGBS mix the increase in curing period from 7 to 28 days resulted in an overall increase of 21% in the UCS value, whereas for soil-GGBS-lime mix the increase in UCS value was observed to be 18%.

3.1.4 Effect of Soaking

Figure 3 shows the effect of soaking on the strength of the treated soil. A comparison was made between the unsoaked samples cured for 7 days and soaked samples cured for 3 days and soaked for 4 days. For both soil-GGBS mix and soil-GGBS-lime mix soaking resulted in a decrement of UCS values by 25%.

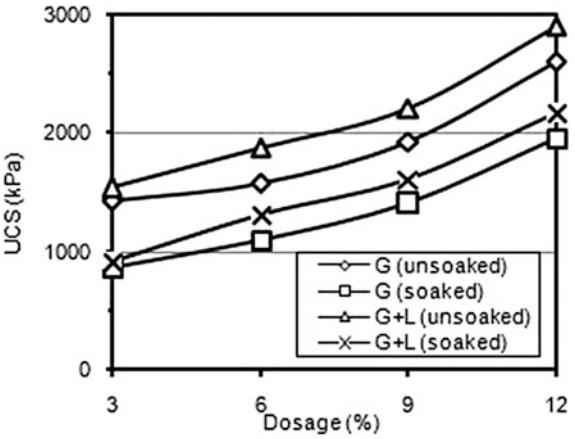

Fig. 3 Variation of UCS with binder content (soaked and unsoaked)

3.1.5 Comparison of Soil-GGBS Mix with Soil-GGBS-Lime Mix

A comparison is made between soil-GGBS mix and soil-GGBS-lime mix and shown in Fig. 4. From the figure it is evident that soil-GGBS-lime mix has got higher UCS value compared to soil-GGBS mix. With the addition of lime as an extra binder the UCS value got increased by 11% after 7 days curing and 9% after 28 days curing.

3.2 Elastic Modulus

The relevant design parameter for chemically stabilized sub-bases is the Elastic Modulus which can be determined from the UCS test. The elastic tangent modulus

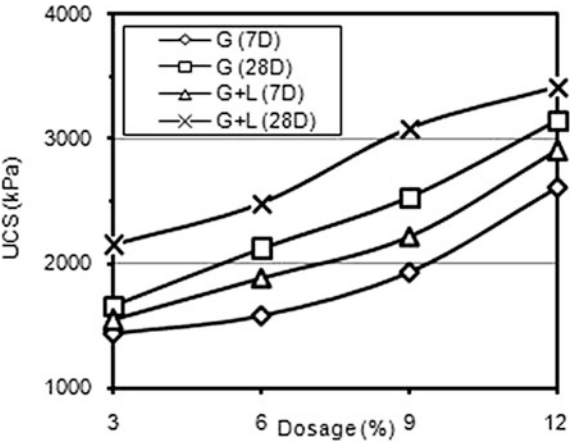

Fig. 4 UCS values of soil-binder mixes for 7 and 28 days curing

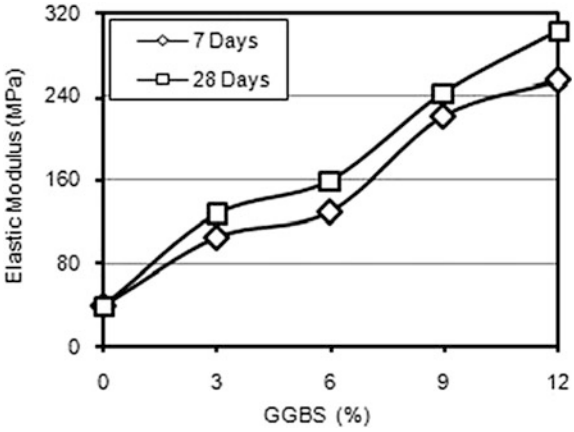

Fig. 5 Variation of elastic modulus with GGBS content

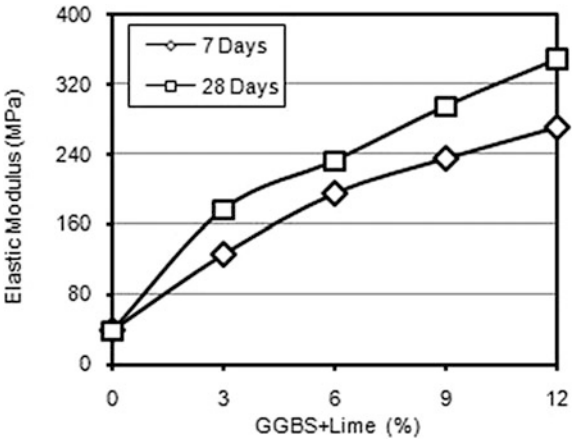

Fig. 6 Variation of elastic modulus with binder (GGBS + Lime) content

corresponding to 50% stress is obtained from the stress–strain curve plotted using the UCS test results.

3.2.1 Effect of Binder Content

The variation of elastic modulus for various soil-binder mixes is shown in Figs. 5 and 6. From the figures it can be observed that there is a considerable increase in the elastic modulus with the increase in binder content.

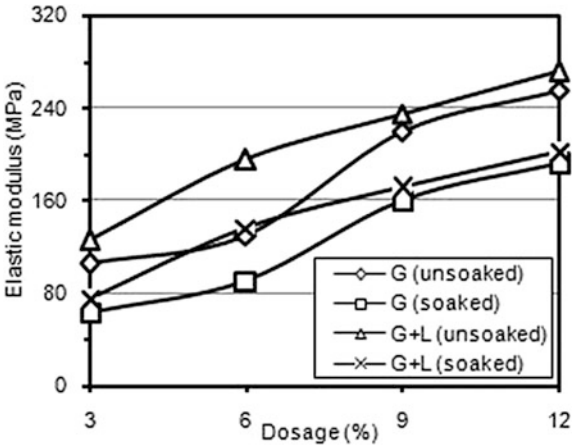

Fig. 7 Variation of elastic modulus with binder content (soaked and unsoaked)

3.2.2 Effect of Curing Period

From both Figs. 5 and 6 it is clearly visible that, with the increase in curing period the elastic modulus was found to be increased.

3.2.3 Effect of Soaking

Figure 7 shows the effect of soaking on the elastic modulus of the treated soil. A comparison was made between the unsoaked samples cured for 7 days and soaked samples cured for 3 days and soaked for 4 days. For both soil-GGBS mix and soil-GGBS-lime mix soaking resulted in a decrement of elastic modulus by 23%.

3.2.4 Comparison of Soil-GGBS Mix with Soil-GGBS-Lime Mix

A comparison is made between soil-GGBS mix and soil-GGBS-lime mix and shown in Fig. 8. From the figure it is evident that soil-GGBS-lime mix has got higher elastic modulus compared to soil-GGBS mix. With the addition of lime as an extra binder the elastic modulus increased by 6% for 7 days curing and 15% for 28 days curing.

3.3 California Bearing Ratio

The CBR value of soil-GGBS-lime mix is more when compared to soil-GGBS mix. The comparison is shown in Fig. 9. The CBR value ranged from 6 to 31% for

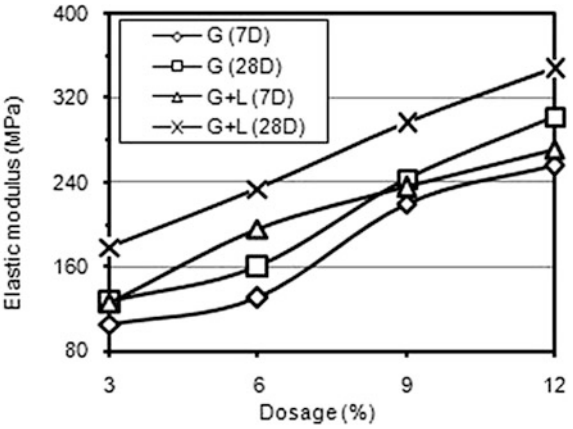

Fig. 8 Elastic modulus of soil-binder mixes for 7 and 28 days curing

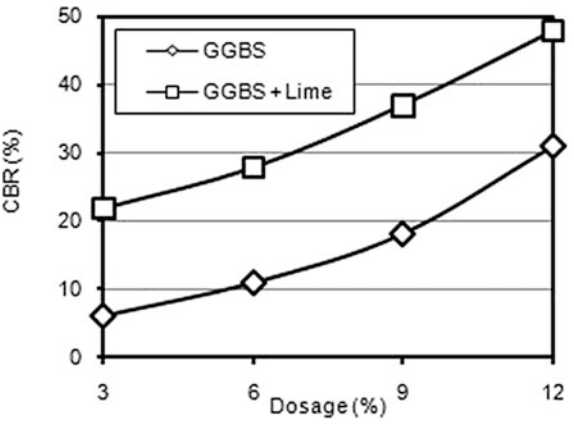

Fig. 9 CBR of soil-GGBS mix and soil-GGBS-Lime mix

soil-GGBS mix and 22 to 48% for soil-GGBS-lime mix for the binder content ranging from 3 to 12%. For maximum dosage of 12% the CBR value of soil-GGBS-lime mix is 48% and that of soil-GGBS mix is 31%. Thus, with the addition of lime as an extra binder the CBR value of treated soil got enhanced by 55%.

4 Conclusions

Following conclusions were drawn from the study:

- The UCS value of soil–binder mixes were found to be increasing with the increase in binder content. Increase in curing period also showed appreciable increase in the UCS values. 28 days cured specimen showed enhanced strength

compared to 7 days cured specimen. The elastic modulus was also found to be increasing with the increase in binder content and increase in curing period.

- The addition of lime improved the strength even more. Soil-GGBS-lime mix showed greater strength when compared to soil-GGBS mix.
- The soaked strength for both soil-GGBS and soil-GGBS-lime mix were found to be lower when compared to the unsoaked strength. The reduction in strength for both the mixes was found to be 25%.
- The CBR values for soil-GGBS and soil-GGBS-lime mixes were found to be increasing with the increase in binder content. The CBR value of soil-GGBS-lime mix was found to be more than that of soil-GGBS mix. With the addition of lime as an additional binder to soil-GGBS mix the CBR value got enhanced by 55%.

References

Bahman, N., Seyed, A. N., & Ehsan, I. (2011). Unconfined compressive strength of clayey soils stabilized with waterborne polymer. *KSCE Journal of Civil Engineering*, 943–949, Springer 12205-012-1388-9.

Gupta, D., & Tare, V. (2014). Influence of randomly distributed nylon fibers mixed with fly ash in black cotton soil. *Indian Highways,* pp. 47–51.

Indian Standard (IS). (1987). Laboratory determination of CBR. *IS 2720 (Part 16)*, New Delhi.

Indian Standard (IS). (1991). Determination of unconfined compressive strength. *IS 2720 (Part X)*, New Delhi.

Islam, S., Haque, A., & Wilson, S. A. (2013). Effect of curing environment on the strength and mineralogy of Lime-GGBS treated acid sulphate soils. *Journal of Materials in Civil Engineering ASCE, 26*(5), 1003–1008.

Joseph, J., & Muthukkumaran, K. (2014). Utilization of industrial waste products in the stabilization of montmorillonite rich expansive soil. *Soil Behavior and Geomechanics*, GSP 236, ASCE, pp. 224–233.

Liska, M., Yi, Y., & Al-Tabbaa, A. (2014). Properties of two model soils stabilized with different blends and contents of GGBS, MgO, lime, and PC. *Journal of Materials in Civil Engineering ASCE, 26*(2), 267–274.

Patil, B. M., & Patil, K. A. (2013). Effect of fly ash and RBI Grade 81 on swelling characteristics of clayey soil. *International Journal of Advanced Technology in Civil Engineering, 2*(2), 27–31, ISSN: 2231-5721.

Yadu, L., & Tripathi, R. K. (2013). Effects of Granulated Blast Furnace Slag in the engineering behavior of stabilized soft soil. In *Chemical, Civil and Mechanical engineering Tracks of 3rd Nirma University International Conference*. Procedia Engineering, 51. Science Direct Elsevier Ltd, pp. 125–131.

Soil Improvement Using Microbial: A Review

R. B. Wath and S. S. Pusadkar

Abstract The various methods are in practice for improving the properties of soil which are neither economical nor eco-friendly. The microorganisms, nutrients, biological processes may prove to eco-friendly solution to soil improvement. This paper aims to review different microbial, their microbiological processes and their geotechnical applications to enhance the properties of soil. The microbial improves different geotechnical properties of soil. The microbiological processes include calcite precipitation, mineral transformation and different pathways. The properties of cohesionless soil or cohesive soil can be improved using microbes. This paper review, the geotechnical applications of cementation of sands to enhance bearing capacity, soil erosion control, groundwater flow control, and remediation of soil and groundwater impacted by metals and radionuclides.

Keywords Soil improvement · Bioclogging · Biocementation · Microbial

1 Introduction

Presently, all civil engineers facing a great challenge of constructing a structure on or with a soil which does not have suitable characteristics even for walking human kind on that soil. The civil engineers cannot avert such site due to presence of weak soil or geotechnical properties. To face these challenges, engineers are working hard to change or reform, the mechanical and physical properties of the soil by using different soil stabilization techniques.

R. B. Wath (✉)
SCOET, Amravati, India
e-mail: wathrb@gmail.com

S. S. Pusadkar
Department of Civil Engineering, Government College of Engineering, Amravati 444604, India
e-mail: ss_pusadkar@yahoo.co.in

T. Thyagaraj (ed.), *Ground Improvement Techniques and Geosynthetics*, Lecture Notes in Civil Engineering 14, https://doi.org/10.1007/978-981-13-0559-7_37

Today, mostly stabilization of soil can be carried with lime, cement, fibres, waste materials and geosynthetic material. Few methods are not only eco-friendly but also toxic, costly, and contaminate the ground water. In order to have green approach for ground improvement, geotechnical engineers are working with environment to find suitable and economical method for soil stabilization using microbes. It is an uncommon alternative for improvement of properties of soil. Microbiological process is more environmentally friendly than other conventional treatment methods.

The bacteria's or microbes found in around are used in the process. The process involved in microbial effect results in the pores of the soil matrix. The formation of mineral precipitate in pores alters the soil properties by cementation called biocementation. The other way is process of filling voids by a product resulting from microbial-induced biochemical process called as bioclogging. Each of the process applied results in influencing different geotechnical properties of soil. Many researchers are working on deployment of microbes for assessing the strength of these bacteria in geotechnical application and also assessing the factors influencing the performance of various microbes. This paper aims to review different microbes, their microbiological processes (Mortensen et al. 2011; Ng et al. 2013; Dhami et al. 2013; Kim et al. 2014) and their geotechnical applications to enhance the properties of soil (Dejong et al. 2006; Whiffin et al. 2007; Chou 2007; Ahmed and Hussain 2008; Ivanov and Chu 2008; Kavazanjian and Karatas 2008; Yasuhara et al. 2012; Ng et al. 2012; Pusadkar 2014; Pusadkar and Chavan 2014; Shahrokhi et al. 2014; Ukken and Krishnan 2015; Maleki et al. 2016). Chang et al. (2016) describe the geotechnical sustainability using microbial treatment for soil improvement.

2 Microbes and Soil

Soil contains microorganisms which are highly adaptable to varying conditions both genetically and physiologically, because they have been in existence for over 3.5 billion years. However, the quantum of efficient bacteria required for cementation or clogging are not sufficient to have the process complete. Hence, adding more microbes to soil which are helpful to enhance geotechnical properties is the need of the hour. It will be helpful to utilize the unused or weak soil area to built suitable infrastructure.

The soil improvement using microbes taking shape and therefore little work is available. Table 1 gives various microbes studied by researchers for enhancing various geotechnical properties. The most of the work is carried out on sand expect few on black cotton soil.

The microbially induced $CaCO_3$ precipitation in porous soil usually occurs by adding the exogenous bacterium *Sporosarcina pasteurii* (*S. pasteurii*) to promote urea hydrolysis via the enzyme urease (Whiffin et al. 2007; Mortensen et al. 2011). The deposition of $CaCO_3$ in the void spaces or around the surfaces of the soil particles contributes to the clogging of the porous medium with a consequent reduction of porosity.

Table 1 Improvement in soil properties

Sr. No.	Soil	Bacteria	Microbial process	Improvement	Disadvantages	Reference
1.	Ottawa 50–70 sand	*Bacillus pasteurii*	Cementation process	Increase in axial capacity, higher elastic capacity	degradation of cementation was detectable	Dejong et al. (2006)
2.	Itterbeck sand	*Sporosarcina pasteurii*	Urease activity	Porosity was decreased to 90%, significant strength increase	$CaCO_3$ (below 60 kg/m^3 or 3.5% w/w) had no significant effect	Whiffin et al. (2007)
3.	Sand	Urease–enzyme-driven mineralization	Enzyme to hydrolyze urea	Unconfined compression strength increases and permeability reduces	–	Yasuhara et al. (2012)
4.	Sand	*Bacillus pasteurii*		Effective size of sand influences the performance	–	Pusadkar and Chavan (2014)
5.	Sand	*Sporosarcina pasteurii*	Calcite precipitation	Significant improvements in the UCS and stiffness values, permeability coefficient values of the treated sands	–	Shahrokhi et al. (2014)
6.	Black cotton soil	Tryptic Soy Broth was used for the cultivation of Fastidious and non-fastidious microorganisms	Use of Tryptic Soy Broth	Plasticity Index decreases, Shrinkage limit increases, Swelling pressure decreased	–	Pusadkar (2014)
7.	Sand	Bacillus, Sporosarcina, Sporolactobacillus, Clostridium and Desulfotomaculum	Urea hydrolysis	Increases in shear strength, confined compressive strength, stiffness and liquefaction resistance	–	Ukken and Krishnan (2015)

Anbu et al. (2016) also reported many urease producing bacteria which are responsible for calcite precipitation such as Aerobacter aerogenes, *B. megaterium*, *B. subtilis*, Bacillus sp. CR2, *B. thuringiensis*, *Deleya halophila*, *Halomonas eurihalina*, *Helicobacter pylori*, *Kocuria flava* CR1, *Lysinibacillus sphaericus* CH5, *Methylocystis parvum*, *Myxococcus xanthus*, *Proteus mirabilis*, *Pseudomonas denitrificans*, Sporolactobacillus sp., *Sporosarcina ginsengisoli* and *S. pasteurii*.

3 Microbiological Mechanism

The mechanisms for microbiological applications to geotechnical engineering can be divided into two main categories: bioclogging and biocementation. Bioclogging is a process where the soil void is filled by the product from microbial-induced biochemical process. Biocementation is to enhance the strength and stiffness properties of soil and rocks by introducing bacteria and cementation reagents into the soil.

Ivanov and Chu (2008) describes different possible microbial processes that can lead potentially to bioclogging and biocementation. Bioclogging includes formation of impermeable layer of algal and cyano bacterial biomass.

The production of slime in soil is caused by aerobic and facultative anaerobic heterotrophic bacteria, oligotrophic microaerophilic bacteria and nitrifying bacteria. The production of undissolved sulphides of metals by sulphate-reducing bacteria and undissolved carbonates of metals are formed by ammonifying bacteria. The ferrous solution and precipitation of undissolved ferrous and ferric salts and hydroxides in soil are formed by iron-reducing bacteria.

Biocementation includes binding of the soil particles with sulphides of metals produced by sulphate-reducing bacteria and binding of the particles with carbonates of metals produced due to hydrolysis of urea. Binding of the particles with ferrous and ferric salts and hydroxides are produced due to activity of iron-reducing bacteria.

Umar et al. (2016) review the biological process of soil improvement considering various factors. The temperature and humidity affect metabolic reactions inside the cells and some physical properties such as viscosity and diffusion. The availability of other microorganisms also restricts the available space for bacterial growth and activity, and limits the population of the bacteria. He also discussed the challenges need to be face for mixing the bacteria in deeper location, flow of bacteria in voids and long-term durability of strength induced by the process.

4 Geotechnical Properties

Mechanical properties of soil are of insufficient and subjected to erosion. Stabilization of soil is highly desirable because of the increasing infrastructure. Conventional chemical grouting techniques are often expensive and require many injection wells for treating large volumes.

Many researchers have evaluated the potential of application of bacterially induced carbonate precipitation by ureolytic bacteria by providing urea and calcium sources in various sand plugs. It is reported that sand consolidation by *B. pasteurii* reduced porosity by up to 50% and permeability by up to 90% in the areas where the cement action took place. Improvement in strength of sand columns upon bacterial carbonates was also reported.

Ureolytic-driven MICCP has also been proposed to suppress dust, reduce permeability in granular media, improve soils, stabilize slopes and strengthen liquefiable soils. Table 1 show the work carried out by various authors and improvement in the geotechnical properties. The bacterial improvement of sandy soil and black cotton soil leads in increasing strength, reducing permeability and swelling characteristics.

5 Applications of Microbial in Geotechnical Engineering

The microbial can be widely used in soil improvement in various ways. In most of process injection mode can be used for bacteria intrusion while in some cases mixing with soil can be taken place before placing in position. Some of the areas where improvement needs are

- Reinforcing or stabilizing soil to facilitate the stability of tunnels or underground constructions;
- Increasing the bearing capacity of piled or non-piled foundations;
- Reducing the liquefaction potential of soil;
- Treating pavement surface;
- Strengthening tailings dams to prevent erosion and slope failure;
- Binding of the dust particles on exposed surfaces to reduce dust levels;
- Increasing the resistance of offshore structures to erosion of sediment within or beneath gravity foundations and pipelines;
- Stabilizing pollutants from soil by the binding;
- Controlling erosion in coastal area and rivers.

6 Field Implementation

To date only a few field trials have been performed in which microbes have been actively used to either increase the strength and stiffness of soil or reduce the hydraulic conductivity. For field implementation required bacterial suspension can be produced in laboratory. Then this suspension is mixed with soil similar to chemical injection methods. For uniform treatment on the field microbiological processes can utilize by using technologies from the ground improvement—

geo-environmental remediation. i.e. grouting methods, including injection well patterns and point injection techniques.

The cost of microbiological treatment schemes are dependent on the processes used, and on details of the specific field project. It also shows that as is common with many other ground treatment processes, the major cost is in delivery. If processes can be developed that enable bio-treatment to be delivered more economically, then strong potential exists.

7 Conclusions

1. Facultative anaerobes could be useful for bioclogging and biocementation methods to improve the mechanical properties of soil.
2. The microbes which precipitates calcium carbonates very useful for increasing bearing capacity, stiffness, susceptibility to liquefaction and decreasing the permeability of soil.
3. The use of microbials for improvement of soil characteristics is not only very cost effective method but also eco-friendly method.
4. MICP process offered a ground improvement method to reduce the liquefaction susceptibility and the damage due to seismic loading.
5. The black cotton soil can also be well treated by microbes to reduce the swelling effects and improve bearing capacity.
6. It is required to observe the performance of microbial treated soil in field or real engineering problem.
7. It will also need to ensure the retention capacity, environmental effect of gained strength and lifelong serviceability.

References

Ahmed, A., & Hussain, I. (2008). Enhancing the stability of fine grained soil using biological approach. *Electronic Journal of Geotechnical Engineering, 1*, 1–11.

Anbu, P., Kang, C.-H., Shin, Y.-J., & So, J.-S. (2016). Formations of calcium carbonate minerals by bacteria and its multiple applications. *Springer Plus, A Springer Open Journal*, *5*(250), 1–26.

Chang, I., Im, J., & Cho, G. (2016). Introduction of microbial biopolymers in soil treatment for future environmentally-friendly and sustainable geotechnical engineering. *Sustainability, 8* (251), 1–23.

Chou, C.-W. (2007). *Bioimprovement of geotechnical properties of sandy soils (Thesis of Master of Science)*, University of Maryland.

Dejong, J. T., Fritzges, M. B., & Nusslein, K. (2006). Microbially induced cementation to control sand response to undrained shear. *Journal of Geotechnical and Geoenvironmental Engineering, 132*(11), 1381–1392.

Dhami, N. K., Reddy, M. S., & Mukherjee, A. (2013). Biomineralization of calcium carbonates and their engineering applications: A review. *Frontiers in Microbiology, 4*, 1–13.

Ivanov, V., & Chu, J. (2008). Applications of microorganisms to geotechnical engineering for bioclogging and biocementation of soil in situ. *Reviews in Environmental Science Biotechnology, 7*(2), 139–153.

Kavazanjian, E., Jr., & Karatas, I. (2008). Microbiological improvement of the physical properties of soil. In *6th International Conference on Case Histories in Geotechnical Engineering* (pp. JKM-3, 1–10), Arlington, VA, August 11–16, 2008.

Kim, D., Park, K., & Kim, D. (2014). Effects of ground conditions on microbial cementation in soils. *Materials*, 143–156.

Maleki, M., Ebrahimi, S., Asadzadeh, F., & Tabrizi, M. (2016). Performance of microbial-induced carbonate precipitation on wind erosion control of sandy soil. *International Journal of Environmental Science and Technology, 13*(3), 937–944.

Mortensen, B. M., Haber, M. J., Dejong, J. T., Caslake, L. F., & Nelson, D. C. (2011). Effects of environmental factors on microbial induced calcium carbonate precipitation. *Journal of Applied Microbiology*, 338–349.

Ng, W.-S., Lee, M.-L., & Hii, S.-L. (2012). An overview of the factors affecting microbial-induced calcite precipitation and its potential application in soil improvement. *International Scholarly and Scientific Research & Innovation, 6*(2), 683–689.

Ng, W.-S., Lee, M.-L., Khun, T. C., & Ling, H. S. (2013). Improvements in engineering properties of soils through microbial-induced calcite precipitation. *KSCE Journal of Civil Engineering, 17* (4), 718–728.

Pusadkar, S. S. (2014). Swelling and shrinkage characteristics of biologically treated black cotton soil. In *National Conference on 'Geo-Environmental Issues and Sustainable Urban Development'* (GEN-2014), October 11–12, 2014, MNNIT, Allahabad.

Pusadkar, S. S., & Chavan, R. (2014). Effect of effective size of sand on behavior of microorganism reinforced sand. In *International Conference on Recent Trends in Engineering and Technology* (pp. 127–132), March 13–14, 2014, Mount Zion College of Engineering, Pudukkottai, Tamilnadu, India, CE-1.

Shahrokhi, R., Zomorodian, S. M., Naizi, A., & O'Kelly, B. C. (2014). Improving sand with microbial-induced carbonate precipitation. *Ground Improvement, Proceeding of the Institution of Civil Engineers*, 1–14.

Ukken, E. T., & Krishnan, A. (2015). Microbial-induced calcite precipitation for soil improvement. *International Journal of Advanced Research Trends in Engineering and Technology (IJARTET), II*(Special Issue X).

Umar, M., Kassim, K. A., Chiet, K. T. P. (2016). Biological process of soil improvement in civil engineering: A review. *Journal of Rock Mechanics and Geotechnical Engineering*, 1–8.

Whiffin, V. S., van Passen, L. A., & Harkes, M. P. (2007). Microbial carbonate precipitation as a soil improvement technique. *Geomicrobiology Journal, 24*, 417–423.

Yasuhara, H., Neupane, D., & Hayashi, K. (2012). Experiments and predictions of physical properties of sand cemented by enzymically-induced carbonate precipitation. *Soil and Foundation, 52*(3), 539–549.

Long-Term Strength Studies on Natural Fibre Composite (N-F-C) Sheets for Use as Separator in Flexible Pavements in Terms of CBR Values

Aathira Vijayan, Leema Peter, P. K. Jayasree and K. Balan

Abstract Coir fibre–polymer composite being economical and ecofriendly, can be considered as a best alternative for the geosynthetic composite. The use of coir fibre–polymer composites can be extended to ground improvement and can be used as a separator in flexible pavement. This paper deals with the long-term performance in terms of strength criteria of natural fibre composite sheets for use as separator in flexible pavements. The study was confined to three types of composites: coir fibre latex composite sheet, woven coir mat and woven coir mat latex composite sheet. In the study the strength characteristics were studied using the California Bearing Ratio (CBR) test method. The tests were conducted at an interval of one month for a period of four months to study the time dependent strength variation on natural fibre composites. A system of soil, aggregate and composite is used for CBR test. The soaked CBR values for various composites developed are studied and compared for their strength characteristics. Several results show that with time the residual strength increases initially and converges to a certain value, after which the rate of deterioration decreases at a small value. Among the three types of composites, woven coir mat latex composite is expected to give better results in terms of strength characteristics.

Keywords Natural fibre-polymer composite · Durability · California bearing ratio test · Deterioration

A. Vijayan · L. Peter (✉) · P. K. Jayasree · K. Balan
Department of Civil Engineering, College of Engineering Trivandrum, Trivandrum 695016, India
e-mail: leema.cet@gmail.com

A. Vijayan
e-mail: aathiravijayan91@gmail.com

P. K. Jayasree
e-mail: jayasreepk@cet.ac.in

K. Balan
e-mail: drkbalan@gmail.com

T. Thyagaraj (ed.), *Ground Improvement Techniques and Geosynthetics*, Lecture Notes in Civil Engineering 14, https://doi.org/10.1007/978-981-13-0559-7_38

1 Introduction

Natural fibre-polymer composites are hybrid materials that combine the mechanical properties of natural fibre with durability and bonding strength of polymer. Coir–latex composites are one such hybrid material developed which have superior mechanical strength to be used as a separator in flexible pavements. Geotextiles will degrade over time. The rate of degradation will depend on the molecular configuration of the geotextile polymer and the nature of the environment to which the geotextile is exposed. Degradation of a polymeric material typically results in a loss of strength.

The long term performance in terms of CBR strength criteria of natural fibre composite sheets for use as separator in flexible pavements is studied in this paper. The study is confined to three types of composites: coir fibre latex composite sheet, woven coir mat and woven coir mat latex composite sheet.

Natural Fibre Composite Sheets were developed (Soumya 2015; Sumesh 2015) for use as a separator in flexible pavements. Composites and natural geotextiles have been used as a separator in flexible pavements by various researchers (Rajagopal and Ramakrishna 2009; Singh and Mittal 2014). CBR strength of the geotextiles/composites is one of the parameters to determine their effectiveness (Kumar and Rajkumar 2012; Michael and Vinod 2009; Sarbaz et al. 2014).

2 Experimental Study

2.1 Preparation of Test Pits

The composites were buried in the soil and the intensity of degradation was studied after a particular interval of time. The tests were conducted for a period of five months. Test pits were prepared in soil for the embedment of samples for the study. The durability of polymers and fibre-reinforced polymer composites under service condition is a critical aspect to be addressed for their robust designs and condition-based maintenance.

2.2 Material

2.2.1 Properties of Soil

The basic properties of soil given in Table 1 were determined from specific gravity test, liquid limit test, plastic limit test, light compaction test, etc., as per IS 2720.

Table 1 Basic properties of soil

Particulars	Values
Specific gravity	2.26
Optimum moisture content (%)	25.25
Maximum dry density (g/cm^3)	1.5
Liquid limit (%)	55
Plastic limit (%)	19
Plasticity index (%)	36

Table 2 Gradation of WMM

IS sieve opening (mm)	Standard values MORTH Table 500-13 (100%)
53	100
45	95–100
26.5	–
22.5	60–80
11.2	40–60
4.75	25–40
2.36	15–30
0.6	8–22
0.075	0–5

2.2.2 Properties of Aggregate Used as Base Course Layer

Wet mix macadam (WMM) was selected as the base course for the pavement. The aggregate used for WMM was from the specified gradation as per Ministry Of Road Transport and Highways (MORTH) Specification for Road and Bridge Works (5th revision) 2013 is shown in Table 2. Aggregate sizes of 45, 22.5, 6 mm and filler are used in the proportion of 25:18:30:27 to get the required gradation.

2.2.3 Natural Fibre Composite Sheet

Coir fibres of length 10 cm showed the maximum performance when used in a coir fibre-latex composite (Sumesh 2015). Coir pith and other undesirable materials were separated from the coir fibre. It was then chopped to about 10 cm in length. In addition, rubber being the most widely available natural polymer, it was decided to use rubber as a polymer matrix. Coir fibres were soaked in sodium hydroxide solution for 48 h. Fibre were taken out, repeatedly washed with water and dried in the air. Latex compound was prepared by mixing 70% of natural rubber latex and 10% of sodium hydroxide solution and 20% of water. The latex compound and the

resin solution were agitated to achieve homogenization. The minimum latex content should be at least equal to the fibre content that is used for the development of composite (Sumesh 2015).

Three types of fibre-latex composites are prepared and tested in this study. Coir fibre latex composite, woven coir mat and non-woven coir mat latex composite are prepared which are relatively thick planar sheets. Woven coir composites are manufactured by interlacing yarns, usually at right angles. The types of fibre latex composites used in the study are shown in Figs. 1, 2 and 3.

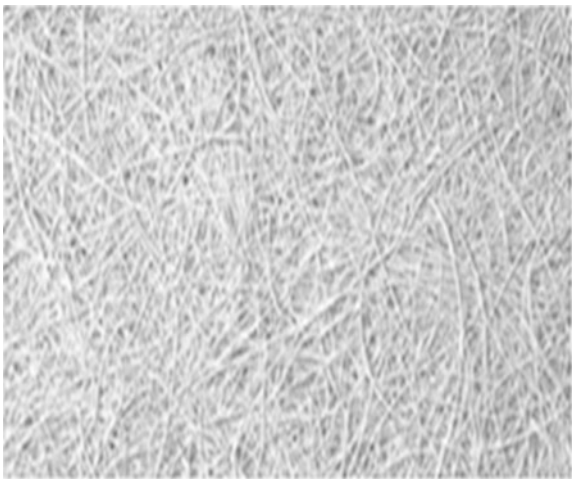

Fig. 1 Coir fibre latex composite

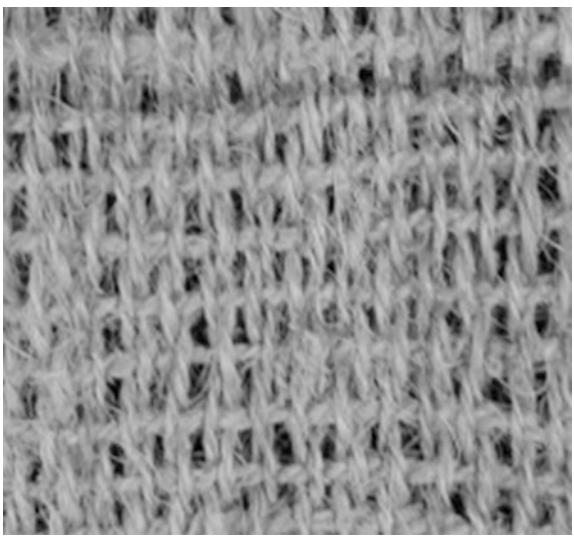

Fig. 2 Woven coir mat

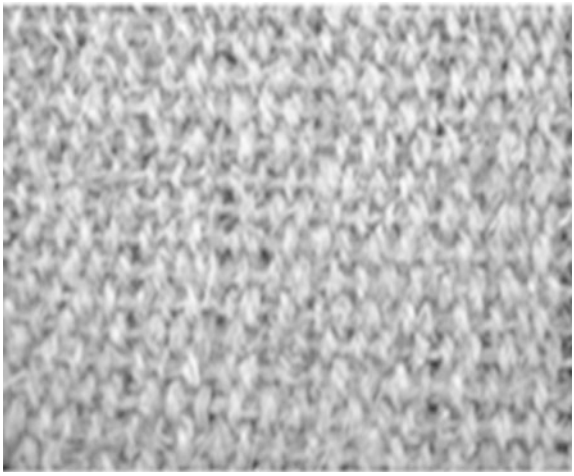

Fig. 3 Woven coir mat latex composite

3 Development of N-F-C Sheets

The composite was developed at Kairali coir mattress industry, Chirayankeezhu, Trivandrum.

3.1 Collection of Coir Fibres

Coir fibres were obtained from a small scale coir industry. The collected coir fibres were then sun dried and manually cut using scissors into length of 10 cm. As per literature reviewed, it was observed that coir fibres of length 10 cm showed the maximum performance when used in a coir fibre-polymer composite.

3.2 Collection and Treatment of Latex

The latex obtained from the rubber trees has high viscosity, a pungent smell and slow setting time. In the present investigation, latex is required to be of medium viscosity for adequate penetration into coir fibres, and should have faster setting time for developing the composite. Hence the latex is to be treated to obtain the required properties.

3.3 *Preparation of NFC Sheets*

Fibres of 10 cm length were spread uniformly by hand in a steel tray into which chemically treated latex was sprayed manually using a standard spray gun having a nozzle diameter of about 1–1.5 mm to obtain a mat shaped composite was compressed in a mechanical compressor to attain required strength and thickness of 5–10 mm.

4 Testing Method

This study was conducted to investigate the beneficial use of different varieties of coir geotextiles as reinforcing material in subgrade. Soaked California Bearing Ratio tests were conducted. CBR is a measure of resistance of a material to penetration of standard plunger under controlled density and moisture conditions. CBR test may be conducted in remoulded or undisturbed sample. The schematic diagram of the reinforced soil aggregate system prepared in conventional CBR mould is shown in Fig. 4.

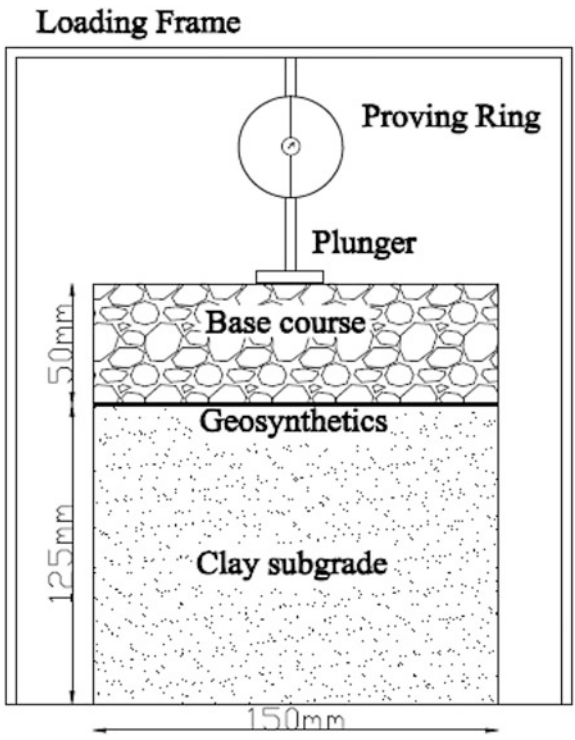

Fig. 4 Schematic diagram of the reinforced soil aggregate system

Test consists of causing a cylindrical plunger of 50 mm diameter to penetrate a pavement component material at 1.25 mm/min. The loads for 2.5 and 5 mm are recorded. This load is expressed as a percentage of standard load value at a respective deformation level to obtain CBR value. The California bearing ratio test is penetration test meant for the evaluation of subgrade strength of roads and pavements. This is the most widely used method for the design of flexible pavement. California bearing ratio is the ratio of force per unit area required to penetrate into a soil mass with a circular plunger of 50 mm diameter at the rate of 1.25 mm/min.

5 Results and Discussions

5.1 Load Characteristics

The CBR of soil aggregate system without the composite was obtained as 4.61%. The load characteristics of the soil aggregate composite system obtained by California bearing ratio test is shown in Table 3.

The CBR strength was found to be higher for woven coir mat latex composite compared to other composites. The variation of load-penetration characteristics of soil aggregate system reinforced with three types of composites were shown in Figs. 5, 6 and 7.

From the load-penetration curves, it is clearly observed that there is an increase in resistance to penetration when woven coir mat latex composite is used as reinforcement in soil aggregate system.

Table 3 CBR of soil aggregate composite system

Particulars	Coir fibre latex composite	Woven coir mat	Woven coir mat latex composite
Initial	6	4.7	23.4
7th day	5.0	2.1	20.9
14th day	5.2	2.0	20.1
28th day	5.0	1.9	20.1
2 months	4.6	1.9	19.3
3 months	3.8	1.5	18.8
4 months	3.6	1.3	18.0

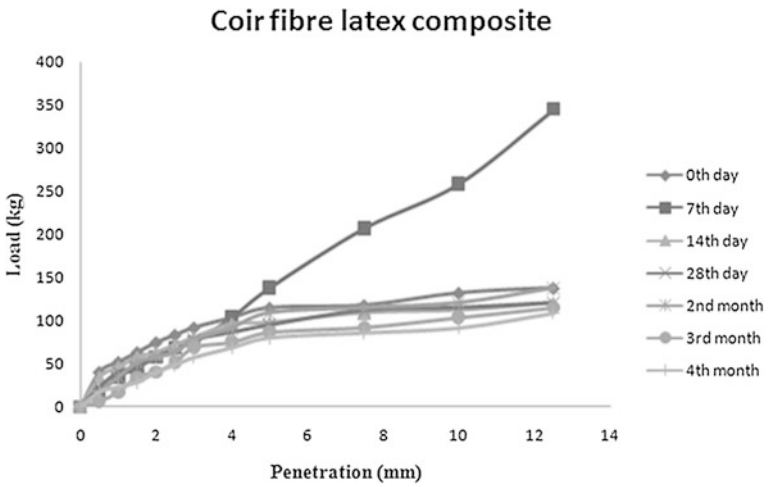

Fig. 5 Load-deformation characteristics of coir fibre latex composite

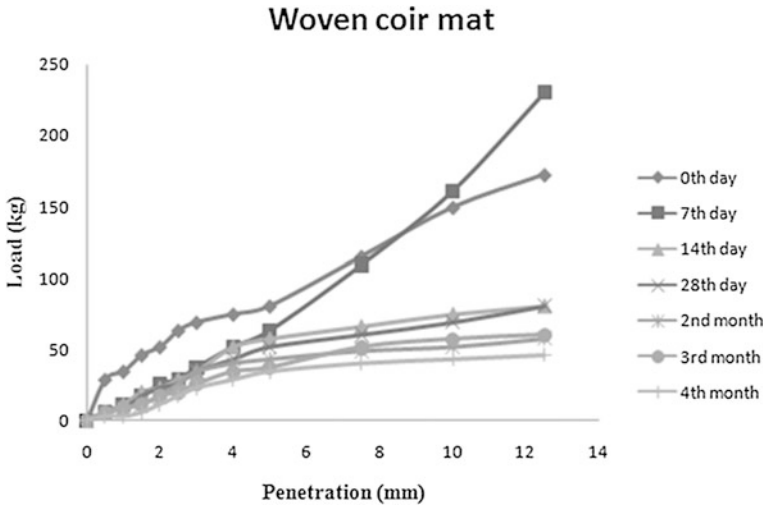

Fig. 6 Load-deformation characteristics of woven coir mat

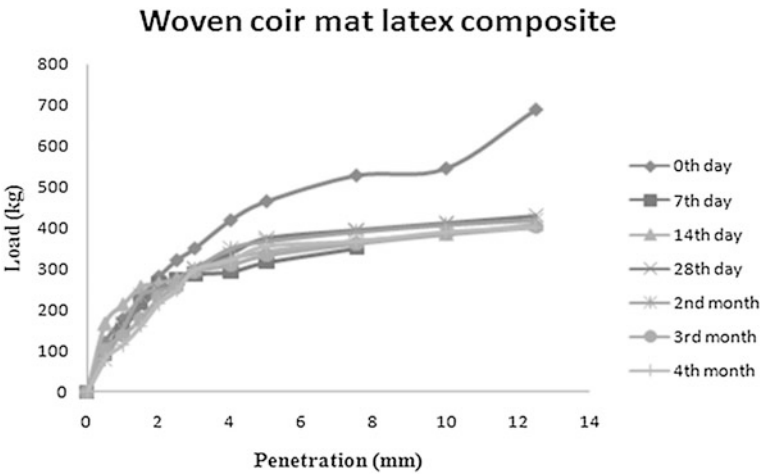

Fig. 7 Load-deformation characteristics of woven coir mat latex composite

6 Conclusions

The long term strength characteristics of natural fibre composites for use as a separator in flexible pavements were studied in this paper.

The latex coating provided increases the strength characteristics of the coir fibre. CBR is found to be higher for soil aggregate system reinforced with woven coir mat latex composite compared to coir fibre latex composite and woven coir mat. For the 28th day, CBR for woven coir mat latex composite was found to be three times higher than that of coir fibre latex composite and ten times higher than that of woven coir mat. The higher load carrying capacity of the composite may be due to the binding property of latex on the coir fibre and also the woven coir fibre will provide a good strength to the composite. Woven coir fibre latex composite has superior strength properties.

Acknowledgements The authors express deep sense of gratitude to Centre for Engineering Research and Development (CERD) for funding the project.

References

Kumar, P. S., & Rajkumar, R. (2012). Effect of geotextile on CBR strength of unpaved road with soft subgrade. *Electronic Journal of Geotechnical Engineering, 17,* 1355–1363.

Michael, M., & Vinod, P. (2009). California bearing ratio of coir geotextile reinforced subgrade. In *10th National Conference on Technological Trends* (pp. 63–67), November 2009.

Rajagopal, K., & Ramakrishna, S. (2009). Coir geotextiles as separation and filtration layer for low intensity road bases. In *Indian Geotechnical Society* (IGS) (pp. 941–946), 2009.

Sarbaz, H., Ghiassian, H., & Heshmati, A. A. (2014). CBR strength of reinforced soil with natural fibres and considering environmental conditions. *International Journal of Pavement Engineering, 15*(7), 577–583.

Singh, R. R., & Mittal, S. (2014). Improvement of local subgrade soil for road construction by the use of coconut coir fiber. *International Journal of Research in Engineering and Technology, 03*(05), 707–711.

Soumya, G. (2015). *Development of a coir polymer composite as a separator in flexible pavements* (Unpublished, Mtech Thesis). University of Kerala.

Sumesh, C. (2015). *Development of a coir fibre-latex composite (CFLC) sheet for use as a separator in flexible pavements* (Unpublished, Mtech Thesis). University of Kerala.

Coefficient of Consolidation for Vertical and Radial Drainage

Aparna R. Pillai and S. R. Gandhi

Abstract The knowledge of the rate at which the settlement of clay layer takes place is very important in the design of vertical drain. The coefficient of consolidation, whether it is vertical or radial drainage (c_v or c_r) plays an important role in the design of vertical drains and it controls accurate prediction of rate of consolidation of soil. This paper presents an overview of different methods used in the past for finding the coefficient of consolidation, using vertical drainage (c_v), as well as with vertical drains (c_r) based on free strain approach as well as equal strain approach. It is noted that free strain approach is complex; a large number of methods were developed based on equal strain approach. In this paper, these methods for the determination of c_v and c_r are summarized and compared. This review will be useful for researchers or practicing engineers for estimating the rate of settlement in the clay layer with/without drains.

Keywords Coefficient of consolidation · Vertical drainage · Radial drainage

1 Introduction

The analysis of consolidation settlement of soil has two main factors, one is the rate at which the settlement takes place, and the other is amount of settlement. The rate of compression can be found out by determining the coefficient of consolidation (c_v or c_r). For low permeable soil, the time required for consolidation is usually long if the drainage path is more. In such cases, in order to accelerate the process of

A. R. Pillai (✉)
Indian Institute of Technology Madras, Chennai, India
e-mail: araparnalachu4@gmail.com

S. R. Gandhi
Department of Civil Engineering, Indian Institute of Technology Madras, Chennai, India
e-mail: srgandhi@iitm.ac.in

T. Thyagaraj (ed.), *Ground Improvement Techniques and Geosynthetics*, Lecture Notes in Civil Engineering 14, https://doi.org/10.1007/978-981-13-0559-7_39

consolidation, vertical drains are installed at the site at a spacing which is less than the thickness of the clay layer. The purpose of vertical drain is to permit drainage in the horizontal direction to the nearest vertical drain which also helps to reduce the length of drainage path. The value of coefficient of consolidation, whether it is radial or vertical, is the most important factor that controls the accurate prediction of the rate of consolidation of the soil. Various methods for finding out the coefficient of consolidation using vertical and radial drainage along with the equations are as summarized in Tables 1 and 2 respectively.

Table 1 Summary of different methods for finding c_v

Method	Year	Author	Plot	Formula to find c_v
Log-time fitting method	1940	Casagrandes	Dial reading versus log*t*	$c_v = \frac{T_v H^2}{t_{50}}$
Root *t* method	1948	Taylors	Dial reading versus $\sqrt{t}$	$c_v = \frac{T_v H^2}{t_{90}}$
Su's Maximum slope	1958	Su	Dial reading versus log *t*	$d_u = [d_0 - (h/0.688 * U_{av})]$ $c_v = \frac{T_v H^2}{t_{50}}$
Velocity method	1978	Parkin	log(δ/t) versus log t	$c_v = \frac{TH^2}{t}$
Rectangular hyperbola	1981	Sridharan et al.	t/δ versus *t*	$c_v = \frac{TH^2}{t}$
Improved rectangular hyperbola method	1985	Sridharan et al.	t/δ versus *t*	$c_v = \frac{B(mH^2)}{c}$, $B = T(A-1)$
log δ/t–log*t* method	1992	Pandian et al.	log(δ/t) versus log *t*	$c_v = \frac{0.793H^2}{t_{88.5}}$
δ-δ/t method	1993	Sridharan et al.	δ versus δ/t	$c_v = \frac{TH^2}{t}$
Improved velocity method	1994	Pandian et al.	log(δ/t) versus log *t*	$c_v = \frac{0.524H^2}{t}$
LogH^2/t versus U_v curve, 1-point method	1995	Sridharan et al.	logH^2/t versus U_v	$c_v = \frac{T_v H^2}{t}$
Early log *t*	1996	Robinson et al.	δ versus log *t*	$c_v = \frac{0.0385H^2}{t_{22.14}}$
Improved root t method	1997	Tewatia et al.	Dial reading versus $\sqrt{t}$	Slope95 $= \frac{U95-U0}{\sqrt{T95}-\sqrt{T0}}$ $c_v = \frac{T_v i H^2}{t_i}$
Inflection point	1971 1997 1999	Cour Robinson Mesri	dδ/d(log *t*) versus log t	$c_v = \frac{0.405H^2}{t_{70}}$

Table 2 Summary of different methods for finding c_r

Method	Year	Author	Plot	Formula to find c_r
Taylors	1996	Sridharan et al.	Dial reading versus $\sqrt{t}$	$c_r = \frac{T_r d e^2}{t_{90}}$
Logde^2/t versus U_r curve, One point	1996	Sridharan et al.	logde^2/t versus U_r	$c_r = \frac{T_r d e^2}{t}$
Inflection point	1997	Robinson	dδ/d(log$t$) versus log t	$c_r = \frac{T_{63.21} * H^2}{t_{63.21}}$ $T_{63.21} = F(n)/8$ $F(n) = n^2/(n^2 - 1)$*ln $(n) - (3n^2 - 1)/4n^2$
Log-Log method	2009	Robinson et al.	Log (S-S_o) versus log$t$	$(S_2\text{-}S_o)/(S_1\text{-}S_o) = t_2/t_1$ $c_r = \frac{T_{66} * H^2}{t_{66}}$
Hyperbolic method	2009	Chung et al.	t/δ versus t	$c_r = (0.1333 \log_e(n) - 0.0906) \times (\beta d e^2/\alpha)$
Steepest tangent fitting method	2010	Vinod et al.	δ versus log t	$d_u = [d_0 - (h/0.848 * U)]$ $c_r = \frac{T_r d e^2}{t}$
Log method	2011	Sridhar et al.	δ versus log t	$c_r = \frac{T_{50} d e^2}{t_{50}}$

2 Coefficient of Consolidation for Vertical Drainage

A theoretical curve was plotted between the degree of consolidation (U) with the time factor (T). The experimental curve was obtained from the standard methods like Casagrande's logarithmic time fitting method (1940) and Taylor's square root time fitting method (1948). In this, dial gauge reading was plotted against the logarithm of time and square root of the time, respectively, is similar to the theoretical curve. In the Casagrande's method, after plotting the curve, a straight line was drawn through the points representing final reading. A second line tangent to the steepest part of the curve was then drawn. Both these lines will meet at a point, and dial gauge reading (δ_{100}) and time (t_{100}) corresponding to 100% consolidation was found out. In order to get compression ordinate at 0% consolidation (δ_0), two earlier times t_1 and t_2 was selected ($t_2 = 4t_1$), and the offset distance between t_1 and t_2 was found out, and plotted above t_1. In order to find the c_v value we need compression ordinate at 50% consolidation, [$\delta_{50} = (\delta_{100} + \delta_0)/2$]. Thus c_v value can be determined using drainage layer thickness H, Time factor T_v, and time t, for achieving 50% consolidation. This method can be used for soils which does not have an initial straight portion, but it takes time for secondary compression portion to establish. Su (1958) and Robinson et al. (1996) developed a method which makes use of the early log$t$, which requires time compression data only for shorter duration, i.e., the end portion of the curve is not important in this case. For the first method, δ – log$t$ plot was made, and δ_0 was determined as explained in log$t$ method. A tangent is drawn through the steepest part of the curve, to determine

the slope "*h*". For a chosen average value of degree of consolidation (U_{avg}), dial gauge reading, δ_u, was computed and corresponding time was noted to find c_v value. In the second method, the point of intersection between the tangent passing through the inflection point and the line passing through the corrected zero was noted and c_v value can be found out. Both the methods are not suitable for samples exhibiting more secondary compression. In the Taylors method, which is suitable for soils having high secondary compression, for the degree of consolidation, $U = 90\%$, the value of $\sqrt{t}$ is obtained by drawing a line 1.15 times the value obtained by the extension of the initial straight line portion of the dial reading versus $\sqrt{t}$ curve and the point where this line touches the curve is noted and thus t_{90} was obtained and c_v was found out. This method was then improved by Tewatia et al. (1997), and c_v value at any U, between 70 and 95% consolidation can be found out. These methods are not applicable for the rapidly consolidating sample.

A method which is more efficient than the standard methods, the velocity method, was developed by Parkin (1978), in which theoretical consolidation rate with time factor was plotted and along with this, experimental settlement rate was plotted with time. By overlaying both the graphs at $T = 1$, the time 't', was found out, from which we will get c_v value. Further studies of Parkins method, were made by Pandian et al. (1992), in which log dδ/dt versus log t was plotted and is divided into three parts, extrapolating the first two straight lines and corresponding t value at 100% consolidation was obtained. These methods do not give emphasis to initial and final parts of consolidation curve. The initial compression was not affected, in Rectangular hyperbola method, developed by Sridharan et al. (1981), in which the theoretical T/U versus T plot was made, and it starts from the origin, in which it is curve for some portion and then straight line over large values of T ($0.25 < T < 0.9$) corresponding to U value ($60 < U < 95$). The experimental t/δ versus t plot was made, when the straight line is fixed, lines through the origin 12.14, 2.02, 1.35 times the slope of the straight line was made. Where the first of the above line meets the straight line portion of the curve, gives t_{10}. Similarly the other two lines, t_{60} and t_{90} can be obtained. From R_{60} and R_{90}, R_0 and R_{100} can be made. Sridharan et al. (1985, 1987) further improved the above method and developed equations with some constants A and B. Values for A and B depends on the degree of consolidation and B value was computed for different U values, and founded as 0.3. Similar to the above method t/δ versus t was plotted, and after identifying straight line portion, slope 'm' and intercept 'c' were noted and thus c_v can be found out. Pandian et al. (1992a) suggested a new method of plotting U/T versus U in which, lines were extended from the initial portion and final portion of the curve, thus getting a T value of 0.793 at $U = 88.5\%$. Since evaluated through the intersection of points, less ambiguous and more accurate. Sridharan et al. (1993), proposed δ-δ/t method, which has a flatter slope than root t which makes it more accurate, in which theoretical curves of U–U/T was plotted and then experimental δ-δ/t was made to get time corresponding to 90% consolidation. From the straight line portion of the curve, a flatter slope of 1.33 times, that of, identified initial straight line is drawn, unlike 1.15 in $\sqrt{t}$ method. It was found that the line intersects the curve at 90%

primary consolidation. Sridharan et al. (1995) developed two methods, (H^2/t) versus U curve as well as One point method in which the experimental curve coincides directly with the theoretical curve. At first, theoretical Log_{10} (H^2/t) versus U curve was plotted by assuming different values of c_v and U, and then the experimental curve was plotted above theoretical curve. The point where the experimental curve coincides with the theoretical curve was noted and corresponding H^2/t value was taken and substituting into the equation to get c_v value. It was found that, the experimental curve coincides with the theoretical curve fairly well in the range of U = 40–60%. In one point method the values between this 40–60% was taken and c_v value was found out directly. Inflection point method, which doesn't require graphical construction was first proposed by Cour (1971), later it was explained by Robinson (1997) and Mesri (1999). dU/d(log$T$) versus log$T$ was plotted and inflection point was found at U = 70.15% and hence T can be evaluated, from that c_v can be determined.

3 Coefficient of Consolidation for Radial Drainage

The basic theory of radial drainage was proposed by Barron (1948). McKinlay (1961) developed a method for determination of c_r based on the linear relationship between U_r versus T_r in the range of U_r from 0 to 50% in the case of peripheral drain. Based on the linear relationship between U_r versus T_r in the range of U_r from 20 to 60%, Berry and Wilkinson (1969) suggested another method in the case with a central drain. Both of these methods are based on free strain hypothesis, which is complex. Based on equal strain conditions, a number of methods have been developed for radial consolidation analysis. Most of the methods used to find c_v were extended to find c_r value. Taylors method, Casagrandes method, Inflection point method, LogH^2/t versus U_v curve, One point method etc. were extended to find c_r value. These methods along with formulas are as shown in Table 2. Robinson et al. (2009) proposed log–log method, which reflects actual ground conditions, Log(S-S_0) versus Log$t$ graph was plotted [(S-S_0 is the corrected settlement and t is the time]. Straight lines were drawn from the initial portion and end portion of the curve. The two lines meet at a point which was taken as the time, t at 66% consolidation. A hyperbolic method was developed for estimating the coefficient of radial consolidation that are only suitable to 60–90% degree of consolidation, based on the hyperbolic relationship of settlement(s) versus time(t) and on the Barron's solution (Chung et al. 2009). Equations are as given in Table 2. α and β are the intercept and the slope of the initial linear line respectively in the t/s versus t plot. Su's method (1958) was extended to the Barron's solution for determining c_r value in tangent fitting method (Vinod et al. 2010).

4 Conclusion

Various methods to find the coefficient of consolidation for vertical as well as radial drainage has been reviewed. It is observed that there are various methods for determination of c_v whereas only a few methods to find c_r. Further Research is in progress to develop new and simple method for estimating the coefficient of consolidation for radial drainage, even by extending the available methods for finding out the c_v value based on a detailed laboratory test.

References

Barron, R. A. (1948). Consolidation of fine grained soils by drain wells. *Transactions of ASCE, 113,* 718–724.

Berry, P. L., & Wilkinson, W. B. (1969). The radial consolidation of clay soils. *Geotechnique, 19* (2), 253–284.

Casagrande, A., & Fadum, R. E. (1940). *Notes on soil testing for engineering purposes*. Soil Mechanics Series No. 8, Pub. No. 268, p. 37. Cambridge: Harvard University.

Chung, S. G., Lee, N. K., & Kim, S. R. (2009). Hyperbolic method for prediction of prefabricated vertical drains performance. *Journal of Geotechnical and Geoenviromental Engineering*, 1519–1528.

Cour, F. R. (1971). Inflection point method for computing Cv. *Journal of Soil Mechanics and Foundations Division, ASCE, 97*(SM5), 827–831.

McKinlay, D. G. (1961). A laboratory study of consolidation in clays with particular reference to conditions of radial pore water drainage. In *Proceedings of the 5th International Conference on SM&FE*, Paris (Vol. 1, pp. 225–228).

Mesri, G., Feng, T. W., & Shahien, M. (1999). Coefficient of consolidation by inflection point method. *Journal of Geotechnical and Geoenvironmental Engineering, ASCE, 125*(8), 716–718.

Pandian, N. S., Sridharan, A., & Kumar, K. S. (1992a). A new method for the determination of coefficient of consolidation. *Geotechnical Testing Journal, ASTM, 15*(1), 74–79.

Pandian, N. S., Sridharan, A., & Kumar, K. S. (1992b). Improved velocity method for the determination of coefficient of consolidation. *Geotechnical Testing Journal, ASTM, 17*(1), 113–118.

Parkin, A. K. (1978). Coefficient of consolidation by the velocity method. *Geotechnique, 28*(4), 472–474.

Robinson, R. G., & Allam, M. M. (1996). Determination of coefficient of consolidation from early stage of log t plot. *Geotechnical Testing Journal, ASTM, 19*(3), 316–320.

Robinson, R. G. (1997). Consolidation analysis by an inflection point method. *Geotechnique, 47* (1), 199–200.

Robinson, R. G. (2009). Analysis of radial consolidation test data using a log-log method. *Geotechnical Testing Journal, ASTM, 32*(2), 119–125.

Sridharan, A., & Sreepada, Rao, A. (1981). Rectangular hyperbola fitting method for one dimensional consolidation analysis. *Geotechnical Testing Journal, 4*(4), 161–168.

Sridharan, A., & Prakash. (1985). Improved rectangular hyperbola method for the determination of coefficient of consolidation. *Geotechnical Testing Journal, ASTM,* 8(1), 37–40.

Sridharan, A., Murthy, N. S., & Prakash, K. (1987). Rectangular hyperbola method of consolidation analysis. *Geotechnique, 37*(3), 355–368.

Sridharan, A., & Prakash, K. (1993). δ-δ/t method for the determination of coefficient of consolidation. *Geotechnical Testing Journal, 16*(1), 131–134.

Sridharan, A., Prakash, K., & Asha, S. R. (1995). Consolidation behaviour of soils. *Geotechnical Testing Journal, ASTM, 18*(1), 58–68.

Sridharan, A., Prakash, K., & Asha, S. R. (1996). Consolidation behaviour of clayey soils under radial drainage. *Geotechnical Testing Journal, ASTM, 19*(4), 421–431.

Sridhar, G., & Robinson, R. (2011). Determination of radial coefficient of consolidation using log t method. *International Journal of Geotechnical Engineering, 5,* 373–381.

Su, H. L. (1958). Procedure for rapid consolidation test. *Journal of the Soil Mechanics and Foundations Division, ASCE, 95*, 1–9 (Proc. paper 1729).

Taylor, D. W. (1948). *Fundamentals of soil mechanics*. New York: Wiley.

Tewatia, S. K., & Venkatachalam, K. (1997). Improved rectangular $\sqrt{t}$ method to evaluate consolidation test results. *Geotechnical Testing Journal, 8*(1), 37–40.

Vinod, J. S., Sridharan, A., & Indraratna, B. (2010). Determination of radial coefficient of consolidation using steepest Tangent fitting method. *Geotechnical and Geological Engineering, 28*, 533–536.

Comparative Analysis of Strength Characteristics of Soil Reinforced with Coir and Polypropylene Fibers

Sajal Pachauri, M. Indu Priya and Ankit Garg

Abstract Ground improvement through fiber-reinforced soil has been in practice in the recent past. However, with increasing concern for sustainable development, researchers are encouraged to investigate alternative forms of reinforcement than the mainstream synthetic fibers. Coir fibers have been in practice as an alternative natural fiber for ground improvement. In this study, fibers extracted from a local coconut plantation were used to improve the strength characteristics of a local hill soil. The strength characteristics of the soil-coir fiber composite have been compared with the same soil reinforced with synthetic polypropylene fiber. The study investigates the strength variation and change in ductility of both soil-fiber composite with respect to bare soil. The fiber percentage added to soil was selected at 0.5, 0.75 and 1% of the dry weight of soil. A series of unconfined compressive strength (UCS) tests were conducted to ascertain the strength characteristics of the soil. The reinforcement strength results of the soil-coir fiber composite show the efficacy of using such a natural fiber to improve the soil strength characteristics.

Keywords Polypropylene · Coir · Unconfined compressive strength
Fiber composition

1 Introduction

In the modern times, when the world is facing an acute problem of land shortage coupled with poor soil property, the need of soil reinforcement has gained traction. Reinforcement of such soils is required to improve the engineering properties, thus increasing the shear strength and ductility (Vidal 1969). In the past, a large range of tensile inclusions ranging from low-modulus polymeric materials to high tensile strength metallic sheets has been used (Hejazi et al. 2012). However, the inherent disadvantages of such planar inclusions are the existence of an inherent plane of weakness. Fiber reinforcement has been popularly used in shallow depth soil

S. Pachauri (✉) · M. Indu Priya · A. Garg
Indian Institute of Technology, Guwahati, Guwahati 781039, India

T. Thyagaraj (ed.), *Ground Improvement Techniques and Geosynthetics*, Lecture Notes in Civil Engineering 14, https://doi.org/10.1007/978-981-13-0559-7_40

reinforcement, due to its inherent advantages (strength isotropy, increased ductility), which is generally not provided by the aforementioned planar reinforcement (Maher and Gray 1990). This soil-fiber composite is conventionally discussed as randomly distributed fiber reinforced soil (RDFS). Among the fibers used in RDFS, they are briefly discussed as natural and synthetic fiber. The common synthetic fibers used are polypropylene fiber, glass fiber and nylon fibers. They are basically by-products of petroleum—thus exhaustive and relatively costly compared to natural fibers (Hejazi et al. 2012). The utility of using natural fibers over synthetic fibers in specific sites is due to its cheap cost, easy availability and its favorability to subsequent vegetation. Such sites, where the mechanical strength provided by this natural reinforcement is required for short-term constructions (1–2 years) such as approach roads, landfill cover system, military roads; this form of reinforcement is ideal and cost effective.

One of the natural fibers used in the current study is coir. Coir is derived from coconut, Cocos Nucifera, and is one of the most popular natural fibers used in soil reinforcement (Faruk et al. 2012). It has remarkable property of adapting to various soil types, and can be found throughout the tropical and subtropical regions of the world. Coir contains high percentage of lignin, which leads to a relative high degradation life of the fiber. According to a study, the service life of coir fiber during its use in field is found to be from 4 to 10 years and thus makes it suitable for soil reinforcement.

The objective of the work was to find out the strength characteristics of coir fiber-reinforced soil. The results based on the stress–strain response from a series of unconfined compressive strength (UCS) test, are compared with polypropylene (PP) fiber-reinforced soil. The tests were carried out for three percentages for both fiber type in the soil viz. 0.5, 1, and 1.5% of the dry soil mass. The effect of compaction state (i.e., the density and water content), on the strength and ductility of soil-fiber composite has been investigated. The density of soil-fiber composite was kept at 0.95 MDD (Maximum Dry Density), MDD and 1.05 MDD; while the moisture content was selected at optimum moisture content (OMC), (OMC −5%) and (OMC +5%). Based on the results obtained from the tests conducted, the effect of compaction on strength characteristics of soil has been discussed. The inclusion of fiber reinforcement and its subsequent effect on the stress strain response has been discussed in detail.

2 Materials and Methods

The soil used in the tests was collected from a local construction site. The grain size distribution of the soil sample was done as per the provisions of IS-2720-Part 4-1985. The percentage of silt in the soil was 53.07% whereas the clay percentage was found to be 24.34%. Various other physical properties of the soil are as listed in Table 1.

Table 1 Physical properties of soil

Properties	Values
Specific Gravity, G_s	2.65
Atterberg limits	
Liquid limit (%)	42.50
Plasticity index (%)	15.59
Size fraction	
Classification[a]	ML
Compaction characteristics	
Optimum moisture content (OMC)	16.72%
Maximum dry density (MDD)	1.75 g/cc

[a]As per USCS

Table 2 Properties of Coir fiber

Properties	Values
Bio-chemical characteristics	
Cellulose	48.2%
Hemicellulose	14.7%
Lignin	39.5%
Ash content	2%
Physical characteristics	
Specific gravity	0.67
Thickness of fiber	0.4 mm
Tensile strength	250 N

Coir used as reinforcement in this study is a natural fiber. Mainly derived from plants, natural fibers are referred to as cellulosic and lignocellulose fibers (Methacanon et al. 2010). The three main constituents of natural fibers are cellulose, hemicellulose, lignin, and ash. Cellulose is responsible for the tensile strength of natural fibers. The hemicellulose plays an important role in moisture absorption by fibers. Ash content acts as a measure of the mineral content and other inorganic matter in a biomass and also provides natural capacity of plant for metal adsorption. Due to relatively high amount of lignin and high resistance to biodegradation, coir is the one of the most popular fibers used for reinforcing soil. The general properties of coir fiber are given in Table 2.

2.1 Sample Preparation and Test Procedure

The fibers of length 15 mm and required fiber content were taken and uniformly mixed with dry soil, and subsequently water was added to the mixed soil. The composite was kept in desiccator for 24 h before UCS samples were made in an in-house developed mould at the selected compaction density. The Proctor's light

compaction technique was used for soil sample testing and determination of MDD and the OMC. The UCS test was performed at a constant strain rate of 1.25 mm/min in accordance with IS-2720 part-10-1991, to determine the strength of the reinforced soil. The addition of fibers was restricted to 1%, to avoid formation of low density pockets in the soil-fiber composite.

3 Results and Discussions

Figure 1 shows the stress–strain curves of plain soil and soil reinforced with coir and PP fibers at 0.5% fiber content. It is evident that the peak strength of the soil is higher after fiber inclusion. This was because fiber interface. Failure of the UCS sample occurs when the alied shear stress exceeds the interarticle friction interface. Failure of the UCS sample occurs when the applied shear stress exceeds the interparticle friction inclusion increased the friction at the fiber-soil causing the soil to fail at a particular failure plane. The increase in friction resisted the shear stress and increased the strength of the fiber reinforced soil samples leading to bridging effect of the fibers (Fig. 1a, b). This bridging effect restricts soil particles to roll over

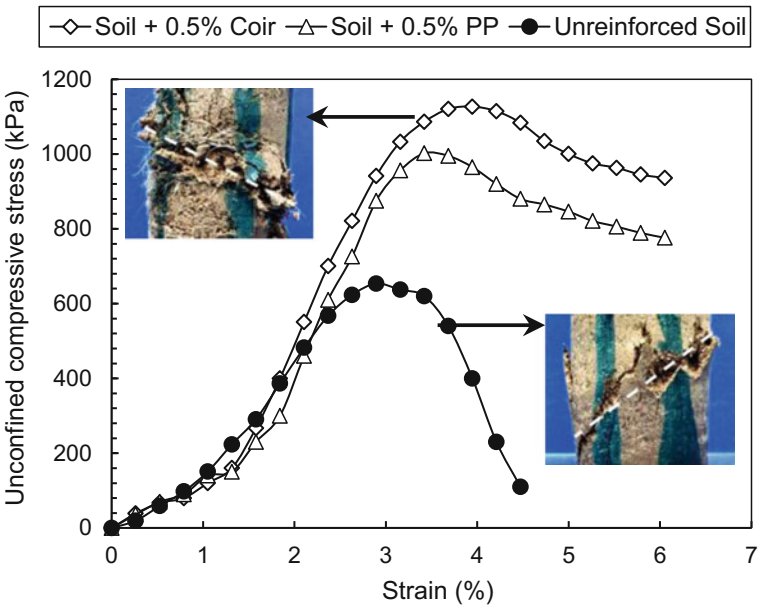

Fig. 1 Stress–strain relationship of soil fiber composite

in the shear plane. Randomly distributed fiber reinforcement also prevented the formation of a single failure plane thus delaying the failure of the UCS sample.

The drop in post peak strength in unreinforced sample was much higher (83%) than coir (16%) and PP (22%). This is because in the absence of fibers, once the unreinforced sample fails, it loses its resistance against shear stress as the only friction acting is due to rolling of the soil particles against each other. The fibers help in interlocking the surrounding soil and resisting slippage. Hence, even after the soil loses its strength, the fiber-soil composite shows residual strength due to the tenacity of the fibers. The peak strain corresponding to the peak strength of the soil increased from unreinforced, PP-reinforced to coir-reinforced indicating the increase in ductility of the samples. Coir sample had higher peak strength and peak strain as well as a lower drop in post peak strength than PP sample.

The variation of mean UCS with density for coir and polypropylene fiber reinforced soil in comparison to unreinforced soil is presented in Fig. 2. It could be observed that the strength of reinforced soil was much higher than that of unreinforced soil for the corresponding water content. UCS of soil increased with the density of the soil sample. As density increased, the packing of soil articles becomes closer which led to a higher abrasion between the particles. Denser packing also increased matric suction, hence, the strength of the sample. Similar trend could be noted with a variation of moisture content in the soil. The strength of soil decreased with increasing water content and the maximum strength values were that of the samples with OMC-5% water content. At a micro-level, water present in the voids reduced the friction between the soil particles because water cannot resist shear force. So as water content increased, the strength of the soil decreased.

From Fig. 2 it can be observed that there is no specific trend followed by the varying fiber content of the soil. However, optimum fiber contents at which the reinforcement was at its highest efficiency for coir and PP fibers were found to be 1 and 0.75% respectively.

While both fibers showed improvement of strength over unreinforced soil samples, coir-reinforced samples exhibited relatively higher values of strength than that of polypropylene-reinforced samples. Due to the rougher surface of the natural fiber, coir fibers offered more shear resistance than the polypropylene fibers and enhanced the strength of the soil sample. Coir also has lesser specific gravity than PP. Therefore, the number of discrete coir fibers in unit volume of the sample was higher than the number of PP fibers. This led to higher friction and cohesion in the coir-reinforced samples. With higher UCS, ductility and tensile strength, coir fibers indicated better reinforcement than PP fibers, reaching its maximum efficiency at OMC-5% water content.

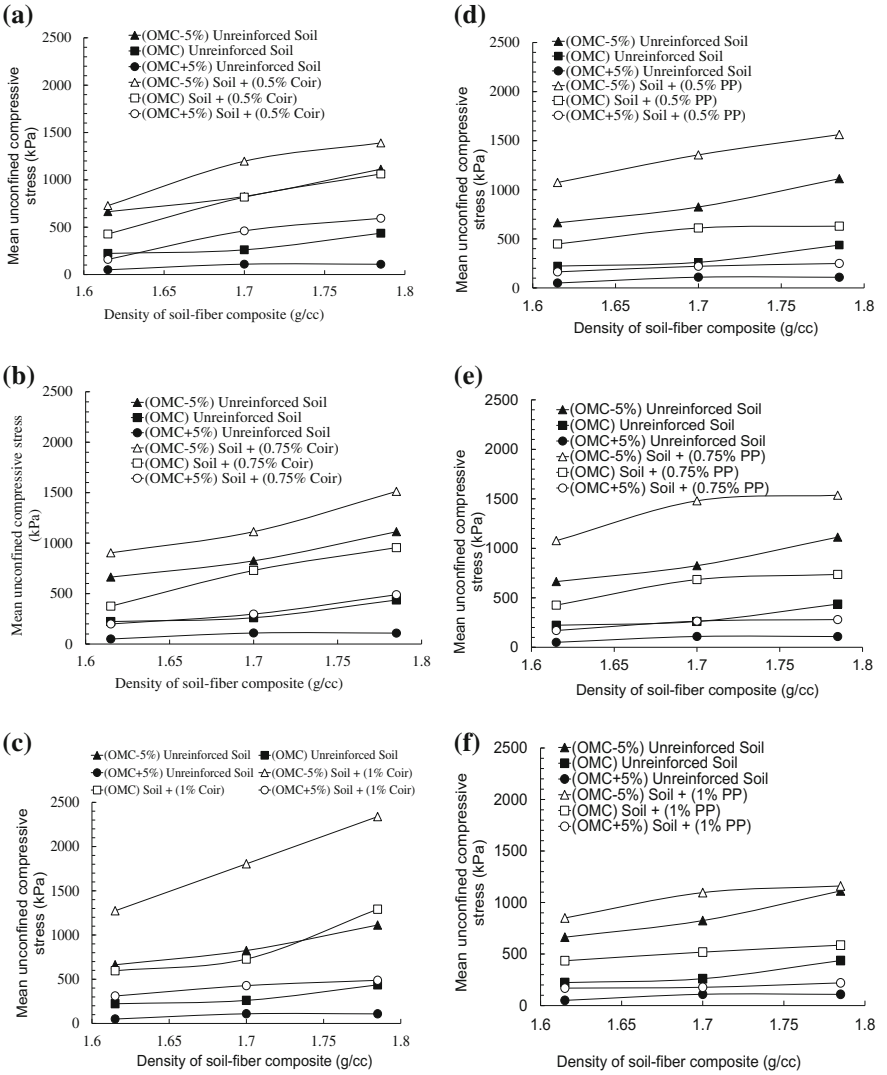

Fig. 2 UCS variation of soil-fiber composite with density and fiber content in **a–c** coir fiber reinforced soil and (**d–f**) PP fiber reinforced soil

4 Conclusions

In this study, UCS tests were done on unreinforced, coir-reinforced, and PP-reinforced samples with varying moisture contents, densities, and fiber contents. It was observed that fiber inclusion increased not only the peak strength of the samples but also its ductility. It was also noted that water content of 5% dry of

optimum moisture content showed the maximum strength. Moreover, soil samples reinforced with coir fibers were equally efficient (if not more) in resisting shear stress and showed higher strength characteristics than conventional polypropylene-reinforced soil samples. Thus, this study concludes that coir as natural fiber reinforcement could be successfully employed in field where short-term and effective fiber reinforcement is desired.

References

Faruk, O., Bledzki, A. K., Fink, H. P., & Sain, M. (2012). Biocomposites reinforced with natural fibers: 2000–2010. *Progress in Polymer Science, 37*(11), 1552–1596.

Hejazi, S. M., Sheikhzadeh, M., Abtahi, S. M., & Zadhoush, A. (2012). A simple review of soil reinforcement by using natural and synthetic fibers. *Construction and Building Materials, 30,* 100–116.

Maher, M. H., & Gray, D. H. (1990). Static response of sands reinforced with randomly distributed fibers. *Journal of Geotechnical Engineering, 116*(11), 1661–1677.

Methacanon, P., Weerawatsophon, U., Sumransin, N., Prahsarn, C., & Bergado, D. T. (2010). Properties and potential application of the selected natural fibers as limited life geotextiles. *Carbohydrate Polymers, 82*(4), 1090–1096.

Vidal, H. (1969). The principle of reinforced earth. *Highway Research Record, 282.*

Geo-engineering Properties of Sedimented Flyash Bed Stabilized by Chemical Columns

Aparupa Pani and Suresh Prasad Singh

Abstract Ash ponds cover up enormous stretches of valuable land and accounts environmental problem. Adaptation of appropriate in-place stabilization technique may bring about enhancement in the geotechnical properties of the ash deposit as a whole, transforming it into a worthy construction site. In this present experimental program, large-scale laboratory model test tank of diameter 105 cm with 120 cm height has been filled with ash slurry at 70% water content with a centrally installed chemical column of sodium hydroxide (1% of NaOH by dry weight of the ash in the bed) having a diameter of 20 cm. Undisturbed samples were collected from different radial distances of 15, 25, 35, and 45 cm after curing periods of 7, 30, 60, and 90 days and the in-situ water content, dry density, unconfined compressive strength, and hydraulic conductivity were measured. This method has been found more efficient in increasing the unconfined compressive strength and reducing hydraulic conductivity of the ash deposits in addition to altering other geotechnical parameters like in-situ water content and dry density. A substantial strength increment was noticed up to a radial distance of $2D$ (where D is the diameter of the chemical column) from the center of the column.

Keywords Flyash · Chemical column · Unconfined compressive strength Hydraulic conductivity

A. Pani (✉) · S. P. Singh
Department of Civil Engineering, National Institute of Technology, Rourkela, Rourkela 769008, India
e-mail: aparupapani@gmail.com

S. P. Singh
e-mail: spsingh@nitrkl.ac.in

T. Thyagaraj (ed.), *Ground Improvement Techniques and Geosynthetics*, Lecture Notes in Civil Engineering 14, https://doi.org/10.1007/978-981-13-0559-7_41

1 Introduction

The exponential increase in the generation of fly ash in India has been reached up to 170 million tons per every year posturing serious disposal problems and environmental issues. It is calculated that, in India, about 20,000 ha of valuable land is covered with abandoned ash ponds. These ash deposits possess very low density, high compressibility, and poor bearing capacity, and are generally considered inappropriate for any construction activity. However, it may be feasible to use some suitable in-situ stabilization techniques to enhance the geotechnical properties of the ash deposits as a whole converting it to a construction worthy site.

In-situ chemical stabilization is a promising method of stabilization to improve the geotechnical parameters of soft compressible ground. Available literature is very scarce. Here are few literatures on in-situ chemical stabilization technique. Rajasekaran and Rao (1997) conducted laboratory tests on stabilization of marine clay by lime column technique. It is reported that a significant enhancement of engineering properties occurred due to migration of lime from lime injection zone. Hua and van Deventer (2002) observed significant increases in compressive strength when NaOH and KOH mixed together with flyash, kaolinite, and albite. It is also observed that when a calcined source material (i.e., fly ash) is added it not only improved the compressive strength, but also a substantial reduction in reaction time. Granizo et al. (2002) observed that the alkali activation of metakaolin (MK) by injecting calcium hydroxide $Ca(OH)_2$ to the raw MK produces a different reaction structure and C–S–H gel form. Kamarudin et al. (2011) studied the early age strength gain for kaolin at day-1 and day-2 of curing. It is noticed that when NaOH concentration increases from 8 to 12 M the strength increases but the strength drops at 14 M of solution due to higher concentration.

Several efforts have been made to enhance the geo-engineering properties of fly ash by mixing lime and chemicals through mechanical mixing method. Joshi et al. (1975), Usmen and Bowders (1990), Malhotra (1994), and Ghosh and Subbarao (2001, 2006) have studied various geo-engineering properties of fly ash mixed with different chemicals. However, mechanically excavating and mixing is cumbersome and expensive. The lime column technique is suitable as an alternative approach but it gives later age strength and very slow migration of lime. Therefore an attempt has been made to improve the geo-engineering properties of sedimented ash deposits by in-place chemical stabilization technique. It may improve the geo-engineering properties of ash deposits at an early age of curing such that the massive ash pond sites become construction worthy site.

2 Materials

2.1 Fly Ash and Alkali

The fly ash used in this experimental work was brought from Adhunik Metaliks Ltd. Rourkela. The specific gravity of flyash was found to be 2.44. The grain size distribution of the fly ash sample was analyzed as per IS: 2720 part (IV), 1975. The percentage of particles <75 μm was found to be 88%. The Cu and Cc values were found to be 8.34 and 2.08 respectively; indicating uniform gradation of the sample shown in Fig. 2. The major constituents of fly ash are silica, alumina, and iron oxide shown in Table 1. Calcium present in the fly ash is less than 20%. So, according to ASTM specification C 618-89 (1992), this fly ash belongs to a Class-F category. Sodium hydroxide (NaOH) pellets from Loba chemicals Mumbai having 99% purity was used in this test programme.

3 Experimental Program

3.1 Preparation of Model Test Tank

In the present study, a large circular galvanized iron test tank is used having diameter 105 and 120 cm height open at the top shown in Fig. 1. In order to prepare the sedimented flyash bed, approximately 1 ton of fly ash sample was used and the quantity of water essential for flowable fly ash slurry is determined from step-by-step water addition. The optimum moisture content without bleeding of water from the fly ash was found to be 70%. The restricted tank boundary of the prepared semi-infinite ash bed may possibly apply a negligible confining pressure which has not much effect over the larger area/ the findings. Before placing slurry in the test tank, a steel casing with GI mesh of small aperture has been placed exactly at the center of test tank. This ash slurry remained in place for an initial sedimentation period of 30 days to facilitate sedimentation and consolidation under self-weight (Fig. 2).

Table 1 Chemical composition of fly ash

Constituents	Percentage	Constituents	Percentage
SiO_2	59.2	MgO	1.3
Al_2O_3	17.9	SO_4	1.2
Fe_2O_3	9.5	Unburnt Carbon	7.0
CaO	3.2	Others	0.7

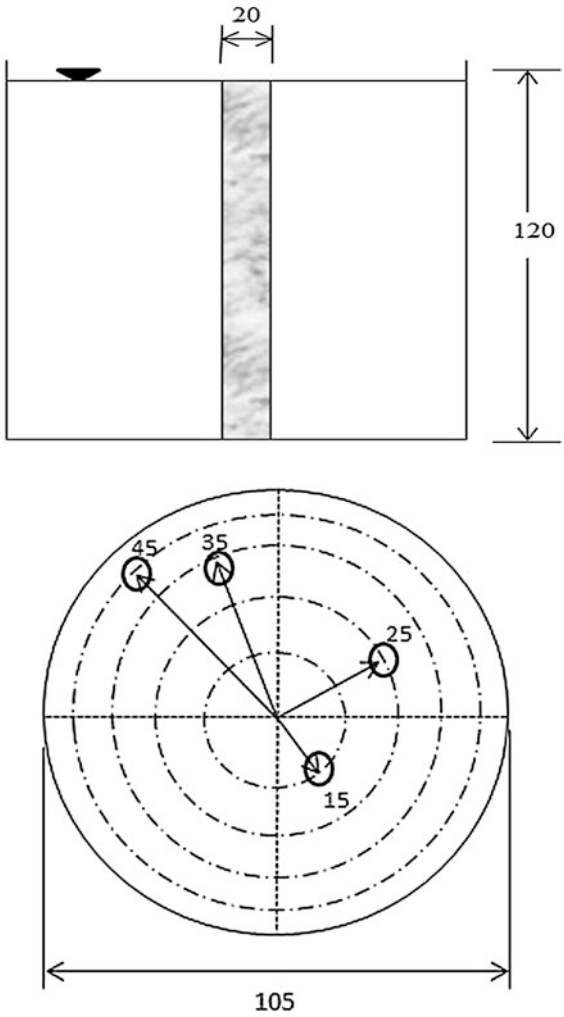

Fig. 1 Details of model test tank showing all sampling locations (all dimensions are in cm)

3.2 Installation of Chemical Column

At the completion of initial sedimentation period of 30 days, the NaOH of 1% by dry weight of flyash was mixed thoroughly with water and poured into the perforated GI mesh having 20 cm diameter has been placed exactly at the center of test tank. Thus, a column of NaOH was neatly installed at the center of the ash bed. The samples were collected at different radial distances 15, 25, 35, and 45 cm from the center of the chemical column after 7, 30, 60 and 90 days of curing.

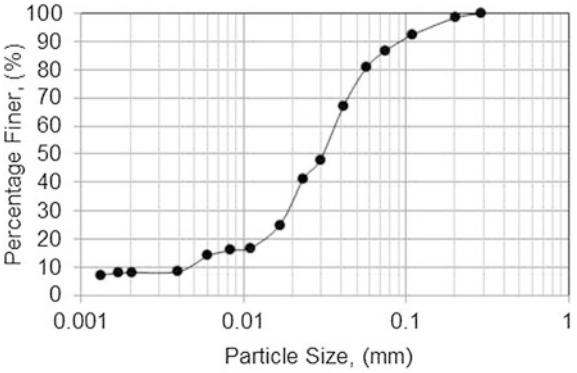

Fig. 2 Gradation curve of flyash

3.3 Details of Test Program

After specified curing period samples were subjected to following laboratory tests in addition to finding out the in-situ density and moisture contents.

3.3.1 Unconfined Compressive Strength Test

Undisturbed samples of 50 mm diameter and 100 mm height were collected by introducing thin wall samples in the test tank at specified locations at the end of each curing period. The tests were conducted according to IS: 2720 (Part-10)—1991 and the average value of three samples are reported.

3.3.2 Hydraulic Conductivity Test

Undisturbed specimens collected from different locations after specified curing periods were subjected to falling head test according to IS: 2720(Part-17)—1987.

4 Results and Discussion

4.1 In-Situ Water Content and Dry Density

The in-situ water content and dry density at different radial distance and curing period are shown in Figs. 3, 4, 5, and 6. It is observed that due to continuous migration of chemicals from the column and formation and deposition of hydration products the dry density continuously increases whereas the in-situ m/c decreases. These changes are more prominent up to a radial distance of 2*D* (where *D* is the diameter of the chemical column).

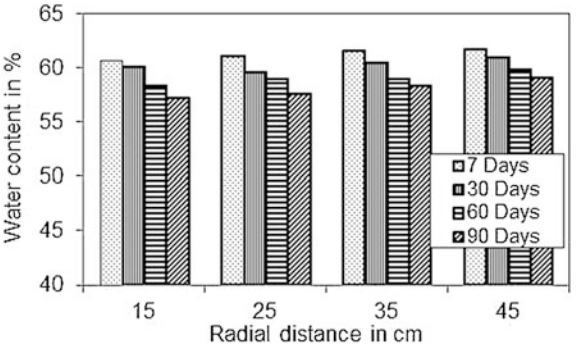

Fig. 3 Variation in in-situ water content at different radial distances

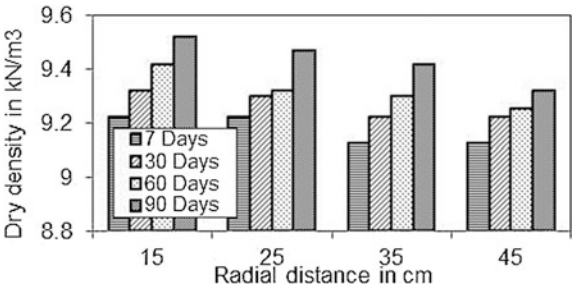

Fig. 4 Variation in in-situ dry density at different radial distances

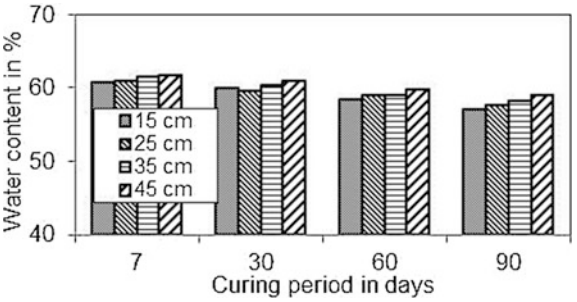

Fig. 5 Variation in in-situ water content at different curing periods

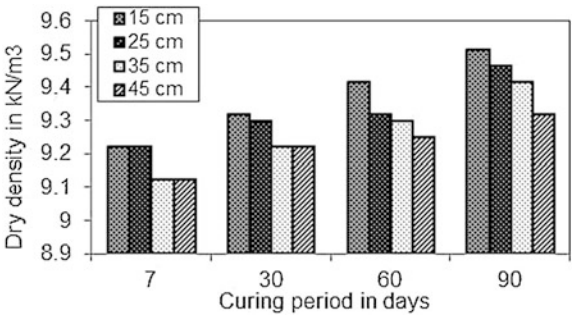

Fig. 6 Variation in in-situ dry density at different curing period

4.2 Unconfined Compressive Strength

The unconfined compressive strength determined at radial distances of 15, 25, 35, and 45 cm after 7, 30, 60, and 90 days of curing are shown in Fig. 7. The flyash mostly contains silica and alumina and the alkali solution migrates from the column; it reacts with the soluble Al–Si present in the fly ash and produces alumino-silicate gel. Therefore, the column ensues quick formation of hydration products which makes the surrounding ash impermeable and results in a gain in strength and a reduction in the hydraulic conductivity. Furthermore, significant increment in strength is observed up to a curing period of 60 days thereafter no appreciable increase in strength is noticed. These changes are more prominent up to a radial distance of 2*D* beyond this no substantial increase in strength is noticed. Correspondingly, in this study about 1 ton of fly ash sample in a large circular galvanized iron test tank has been used and surely this cannot represent a semi-infinite ash bed. However, as the diameter of the tank is more than five times the column diameter; the boundary effects can be neglected.

4.3 Hydraulic Conductivity

The hydraulic conductivity of sedimented ash deposits collected from radial distances of 15, 25, 35, and 45 cm after 7, 30, 60 and 90 days of curing are determined and these are presented in Figs. 8 and 9. It is observed that at a given curing period the hydraulic conductivity is the minimum at locations closer to the column and the same increases with increase in the radial distance. Further as expected the hydraulic conductivity at a given location decreases with the increase in curing period. This is due to the reaction of NaOH with flyash and formation alumina-silicate gel which reduces the capillary voids. This in turn reduces the hydraulic conductivity.

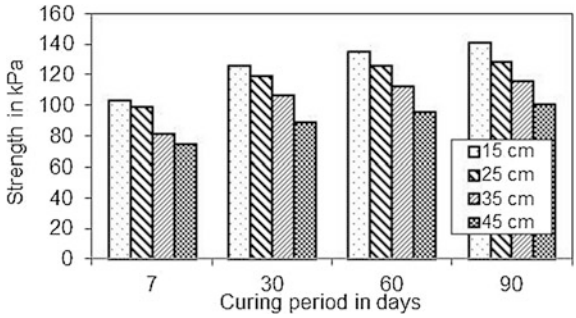

Fig. 7 Compressive strength variation at different curing periods

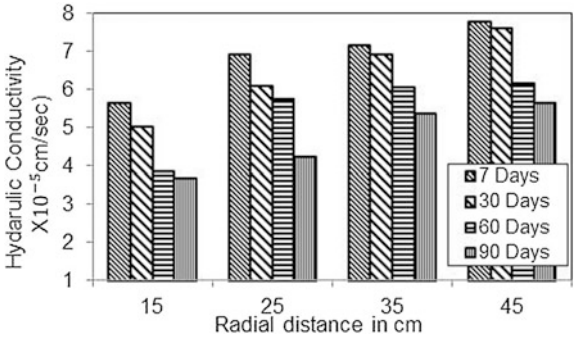

Fig. 8 Variation of coefficient of permeability value with radial distance

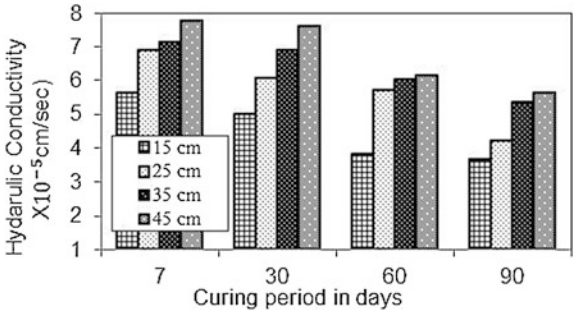

Fig. 9 Variation of coefficient of permeability value with curing period

5 Summary and Conclusions

Chemical stabilization of sedimented ash deposits by mechanical mixing is cumbersome and expensive; emphasis has been done in the application of the in-place chemical column technique for stabilization of sedimented flyash deposits.

It is observed that at a given location the in-situ dry density increases whereas the in-situ moisture content and permeability value is found to decrease with curing period. A substantial increment in strength is observed up to a radial distance of $2D$ from the center of the column. No substantial increase in strength is noticed after a curing period of 60 days.

This technique is found effective in increasing the unconfined compressive strength and reducing hydraulic conductivity of the ash deposits in addition to altering other geotechnical parameters like in-situ water content and dry density.

The chemicals migrate from the column in radial directions. The concentration of the chemical diminishes with radial distance and curing period. Furthermore, the hydration products make the surrounding ash impermeable so it prevents the migration of substantial amount of chemicals beyond a radial distance of $2D$ which regulates the environmental harmfulness.

References

Ghosh, A., & Subbarao, C. (2001). Microstructural development in fly ash modified with lime and gypsum. *Journal of Materials in Civil Engineering, 13*(1), 65–70.

Ghosh, A., & Subbarao, C. (2006). Tensile strength bearing ratio and slake durability of class F fly ash stabilized with lime and gypsum. *Journal of Materials in Civil Engineering, 18*(1), 18–27.

Granizo, M. L., Alonso, S., Blanco-Varela, M. T., & Palomo, A. (2002). Alkaline activation of metakaolin: Effect of calcium hydroxide in the products of reaction. *Journal of the American Ceramic Society, 85*(1), 225–231.

Joshi, R. C., McMaster, H. M., & Duncan, D. M. (1975). New and conventional engineering uses of fly ash. *Transportation Engineering Journal, 101*(4), 791–806.

Kamarudin, H., Al Bakri, A. M., Binhussain, M., Ruzaidi, C. M., Luqman, M., Heah, C. Y., et al. (2011). Preliminary study on effect of NaOH concentration on early age compressive strength of kaolin-based green cement. In *Proceedings of International Conference on Chemistry and Chemical Process (ICCCP 2011).*

Malhotra, V. M. (1994). *Fly ash in concrete* (2nd ed.). Ottawa, Canada: CANMET Publication on Concrete.

Rajasekaran, G., & Narasimha Rao, S. (1997). Lime stabilization technique for the improvement of marine clay. *Soils and Foundations, 37*(2), 97–104.

Usmen, M. A., & Bowders, J. J. (1990). Stabilization characteristics of class F fly ash. *Transportation Research Record, 1288*, 59–69. Washington, D.C.: Transportation Research Board.

Xu, H., & Van Deventer, J. S. (2002). Geopolymerisation of multiple minerals. *Minerals Engineering, 15*(12), 1131–1139.

A Short Review of Geosynthetic Granular Column Treatment of Soft Clay Soils

J. Jayapal and K. Rajagopal

Abstract In urban areas scarcity of land to build infrastructure has driven the geotechnical engineers to improve poor subsoil conditions through different techniques. Granular column treatment is one of the most promising ground improvement techniques widely practiced all over the world. This paper discusses briefly the status of research on this topic. Focus is on the recent advancement of encasing these columns with geosynthetic products to enhance their performance in load bearing capacity and reducing the foundation settlements. This paper is divided into analytical, experimental, numerical and field studies on the aspect of encased granular columns (EGCs) which have been published in the past three decades. The primary objective of this study is to compile the above said aspects of EGCs into one single source of information to interested researchers in this field. Lot of studies have been conducted mainly on the laboratory aspects of EGCs. Very few attempts have been made by researchers to study the mechanism of granular columns at full-scale levels through field tests. Finally a brief summary with necessary discussions is provided on the efforts made so far in studying the behavior of EGCs.

Keywords Ground improvement · Granular column · Encased granular column Geosynthetics · Field study

J. Jayapal (✉) · K. Rajagopal
Department of Civil Engineering, Indian Institute of Technology Madras, Chennai 600036, India
e-mail: jayapal.jp@gmail.com

K. Rajagopal
e-mail: gopalkr@iitm.ac.in

T. Thyagaraj (ed.), *Ground Improvement Techniques and Geosynthetics*, Lecture Notes in Civil Engineering 14, https://doi.org/10.1007/978-981-13-0559-7_42

1 Introduction

Enhancing the infrastructure facilities has become essential for improving the economic conditions in different parts of the country. Due to increasing pressure on the land availability the engineers are forced to develop these projects even in areas with poor sub-soil conditions. Granular column treatment is one such technique widely practiced to overcome the problematic soils. The characteristic features of problematic soils include low shear strength, high settlement and their susceptibility to liquefaction. Soft clays and loose sands are the predominant problematic soils where no construction is possible without ground improvement. Granular columns are cylindrical columns made up of either stone aggregate or coarse grained sand installed in the soft clay soils to support flexible structures by reinforcing the ground and accelerating the consolidation. They improve the shear strength and reduce the settlement of the in situ soft soil and also in loose sandy deposits they reduce the potential of liquefaction (Mitchell and Huber 1985). The main focus of this paper is on the performance of encased granular columns (EGCs). A brief limitation of granular columns installed in homogeneous clay sub grades and the need for an EGC are discussed below.

1.1 Limitations of Ordinary Granular Columns

Soil conditions for which the granular columns are in general not suited include sensitive clays and silts whose sensitivity is greater than 4 which normally tend to lose strength when vibrated. The granular column foundations are suited only for flexible structures like highway and railway embankments, Oil storage tanks etc., which can tolerate some total and differential settlements. Most of all, the bearing aspects of the granular column depend on the strength of the soil around them. The construction of granular columns becomes difficult when the undrained cohesion (C_{uu}) values drop down to 25 kPa or even less. In that case, the aggregates penetrate laterally into the soft clay soil. The soft clay also may flow and contaminate the stone aggregate in the column thus reducing the drainage capacity of the column. This may lead to a reduced load bearing capacity also leading to failure of the same by bulging. All the above discussed problems encountered in granular columns have paved the way for enhancing their performance by encasing with geosynthetics. The granular columns without encasement are referred as Ordinary Granular Column (OGC) and with encasement as EGC respectively from here on.

2 Encased Granular Columns

As mentioned above, the encasement of granular columns enhances their performance in several ways including *by offering confinement, easy pore water pressure dissipation, load transfer to deeper depths, less compression and lateral bulging, quick installation by allowing higher degree of compaction of aggregates, by preserving the strength properties of aggregates, improving the economy of construction*.

The EGCs have been an efficient alternative to traditional piles or compacted granular columns, Due to the confining effect, encasement of the compacted sand or gravel/granular columns in the EGC-system it can be applied even in extremely soft soils with Su < 2 kPa, which is in fact more a suspension than a soil (Alexiew et al. 2005).

The studies conducted so far on EGCs are presented below under different heads, analytical and numerical studies, experimental and field studies.

2.1 Analytical and Numerical Studies

The analytical procedures for EGC was first initiated by Van Impe (1989) in which estimation of required tensile strength of reinforcement was carried out. However, the method is not able to calculate the strains and settlements. Raithel and Kempfert (2000) presented two analytical design procedures, simplified and precise, based on vibro-displacement method of Priebe (1995). The procedures not only included a confining force in the ring direction but also complete stress–strain behavior of geosynthetic encasement. Due to the complexity involved in the load bearing aspects of EGCs, iterative procedures were suggested in the calculations. Wu and Hong (2008, 2014) have proposed an analytical procedure based on normalized relation between volumetric and axial soil strains for column expansion in line with the observations from triaxial compression tests. The authors have finally concluded that stiffer the inclusion, lower is the axial strain at which reinforcement slippage occurs. Pulko et al. (2010) developed a design chart for the practical use of the proposed analytical method which helps to select column spacing and encasement stiffness on a preliminary basis to achieve the desired settlement reduction. Analytical closed form solution for EGCs in the aspects of reducing both settlement and consolidation time was studied by Castro and Sagaseta (2011, 2013). They concluded that settlement reduction provided by the encasement does not depend on the area replacement ratio. Further the encasement effect of the granular column comes into picture only after column yields. Zhang and Zhao (2014) worked on the geotextile-EGCs and provided analytical solutions based on unit cell concept. The solutions provided were compared with analytical solutions of Pulko et al. (2010) and Raithel and Kempfert (2000). The bulging behavior was taken into consideration along with the shear stress existing between EGC and the surrounding soil in

the vertical direction. Through parametric studies it was observed that with increase in stiffness of the encasement, the bulging and settlement gets reduced.

Raithel and Kempfert (2000) investigated numerically the use of compacted sand columns in peaty soils and brought out models based on numerical and analytical forms. For single columns, axisymmetric model and for a deformation behavior of the whole system a cross model was preferred and used.

Murugesan and Rajagopal (2006) have numerically investigated the advantages of EGC over OGCs using the program GEOFEM and concluded that the elastic modulus of the geosynthetic encasement plays an important role in enhancing the load carrying capacity and stiffness of the encased columns. Yoo and Kim (2009) worked on the numerical aspects of the EGC using different FE approaches viz. axisymmetric, 3D column, Full 3D model for a rapid embankment construction. The axisymmetric model was found to predict approximately 20% higher results on vertical effective stress and lateral deformation when compared to 3D models. A numerical study of geosynthetic EGCs in soft clay was carried out by Lo et al. (2009). The analysis models the time dependent interaction of the EGC and surrounding soft clay by a fully coupled analysis. The results obtained were in line with the previous results published by the same authors. Khabbazian et al. (2010, 2011) numerically investigated on the aspects of single EGC which provides adequate lateral support thereby increasing its load bearing aspect through 3D analysis by ABAQUS Program. For partially encased columns, the authors suggest that optimum length of encasement was found to be a function of the stress that is applied to the column. The stress settlement response is improved for a shorter diameter encased column rather than the larger one. Keykhosropur et al. (2012) observed the behavior of group of EGC numerically on a 3D basis and found that there was no necessity to encase all the columns in a group rather for an optimum design encasing only the outer columns in a group is sufficient. Almeida et al. (2013, 2015) presented the behavior of granular column numerically and compared it with the analytical model developed. Unlike the analytical model the FE result indicated that the settlement in the soft soil is not the same as that of the encased column. As observed from the previous observations of the researchers, Yoo et al. (2010), have observed that the influence of geosynthetic modulus on the settlements is constant beyond a modulus value of 2000 kN/m.

2.2 *Laboratory and Field Studies*

A good amount of laboratory-based research work has been carried for understanding the behavior of EGCs in the past decades.

Malarvizhi and Ilamparuthi (2004) observed the load versus settlement relationship of ordinary and EGC through laboratory studies. The settlement decreased with increase in stiffness of the encasement. For lesser and higher loads the settlement reduction is observed better for ordinary and EGCs. Murugesan and Rajagopal (2006, 2007, 2010) conducted laboratory model tests on ordinary and

EGCs extensively for both single as well as group and found that the EGC exhibited a stiffer response whereas the ordinary columns showed significant strain softening behavior. Gniel and Bouazza (2009, 2010) conducted laboratory experiments to verify the effect of partial encasement in both single and group of granular columns. A steady reduction in vertical strain was observed for increase in length of encasement for the above mentioned categories of granular columns. Ali et al. (2010, 2014) conducted laboratory experiments on granular columns with and without encasement on floating and full penetration basis. Parametric studies revealed that smaller diameter columns gave better performance and there was no improvement in bearing capacity for a granular column length greater than six times diameter in the study conducted. The authors observed that full encasement increases the failure stress in the columns when compared to partial encasement.

Dash and Bora (2013) investigated the effect of reinforcement length on bearing capacity through laboratory tests on floating and end bearing granular columns. The floating columns exhibited a fivefold increase in capacity with 60% coverage length of column, whereas the improvement was threefold for full coverage (length) of encasement. For end bearing columns full encasement showed a better response than partial encasement.

Indicated below are the few attempts that have been made so far in the field aspects of EGCs.

Raithel and Kempfert (2000) worked on the practical aspects of the design of deep geotextile-encased sand columns for the foundation of a dike on very soft soils. The authors presented the implementation of a new foundation system "Geotextile-Encased Columns" (GEC) for the foundation of a dike on very soft sludge for land reclamation in Hamburg, Germany. The necessary dike foundations were realized by about 60,000 encased sand columns with a diameter of 800 mm. Due to the foundation system the dike was constructed on the subsoil with very small shear strength and high deformability in a construction time of approximately 9 months.

Raithel et al. (2005) assessed the effectiveness of encased columns in relation to the conventional column foundation. By combining geotextile encasement and horizontal reinforcement (load transfer mat) it is proved that foundations can be constructed even in sludge. *The authors insist a full-scale field study coupled with laboratory measurements to forecast settlement reduction.*

Yoo and Lee (2012) conducted field load tests at two different sites to test the performance of geogrid encased columns in soft ground. The effect of the geogrid encasement length and column strain was investigated. By measuring hoop strains at different depths, it was observed that the critical encasement length of geogrid is 2–3 times the diameter of the column. The authors conclude that the encasement effect in EGC differs according to the site conditions and to achieve optimum reinforcement in EGC the encasement length and geogrid modulus should be based on ground conditions and geogrid ring tension force.

Alexiew et al. (2014) monitored a full-scale bridge abutment on soft soil supported by geosynthetic encased sand columns. The field performance was monitored with pressure cells, electrical piezometers, inclinometers and settlement

plates. Sand columns have proven to be useful in providing drainage to reduce the potential for buildup of excess pore water pressures in the clay layer, in reducing the magnitude of settlements and in reducing the maximum horizontal earth pressure acting on the structures.

Almeida et al. (2015) conducted field studies by constructing an embankment of height 5.35 m in soft soil by geotextile-encased sand columns. Results showed that the differential settlement increased as the embankment height increased and when the excess pore pressure was being dissipated. Due to soil arching, the vertical stress supported by the encased column was two times greater than the stress transmitted to the soft soil.

3 Discussion on the Need for Field Studies

From the topics discussed above in various heads, we can find that extensive research work has been done on the topic of granular and geosynthetic EGCs. Looking at the key components that influence the performance of EGCs say *soil shear strength, length, spacing, diameter of the column, pattern of arrangement, stiffness and length of the geosynthetic encasement and its deformation behavior* various findings are observed from the review conducted so far. Many researchers have reported similar findings on the aspect of the column encasement. A very few have reported results contradicting the previous findings. *These conflicts can finally be sorted out on the basis of controlled full-scale field studies*. Few cases are stated below.

Case 1 Alexiew et al. (2005) observed that encasement stiffness of 4000 kN/m can reduce the settlements by two fold (or >1 m) compared to lower moduli encasement. Similar investigations were conducted by Murugesan and Rajagopal (2006) who on the other hand had investigated the geosynthetic stiffness up to 10,000 kN/m and observed similar findings. Castro and Sagaseta (2011) have also found that the encasement stiffness dominates over the soil stiffness. On the contrary, numerical studies conducted by Yoo (2010), Almeida et al. (2013) has revealed that the critical encasement modulus for settlement performance is around 1500–2000 kN/m beyond which no appreciable additional improvement is found.

Case 2 Ali et al. (2014) reported that the floating columns are in need of full encasement for better load transfer behavior. On the other hand, Dash and Bora (2013) have reported that full encasement has actually reduced the load carrying performance by twofold when compared to partial encasement (60%).

Case 3 Keykhosropur et al. (2012) based on their three-dimensional numerical investigations have suggested that in a group of granular columns, it is advantageous to encase only the peripheral columns.

Case 4 Almeida et al. (2013) have reported that the analytical models predict that the settlement in both column and soil to be the same but it is not so as observed from FE studies.

The cases indicated above point to the need for more field trials for developing better understanding of the strength and settlement behavior of these granular columns. Based on the discussions above it is therefore recommended to perform systematic field trials on EGCs to understand their load carrying capacity. The ultimate aim of any such research should be towards formalizing the response and inclusion of the guidelines in Design Codes for their widespread usage.

References

Alexiew, D., Brokemper, D., & Lothspeich, S. (2005). Geotextile encased columns (GEC): Load capacity, geotextile selection and pre-design graphs. In *Geo-Frontiers*, Geotechnical Special Publication, No. 130–142 (pp. 497–510).

Alexiew, D., Kuster, V., Hebmuller, A., Silva, A. E. F., Winter, D., & Schnaid, F. (2014). Geotextile encased columns (GEC) under bridge approaches as a pressure relief system: Concept, experience, measurements. In *Proceedings of the 10th International Conference on Geosynthetics*, Berlin, Germany (pp. 2205–2208).

Ali, K., Shahu, J. T., & Sharma, K. G. (2010). Behaviour of reinforced stone columns in soft soil: An experimental study. In *Indian Geotechnical Conference 2010 Geotrendz* (pp. 292–305).

Ali, K., Shahu, J. T., & Sharma, K. G. (2014). Model tests on single and groups of stone columns with different geosynthetic reinforcement arrangement. *Geosynthetics International, 21*(2), 103–118.

Almeida, M. S. S., Hosseinpour, I., & Riccio, M. (2013). Performance of geosynthetic-encased column (GEC) in soft ground: Numerical and analytical studies. *Geosynthetics International, 20,* 252–262.

Almeida, M. S. S., Hosseinpour, I., Riccio, M., & Alexiew, D. (2015). Behaviour of geotextile-encased granular columns supporting test embankment on soft deposit. *Journal of Geotechnical and Geoenvironmental Engineering, 141*, 04014116, 1–9.

Castro, J., & Sagaseta, C. (2011). Deformation and consolidation around encased stone columns. *Geotextiles and Geomembranes, 29*(3), 268–276.

Castro, J., & Sagaseta, C. (2013). Influence of elastic strains during plastic deformation of encased stone columns. *Geotextiles and Geomembranes, 37,* 45–53.

Dash, S. K., & Bora, M. C. (2013). Improved performance of soft clay foundations using stone columns and geocell-sand mattress. *Geotextiles and Geomembranes, 41,* 26–35.

Gniel, J., & Bouazza, A. (2009). Improvement of soft soils using geogrid encased stone columns. *Geotextiles and Geomembranes, 27*(3), 167–175.

Gniel, J., & Bouazza, A. (2010). Construction of geogrid encased stone columns: A new proposal based on laboratory testing. *Geotextiles and Geomembranes, 28*(1), 108–118.

Keykhosropur, L., Soroush, A., & Imam, R. (2012). 3D numerical analyses of geosynthetic encased stone columns. *Geotextiles and Geomembranes, 35,* 61–68.

Khabbazian, M., Kaliakin, V. N., & Meehan, C. L. (2010). Numerical study of the effect of geosynthetic encasement on the behaviour of granular columns. *Geosynthetics International, 17*(3), 132–143.

Khabbazian, M., Kaliakin, V. N., & Meehan, C. L. (2011). Modeling the behavior of geosynthetic encased columns: Influence of granular soil constitutive model. *Computers and Geotechniques, 12,* 357–369. 2012.

Lo, S. R., Zhang, R., & Mak, J. (2009). Geosynthetic-encased stone columns in soft clay: Numerical study. *Geotextiles and Geomembranes, 28,* 292–302.

Malarvizhi, S. N., & Ilamparuthi, K. (2004). Load versus settlement of clay bed stabilized with stone and reinforced stone columns. In *Asian Regional Conference on Geosynthetics, GeoAsia —2004* (pp. 322–329).

Mitchell, J. K., & Huber, T. R. (1985). Performance of a stone column foundation. *Journal of Geotechnical Engineering, 111*(2), 205–223.

Murugesan, S., & Rajagopal, K. (2006). Geosynthetic-encased stone columns: Numerical evaluation. *Geotextiles and Geomembranes, 24*(6), 349–358.

Murugesan, S., & Rajagopal, K. (2007). Model tests on geosynthetic encased stone columns. *Geosynthetics International, 24*(6), 349–358.

Murugesan, S., & Rajagopal, K. (2010). Studies on the behavior of single and group of geosynthetic encased stone columns. *Journal of Geotechnical and Geoenvironmental Engineering, 136*(1), 129–139.

Priebe, H. J. (1995). The design of vibro replacement. *Ground Engineering, 28*(10), 31–37.

Pulko, B., Majes, B., & Logar, J. (2010). Geosynthetic-encased stone columns: Analytical calculation model. *Geotextiles and Geomembranes, 29*(1), 29–39.

Raithel, M., & Kempfert, H. G. (2000). Calculation models for dam foundations with geotextile coated sand columns. In *Proceedings of the International Conference on Geotechnical and Geological Engineering*, Melbourne, GeoEng (pp. 347–350).

Raithel, M., Kirchner, A., Schade, C., & Leusink, E. (2005). Foundation of constructions on very soft soils with geotextile encased columns—State of the art. Geotechnical Special Publication, No. 130–142 (pp. 1867–1877).

Van Impe, W. F. (1989). *Soil improvement techniques and their evolution* (pp. 63–66). Rotterdam, Netherlands: Balkema.

Wu, C. S., & Hong, Y. S. (2008). The behavior of a laminated reinforced granular column. *Geotextiles and Geomembranes, 26*(4), 302–316.

Wu, C. S., & Hong, Y. S. (2014). A simplified approach for evaluating the bearing performance of encased granular columns. *Geotextiles and Geomembranes, 42,* 339–347.

Yoo, C. (2010). Performance of geosynthetic-encased granular columns in embankment construction: Numerical investigation. *Journal of Geotechnical and Geoenvironmental Engineering, 136*(8), 1148–1160.

Yoo, C., & Kim, S.-B. (2009). Numerical modeling of geosynthetic-encased granular column-reinforced ground. *Geosynthetics International, 16*(3), 116–126.

Yoo, C., & Lee, D. (2012). Performance of geogrid-encased stone columns in soft ground: Full-scale load tests. *Geosynthetics International, 19*(4), 480–490.

Zhang, L., & Zhao, M. (2014). Deformation analysis of geotextile encased stone column. *International Journal of Geomechanics, 15*, 04014053-1–10 (2015).

Engineered Anti-erosion Works Along the Right Bank of Jiabharali River in Assam

Suresh Maurya, Manish Gupta and R. Chitra

Abstract Erosion and flood are the two major problems of lower plain reach of Jiabharali River and hence become a matter of concern due to its devastating impact on life and property. The River Jiabharali carries substantial quantity of silt along with discharge of 4429.73 cumec. Due to deposition of sediments, the sand chars forms in the river bed at random, creating spill channels making bank erosion more vulnerable. River also has a natural gradient to shift its courses towards the western side and there is formation of offshoot channels after each flood, thereby widening its waterway and making the problem more intense. This paper describes the case study where Geosynthetics materials and Gabions are used in erosion control and flood protection measures at two different reaches (Dikoraijan and Kurukani) along the Jiabharali River by construction of bank revetment with launching apron and raising and strengthening of embankment at places which are prone to floods. The project is located in the Sonitpur District of Assam from Ch: 9490 m (Dikoraijan) to 14,397 m (Kurukani). The laboratory investigations undertaken for Geosynthetics materials and Gabions for the above project are presented in this paper along with advantages of using Geosynthetics materials.

Keywords Protection · Erosion · Geosynthetics · Quality control

S. Maurya (✉) · M. Gupta · R. Chitra
Central Soil and Materials Research Station, New Delhi 110016, India
e-mail: maurya_suresh@yahoo.co.in

M. Gupta
e-mail: manishgupta@nic.in

R. Chitra
e-mail: rchitra@nic.in

T. Thyagaraj (ed.), *Ground Improvement Techniques and Geosynthetics*, Lecture Notes in Civil Engineering 14, https://doi.org/10.1007/978-981-13-0559-7_43

1 Introduction

Jiabharali is one of the tributary of Brahmaputra which originates from Himalaya and after traveling through Arunachal Pradesh and Sonitpur District of Assam, it finally outfalls at mighty river Brahmaputra. Broadly Jiabharali River can be divided into three main reaches i.e., upper (hilly), central reach and lower plain reach.

In the hilly region, rivers tend to erode their beds and banks resulting in deepening and widening of rivers. The bed of the basin is built up of rock boulders, gravels, etc. When river enters the flood plains, it shows a tendency to braid and develop number of channels causing silting of the riverbed, change in course and bank erosion. In the lower plain reach, a river shows a meandering tendency with meander moving d/s causing erosion on the concave and deposition on the convex side as shown in Fig. 1. Thus bank erosion and consequent loss of land and properties are normal phenomenon all along the course of the river and new areas get affected by erosion every year.

Anti-erosion works are normally taken up only where re-location is not possible on socio-techno-economic grounds, long lengths of embankment benefitting large areas and agriculture lands where cost–benefit ratio justifies such works (Gupta et al. 2015). Use of Geosynthetics material has gained importance for immediate protection measures where flood is a regular phenomenon and construction is to be completed in a limited time period.

2 Bank Erosion Problem

The behavior of river Jiabharali in lower plain reach is found to be very critical due to its natural gradient towards western side and formation of offshoot channels after each flood, thereby widening its waterway. Within the last few years, river has migrated kilometers and shifted its channel running parallel to the extreme western side on its right bank. Also the soil forming the bank in this area vary from medium to fine sand and is very unstable and easily erodible by the flood water as shown in Fig. 2.

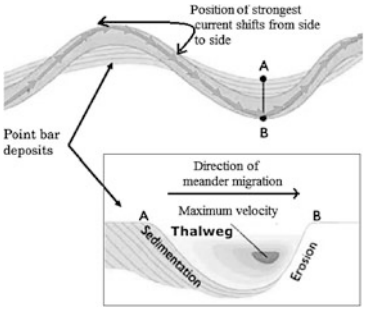

Fig. 1 Erosion and deposition in meandering stream

Fig. 2 Eroded river bank at Jiabharali lower plain reach

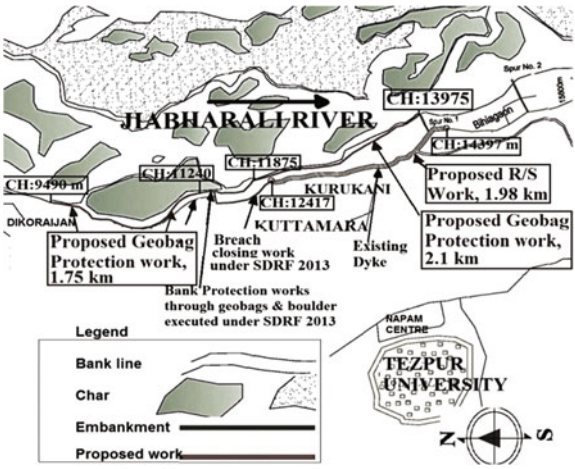

Fig. 3 Location of affected reach and protection works

The river Mansiri, a sub-tributary meet the river Jiabharali at Ch: 6000 m and boosts the erosion problem at Dikoraijan, Kuttamara and Kurukani area as shown in Fig. 3. Due to the combined discharge of both the rivers, there is severe bank erosion for a reach of about 4 km and the river has formed a sharp concave bend. In fact, the flood of 2010, 2012, and 2013 has devastated the entire area due to severe bank erosion. As a result of these, more than 3000 ha of fertile and homestead land has already been eroded and in case the erosion problem continues, there is every possibility of collapse of the infrastructure of the entire locality including Tezpur University Campus.

3 Flood Management Scheme and Benefit

The scheme is to protect Tezpur University and its adjoining area against erosion of the River Jiabharali as shown in Fig. 3. The scheme is executed by Tezpur Water Resources Division, Assam under the Flood Management Programme to benefit

thickly populated villages, other public and private properties and protect 15,000 ha of cultivated and homestead land. Geosynthetics materials and Gabions used in the above scheme were evaluated for their quality at CSMRS, New Delhi.

4 Solution Implementation

In order to firmly arrest the erosion, prevent migration of the river and to provide protection to the Tezpur University and its adjoining areas, Geosynthetics materials and Gabions are adopted in construction of bank revetment with launching apron covering the most affected reach for a total length of 3.85 km and raising and strengthening of the existing embankment for a length of 1.98 km as shown in Fig. 3. Such application can be rapidly deployed to achieve maximum benefit to the community, typically through the use of on-site materials, innovative Geosynthetics materials and construction techniques.

In the present cases the following advantages of Geosynthetics materials are outlined:

- Filling, transportation and installing the Geotextile bags and Geo-mattress is quick, simpler and economic when required in-filling sand material is abundantly available at site. Locally available unskilled labors for filling the bags can bring more economy to the project.
- It takes less time in the procurement of the Geosynthetics materials and Gabions than the boulders and aggregates. Therefore huge cost for carriage of rock boulders would be saved.
- Conventionally used boulders for protection works have become scarce and their continuous use also disturbs the ecological balance. Use of sand filled geotextile bags and Geo-mattress in various forms, size, and shape is found perfect replacement for boulder and causes lesser environmental damage.
- Satisfying the filter and drainage criterion for conventional graded granular design is extremely expensive, difficult to obtain, time consuming to instal and involves problem of segregation during placement. The conditions can easily and cheaply be achieved using a Geotextile to perform filtration. Specially, a single layer of Geotextile fabric can replace a graded filter comprising two or three layers.
- Restoration and maintenance work is easier than other conventional methods.
- Being light in weight, it is easy to handle and can be installed quickly. Also, working under water becomes much easier because the bags and filter system can be assembled above the water and lowered into position.
- They are made up of Polypropylene materials, so they are durable and chemical resistant. Since they are factory manufactured products, high quality can be assured. Also, uniformity in material specification can be maintained throughout the project.

- Construction of bank revetment can be used to restrict the flow towards habitat area, thereby delaying the problem to complete the permanent structure higher than the flood plain.

4.1 Bank Revetment with Launching Apron

Pitching of Geotextile bags and launching of apron is carried out for a total length of 3.85 km where the river bank is dressed to the inclination of 1V: 2H and over this a layer of non-woven geotextile of 400 gsm is laid as filter media, anchored at the top and bottom of bank slope. After the placement of geotextile filter on the bank slope, sand filled geotextile bags of Type-A (size 1.03 × 0.70 m) made of non-woven geotextile are placed all along the length of the bank. Thickness of the pitching on bank slope is 0.45 m (three layers) and top height of bank is maintained with respect to HFL of 71.82 m. Geotextile bags are filled with sand to the specified height to ensure that appropriate density is achieved and open ends of the bags is closed by stitching the bags with the help of hand stitching machines. Total quantity of filter material applied is 46,489 m^2 and geotextile bags for the protection works is approximately 761,115 nos. Figure 4 shows the cross section of the launching apron and bank pitching work.

Launching of apron is carried out with multiple layers of geotextile bags (6 layers) having thickness of 0.90 m and width of 10.80 m. At the junction of the bank and apron, toe-key is formed from strips of zinc coated wire mesh gabion box (size 2 × 1 × 0.45 m) filled with three layers of sand filled geotextile bags of Type-A (size 1.03 × 0.70 m) all along the length of apron. Intermediate key is

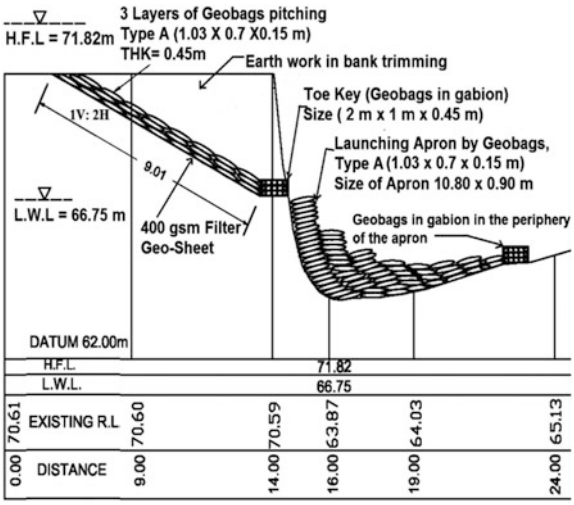

Fig. 4 Cross section of launching apron and bank pitching work

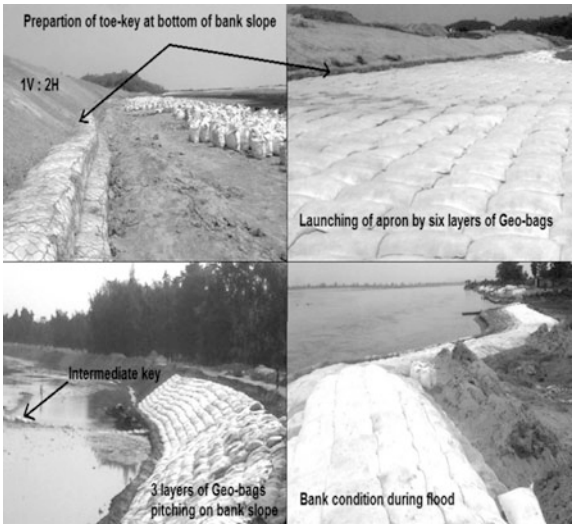

Fig. 5 Installation of Geosynthetics materials and Gabions at various stages

placed at regular intervals of 50 m across the length of the apron and it is formed from two layers of strips of zinc coated gabion box (size 2 × 1 × 0.45 m) filled with three layers of sand filled geotextile bags each. Further, the strip of gabion box filled with geotextile bags are also placed at the periphery of the apron where the scour of the bed initiates. Here, the revetment is a part of bank protection work, while launching apron and toe-key are part of bed protection work. Bank protection followed by a suitable bed protection can be considered as the key success for any anti-erosion work. Strips of Gabion box placed along the length of the apron in toe-key, at specified intervals across the apron and at the periphery of apron impart further stability to the scour protection measure. Total quantity of Gabion boxes used in launching apron and toe-key is 16,822 nos. Figure 5 shows installation of Geosynthetics materials and Gabions at various stages.

4.2 Raising and Strengthening of the Embankment

Raising and strengthening of the embankment is carried out for the total length of 1.98 km. Crest width is kept 7.50 m and top height is maintained at RL 73.30 m with respect to HFL of 71.82 m with freeboard of 1.80 m. Filling of earthwork is done in uniform layers not exceeding 22.50 cm thick with profiling to achieve a slope of 1V: 3H. Total quantity of earth work materials in use is 66,029 m^3. Embankment slope is protected by turfing with grass sods of largest possible rectangles of 12 cm minimum thickness. The total quantity of turfing with grass sods is 23,746 m^2.

5 Laboratory Investigation

Considering the advantages of Geosynthetics materials, its use may rapidly increase in future and the importance of material evaluation should therefore be emphasized to ensure that the Geosynthetics materials and Gabions meet the qualifying criteria. The Geosynthetics materials and Gabions are tested for physical, mechanical, hydraulic, and survivability properties in accordance with ASTM D (5261, 4595, 6241, 4751, and 4491) and IS: 1608 (2005). The tests results (CSMRS 2015) are presented in Tables 1, 2 and 3.

Table 1 Tests results for non-woven Geotextile bags

Properties	Values
Mass per unit area, g/m^2	401
Tensile strength (MD), kN/m	21
Elongation (MD), %	72
Tensile strength (CD), kN/m	20
Elongation (CD), %	79
CBR puncture resistance, N	4010
Apparent opening size, mm	0.075
Permeability, m/s	$>2 \times 10^{-3}$

Table 2 Tests results for non-woven Geo-fabric filter media

Properties	Values
Mass per unit area, g/m^2	402
Tensile strength (MD), kN/m	23
Elongation (MD), %	71
Tensile strength (CD), kN/m	21
Elongation (CD), %	74
CBR puncture resistance, N	4015
Apparent opening size, mm	0.075
Permeability, m/s	$>2 \times 10^{-3}$

Table 3 Tests results for Gabion wires

Properties	Values
Tensile strength (Mesh wire), N/mm^2	481
Elongation (Mesh wire), %	17
Tensile strength (Selvedge wire), N/mm^2	450
Elongation (Selvedge wire), %	15
Tensile strength (Lacing wire), N/mm^2	470
Elongation (Lacing wire), %	17

6 Conclusions

The paper presents the problems and the remedial works along the vulnerable reaches of River Jiabharali. The flood protection and erosion control method adopted with composite Geosynthetics is a highly engineered solution. Such application replaces all other conventional methods (e.g., Boulders, RCC, etc.) for immediate protection where flood is a regular phenomenon and construction is to be completed in a limited time period. The use of Geosynthetics materials permits to carry out the protection works at a faster rate. The use of the mechanically zinc coated wire mesh Gabion box ensured the stability of the geotextile bags by providing the peripheral confinement to the bank structures. Creating such type of protection work with greater area and uniformity in construction reduces damage to the base of structure and chance of sinking considerably. But the performance of restoration work is still to be observed in coming years as a long term measure and thereafter further decision can be taken for execution for similar vulnerable reaches.

Sometimes conventional system for solution will not be sufficient for desired results. Use of a composite Geosynthetics solution may prove effective and economically viable. To enable this system perform in the long run, it is necessary to prevent the erosion from bed and for that geotextile bags, filled with the locally available material, is an ideal option. While designing the protection works and choosing the products, due care has to be taken for proper design, structural integrity of the system, experienced designer and contractors who instal the system.

Protection work increase resistance of river banks to erosion and deflecting the current away. These generally shift the problem in the u/s or the d/s and necessitate further works to safeguard the land against erosion.

Acknowledgements The authors acknowledge the contributions of the Tezpur Water Resources Division, Assam and CSMRS team by way of active cooperation at the time of laboratory investigation and testing.

References

ASTM D 5261. *Test methods for measuring mass per unit area of geotextiles*. Pennsylvania, USA: ASTM.

ASTM D 4595. *Test method for tensile properties of geotextiles by the wide-width strip method*. Pennsylvania, USA: ASTM.

ASTM D 6241. *Test method for the static puncture strength of geotextiles and geotextile-related products*. Pennsylvania, USA: ASTM.

ASTM D 4751. *Test method for determining apparent opening size of geotextile*. Pennsylvania, USA: ASTM.

ASTM D 4491. *Test methods for water permeability of geotextiles by permittivity*. Pennsylvania, USA: ASTM.

CSMRS. (2015). *Report on 'Laboratory testing of geosynthetics materials and gabion for protection of Tezpur University and its adjoining areas from the erosion of River Jiabharali'*. India: New Delhi.

Gupta, M., Chitra, R., & Ratnam, M. (2015). Geosynthetics in engineered anti-erosion works—A new perspective. In *International Symposium on Geosynthetics—The Road Ahead*, 5–6 November 2015, CBIP, New Delhi, India (pp. 202–219).

IS: 1608. (2005). *Metallic materials—Tensile testing at ambient temperature*. New Delhi, India: Bureau of Indian Standards.

Static and Cyclic Properties of EPS Geofoam

Vinil Kumar Gade and Satyanarayana Murty Dasaka

Abstract This paper presents static and cyclic behavior of geofoam specimens of 100 mm cube and 15 kg/m^3 density (D). To understand cyclic behavior of Geofoam, a factor "R", defined as ratio of combined axial static and cyclic stress component to the yield strength of geofoam, is used in cyclic uniaxial compression (CUC) tests. CUC tests are conducted at three frequencies (f) of 0.5, 1 and 3 Hz, R values of 0.4, 0.6, 0.8, 1 and 1.2, and for 5000 cycles. Static tests on geofoam exhibited a bi-linear axial stress–strain response. From CUC tests, it is noted that effect of number of cycles is insignificant on cyclic modulus, and effect of testing frequency on cyclic modulus is found marginal, for lower values of R. As the value of R increases, the cyclic axial strain increases, which decreases cyclic modulus of geofoam, irrespective loading frequency and number of cycles. Previous studies, while modeling Geofoam behavior, assumed positive values of Poisson's ratio and linear regression models relating Poisson's ratio and density of geofoam. In contrary, the present study revealed that Poisson's ratio of geofoam not only depends on its density, but also strongly influenced by number cycles and axial strain of geofoam, and can also take negative values.

Keywords Geofoam · CUC tests · Young's modulus · Poisson's ratio

1 Introduction

Various geosynthetic materials had been used for civil engineering application for nearly four decades, to improve serviceability and economize the cost of projects. Geosynthetic materials, such as geotextiles, geomembranes, geogrids, geonets, clay

V. K. Gade (✉) · S. M. Dasaka
Department of Civil Engineering, Indian Institute of Technology Bombay, Mumbai 400076, India
e-mail: gadevinilkumar23@gmail.com

S. M. Dasaka
e-mail: dasaka@civil.iitb.ac.in

T. Thyagaraj (ed.), *Ground Improvement Techniques and Geosynthetics*, Lecture Notes in Civil Engineering 14, https://doi.org/10.1007/978-981-13-0559-7_44

liners, geocells, geocomposites, geofoam, etc., were developed for specific applications. Among the above, geofoam is a three-dimensional material, with considerable thickness compared to its length and width. Geofoam classified into two types based on the manufacturing process viz., expanded polystyrene geofoam (EPS) and extruded polystyrene geofoam (XPS). EPS geofoam is widely used compared to XPS because of higher compressibility, environmentally safe manufacturing process, easy laying in the field, etc. In the past, EPS geofoam was used in civil structures as thermal insulators, small wave damping, etc. Geofoam density is nearly 100 times lower than the soil, but its Young's modulus is only 10 times lower than soil. With low density and higher stiffness, it can be effectively used in many applications, such as light weight backfill, embankment over soft soils to reduce overburden pressure, etc. Recently, geofoam has been used for reducing the earth pressure on retaining wall (Purnanandam and Rajagopal 2008; Zarnani and Bathurst 2008; Dave and Dasaka 2012), buried pipes (Kim et al. 2010) and to reduce swelling pressure in expansive soils (Ikizler et al. 2009). Properties of geofoam and its behavior must be thoroughly studied to augment its use in various infrastructure projects, to effectively reduce cost and time of construction. In the present study, geofoam behavior under different loading conditions has been performed. The experimental program adopted and the relevant results are discussed briefly in this paper.

2 Experimental Program

In the study, static and stress controlled cyclic uniaxial compression (CUC) tests are conducted on 100 mm cube samples of 15*D* geofoam to evaluate static and cyclic behavior of geofoam. Servo-Hydraulic actuator located at IIT Bombay has been used for performing both static and CUC tests. During the testing, two LVDTs are used to measure lateral deformation of geofoam and they are positioned at middle height of the sample. A small fixture of 10 mm × 10 mm × 2 mm is attached to LVDT tip to avoid any indentation on geofoam sample by spring force of LVDT.

Static tests on geofoam samples are conducted at 10 mm/min displacement rate in accordance with Stark et al. (2004). CUC tests are performed at three loading frequencies (*f*) viz., 0.5, 1, and 3 Hz, 5000 number of loading cycles and different *R* values, viz., 0.4, 0.6, 0.8, 1 and 1.2, where factor "*R*" is defined as ratio of combined static and cyclic deviatoric stress component to the yield strength of geofoam. *R* factor adopted in the study is similar to Ossa and Romo (2011) to understand behavior of geofoam with respect to yield strength of geofoam. Unlike soil samples, failure in geofoam samples does not occur, rather the samples exhibit strain softening after the yield point. This behavior necessitates researchers to choose a wide range of *R* values with respect to yield point. Pictorial view of Static and CUC testing set-ups used in the study are shown in Fig. 1. A loading plate of 150 mm × 150 mm × 6 mm is used to transfer load uniformly on geofoam samples from actuator. Schematic representation of CUC testing procedure and

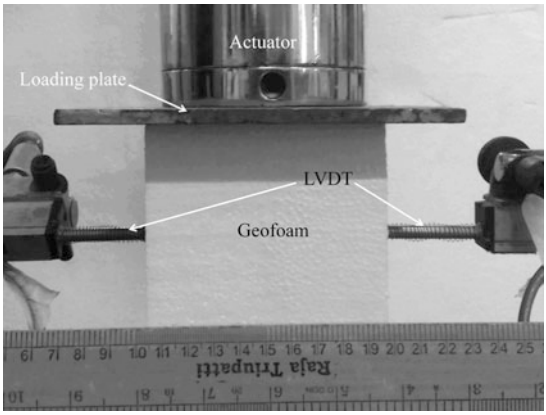

Fig. 1 Pictorial view of static and CUC tests configuration

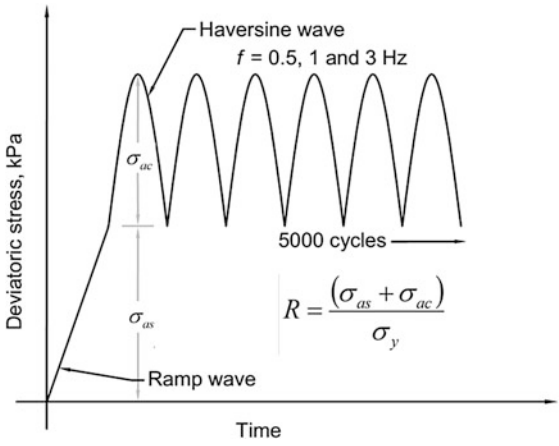

Fig. 2 Schematic representation of CUC tests

definition of R are shown in Fig. 2. Application of axial load on geofoam samples in CUC test is divided into two parts viz., (a) static component (σ_{as}) is applied by using a ramp wave mode, followed by (b) application of cyclic component (σ_{ac}) using haversine wave mode. For each combination of testing program, tests are performed on minimum three identical samples and respective average values are reported.

3 Results and Discussions

From static tests on 15D geofoam, bi-linear axial stress–strain response is observed, as shown in Fig. 3. Horvath (1994) reported bi-sigmoidal behavior of geofoam at 90% axial strain, but in the present study axial strain is limited to 30%. Observed

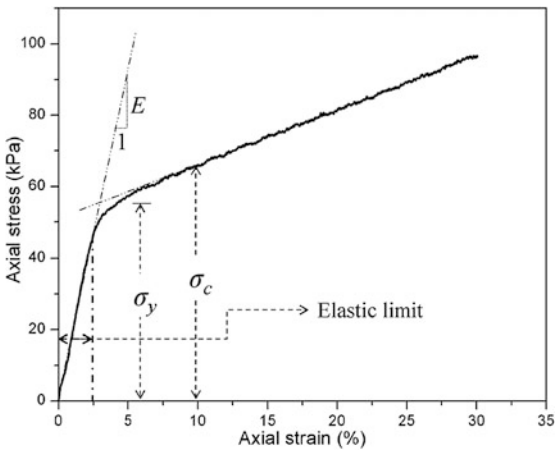

Fig. 3 Axial stress–strain behavior of 15D geofoam

stress–strain behavior and some salient properties of geofoam from static tests are schematically described in Fig. 3. The transition point, where axial stress–strain curve of geofoam is deviates from the initial tangent, is defined as elastic limit. Slope of initial tangent which is drawn from the origin is defined as Young's modulus (E). Axial stress corresponding to 10% axial strain from stress–strain curve is defined as compressive strength (σ_c). Intersection point of initial and back tangent of stress–strain curve and its corresponding axial stress is defined as yield strength (σ_y). Elastic limit, Young's modulus (E), compressive strength (σ_c) and yield strength (σ_y) of 15D geofoam are obtained as 2.4%, 2.1 MPa, 65 kPa and 55 kPa, respectively. The observed stress–strain behavior of geofoam in the present study matches well with Duskov (1997), Athanasopoulos et al. (1999), and Ossa and Romo (2009).

From CUC tests, secant modulus (E_{dyn}) and damping ratio of hysteresis cycles are evaluated according to ASTM D3999-91 (2003). E_{dyn} is evaluated for selected few number of loading cycles. Effect of number of cycles, R and loading frequency on E_{dyn} of 15D geofoam is shown in Fig. 4. It is observed that effect of number of cycles is insignificant on cyclic modulus, and effect of testing frequency on cyclic modulus is found marginal for lower values of R. As the value of R increases, the cyclic axial strain increases, this in turn decreases cyclic modulus of geofoam, irrespective of loading frequency and number of cycles. Effect of cyclic axial strain on cyclic modulus is shown in Fig. 5. Damping ratio of each sample is also calculated and reported with respect to cyclic axial strain shown in Fig. 5. Observed damping ratio increases with increase in cyclic axial strain, and cyclic axial strain depends on R values and loading frequency. Decreasing trend of E_{dyn} and increasing trend of damping ratio with respect to cyclic axial strain of geofoam is more effective in reducing lateral earth pressure on retaining walls and buried pipes during the seismic events.

Effect of number cycles, R and loading frequencies on cyclic axial strain of 15D geofoam from CUC tests is shown in Fig. 6. For lower R values (0.4 and 0.6)

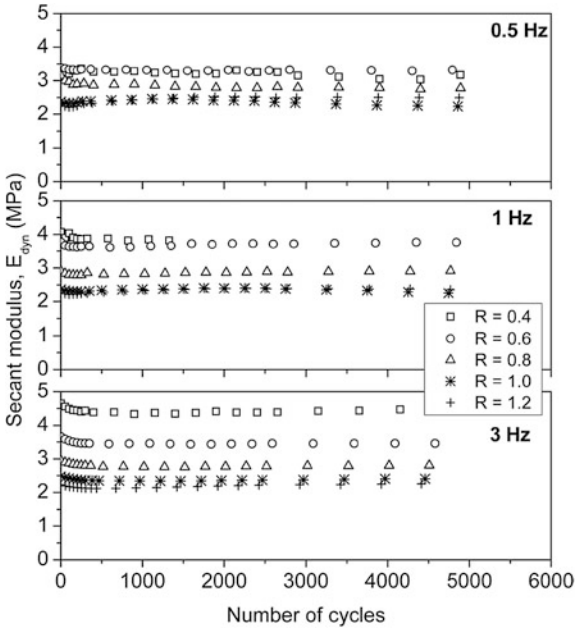

Fig. 4 Effect of loading frequency, number of cycles and R value on secant modulus of 15D geofoam

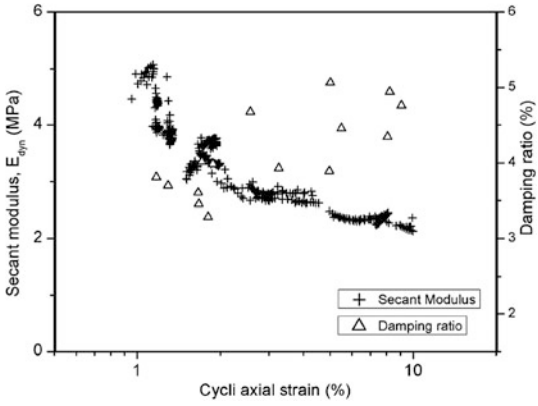

Fig. 5 Effect of cyclic axial strain on secant modulus and damping ratio

loading frequency has insignificant effect on the cyclic axial strain of 15D geofoam, whereas, it is observed significant at higher R values (≥ 0.8). For R value less than 0.6, cyclic axial strain is always within elastic limit of geofoam and same can be observed from Fig. 6. For higher R values, cyclic axial strain increases with increase in number of cycles and irrespective of loading frequencies. This observation might have led Stark et al. (2004) to limit design strength of geofoam to 50% of its compressive strength.

Poisson's ratio is calculated as negative ratio of measured transverse strain to axial strain from testing. From the static tests, the variation of Poisson's ratios with

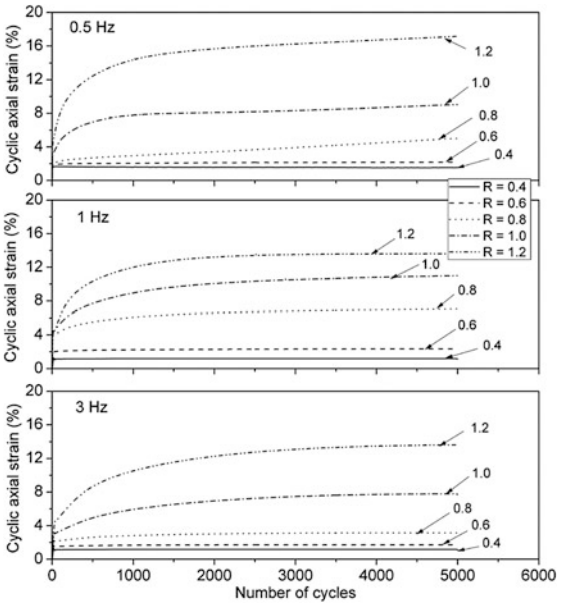

Fig. 6 Effect of number of cycles on cyclic axial strain

respect to axial strain of geofoam is shown in Fig. 7. The observed Poisson's ratio continuously decreased with increase in axial strain, and at 6.5% axial strain, Poisson's ratio reduces below zero. Effect of *R* values, loading frequency and cyclic axial strain on Poisson's ratio of geofoam from CUC tests are reported in Fig. 8. For better representation, an axis with dotted line corresponding to zero Poisson's ratio is shown in Fig.8a–c. For lower *R* values (0.4 and 0.6), Poisson's ratio values are observed positive, irrespective of loading frequency and cyclic axial strain. For *R* values equal to or greater than 0.8, Poisson's ratio is observed negative for all three loading frequencies. From CUC tests, it is observed that Poisson's ratio reaches zero value at 1–2% cyclic axial strain, which is much lower compared to that of static tests (6.5%). Abdelrahman et al. (2008) reported Poisson's ratio decreases from positive to negative from experimental studies and only limited to 1% axial strain. Previous studies assumed positive values of Poisson's ratio for geofoam, and linear regression models are assumed to relate Poisson's ratio and density of geofoam, while modeling Geofoam behavior. In contrary, the present study revealed that Poisson's ratio of geofoam not only depends on its density, but also strongly influenced by number cycles, *R* values and axial strain of geofoam, and can also take negative values, as shown in Figs. 7 and 8.

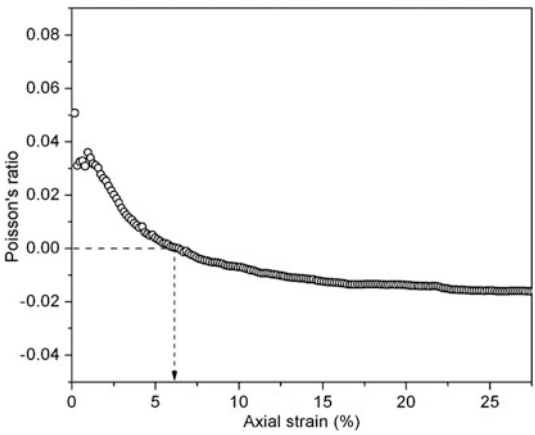

Fig. 7 Effect of axial strain on 15*D* geofoam Poisson's ratio

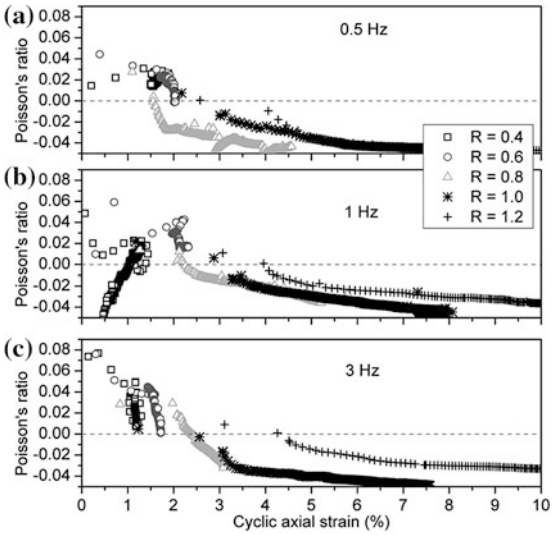

Fig. 8 Poisson's ratio versus axial strain from CUC tests **a** 0.5 Hz, **b** 1 Hz, **c** 3 Hz

4 Conclusions

From the series of static and CUC tests on 15*D* geofoam specimens, the following conclusions are drawn:

- Bi-linear axial stress–strain response of geofoam is observed from static tests.
- Secant modulus (E_{dyn}) of geofoam decreases with increase in cyclic axial strain, irrespective of density of geofoam.
- Damping ratio increases with increase in cyclic axial strain.
- Poisson's ratio of geofoam varies from positive to negative values, depending on loading type and number of cycles.

- Poisson's ratio reaches zero value at low axial strain (<2%) and higher R values from CUC tests, compared to that of static tests (6.5%).
- For R values near to or above unity, cyclic axial strain increases abruptly with number of cycles compared that at lower R values.

References

Abdelrahman, G. E., Kawabe, S., Tsukamoto, Y., & Tatsuoka, F. (2008). Small-strain stress-strain properties of expanded polystyrene geofoam. *Soils and Foundations, 48*(1), 61–71.

ASTM D3999-91. (2003). Standard Test Methods for the determination of the modulus and damping properties of soils using the cyclic triaxial apparatus, West Conshohocken, PA. https://doi.org/10.1520/d3999-91r03.

Athanasopoulos, G. A., Pelekis, P. C., & Xenaki, V. C. (1999). Dynamic properties of EPS geofoam: An experimental investigation. *Geosynthetics International, 6*(3), 171–194.

Dave, T. N., & Dasaka, S. M. (2012). Transition of earth pressure on rigid retaining walls subjected to surcharge loading. *Indian Geotechnical Journal, 6,* 427–435.

Duskov, M. (1997). Material research on EPS20 and EPS15 under representative conditions in pavement structures. *Geotextiles and Geomembranes, 15,* 147–181.

Horvath, J. S. (1994). Expanded polystyrene (EPS) geofoam: An introduction to material behaviour. *Geotextiles and Geomembranes, 23,* 263–280.

Ikizler, S. B., Aytekin, M., & Vekli, M. (2009). Reductions in swelling pressure of expansive soil stabilized using EPS geofoam and sand. *Geosynthetics International, 16*(3), 216–221. https://doi.org/10.1680/gein.2009.16.3.216.

Kim, H., Choi, B., & Kim, J. (2010). Reduction of earth pressure on buried pipes by EPS geofoam inclusions. *Geotechnical Testing Journal, 33*(4), 1–10.

Ossa, A., & Romo, M. P. (2009). Micro- and macro-mechanical study of compressive behavior of expanded polystyrene (EPS) geofoam. *Geosynthetics International, 16*(5), 327–338.

Ossa, O., & Romo, M. P. (2011). Dynamic Characterization of EPS Geofoam. *Geotextiles and Geomembranes, 29*(1), 40–50, https://doi.org/10.1016/j.geotexmem.2010.06.007

Purnanandam, K., & Rajagopal, K. (2008). Lateral earth pressure reduction due to controlled yielding technique. *Indian Geotechnical Journal, 38*(3), 317–333.

Stark, T. D., Arellano, D., Horvath, J. S., & Leshchinsky, D. (2004). *Geofoam applications in the design and construction of highway embankments*. NCHRPWeb Document 65, Transportation Research Record, Washington, DC.

Zarnani, S., & Bathurst, R. J. (2008). Numerical modelling of EPS seismic buffer shaking table tests. *Geotextiles and Geomembranes, 26,* 371–383.

Swell Behavior of Expansive Soils with Stabilized Fly Ash Columns

F. Darikandeh and B. V. S. Viswanadham

Abstract In this study, an attempt has been made to investigate the influence of flyash columns (FACs) on the expansive soil using different percentages of flyash and calcium carbide residue (CCR) to reduce heave of expansive soil bed. Puzzolanic activity of the binder admixture has been studied by replacing the columns admixture by sand in the vertical columns in the soil specimen. Conventional Oedometer tests have been performed. Free swell index (FSI) and particle size distribution tests have also been conducted as post-tests. It has been observed that swell properties considerably reduce with vertical fly ash columns in the expansive soil bed.

Keywords Expansive soil · Swell · Fly ash · Calcium carbide residue (CCR)

1 Introduction

Expansive soil has a potential for shrinkage or swelling under changing moisture condition. The volumetric changes in expansive soils have been observed to cause many structural problems construction works. Which leads to structural damages and the annual cost of damages is estimated £150 million in the UK, $1000 million in the USA and many billions of pounds worldwide (Viswanadham et al. 2009). To overcome this, different foundation techniques have been suggested like granular pile anchors (Phanikumar et al. 2004; Phanikumar et al. 2008; Aljorany et al. 2014), lime pile technique for the improvement of clayey soil (Malekpoor and

F. Darikandeh (✉) · B. V. S. Viswanadham (✉)
Department of Civil Engineering, Indian Institute of Technology Bombay, 400076 Powai, Mumbai, India
e-mail: farahnaz@iitb.ac.in

B. V. S. Viswanadham
e-mail: viswam@civil.iitb.ac.in

T. Thyagaraj (ed.), *Ground Improvement Techniques and Geosynthetics*, Lecture Notes in Civil Engineering 14, https://doi.org/10.1007/978-981-13-0559-7_45

Poorebrahim 2014; Abiodun and Nalbantoglu 2015) and improving the expansive soil behavior by fly ash columns (Phanikumar et al. 2009; Palaniappan and Prabhu 2013).

An experimental investigation has been carried out in this study, with vertical fly ash columns in the expansive clay bed.

Das and Yudhbir (2005) pointed out the poor performance of the typical Indian low calcium fly ashes and (Du et al. 2016; Jiang et al. 2015) pointed out calcium carbide residue (CCR) as an environmentally friendly binder for the stabilization. Due to these reasons, the amount of calcium in fly ash columns has been increased with different percentages of CCR. This paper explores the reaction of fly ash columns in expansive clay specimens and represents the effect on swell properties of expansive soils by analyzing the results of laboratory oedometer tests, free swell index (FSI) and grain size distribution tests (PSD).

2 Experimental Investigation

A laboratory oedometer test has been conducted on expansive clay soil stabilized by FACs to study the efficacy of FACs in reducing the swell characteristics of expansive soil.

2.1 Test Materials

2.1.1 Expansive Soil

The expansive soil used for experimental work has been collected from Nanded city, located in Sinhagad road in Pune, Maharashtra, India from a depth of 0.5 to 1.5 m below the ground level. The basic physical and engineering properties of the parent soil have been listed in Table 1. Soil is classified as fine grained soil, which has been further classified as MH-CH as per Casagrande's plasticity chart (IS-1498-1970). According to IS: 1498-1970, the degree of expansion has been classified as high to very high. The X-ray diffraction (XRD) spectrometer (Phillips 2404, the Netherlands), indicates montmorillonite as the dominant mineralogical constituent of this soil and the basal spacing, height and position of the 001 peak of the clay has been observed to be 16.24 Å, 7075 cts, and 5.43°2θ.

2.1.2 Binders

Fly ash for the present study has been supplied by NTPC Limited. CCR has been collected from Acetylene plant, Murbad, Mumbai. The basic physical and engineering properties of the Flyash and CCR have been listed in Table 2. Chemical

Table 1 Properties of soils tested

Index	Value
Hygroscopic water content, w_h (%)	13.4
Specific gravity, G_s	2.69
Liquid limit, w_L (%)	92
Plastic limit, w_p (%)	45
Maximum dry density, ρ_d, max (kN/m^3)[a]	12.6
Optimum moisture content, w_{opt} (%)[a]	35.5
Free swell index (%)	135
Particle size distribution (%)	
Clay (< 0.002 mm)	66
Silt (0.002 to 0.74 mm)	26
Sand (0.74 to 4.75 mm)	7
Gravel (> 4.75 mm)	1

[a]Standard Proctor Compaction

Table 2 Basic physical properties of CCR and fly ash

Index	Value	
	CCR	Fly ash
Specific gravity, G_s	2.26	2.24
Void ratio in the loosest state e_{max}	3.16	1.11
Void ratio in the densest state e_{min}	2.36	0.69
Particle size distribution (%)		
Clay (< 0.002 mm)	0.28	10
Silt (0.002 to 0.74 mm)	99.7	54
Sand (0.74 to 4.75 mm)	1	35

composition of the materials in oxide form has been determined by using the X-ray fluorescence (XRF) setup (PW2404-Panalytical). Results indicate fly ash contains 18.2% Aluminum oxide, 37% Silicon dioxide, 33.6% Iron (III) oxide, 0.66% Calcium oxide and CCR contains 56.8% Calcium oxide.

3 Test Program

Swell and swell pressure of expansive soil has been measured by one-dimensional swelling pressure test with fixed type ring. In order to experimentally figure out that swell reduction is because of influence of admixture binder FACs and not due to soil removal of the columns, swell test has been conducted for the same orientation as FACs with vertical sand drains.

To study the effect of binder on soil texture, post-test observation has been done by conducting particles size distribution and free swell test. Tests carried on

untreated soil and treated soil with vertical columns on 3 mm diameter with 30 mm distance of columns in rectangular pattern while fly ash and CCR ratio was 95 and 5% which designated by 95F5CCR and likewise 90F10CCR, 80F20CCR, 50F50CCR, and 25F75CCR.

4 Experimental Investigation

4.1 Preparation of Specimens

All the tests have been conducted on OMC and MDD in the specimen of diameter 75 mm and height of 20 mm. Oven dried soil <4.75 mm has been used. Samples have been prepared as Nagaraj et al. (2009). The vertical holes have been carefully filled with sand of particle size of less than 425 μm (fine sand) with 85% relative density or by 85% relative density purposed binder. A seating load of 6.25 kPa has been applied on the hanger. Figure 1 shows the compacted specimen with seven vertical drains.

4.2 Tests Conducted

On applying the seating pressure of 6.25 kPa and giving free water access to the top and bottom, swell has been measured. The free swell reading has been recorded over a period of 10 days. Afterwards, the swell sample has been subjected to

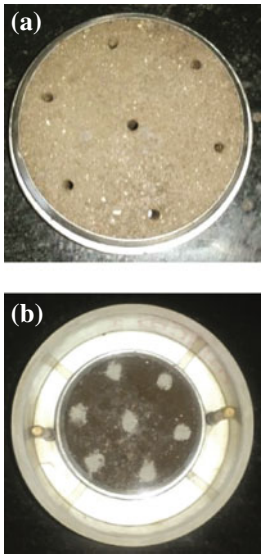

Fig. 1 (a) Final stage of drilling seven vertical holes. (b) Final view of specimen filled up with fly ash and CCR admixture

consolidation under different pressures. For each load specimen, the compression deformation has been recorded for 24 h. The consolidation loads have been applied till the specimen attained its original volume. After determining the swelling pressure, unloading has been done in stages. Every sample has been preserved in a different box for post investigation tests.

The post-test investigation has done on air-drying of specimen, after removal of binder from columns and grinding. FSI has been obtained by passing soil through 425 μm sieve. Two samples of soil have been taken each weighing ∼10 g. One has been put in 50 cc graduated glass cylinder containing kerosene oil and the other sample has been put in a similar cylinder containing distilled water. Both the samples have been left undisturbed for 24 h and then their volumes were noted. In case of particle size distribution analysis, grinded soil has been passed through 0.3 mm sieve. Then has been mixed with sufficient quantity of distilled water and subjected to the laser particle size analyzer.

5 Results and Discussion

The influence of vertical sand drains on swell behavior has been earlier reported by (Nagaraj et al. 2009). The swell and swell pressure has increased because of better saturation of the soil specimen with improved drainage. A similar trend has been observed from Fig. 2, that is, the amount of swell magnitude has increased from 2.11 to 2.26 mm (∼6.7% increase) and swell pressure has increased from 190 to 210 kPa (∼10.5% increase) with the introduction of vertical sand drains. Figure 2 also shows FAC-reinforced expansive clay bed, compacted at initial dry unit weight of 12.6 kN/m^3 with binder stabilized of 95F5CCR, 90F10CCR, 80F20 CCR, 50F50CCR and 25F75CCR, underwent an equilibrium heave of 1.494, 1.206, 1.108, 1.374, and 1.129 mm respectively, resulting in a respective reduction in

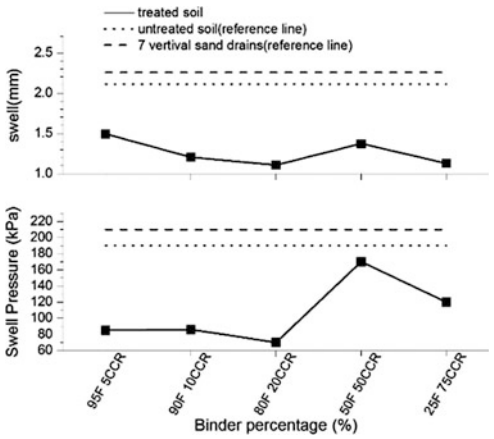

Fig. 2 Variable of swell and swell pressure, with and without vertical drains

heave of 29, 43, 48, 35 and 46%. Swell pressure of above mention sample reduced from 190 to 85, 86, 70, 170, and 120 kPa respectively, resulting in a respective reduction in pressure of 52, 54, 63, 10, and 36%.

Thus heave and swell pressure decreased in all FACs reinforced clay bed. Maximum reduction of heave and swell pressure has been observed on reinforced clay bed of 80F20CCR. This has been attributed to the migration of pozzolanic material and Ca^{2+} ions from the FACs into the soil, flocculation of particles and pozzolanic reactions take place in FACs reinforced clay bed which pointed by Abiodun and Nalbantoglu (2015). As pH value of calcium base stabilized soil increases for pozzolanic reaction, visual observation of pH value of untreated soil and treated soil has done by using 1% phenolphthalein solution indicator. It has been observed that solution of untreated soil becomes pink in color while all combination of treated soil solutions turned colorless. Colorless solution of treated soil may indicates pozzollanic reaction which takes place for pH > 12. The results of PSD test have been shown in Fig. 3. The aim of this test has been to determine whether there was a shift of particle size due to influence of fly ash and CCR to soil. It has been observed that the addition of 80% flyash 20% CCR leads to reduction of clay-sized particle percentages from 66% on untreated soil to less than 5%, higher than the other combinations of binder mixtures. The silt-sized particle percentage of the addition of 80F20CCR increased substantially from 26 to 90% on treated soil.

The change in particle size percentages in the stabilized soils has been inferred mainly due to the some chemical reaction that causes flocculation of clay particle by cation exchange (Cokca 2001).

Table 4 shows variation of the FSI according to different percentages of fly ash and CCR binder admixture.

The free swell index decreased for all combination. Average reduction has been found to be 14% which has been attributed to change of clay particle size to non-plastic silt size, leading to reduction of swelling behavior. Fly ash and CCR are compounds of silicate, alumina, iron oxide and calcium, which promote flocculation of clay particle. The surface area of the samples and affinity for water has been observed to decrease and causes reduction in FSI. (Mir and Sridharan 2013;

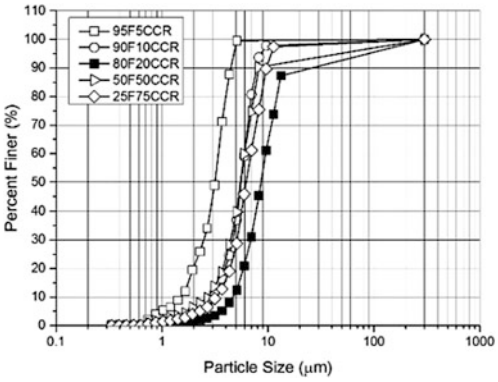

Fig. 3 Results of particle size distribution test in different percentages of binder

Table 4 Results of free swell test in different percentages of binder

Soil state	95F5CCR[a]	90F10CCR	80F20CCR	50F50CCR	25F75CCR
Treated soil	131.5	117.5	113	118	100
Ave. 116 14% reduction					

[a]95F5CCR; 95 percentage fly ash and 5 percentages CCR

Phanikumar and Sharma 2004). Higher values of FSI for 50F50CCR compared to 80F20CCR can be explained as fly ash decreases from 80 to 50%, it causes the reduction of water influence and calcium to clay bed, hence, FSI, swell pressure and heave were attributed to increase. The tests for the other cases like 25F75CCR are ongoing and awaiting results. From our current observations and analysis, it can be clearly stated that the technique of FACs reinforced soil has proved to be a very effective method and helped to reduce the swell behavior of expansive soil. The use of fly ash and CCR as civil engineering construction material has ceased their hazardous environmental effects and has also proved out to be very economical.

6 Conclusions

From the laboratory study the following conclusion have been drawn:

With the vertical sand drains into the clay bed, the measured heave has been observed to increase by 6.7% and increase in swell pressure by 10.5%.

With the vertical FACs, the measured heave has been observed to reduce for all combination of fly ash and CCR admixture. Maximum reduction of 48% in 80F20 CCR has been found. Swell pressure has been observed to reduce for all combination of fly ash and CCR admixture. Maximum reduction of 63% in 80F20CCR has been observed. Maximum clay fraction reduction has been observed by 80F20CCR. The free swell index has been found to decrease for all the combinations.

To investigate the optimum spacing, micro structure, and soil mineralogy, further study is required with different column orientations, along with shrinkage limit studies, XRD and SEM as post-tests.

References

Aljorany, A. N., Ibrahim, S. F., & Al-Adly, A. I. (2014). Heave behaviour of granular pile anchor-foundation system (GPA-foundation system) in expansive soil. *Journal of Engineering, 20*(4), 1–22.

Abiodun, A. A., & Nalbantoglu, Z. (2015). Lime pile techniques for the improvement of clay soils. *Canadian Geotechnical Journal, 52*(6), 760–768.

Cokca, E. (2001). Use of class C fly ashes for the stabilization of an expansive soil. *Journal of Geotechnical and Geoenvironmental Engineering, ASCE, 127*(7), 568–573.

Das, S. K., & Yudhbir. (2005) Geotechnical characterization of some Indian fly ash. *Journal of Material in Civil Engineering, ASTM, 17*(5), 544–552.

Du, Y. J., Jiang, N. J., Liu, S. Y., Horpibulsuk, S., & Arulrajah, A. (2016). Field evaluation of soft highway subgrade soil stabilized with calcium carbide residue. *Soil and Foundation, 56*(2), 301–314.

Jiang, N. J., Du, Y. J., Liu, S. Y., & Wei, M. L. (2015). Multi-scale laboratory evaluation of the physical, mechanical and microstructural properties of soft highway subgrade soil stabilized with calcium carbide residue. *Canadian Geotechnical Journal*. Published on the web 28 August 2015.

Mir, A., & Sridharan, A. (2013). Physical and compaction behaviour of clay soil-fly ash mixtures. *Geotechnical and Geological Engineering, 31*(4), 1059–1072.

Malekpoor, M. R., & Poorebrahim, Gh R. (2014). Behavior of compacted lime-soil columns. *International Journal of Engineering, 27*(2), 315–325.

Nagaraj, H. B., Mohammed Munnas, M., & Sridharan, A. (2009). Critical evaluation of determining swelling pressure by swell-load method and constant volume method. *Geotechnical Testing Journal, ASTM, 32*(4), 1–10.

Phanikumar, B. R., Sharma, R. S., Rao, A. S., & Madhav, M. R. (2004). Granular pile anchor foundation (GPAF) system for improving the engineering behaviour of expansive clay bed. *Geotechnical Testing Journal, ASTM, 27*(3), 1–9.

Phanikumar, B. R., & Sharma, R. S. (2004). Effect of fly ash on engineering properties of expansive soils. *Journal of Geotechnical and Geoenvironmental Engineering, ASCE, 130*(7), 764–767.

Phanikumar, B. Srirama, Rao, A., & Suresh, K. (2008). Field behavior of granular pile-anchors in expansive soils. *Journal of Ground Improvement, 161*(GI4), 199–206.

PhaniKumar, B. R., Mani, A. R., Sathiyasheelan, S., & Reddy, P. R. (2009). Fly ash columns (FAC) as an innovative foundation technique for expansive clay beds. *Journal of Geomechanics and Geoengineering, 4*(3), 183–188.

Palaniappan, K. E. A., & Prabhu, S. (2013). Improving soft clay soil using fly ash as material of column. *International Journal of Engineering Research & Technology (IJERT), 2*(4), 1458–1464. ISSN: 2278-0181.

Viswanadham, B. V. S., Phanikumar, B. R., & Mukherjee, R. V. (2009) Swelling behaviour of a geofiber-reinforced expansive soil. *Geotextiles and Geomembranes, 27*(1), 73–76.